To the Graduate Council:

I am submitting herewith a dissertation written by Ahamad Yacub A. Khan entitled " A FUNDAMENTAL INVESTIGATION OF THE EFFECTS OF DIE GEOMETRY AND PROCESS VARIABLES ON FIBER DIAMETER AND QUALITY OF MELT BLOWN POLYPROPYLENE WEBS." I have examined the final copy of this dissertation for form and content and recommend that it be accepted in partial fulfillment of the requirements for the degree of Doctor of Philosophy, with a major in Human Ecology.

Larry C. Wadsworth, Major Professor

We have read this dissertation and recommend its acceptance:

Accepted for the Council:

Associate Vice Chancellor and Dean of the Graduate School

A FUNDAMENTAL INVESTIGATION OF THE EFFECTS OF DIE GEOMETRY AND PROCESS VARIABLES ON FIBER DIAMETER AND QUALITY OF MELT BLOWN POLYPROPYLENE WEBS

A Dissertation Presented for the Doctor of Philosophy Degree

The University of Tennessee, Knoxville

Ahamad Yacub A. Khan

May 1993

DEDICATION

This dissertation is dedicated to my loving parents, brothers, sister, and all my near and dear ones.

ACKNOWLEDGMENTS

I would like to express my deepest gratitude and appreciation to my advisor and major professor, Dr. Larry Wadsworth, for providing encouragement and guidance over the past three years. I feel indebted to him for having inculcated in me a sense of perfection.

I would like to thank Dr. Kermit Duckett, Dr. Gajanan Bhat, Dr. Marion Hansen, and Dr. Mancil Milligan for taking the time to serve on my graduate committee and for the helpful suggestions they made in reviewing this dissertation and Dr. William Sanders for the help in statistical analyses and experimental design. I would like to thank Mr. Larry Spires and Mr. Richard Meade at the Textile Processing Laboratory for all the help and valuable suggestions offered during melt blowing trial runs.

I owe a great deal to my parents, brothers and sister for their support and encouragement through all these years of college. I am grateful to all my friends, especially Dr. Charles Hassenboehler, Jr. for lending a friendly ear to my problems and help overcome occasional disappointments during this research. II would like to express my special thanks to Mr. Nataraj Gosavi for his help in preparing tables, and proof reading this dissertation for consistency and continuity.

I sincerely thank Exxon Chemical Company for their financial support and assistance throughout this work. I would also like to thank Mr. Chris Davey and Dr. Robert Buntin for their valuable suggestions during the course of this research.

ABSTRACT

An elaborate investigation was carried out to study the effects of die geometry and process variables on fiber diameter and shot formation of melt blown polypropylene webs. This four part investigation included the study of die orifice dimensions such as diameter and L/D ratio, die geometry variables such as nosetip angle, air gap, nosetip setback, face gap, and process variables such as polymer throughput rate, volumetric flow rate of primary air, die-to-collector-distance, resin melt flow rate (MFR), and melt shear viscosity. Also the effects of different process variables on physical and mechanical properties of the webs were studied during phase I. The 6-inch pilot line at UTK was used to melt blow a series of homopolypropylene resins provided by Exxon Chemical Company.

Statistical techniques used to analyze the data in Phase I concluded that polymer throughput was the only variable to have an independent main effect on average fiber diameter when the primary air flow rate was maintained constant while air knife gap and the corresponding nosetip setback, orifice diameter, orifice L/D, polymer MFR, and polymer throughput rate were varied. Orifice diameter, resin MFR, air gap, and L/D ratio all had a statistically significant effect (interactive) on average fiber diameter and shot formation. It was also found that under the processing conditions employed, 400 MFR was more sensitive to orifice length than 35 MFR. During Phase II with 650 MFR, the air-to-polymer flow rate ratio and air knife gap were maintained constant while polymer throughput rate and nosetip setback were varied. It was learned that the average fiber diameter could be maintained over a range of only 0.46 μm with increasing polymer throughput rate from 0.4 to 2.0 g/hole/min. Under the resin and processing conditions employed, the effect of nosetip setback on fiber diameter

was not statistically significant. Orifice L/D did not show a statistically significant effect on average fiber diameter. It was also found during phase II that shot notably increased with the increase in polymer throughput rate, nosetip setback and orifice diameter. The general conclusion from phases I and II was that orifice diameter in the range of 15-20 mils had no practical effect on final fiber diameter.

During Phase III of this research, 800 MFR webs produced with a 60^0 nosetip angle were compared to ones made with a 90^0 tip. The results indicate slightly smaller average fiber diameter for webs obtained with a 60^0 nosetip. However, the coefficient of variation of fiber diameter was found to be smaller in the case of 90^0 nosetip angle. The key properties of melt blown webs such as air permeability, bursting strength, and aerosol filtration efficiency to 0.1 μm sodium chloride particles were all higher for the 90^0 nosetip angle compared to 60^0 nosetip angle.

Phase IV was carried out to explain the effects of orifice diameter and L/D ratio on fiber diameter in terms of viscosity response obtained under different processing conditions. Both the 35 and 800 MFR resins used this part of the research exhibited a linear response between shear stress and shear rate under actual melt blowing conditions with the chosen temperatures, orifice dimensions, and polymer throughput rates.

TABLE OF CONTENTS

CHAPTER		PAGE
1	INTRODUCTION	1
	BACKGROUND	1
	OBJECTIVES	4
	PRESENT STUDY	6
2	REVIEW OF LITERATURE	8
3	EXPERIMENTAL DESIGN	19
	MATERIALS	19
	DIE SWELL STUDIES - INSTRON RHEOMETER	19
	WEB PREPARATION	21
4	EXPERIMENTAL PROCEDURES	34
	DIE SWELL MEASUREMENTS	34
	AIR PERMEABILITY	34
	BURSTING STRENGTH	35
	FIBER DIAMETER	35
	FILTRATION EFFICIENCY	35
	WEB TENACITY AND ELONGATION-AT-BREAK	36
	MOLECULAR WEIGHT DETERMINATION	37
	SHOT LEVEL	37
	FLY RATING	37
	MELT SHEAR VISCOSITY	38
	PACKING FACTOR	38
	SODIUM CHLORIDE AEROSOL FILTRATION EFFICIENCY	39

CHAPTER PAGE

5 RESULTS AND DISCUSSION 41

DIE SWELL STUDIES - INSTRON RHEOMETER 41

PHASE I - PRELIMINARY STUDY 42

Process Conditions 47

Shot and Fly Formation 48

Effect of Production Variables on Shot Generation 48

Effect of Production Variables on Fly Generation 52

Effect of Production Variables on Fiber Diameter 56

Effect of Die-to-Collector Distance on Fiber Diameter 64

Effect of Production Variables on Physical and Mechanical Properties of Webs 64

Effect of Production Variables on the Weight Average Molecular Weight of the web 93

PHASE II - NOSETIP SETBACK STUDY 98

Effect of Production Variables on Fiber Diameter 102

Effect of Production Variables on Shot Generation 112

Effect of Primary Air Velocity and Momentum on Fiber Diameter and its Variability 119

PHASE III - NOSETIP ANGLE (60^0 vs 90^0) STUDY 128

Effect of Nosetip Angle on Fiber Diameter and its Variability 128

Effect of Nosetip Angle on the Physical and Mechanical Properties of Melt blown Webs 134

PHASE IV - MELT SHEAR VISCOSITY STUDY OF 35 AND 800 MFR POLYPROPYLENE MELTS 139

CHAPTER **PAGE**

6 CONCLUSIONS 146

LIST OF REFERENCES 150

APPENDIXES 155

APPENDIX A - DIE SWELL STUDIES (INSTRON RHEOMETER) 156

APPENDIX B - STATISTICAL ANALYSES 161

APPENDIX C - PRIMARY AIR FLOW RATE AND VELOCITY DETERMINATION 186

APPENDIX D - MELT SHEAR VISCOSITY DATA [PHASEIV] 192

APPENDIX E - MASTER DATA TABLE 203

VITA 211

LIST OF TABLES

TABLE		PAGE
3.1	Melt Blown Processing Conditions (6" Line) [Phase I], Air Valve Setting 40%	24
3.2	Melt Blown Processing Conditions (DCD Study) - Phase I. 35 MFR, 0.4 g/hole/min Throughput, 20 mil Orifice Diameter, 5 psi Pressure, and 15/1 L/D	27
3.3	Melt Blown Processing Conditions (6 " line), Phase II, PD 3495 G (650 MFR) Polypropylene Resin	30
5.1	Results Table - Phase I	43
5.2	Shot and Fly Rating of MB PP Webs - Phase I	49
5.3	Average Fiber Diameter and Shot Rating of 650 MFR Melt Blown PP Webs	99
5.4	Actual CFM and Air Velocity Data for 0.4, 0.8, and 1.2 g/hole/min Polymer Throughput Rates - Phase II	108
5.5	Results of the 60^0 versus 90^0 Nosetip Angle Study [Phase III] Primary Air Flow Rate = 130 Standard ft^3/min at 14.5 psi, 70^0 F	129
5.6	ACFM, Primary Air Velocity, And Momentum Calculations-60^0 versus 90^0 Nosetip Angle Study - Phase III Primary Air Flow Rate = 130 Standard ft^3/min at 14.5 psi, 70^0 F	132
5.7	Melt Shear Viscosity (Newt) Data - Phase IV [Parameters Measured During Actual Melt Blowing]	143
A.1	Die Swell Data for Different Polymer Throughputs and L/D Ratios - Instron Rheometer Temperature=240 ^{0}C; 400 MFR Polypropylene	157

TABLE **PAGE**

B.1 Summary of Main Effects and Interactive Effects on the Response Variables - Phase I 162

B.2 Summary of Main Effects and Interactive Effects on the Response Variables - Phase II 163

D.1 Melt Shear Viscosity Data (Newtonian) for 35 (PP 3445) and 800 (PD 3545G) MFR Polypropylene Resins - Phase IV [Parameters Measured Under Actual Melt Blowing] 193

E.1 Master Data Table 204

LIST OF FIGURES

FIGURE		PAGE
1.1	Schematic of a melt blowing process	5
3.1	Flow chart of experimental design - Phase I	22
3.2	Flow chart of experimental design - setback study	29
3.3	Flow chart of experimental design - nosetip angle study	31
5.1	Effect of orifice L/D ratio, orifice diameter, and air knife gap on average fiber diameter showing the 96 % upper and lower confidence limits	57
5.2	Effect of orifice L/D ratio, orifice diameter, and air knife gap on average fiber diameter showing the 96 % upper and lower confidence limits	58
5.3	Effect of orifice L/D ratio, orifice diameter, and air knife gap on average fiber diameter showing the 96 % upper and lower confidence limits	59
5.4	Effect of orifice L/D ratio, orifice diameter, and air knife gap on average fiber diameter showing the 96 % upper and lower confidence limits	60
5.5	Effect of air knife gap on average fiber diameter at constant primary air stagnation pressure	65
5.6	Effect of volumetric flow rate of air on average fiber diameter at constant primary air stagnation pressure	66
5.7	Effect of DCD on average fiber diameter	67
5.8	Effect of L/D ratio, orifice diameter, and air knife gap on filtration efficiency	69

FIGURE **PAGE**

5.9 Effect of L/D ratio, orifice diameter, and air knife gap on filtration efficiency 70

5.10 Effect of L/D ratio, orifice diameter, and air knife gap on filtration efficiency 71

5.11 Effect of L/D ratio, orifice diameter, and air knife gap on filtration efficiency 72

5.12 Effect of L/D ratio, orifice diameter, and air knife gap on air permeability 73

5.13 Effect of L/D ratio, orifice diameter, and air knife gap on air permeability 74

5.14 Effect of L/D ratio, orifice diameter, and air knife gap on air permeability 75

5.15 Effect of L/D ratio, orifice diameter, and air knife gap on air permeability 76

5.16 Effect of L/D ratio, orifice diameter, and air knife gap on bursting strength 78

5.17 Effect of L/D ratio, orifice diameter, and air knife gap on bursting strength 79

5.18 Effect of L/D ratio, orifice diameter, and air knife gap on bursting strength 80

5.19 Effect of L/D ratio, orifice diameter, and air knife gap on bursting strength 81

5.20 Effect of L/D ratio, orifice diameter, and air knife gap on MD web tenacity 83

5.21 Effect of L/D ratio, orifice diameter, and air knife gap on MD web tenacity 84

FIGURE **PAGE**

5.22 Effect of L/D ratio, orifice diameter, and air knife gap on MD web tenacity 85

5.23 Effect of L/D ratio, orifice diameter, and air knife gap on MD web tenacity 86

5.24 Effect of L/D ratio, orifice diameter, and air knife gap on M D breaking elongation 88

5.25 Effect of L/D ratio, orifice diameter, and air knife gap on MD breaking elongation 89

5.26 Effect of L/D ratio, orifice diameter, and air knife gap on M D breaking elongation 90

5.27 Effect of L/D ratio, orifice diameter, and air knife gap on M D breaking elongation 91

5.28 Effect of L/D ratio, orifice diameter, and air knife gap on weight average molecular weight of the web 94

5.29 Effect of L/D ratio, orifice diameter, and air knife gap on weight average molecular weight of the web 95

5.30 Effect of L/D ratio, orifice diameter, and air knife gap on weight average molecular weight of the web 96

5.31 Effect of L/D ratio, orifice diameter, and air knife gap on weight average molecular weight of the web 97

5.32 Effect of nosetip setback on average fiber diameter 104

5.33 Effect of nosetip setback on average fiber diameter 105

5.34 Effect of nosetip setback on average fiber diameter 106

5.35 Effect of nosetip setback on average fiber diameter 107

5.36 Effect of nosetip setback on shot 113

FIGURE PAGE

5.37 Effect of nosetip setback on shot 114

5.38 Effect of nosetip setback on shot 115

5.39 Effect of nosetip setback on shot 116

5.40 Effect of primary air momentum on average fiber diameter 121

5.41 Effect of primary air momentum on average fiber diameter 122

5.42 Effect of primary air momentum on average fiber diameter 123

5.43 Effect of primary air momentum on C.V% of fiber diameter 124

5.44 Effect of primary air momentum on C.V% of fiber diameter 125

5.45 Effect of primary air momentum on C.V% of fiber diameter 126

5.46 Effect of nosetip angle on average fiber diameter 130

5.47 Effect of nosetip angle on C.V% of fiber diameter 131

5.48 Effect of nosetip angle on air permeability 135

5.49 Effect of nosetip angle on NaCl aerosol filtration efficiency 136

5.50 Effect of nosetip angle on bursting strength 137

5.51 Effect of nosetip angle on web packing factor 138

5.52 Effect of shear rate on shear stress of 35 MFR PP melt 140

5.53 Effect of shear rate on shear stress of 800 MFR PP melt 142

A.1 Effect of polymer throughput and L/D ratio on die swell ratio 159

A.2 Effect of polymer throughput and L/D ratio on melt pressure 160

CHAPTER 1

INTRODUCTION

BACKGROUND

Although nonwovens have been manufactured for only five decades, they account for 10% of all textiles manufactured in the United States within this relatively short period of time [1,2]. In spite of their significant market penetration, the awareness of their existence among the general public is quite poor. Though the term "nonwoven" is well accepted, the word is not a satisfactory descriptor of this class of textiles. "Nonwovens" does not indicate how these textile materials are made, but rather how they are not made. The average person uses nonwovens in every day life without even being aware of it. Nonwoven materials have found applications in a variety of diverse areas ranging from clean room garments to baby diapers. Nonwoven fabrics are used in disposable diapers, adult incontinence products, feminine hygiene products, surgical supplies, protective apparel for doctors and health care professionals, wipes, garment interlinings, automobile interiors, substrates for synthetic luggage materials, geotextiles, floppy disk liners, carpet backings, thermal insulation [3], tea bags, filtration media, and various other household and industrial applications.

Nonwoven fabrics are "porous, textile like materials, usually in flat sheet form, composed primarily or entirely of fibers assembled in webs. These fabrics, also called bonded fabrics, formed fabrics, or engineered fabrics, are manufactured by processes other than spinning, weaving, or knitting [3]." The primary elements of all nonwoven technologies are fiber selection, web

formation, and bonding. On the basis of web formation techniques, nonwovens can be broadly classified into dry laid, wet laid, or direct-bulk polymer to web technologies. Melt blown nonwovens fall into the third category, along with spunbond webs. In this class, the fiber and web formation occur in one continuous step compared to dry laid and wet laid where the fiber and web formation are two very different independent processes.

The melt blowing process as it stands today has advanced greatly since the 1951 project initiated at the Naval Research Laboratory to investigate the various possibilities to manufacture submicron diameter organic fibers. The results of the study were documented by Wente [4] in a publication titled "Superfine Thermoplastic Fibers". Wente's study paved the way for the present day melt blowing technology. According to Wente, a series of molten polymeric jets issuing from fine orifices were attenuated using two, convergent high velocity heated air streams and the resulting superfine fibers were made to pass over a 16-mesh collecting screen resulting in a random and cohesive network of fibers.

In 1974 Esso Research and Engineering Company (presently, Exxon Chemical Company) obtained a patent titled "Nonwoven Mats by Melt blowing" [5]. Although research and development work was carried out prior to 1974, it is only since 1974 that large scale commercialization of the melt blowing process began. Since then melt blowing has become an important industrial technique to manufacture micro-fibered webs (1-5 μm average fiber diameter). The fine fibers in a melt blown web result in soft, drapable, and breathable fabrics used in filtration media, medical supplies, thermal insulation, and several other applications.

The basic components of a melt blowing process are:

(a) a polymer feed system, generally a hopper fed screw extruder,

(b) a metering pump to vary the polymer throughput rate,

(c) a polymer feed distribution system to provide even polymer flow and residence time across the whole width of the die,

(d) a die block that consists of a nosetip with closely arranged holes (typically 15 mil in diameter and 20-30 holes per inch), with an including angle, usually 60^0 and two air bars (air knives) with their inside surfaces following the contour of the nosetip. The gap between the inside surface of the air knife and the nosetip (commonly referred to as the air gap) can be varied to change the air velocity. Relative to the face of the orifice plane the air knives can be pushed in or out to create an offset referred to as the setback. The die can either be horizontal (in which case the fibers are blown parallel to the floor) or vertical (in which case the fibers are blown perpendicular to the floor),

(e) a collection device (collector) for collecting the attenuated filament streams thus forming a web with almost random network of fibers. It also serves as a device to separate the fibers from the air blast. In the case of a horizontal melt blowing system, typically the collector is a cylindrical wire mesh screen. A vertical melt blowing system, typically has an endless forming belt running flat over the collection area below the die block, although either type of collector device may be used with either melt blowing system, and

(f) a winding system to wind the formed nonwoven web into a cylindrical package for easier subsequent handling.

A thermoplastic, fiber forming resin (granules, pellets, or flakes) is fed to the extruder by a hopper. The molten polymer is metered by a gear pump to the orifices through a polymer feed distribution system. As the molten polymer jets

exit the orifices, convergent streams of high velocity hot air on either side of the nosetip attenuate them to superfine fibers. As the turbulent air stream expands, the ambient air is entrained into the flow field which provides a convective medium of heat transfer for the polymer jets to cool. The attenuated filaments are carried by the air stream and deposited on the rotating collector. The speed of the collector can be varied to obtain the desired web basis weight. A schematic diagram of the melt blowing process is shown in Figure 1.1.

OBJECTIVES

The primary objective of this dissertation was to investigate the effects of die geometry, specifically the orifice diameter, orifice L/D ratio, air knife configuration (air gap and setback), air injection angle, and various process variables on the fiber diameter and web quality (in terms of shot and fly generation) of melt blown webs produced with different melt flow rate (MFR) polypropylene resins. Ever since the commercialization of melt blowing technology, the industry has been pushing for higher production speeds. Production rates greater than 1.0 g/hole/min appeared impossible a decade ago because of the need to obtain sufficiently low viscosity in the melt blowing process. Although the developments in higher melt flow rate (MFR) resins have made processing at greatly increased production rates possible, the quality of the web has generally been found to deteriorate with increasing polymer throughput rate. The success of melt blowing can be attributed mostly to the extremely fine fiber diameters (1-5 μm) and the way they are arranged in the web. Processing at high polymer throughput rates requires a thorough understanding of the various machine variables and production parameters and their effect on fiber diameter

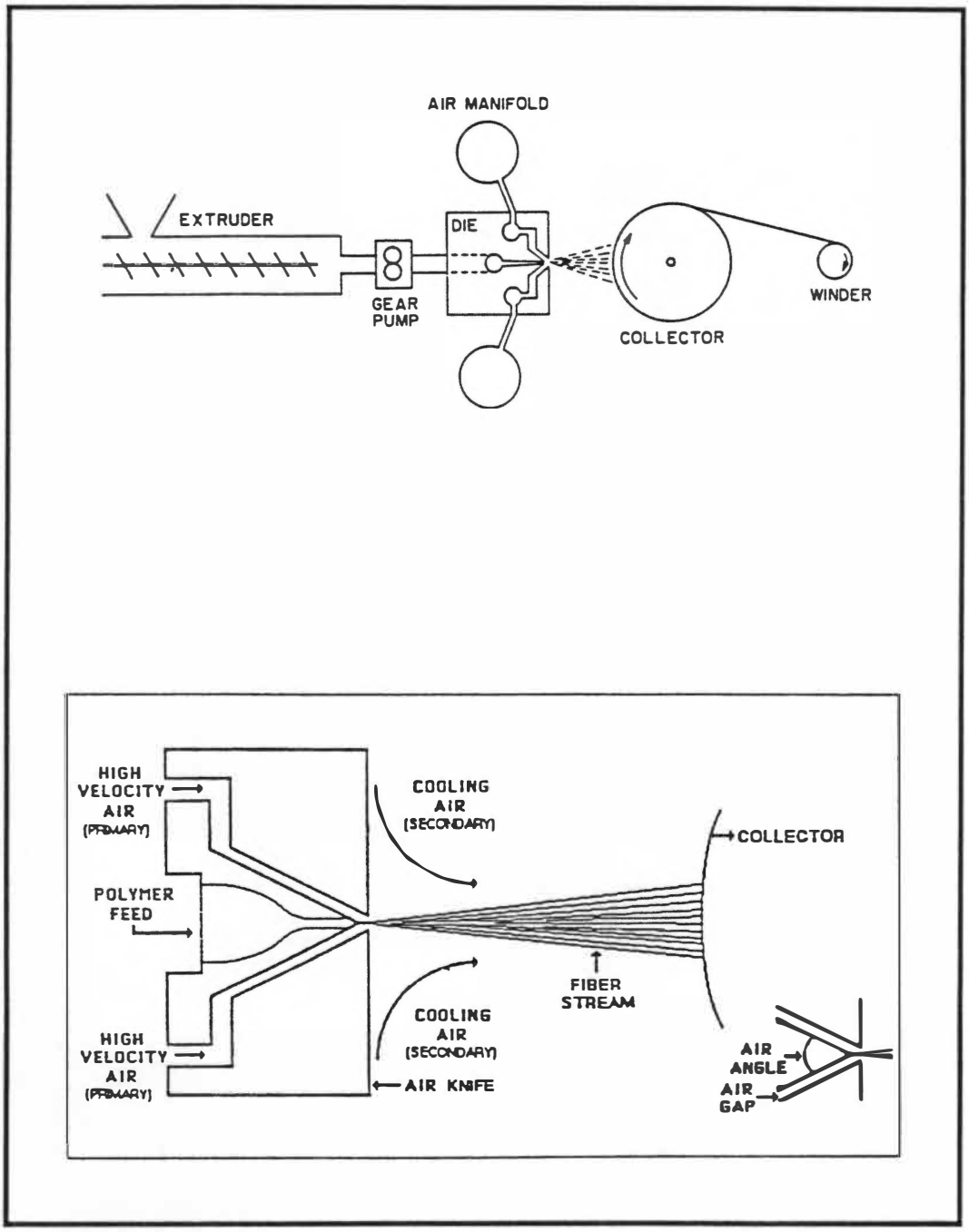


Figure 1.1 Schematic of a melt blowing process [16]

and web quality. This research was an attempt to help gain a better handle on the various factors affecting the fiber diameter and web quality of melt blown polypropylene webs. An attempt was made to theoretically explain the results obtained, using the well-known fundamentals of polymer rheology.

PRESENT STUDY

The research presented in this dissertation is concerned with the investigation of the effects of die geometry variables, air knife configuration, and process parameters on the fiber diameter and web quality in melt blowing. As a precursor to Phase I die swell measurements were carried out with the 400 MFR PP resin using a Instron Capillary Rheometer on single orifice dies with different orifice diameter and L/D ratio combinations. The primary motivation for this study was to determine the magnitude of die swell with high MFR (low molecular weight) PP resins and if increasing orifice L/D would result in decreasing die swell ratio. Phase I of the research was concerned with studying the effects of orifice diameter, orifice L/D ratio, air gap, resin MFR, polymer throughput rate, and their interactions on fiber diameter, shot and fly generation.

Polypropylene resins with two different melt flow rates (MFR) 35 and 400 were melt blown at two levels each of air gaps, orifice L/D ratio, orifice diameter, and polymer throughput rate. The melt blown web properties determined were average fiber diameter, filtration efficiency, shot and fly generation, breaking strength, elongation-at-break, air permeability, and bursting strength, as well as the web weight average molecular weight of the PP in the web.

Phase II was designed to investigate the effect of nosetip setback, and constant air-to-polymer flow rate ratio at increasing polymer throughput rates on

fiber diameter and shot generation. A different MFR polypropylene resin (650) than the one used in first part of this research was melt blown at two levels each of orifice diameters, orifice L/D ratio, five levels each of nosetip setbacks, and polymer throughput rate.

All the runs were carried out at a constant nominal air gap of 31 mil. The webs were characterized in terms of average fiber diameter and incidence of shot. A different MFR polypropylene resin was chosen for two reasons, one being a means of verification of the results obtained in the first part of the research and the other being the fact that the MFR (650) chosen, is largely used in the industry for melt blowing, as compared to lower MFR resins.

Phase III of this research dealt with the effect of air injection angle on fiber diameter and web quality. The study consisted of runs comparing webs obtained from the traditional 60^0 nosetip (30^0 air injection angle) with that of the 90^0 experimental nosetip. A 800 MFR resin was used for this study.

In Phase IV, an attempt was made to theoretically explain the experimental results obtained using well known fundamentals of polymer rheology. Using accurate melt pressure measurements from the actual melt blowing operation with different polymer throughput rates, orifice diameters, and orifice L/D ratios, shear viscosities were computed. The calculated shear viscosity data was used to explain the effects of changes in orifice diameter and L/D ratio on fiber diameter during Phase I and Phase II.

CHAPTER 2

REVIEW OF LITERATURE

The earliest nonwovens were believed to have been produced in prehistoric times by cave men beating wet wool fibers with a rod. Although, the felting process has become mechanized in more recent history, some of the definitions of nonwovens do not include felting as a nonwoven process [6]. In the ever controversial area of defining nonwovens, some definitions are well accepted than the others. The American Society of Testing and Materials (ASTM) [6] has defined the term "nonwoven" as "a structure produced by bonding or the interlocking of fibers, or both, accomplished by mechanical, chemical, thermal, or solvent means and the combination thereof. The term does not include paper or fabrics that are woven, knitted, tufted, or those made by wool or other felting processes." TAPPI has taken a more generalized approach and the definition states, "a nonwoven is a fabric-like structure consisting of a conglomeration of fibers that are bonded in some way or the other" [7].

Traditionally melt blowing is defined as "a process for producing micro fibrous webs or articles directly from polymer or resin using high velocity air to attenuate the filaments" [8]. According to Trimble, "melt blowing is a process for producing fibrous webs or articles directly from polymers or resins using high-velocity air or another appropriate force to attenuate the filaments" [8]. This expanded melt blowing process definition accommodates processes where the attenuating force may be provided by some media other than air. Both these definitions fail to make a note of the fact that high-velocity air is normally at a high temperature as well. Therefore it may be necessary to include a descriptor for the

high temperature attenuating air stream to make the above definitions clearer and more representative of the present practice in melt blowing processes.

Although much research and development has been done in the area of melt blowing the amount of existing published research articles is limited. One of the primary reasons for this limited amount of published literature is the highly commercial and proprietary nature of melt blowing technology. Most of the research in melt blowing is geared towards product development work which either gets patented or maintained as trade secret. This has lead to the availability of a large amount of patent literature and relatively very small volume of published research. An extensive review of patents relating to melt blowing is given by Moore [9]. Also, the majority of the published papers are experimental in nature with the exception of a few analytical studies.

Wente first reported the feasibility of manufacturing submicron fibers from a variety of thermoplastic materials [10]. It has been stated that the greatest amount of attenuation occurs at the point of exit of the polymer jet. This conclusion has since been disputed [11]. Wente has stated that fiber diameters as low as 0.1 micron can be obtained from linear polyamides and polyesters. Wente reported that a steeper air angle [90^0] gave a higher degree of fiber dispersion and the fiber mat is deposited on the screen with the most random fiber distribution whereas a 30^0 air angle resulted in increased ropiness, but produced greater fiber attenuation for a given air velocity. These findings appear to imply a streamline attenuation behavior such as in air drag melt spinning. But according to Milligan and Haynes [12], the attenuation of fibers in melt blowing is primarily due to the shape they assume during their flight from the die face to the collector screen, otherwise known as "form drag".

Wente's work formed the basis for early research activity in melt blowing at Esso Research and Engineering Company [13]. Buntin and Lohkamp [13] have stated that during the normal operation of melt blowing process, fiber breakage occurred continuously and that fiber lengths were on the order of a few inches. The current understanding of the melt blowing process provides a better picture of the process. Some believe that melt blown fibers are continuous under normal operating conditions (without fly generation) [15], whereas a few others describe the fibers at the best as semicontinuous [15]. Buntin and Lohkamp [13] associated the incidence of "shot" (they defined shot as a particle of polymer, considerably larger than the fibers, which is formed by the elastic "snap back" of the fiber ends upon breaking) to fiber breakage. With much emphasis placed nowadays on the continuous nature of melt blown filaments under normal operating conditions the origin and nature of shot remains debatable. Malkan has reported that the most likely causes for shot across the total width of the web are either too low temperatures or an air flow rate too low for the chosen processing conditions [16]. Private communications with Textile Processing Laboratory staff at the University of Tennessee, Knoxville have indicated that the primary reason for increased shot is excessive primary air temperatures [17]. Lau [18] without giving reasons has stated that excessive air temperatures resulted in increased incidence of shot in melt blown webs.

Buntin and Lohkamp [13] have described the development of the melt blowing process for converting polypropylene into low cost fine fibrous webs. The advantages of using multiple dies in series to achieve high production rates instead of increased polymer throughput with a single die, have been discussed in terms of web uniformity and reduction of defects.

Jones [19] reported the effects of resin MFR and polydispersity on the mechanical properties of melt blown webs. It has been stated that melt blown web tenacity initially increased with MFR, peaked at 300 MFR, and started decreasing at higher melt flow rates. Jones postulated that the fabric strength was a combination of individual fiber strength and fiber bonding and/or fiber entanglements. The results of Jones agree with the findings of earlier studies [20, 21]. This was in contrast to the findings of Malkan [16]. Malkan reported that breaking stress decreased non-linearly with increase in melt flow rate in both machine and cross directions and attributed the reasons for decreased strength at higher melt flow rates to the lower molecular weight of the resin. Jones [19] also reported that increasing the polydispersity (molecular weight distribution) did not affect the web strength to any great extent.

Warner, Perkins, and Abhiraman [15] have reported that fibers larger than 10 μm have essentially no molecular orientation. This implies that these fibers do not contribute to melt blown web strength in any significant manner. It should also be noted that the mass of a fiber per unit length is proportional to the square of its diameter. Therefore the mass diameter distribution of the web will be more appropriate than the number diameter distribution as a means to calculate the fiber strength realization in a melt blown web. The results of Shambaugh [22], when replotted in terms of a mass-diameter distribution, indicate an increase in the mass fraction (comprised of fibers with diameters 10 μm and above), with increasing the resin polydispersity. This should result in decreased web strength as the molecular weight distribution becomes wider. Malkan's results [16] on bursting strength agree well with the findings of Jones [19]. Bursting strength decreased with increase in melt flow rate of polypropylene resin. Jones also found that the extruder temperatures and polymer throughput rates have a

significant effect on the strength properties of the webs. Tenacity of melt blown webs increased with decreased extruder temperatures; increasing throughputs decreased the bursting strength.

Jones and Wadsworth [20] have reported results of a study which consisted of melt blowing a variety of polypropylenes and a number of experimental polypropylene random copolymers. The key objective of this study according to the authors was to enhance the physical performance properties and develop new product applications. The results show that some webs compared favorably to standard polypropylene webs and had improved drapability. These webs exhibited equal bursting strength, appreciably increased gamma radiation resistance, with only a slight decrease in tenacity when compared to webs of standard polypropylene.

Wadsworth and Jones [23] reported the effects of die-to-collector (DCD) distance, polymer throughput rate, and die orifice diameters on melt blown web properties. The results of the study indicate a decrease in MD tenacity with an increase in DCD whereas the CD tenacity remained relatively constant. The MD tenacity increased with increasing polymer throughput rate and the bursting strength decreased with increasing polymer throughput rate. These results appear to follow the trends of Malkan [16]. Wadsworth and Jones [23] also reported that the smaller orifice die tip appeared to result in slightly larger fiber diameters compared to the standard nosepiece under similar processing conditions. Wadsworth and Muschelewicz [24] have reported the results of a study designed to produce extremely fine melt blown fibers (<2 μm) using 35, 300, and 700 MFR polypropylene resins. The study involved the optimization of melt blown processing conditions to obtain those extremely fine melt blown fibers. Statistical analyses of their data indicated that under some resin and

processing conditions, die orifice diameter had a small but significant effect on fiber diameters [23].

Eaton et al. [21] have studied the effect of pigments on the physical properties of melt blown polypropylene webs. The primary objective of the study was to demonstrate the feasibility of melt blowing pigmented polypropylene resins. Eaton, Wadsworth, and Potnis [25] studied the implications of key performance parameters of melt blown webs in healthcare products. The study suggested that it was possible to carefully control the process parameters to produce webs with physical properties designed to meet the end-use requirements of healthcare products. The results indicated that the flexural rigidity was a good descriptor of softness for optimized melt blown webs, whereas, for coarse, non-optimized webs, a high degree of fiber bunching was observed and flexural rigidity had a poor agreement with tactile hand.

Wadsworth et al. [26] have studied polypropylene melt blown webs in terms of relationships among the processing conditions, structure, and filtration efficiency. The emphasis was on the effect of die-to-collector distance (DCD) and smooth roll thermal calendering on filtration efficiencies of water aerosols containing 0.5 and 0.8 μm latex spheres. It was found that filtration efficiencies for 0.5 and 0.8 μm latex spheres and bacteria were dependent on mean pore diameter and on the parameter "basis weight/the square of the average fiber diameter". It has been reported that calendering reduced web thickness, maximum pore diameters, and air permeability regardless of the original values. Interestingly the DCD of the samples before calendering did not appear to affect the performance values after calendering. A sample made with 12 inches DCD and another made at 15 inches DCD had almost identical air permeability values, and similar latex and bacteria filtration efficiencies after calendering.

Choi et al. [27] have reported a method to obtain the tenacity and Young's modulus of melt blown webs without direct measurement of web thickness. The effect of processing conditions on the strength properties of the webs was discussed. Malkan et al. [28] demonstrated the effects of increasing the throughput rate of 300 and 1400 MFR polypropylene resins while in his first study maintaining air flow rate constant and in his second study by increasing air flow rate with increased polymer throughput on the physical and morphological properties of melt blown fibers and webs. The deterioration of web properties with an increase in polymer throughput rate was discussed. The evidence from differential scanning calorimetry and x-ray diffraction pointed to the presence of more than one morphological form of a single crystal structure. Malkan [16] reported the process-structure-property relationships in melt blowing for different polypropylene resins. The study was extensive and various aspects of melt blowing ranging from process and resin variables to the characterization of web and single fibers have been discussed. It was hypothesized that the reason for increase in fiber diameters with increasing polymer throughputs was because of the increased die swell and the change in air-to-polymer ratio at higher polymer throughput rates. A "processing window" was established to optimize the processing parameters to ensure good web quality.

On the basis of DSC and X-ray diffraction results, Malkan [16] hypothesized that the higher polymer throughput rate condition caused a change in morphological or crystalline structure of melt blown polypropylene fibers. It has been shown that water-quenched polypropylene fibers have a para-crystalline structure and the air-quenched fibers have a regular monoclinic crystal structure. Samuels [30] argued against the possibility of different morphologies (folded chain crystals or extended chain crystals) since the double endotherms were

produced at an isothermal crystallization temperature as low as 130^0 C. This temperature appears to avoid the possibility of extended chain crystal formation. Samuels [30] concluded that two crystalline species are involved, either different disordered crystals, different crystal sizes, or different crystal types as a reason for the double endotherms. Malkan [16] indicated that the presence of double endothermic peaks might have been due to the presence of different crystal forms, namely: a-form (monoclinic) and b-form (hexagonal). Bodahgi [29] has reported several techniques to characterize melt blown microfibers. It has been shown that water-quenched polypropylene fibers have a para-crystalline structure and the air-quenched fibers a regular monoclinic crystal structure.

Straeffer and Goswami [31] reported that 1100 MFI (melt flow index) resin degraded more than the 300 MFI resin. This finding is in conflict with Malkan's [16] results, wherein the lower MFR (melt flow rate, same as MFI) resin degraded more than the higher MFR resin. Warner, Perkins, and Abhiraman [15] claim to be able to see spherulitic crystalline morphology of melt blown fibers using scanning electron microscopy. The procedure used by the authors has not been listed in the article. By comparing the dimensions of a spherulite it appears that a very high magnification (perhaps a few orders of magnitude higher) may have been used. The rest of the conclusions drawn by the above study were more or less similar to conclusions drawn by other studies.

Milligan et al. [32] have reported the use of a stream of unheated cross flow air to make finer melt blown fibers. The authors claim that in addition to finer fiber diameters the variation in fiber diameter was smaller with the use of cross flow air. The motivation for this research was the earlier finding by Milligan and Haynes [33] that the fiber form drag, due to large amplitude flapping of the molten polymer jet as it gets blown away from the die, played a significant role in

contributing to the total air drag force necessary for fiber attenuation during melt blowing. Milligan et al. [32] have pointed out the possibility of substituting unheated cross flow air for a portion of the primary hot air, resulting in energy savings.

Haynes' [34] data on a single hole orifice melt blowing die indicates that at constant volumetric flow rate of primary air, the average fiber diameter is not affected by its velocity (the velocity change had been brought about by the change in air gap). Although the velocity changed more than 200% the average fiber diameter stayed the same. In one case the air velocity was ~220 m/sec and in the other case it was ~520 m/sec. In both cases a similar magnitude fiber with an average diameter of 7.08 μm was obtained. According to Haynes [34], the smaller air gap (higher air velocity) gave a standard deviation of 5.53 μm, while with the larger gap (lower air velocity), the standard deviation was 3.4 μm. It appears that the larger air gap (lower air velocity) produced a narrower fiber diameter distribution. This indicates that the velocity of primary air in itself does not affect the average fiber diameter significantly in the range of velocities discussed here (high end of the possible velocity scale). A careful examination of average fiber diameters produced at low air velocities indicates a notable effect of air velocity on average fiber diameter, even at constant SCFM. Further evidence to this observation is presented elsewhere by Haynes [34]. The fiber diameter decreased when the velocity was increased by increasing the mass flow rate of air at constant air gap. This result implies that the primary controlling variable of fiber diameter is the mass flow rate of air and therefore increasing the velocity alone, without increasing the mass flow rate of primary air is not of much significance with respect to fiber diameter. This finding was in contrast to popular belief that a smaller air gap gave finer fibers at a constant primary air flow rate.

Apart from the experimental studies mentioned above, a few analytical studies have been reported in the literature. Shaumbagh and co-workers [35, 36] have reported various studies conducted in order to mathematically model the melt blowing process. Majumdar and Shaumbagh [37] have calculated the air drag on fine filaments in the melt blowing process using a wide range of filament diameters, gas velocities (primary air velocity), and Reynolds number. Milligan and Haynes [38] studied the air drag on monofilaments simulating the actual melt blowing conditions, except that the high velocity air was at room temperature and one end of the monofilament was secured to a tensiometer. It was found from the investigation that smaller air injection angles gave larger drag with the other parameters remaining constant.

Milligan et al. [39] have suggested design rules to minimize energy cost, specifically by reducing the pressure losses associated with the air piping and efficient location of air heaters. Milligan et al. [40] investigated the energy requirements for melt blowing different polymers. Polypropylene, linear low density polyethylene, Nylon, and polyester were studied and the energy requirements were reported in KW-hr/Kg of polymer.

As is evident from the literature there has not been any study reported on the effects of orifice L/D ratio, setback, polymer throughput rate at constant air-to-polymer flow rate ratio, their interrelationships, and their interactions with the resin and other production variables on the fiber diameter and web quality of melt blown webs. Since the average fiber diameter of melt blown webs is of paramount importance in enhancing their functionality, a study of the effects of above variables on fiber diameters was worthwhile carrying out. The present study was designed to be in tune with attempts in the industry to substantially

increase polymer throughput rates while still trying to keep fiber diameters constant.

CHAPTER 3

EXPERIMENTAL DESIGN

MATERIALS

The polymers used in this research were commercial grade Exxon homo-polypropylene resins with nominal melt flow rate (MFR) values ranging from 35 to 800. They were Exxon grades PP 3445 (35 MFR), PD 3505 G (400 MFR), PD 3495 G (650 MFR), and PD 3545 G(800 MFR). The resins were supplied by Exxon Chemical Company.

DIE SWELL STUDIES - INSTRON RHEOMETER

Six single orifice dies were fabricated at The University of Tennessee, Knoxville (UTK) for experiments using the Instron Capillary Rheometer with the following specifications:

(1) Four dies with orifice diameter of 0.4 mm and L/D values of 5/1, 10/1, 15/1, and 20/1, respectively.
(2) One die with L/D value of 10/1 and orifice diameter of 0.25 mm.
(3) One step die with a L/D of 10/1 and orifice diameter of 0.25 mm in the entry region and a L/D value of 5/1 and orifice diameter of 0.4 mm in the exit region.

The experiments were carried out with 400 MFR PP using these single orifice dies on the Instron rheometer at polymer throughput rates of 0.24, 0.64,

1.34, and 2.68 g/min. The die swell was measured using photographic techniques.

The motivation for this study came from earlier research by Malkan [16], where he concluded that the increase in fiber diameters with increase in throughput, even with increased primary air flow rate may be due to increased die swell. It has been known in classical polymer processing [45], that the length-to-diameter ratio of an orifice affects the amount of die swell. It has been known for a long time that for a particular orifice diameter, as the L/D ratio increases the amount of die swell decreases. But the previous studies were primarily carried out on high molecular weight (low MFR) polymers.

To determine the magnitude of die swell which occurs in low molecular weight PP resins typically used for melt blowing, five single hole dies were fabricated. Four of them had an orifice diameter of 0.4 mm and L/D ratios of 5, 10, 15, and 20 respectively. The other die had an orifice diameter of 0.25 mm and an L/D ratio of 10. These dies were fitted on to a Instron Rheometer. The throughput rate was varied in steps from 0.24 g/min to 2.68 g/min. A 400 MFR homo-polypropylene was used and the temperature was maintained constant at 240 ^{0}C. It was then decided to fabricate a step die with an entry region diameter of 0.25 mm and L/D ratio of 10 and an exit region diameter of 0.4 mm and L/D of 5. The die swell ratio was determined as before. In all the cases the melt pressure was also determined from the plots recorded from the load cell of the Instron Rheometer.

WEB PREPARATION

The melt blown webs needed for this research were produced on the 6-inch melt blown pilot line at The University of Tennessee, Knoxville. The line features a 6-inch die, an electric furnace for heating the air, and an Ingersoll-Rand air compressor rated at 650 ft^3/min.

The first phase of this research consisted of melt blowing 35 and 400 MFR PP resins in accordance with the experimental flow chart shown in Figure 3.1. The webs were prepared using 6" die tips (121 holes) at a basis weight of 1 oz/yd^2. The air flow rate was maintained constant at 40% air valve opening (nominal 14.9 scfm/inch of air slot width). Each resin was melt blown at two different throughputs (0.4 and 0.8 g/hole/min), two different orifice diameters (0.015" and 0.020"), two different nominal air gaps (0.035" and 0.110") and two different L/D ratios (10/1 and 15/1). The 35 mil nominal air gap had a corresponding nominal setback of -34 mil and the 110 mil nominal air gap had a corresponding setback of -80 mil. Thus, for each resin sixteen webs were prepared, for a total of thirty two webs.

Also to determine if DCD had an effect on average fiber diameter, 35 MFR PP resin was melt blown using a 0.020" orifice die tip (L/D of 15), 0.035" nominal air gap, 0.4 g/hole/min throughput and five different DCDs (8", 12", 16", 20", and 24") as shown in Figure 3.1. The air flow rate was maintained constant at 40% air valve opening (14.9 scfm/inch of air slot width).

Finally to investigate the effect of volumetric flow rate of air on average fiber diameter at constant air velocity, 35 MFR PP resin was melt blown using a 0.020" orifice die tip (L/D of 15), 0.10" air gap, 0.4 g/hole/min throughput and 20" DCD with a 70% air valve opening (24.9 scfm/inch of air slot width) in order to

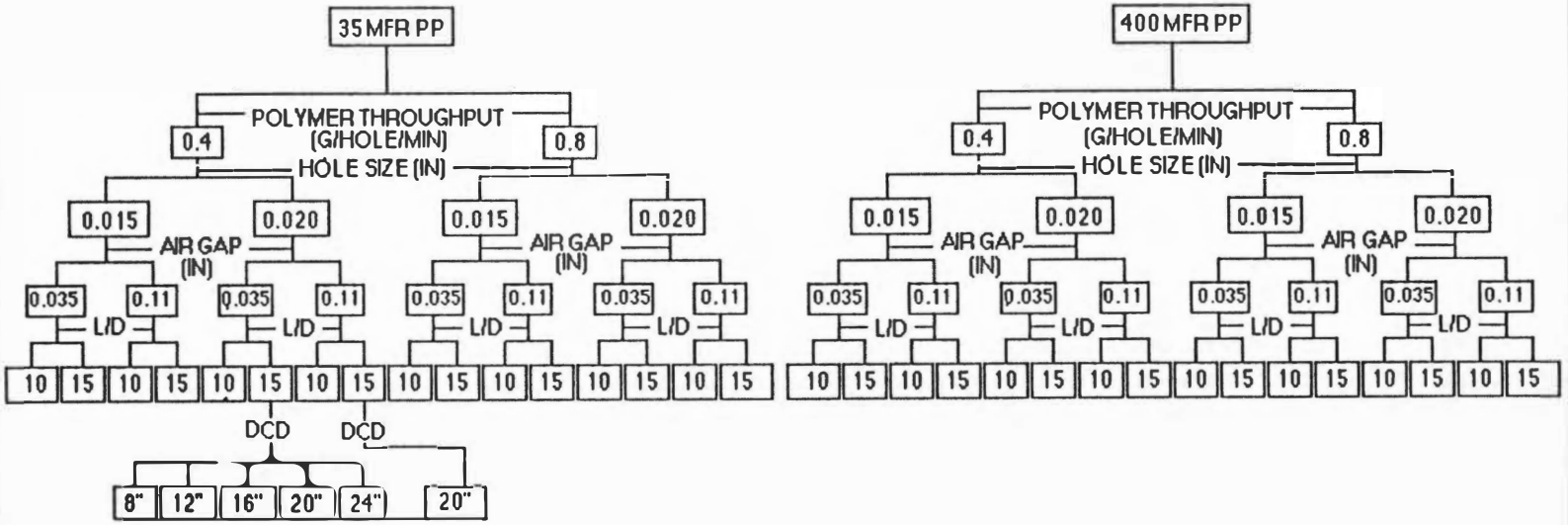


Figure 3.1 Flow chart of experimental design - Phase I

maintain the same air pressure (5 psi) in the manifold as with the 0.035" air gap which was 40%. In other words the air velocities were the same for both 0.035" and 0.110" air gaps but the volumetric flow rates will be very different. The processing conditions used for this study are given in Tables 3.1 and 3.2. Although the nominal air gaps were 35 and 110 mils with corresponding nosetip setbacks of 34 and 80 mils, the exact air gaps and setbacks which were measured on the heated die are given in Tables 3.1 and 3.2.

The main focus of this study was to investigate the effects of different PP melt flow rates (MFRs), polymer throughput rates, die orifice diameter, orifice L/D, and air gap settings on the average fiber diameters in the webs, mechanical properties, and filtration efficiencies of the webs. The DCD was generally maintained at 12" for the 35 mil air knives and 17" for the 110 mil air knives. The longer DCD was required in the latter case to reduce fly formation. In some cases because of fly generation the DCDs were increased (up to 30"). The temperatures (both die and air) were varied, even for the same MFR resin depending on the die tip and air knife combination, consistent with as little shot and fly as possible. For example, the 400 MFR resin resulted in much fly generation when processed with a 20 mil orifice, a 15/1 L/D and a 110 mil air gap. The temperature of the air was lowered. Primarily, the temperatures were selected between the temperature where the shot starts disappearing and the fly started appearing. During Phase I melt pressure at the die was measured using a GENTRAN analog diaphragm pressure probe. The accuracy of the probe was limited and therefore the values were not used to calculate shear viscosities.

The air flow rate in SCFM was determined according to the American Society of Mechanical Engineers Power Test Code (41). The procedure to determine the air flow rate is given in Appendix C.

Table 3.1 Melt Blown Processing Conditions (6" line) [Phase I], Air Valve setting 40%

Sample No.	Sample ID*	Die Temp, °F	Adapter Temp, °F	Air Temp at Die, °F	Screw Speed, rpm	DCD, Inches	SCFM/ Inch	Melt Pressure, psi
1	$27^1/23^2$/0.4/400/15/10	504	-	582	14	12	15.53	200
2	$36^1/39^2$/0.4/400/15/15	525	500	595	14	12	15.08	200
3	$39^1/39^2$/0.4/400/20/10	527	500	594	12	12	16.96	200
4	$36^1/35^2$/0.4/400/20/15	527	500	540	12	17	16.20	200
5	$99^3/64^4$/0.4/400/15/10	525	450	596	12	23	15.78	200
6	$118^3/93^4$/0.4/400/15/15	525	500	595	14	23	15.08	200
7	$111^3/85^4$/0.4/400/20/10	527	500	594	12	17	14.90	200
8	$108^3/80^4$/0.4/400/20/15	527	500	459	12	30	16.56	200
9	$27^1/23^2$/0.8/400/15/10	558	550	577	21	12	15.90	200
10	$36^1/39^2$/0.8/400/15/15	560	550	578	22	12	15.88	250
11	$39^1/39^2$/0.8/400/20/10	561	550	578	19	12	16.84	200
12	$36^1/35^2$/0.8/400/20/15	561	550	488	19	17	16.17	200

1-nominal air gap, 35 mil; 2-nominal setback, 34 mil; 3-nominal air gap, 110 mil; 4-nominal setback, 80 mil. * Air knife gap, mil/Setback, mil/Polymer throughput, g/hole/min/MFR/Orifice dia, mil/L/D ratio.

Table 3.1 (Contd.)

Sample No.	Sample ID*	Die Temp, °F	Adapter Temp, °F	Air Temp at Die, °F	Screw Speed, rpm	DCD, Inches	SCFM/ Inch	Melt Pressure, psi
13	99[3]/64[4]/0.8/400/15/10	560	551	577	20	20	16.33	200
14	118[3]/93[4]/0.8/400/15/15	560	550	578	22	12	15.88	300
15	111[3]/85[4]/0.8/400/20/10	561	550	578	19	20	14.56	200
16	108[3]/80[4]/0.8/400/20/15	561	550	484	19	30	16.17	200
17	27[1]/23[2]/0.4/35/15/10	595	580	608	12	12	15.81	275
18	36[1]/39[2]/0.4/35/15/15	595	580	608	12	12	16.35	275
19	39[1]/39[2]/0.4/35/20/10	597	580	608	12	12	16.40	250
20	36[1]/35[2]/0.4/35/20/15	597	580	608	12	12	16.40	250
21	99[3]/64[4]/0.4/35/15/10	596	580	609	17	17	15.71	275
22	118[3]/93[4]/0.4/35/15/15	596	580	608	17	17	15.81	275
23	111[3]/85[4]/0.4/35/20/10	597	580	609	17	17	15.71	250
24	108[3]/80[4]/0.4/35/20/15	597	580	609	17	17	16.13	250

1-nominal air gap, 35 mil; 2-nominal setback, 34 mil; 3-nominal air gap, 110 mil; 4-nominal setback, 80 mil.

* Air knife gap, mil/Setback, mil/Polymer throughput, g/hole/min/MFR/Orifice dia, mil/L/D ratio.

Table 3.1 (Contd.)

Sample No.	Sample ID*	Die Temp, ^{0}F	Adapter Temp, ^{0}F	Air Temp at Die, ^{0}F	Screw Speed, rpm	DCD, Inches	SCFM/ Inch	Melt Pressure, psi
25	27[1]/23[2]/0.4/35/15/10	625	600	640	22	12	15.88	350
26	36[1]/39[2]/0.4/35/15/15	625	600	645	20	12	16.28	475
27	39[1]/39[2]/0.4/35/20/10	624	600	645	20	12	15.29	375
28	36[1]/35[2]/0.4/35/20/15	624	600	644	21	12	15.29	375
29	99[3]/64[4]/0.4/35/15/10	627	600	645	20	17	16.40	475
30	118[3]/93[4]/0.4/35/15/15	625	600	645	22	17	15.95	475
31	111[3]/85[4]/0.4/35/20/10	624	600	645	20	17	16.13	375
32	108[3]/80[4]/0.4/35/20/15	624	600	643	21	17	16.13	375

1-nominal air gap, 35 mil; 2-nominal setback, 34 mil; 3-nominal air gap, 110 mil; 4-nominal setback, 80 mil.

* Air knife gap, mil/Setback, mil/Polymer throughput, g/hole/min/MFR/Orifice dia, mil/L/D ratio.

Table 3.2

Melt Blown Processing Conditions (DCD Study) - Phase I. 35 MFR, 0.4 g/hole/min Throughput 20 mil Orifice Diameter, 5 psi Pressure, and 15/1 L/D

Sample No.	Air Valve Setting, %	Airgap/setback mils	DCD, Inches	Die temp, ^{0}F	Adapter Temp, ^{0}F	Air Temp at Die, ^{0}F	Screw speed, rpm
33	40	36/35	8	553	530	592	15
34	40	36/35	12	553	530	592	15
35	40	36/35	16	553	530	592	15
36	40	36/35	20	553	530	592	15
37	40	36/35	24	553	530	592	15
38	70	108/80	20	553	530	590	15

During Phase II of this research 650 MFR polypropylene resin was melt blown in accordance with the experimental flow chart in Figure 3.2. The webs were prepared using 6" die tips (121 holes) at a basis weight of 1 oz/yd^2. The primary air flow rate was selected such that the ratio of volumetric flow rate of air and the polymer throughput remained constant at all polymer throughput rates. For example, a polymer throughput of 0.4 g/hole/min was processed using 100 scfm of air, when the polymer throughput was increased to 0.8 g/hole/min the air flow rate was 200 scfm and so on, thus maintaining the air-to-polymer flow rate ratio constant. Since the air slot width on both the upper and lower sections of the die was 8 inches compared to the 6-inch die tip width containing the holes, the values for scfm per inch of die width at 0.4, 0.8, 1.2, 1.6, and 2.0 g/hole/min were 12.5, 25.0, 37.5, 50.0, and 62.5 scfm/inch die width, respectively. For all runs the die and air temperatures were maintained constant at 500 and 520^0 F respectively. The die-to-collector distance (DCD) was held at 12 inches and the nominal air gap was 31 mils for all the runs.

The full experimental plan called for 100 runs (2 orifice diameters X 2 L/D ratios X 5 nosetip setbacks X 5 polymer throughput rates). A fractional factorial design was utilized to reduce the number of runs from 100 to 40 and still obtain a representative data set from which information on all the desired 100 runs could be obtained. The design involved two different orifice diameters (15 and 20 mil), each at two different L/D ratios (10/1 and 15/1), five different nosetip setbacks (+5, -5,-18, -28, and -39 mils), and five different polymer throughput rates (0.4, 0.8, 1.2, 1.6, and 2.0 g/hole/min). Although the nominal air gap was 31 mils, the actual air gaps were measured and recorded for each of the four different nosetips after the assembled die was heated to 400^o F. In addition the face gaps were measured under the same condition for all the setback/air gap combinations

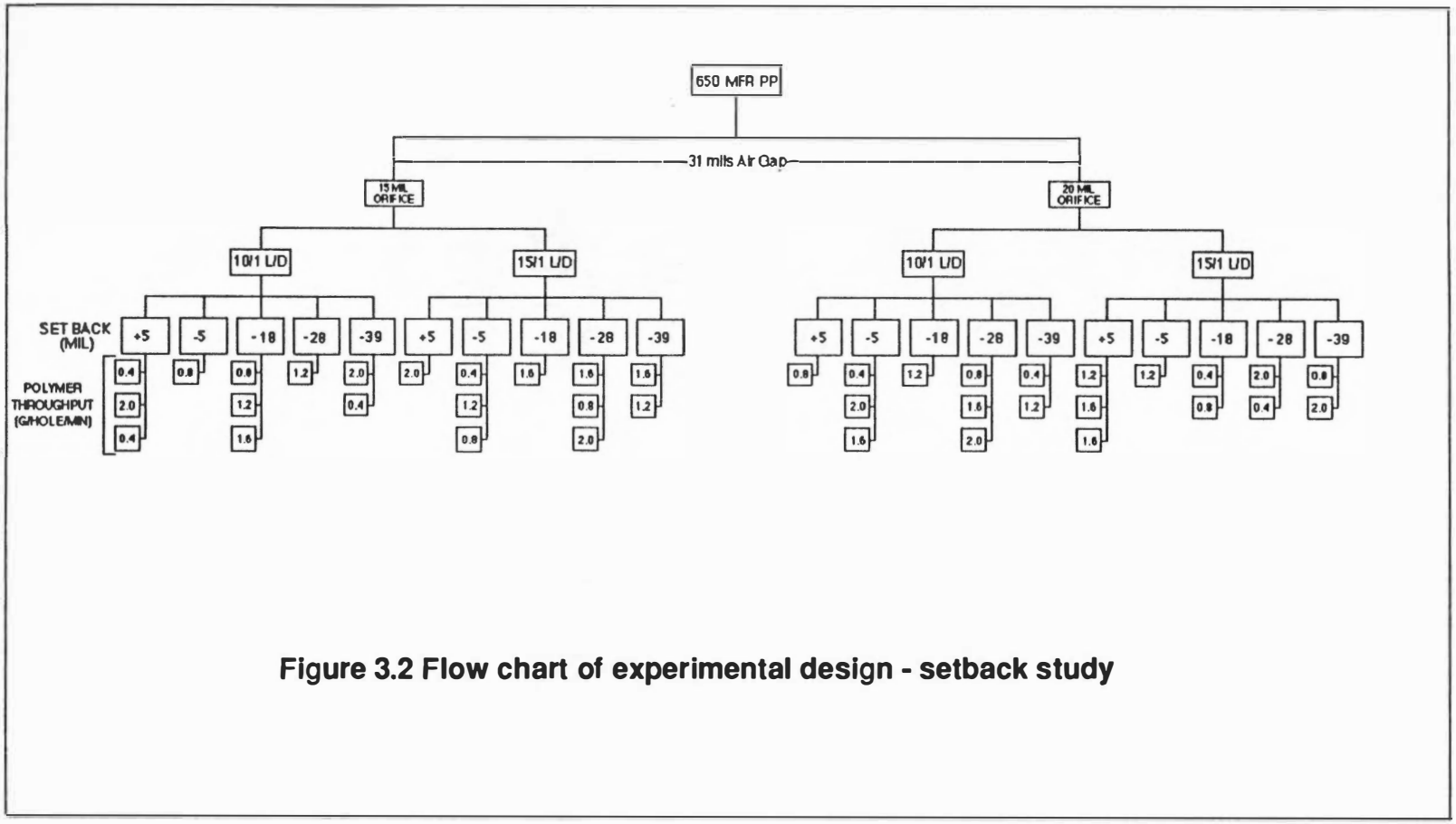


Figure 3.2 Flow chart of experimental design - setback study

and recorded. In the case of positive setbacks, the portion of the die tip that protruded beyond the air knife edge was subtracted from the face gap measurements.

For each run, the process conditions were set and after 10 minutes the polymer throughput rate was checked by weighing the web produced per minute. It was checked twice before collecting a sample web. Then the collector speed was adjusted in order to maintain an average basis weight of 1 oz/yd^2 (33.9 g/m^2). The processing conditions for the second study are shown in Table 3.3.

Table 3.3

Melt blown Processing Conditions (6" line), [Phase II], PD 3495 G (650 MFR) Polypropylene Resin

Die temperature, ^{0}F	500
Primary air temperature at die, ^{0}F	520
DCD, inch	12
Air-to-polymer flow rate ratio, scfm/g of resin	2.07
Nominal air gap	31 mil

The third phase (Phase III) of this research consisted of melt blowing 800 MFR PP (PD 3545 G) resin using nosetips with angles of 60^0 (injection angle, 30^0) and 90^0 (injection angle 45^0) respectively on the 6-inch die. The webs were made according to the experimental flow chart in Figure 3.3. The primary air flow rate and DCD were maintained constant at 130 scfm/8 inches of air slot width, and 12 inches, respectively, for all the runs in this study. With the 60 mil air gap, two polymer throughputs were used (0.4 and 0.8 g/hole/min), whereas with the

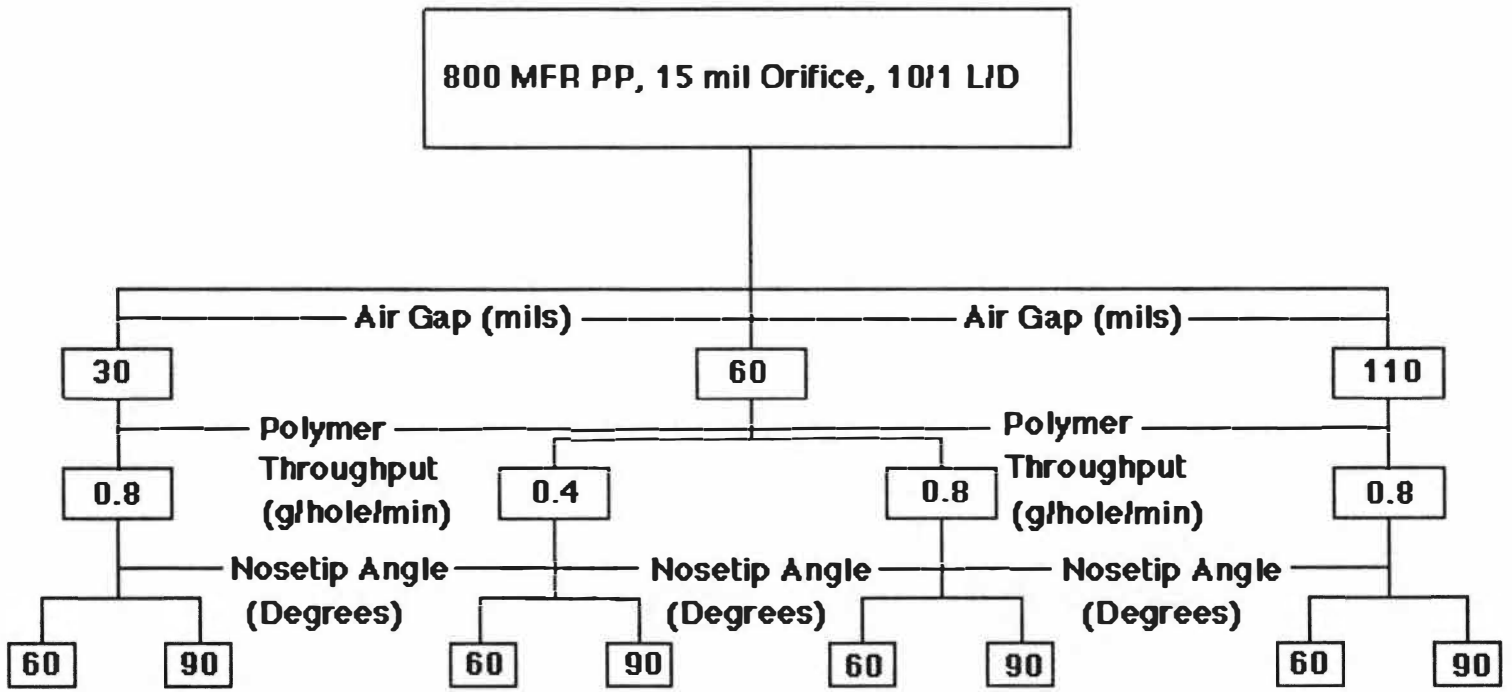


Figure 3.3 Flow chart of experimental design - nosetip angle study

30 and 110 mil air gaps the polymer throughput was maintained constant at 0.8 g/hole/min. Both the 60^0 and 90^0 nosetips had an orifice diameter of 15 mils and a L/D ratio of 10/1. Three sets of air knives were used for this phase of the research (27 mils air gap/23 mils setback, 56 mils air gap/54 mils setback, and 100 mils air gap/64 mils setback). The die and primary air temperatures were maintained constant at 500^0 F for the duration of the study.

The final phase (Phase IV) of this research comprised of accurate on-line melt pressure measurements on the melt blowing die assembly with both 15 and 20 mil orifice diameter nosetips in place. The procedure for melt pressure measurements is described in detail in the following chapter (Ch. 4. Experimental Procedures). The melt pressure was measured on 10/1 and 15/1 L/D ratios for each orifice diameter. Thus four nosetips were used for this study. It involved melt blowing 35 (PP 3445) and 800 (PD 3545 G) MFR resins at different polymer throughput rates and temperatures, for each orifice diameter/L/D ratio combination. The 800 MFR resin was melt blown at a die temperature of 480, 500, 520, 540, and 560^0 F, each at five different polymer throughput rates (0.4, 0.8, 1.2, 1.6, and 2.0 g/hole/min) using all the four nosetips (15 mil, 10/1, 15 mil 15/1, 20 mil, 10/1, 20 mil, 15/1).

With the 35 MFR resin due to the pressure limitations imposed by the system design (because of higher molecular weight compared to 800 MFR) and practical melt blowing considerations (the viscosity has to be low enough to enable attenuation to fine fibers), it was not possible to replicate the experimental design used for 800 MFR resin. The die temperatures employed for the 35 MFR resin were 540, 560, 580, 600, and 620^0 F. With the 15 mil orifice, 10/1 L/D nosetip the polymer throughputs used at each temperature were 0.2, 0.4, 0.8, 1.2, and 1.6 g/hole/min. With the 15 mil orifice, 15/1 L/D nosetip, polymer

throughput rates of 0.2, 0.4, 0.8, and 1.0 g/hole/min were used at each of the above temperatures. With the 20 mil orifice (both 10/1 and 15/1 L/D ratio), polymer throughput rates of 0.2, 0.4, 0.8, and 1.2 g/hole/min were employed.

The melt pressure was used to calculate the shear stress. The shear rates were obtained from orifice diameter and polymer throughput rate. An accurate pressure transducer (1-1500 psi, least count=1 psi) was used for melt pressure measurements. The melt shear viscosity in the orifice was calculated according to procedure described in chapter 4.

CHAPTER 4

EXPERIMENTAL PROCEDURES

Before carrying out any tests, the melt blown specimens were conditioned under standard textile testing conditions (20 ^{0}C and 65% relative humidity) for a minimum period of 24 hours.

DIE SWELL MEASUREMENTS

The extrudate was photographed close to the die (1/2" to 1" from the die face) and from the photograph the true maximum swell diameter was computed using the magnification ratio of the camera (the magnification ratio of the camera was obtained from the ruler placed perpendicular to the camera lens when photographing the extrudate), the print magnification, and by measuring the maximum swell diameter from the photograph. The ratio of the maximum swell diameter to the orifice diameter is the die swell ratio. For each die tip five cross head speeds were used, corresponding to five throughput rates- viz. 0.24, 0.64, 1.32, and 2.68 g/min and a photograph was taken for each throughput rate.

AIR PERMEABILITY

The air permeability of the webs was determined according to the ASTM Standard D737-75 at a pressure drop of 0.5 inches of water. A Frazier Air Permeameter was used to perform the test.

BURSTING STRENGTH

The Bursting Strength was determined using a Mullen Bursting tester (Diaphragm type) according to the ASTM Standard D3786.

FIBER DIAMETER

Fiber diameters were determined from the photomicrographs taken using the ETEC Auto Scan electron microscope. The specimens were cut and mounted on a circular holder (8 mm in diameter). Five specimens were mounted for each sample, making sure that their positions on the web were randomly selected. All the specimens were coated with gold by a diode sputtering technique. The pictures were taken at 20 kilo volt accelerating setting and the magnification was 600X. Five photomicrographs were taken for each web type (one per mount).

Two diagonal lines were drawn across each picture. The diameters of all the fibers at the points where the lines crossed them were measured with a scale under a lighted magnifying glass. Fibers which crossed the lines more than once were measured at only one cross-over point. Typically, an average of 125-150 fiber diameter values for each web type was reported. Finally a number average fiber diameter for each web was computed.

FILTRATION EFFICIENCY

The filtration efficiency of the web samples was determined using a Latex Filtration Efficiency Tester developed by Wadsworth and Davis for Johnson &

Johnson [44]. The test procedure developed at the University of Tennessee was followed.

Nebulized water emulsion of polystyrene microspheres were used to determine filtration efficiency. Monodispersed latex particles with a diameter of 0.8 μm were used. The nebulizer was utilized under air flow rate conditions which gives water droplets of 2-3 μm according to the manufacturer. The flow rate of dried, micro-filtered air to the nebulizer and the dilution air flow rate were maintained at 3.5 and 61.4 liters per minute, respectively. The air pressure of the nebulizer and the pressure drop across the sample were monitored. A Hiac/Royco Airborne Particle Counting System consisting of a Model 4100 Particle counter and a Model 1200 Sensor was used to determine the filtration efficiency.

WEB TENACITY AND ELONGATION-AT-BREAK

The breaking load and elongation-at-break were determined on strips of 7" x 1" (gauge length 5") following the procedure given in ASTM Test Method D1682. A table model Instron tester with a tensile load cell was used for this test. The tenacity was then calculated by taking the breaking load in grams and dividing it by the denier of the strip used for the test and reported in g/denier. Since the samples were prepared on the 6" line, only the machine direction tenacity and elongation-to-break could be determined, since the samples were not wide enough for the required specimen length of 7 inches in the cross direction.

MOLECULAR WEIGHT DETERMINATION

The weight average molecular weight of the web was determined by gel permeation chromatography technique (GPC) at the Baytown Polymer Research Center by the Exxon Chemical Company, according to ASTM Standard D3593.

SHOT LEVEL

Each sample web was visually rated on a relative five level subjective scale for incidence of shot formation. The scale had levels for none, low, medium, high, and extremely high incidence. A value of 1 indicated the no shot condition and a value of 5 indicated an extremely high shot condition. A no shot condition does not necessarily mean an absolute shot free condition. It only means that on the relative scale that particular web had the least amount of shot. There were three independent observers who rated each web. Most of the time all three were consistent. Each web was back lighted with an array of fluorescent lights and also daylight from a window. The web was observed with the naked eye and given a rating.

FLY RATING

Each sample was rated for fly on a relative scale similar to the one used for rating shot. The fly rating was assigned using a combination of observations during melt blowing and visual examination of the sample web after melt blowing. The rest of the procedure was identical to the method used to rate the shot level.

MELT SHEAR VISCOSITY

The shear viscosity of PP melt under actual melt blowing conditions was calculated using sensitive pressure drop measurements across the die orifices. A Dynisco pressure probe (diaphragm type) was inserted as close to the flow channel prior to the orifice entry as possible. Since the maximum pressure drop occurs across the orifice, the pressure drop between the point where the probe was inserted and the entry of the orifice was neglected. The pressure probe had a least count of 1 psi and was connected to a μPR 690 microprocessor readout. The pressure drops for different polymer throughput rates were recorded. This pressure drop was used to compute the shear stress as follows:

$$\text{Shear Stress}_{Newt} = [\text{Diameter of orifice X Pressure drop across orifice}]/[4 \text{ X Length of the orifice}].$$

The shear rate was calculated using the formula,

$$\text{Shear rate}_{Newt} = [8 \text{ X Velocity inside the orifice}]/[\text{Diameter of orifice}].$$

From the shear stress and shear rate the Newtonian shear viscosity was calculated (Shear Viscosity_{Newt} = Shear stress/ Shear rate). The viscosity data was corrected for shear thinning nature of polymer melts. Corrected shear viscosity (non-Newtonian) = Shear $\text{Viscosity}_{Newt}/[(3n'+1)/4n']$, where n' is the slope of the shear stress versus Newtonian shear rate plot.

PACKING FACTOR

The packing factor of a fibrous structure is the fraction of total volume of the structure occupied by the fibers. In other words, the packing factor is a measure of the amount of "solidness" in a web. Packing factor is also referred to

as the solidity or packing fraction. For the purposes of this research the packing factor was calculated using web thickness measurement. For each sample four individual web thickness measurements were made on four pieces (3"x3") of the sample using a TSI thickness tester (1 Psi pressure) calibrated in mils. The four thickness readings were then averaged. Each of the four 3"x3" pieces were weighed and an average mass computed for the sample. Using the average thickness, the area of a piece (3"x3"=9 inch^2, 58 cm^2), and density of bulk polypropylene resin (0.91 g/cc), the mass of a PP sheet of the same dimensions as one piece from a sample web was calculated. The ratio of the actual average mass of a 3"x3" piece to the calculated mass of a piece of same dimensions assuming it were a solid PP sheet was reported as the packing factor of that particular sample.

$$\text{Packing factor} = \frac{\text{Actual average mass of 3"X3" piece of MB web}}{\text{Calculated mass of a piece of same dimensions assuming a 100\% solid PP sheet}}$$

SODIUM CHLORIDE AEROSOL FILTRATION EFFICIENCY

The filtration efficiency of the web samples for the 60 versus 90^0 nosetip study was determined using a TSI model 8110 automated filter tester. The test procedure developed at the University of Tennessee based on the recommendations of the manufacturer was followed.

Sodium chloride aerosol was used to determine filtration efficiency. The aerosol was generated from a 20 g/l sodium chloride solution in water. The instrument generates sodium chloride crystals measuring 0.1 μm by passing the aerosol through a heater. An air stream carries the dried crystals to the filter test

assembly. The mass concentration of NaCl in air was 101 mg/m^3. Photometry was used to detect the volume concentration of the air in the upstream volume of the media and the volume concentration of the air in the downstream volume of the media. The nominal air flow rate used was 32 l/min. The effective filter test area was 100 cm^2. Therefore the face velocity will be 5 cm/sec.

The melt blown sample was mounted in the filter test assembly with the screen side facing up. The flow direction is from bottom to top. Thus the initial contact between the sodium chloride crystal laden air stream and the sample will occur on the face side of the fabric (side of the web in contact with the collector screen during melt blowing). The instrument is fully automated and at the end of each test a print out showing the percent penetration, air flow rate (in l/min), and the pressure drop (in mm of H_2O) was obtained. Four or five individual measurements (depending on the variability) were made for each sample and the average penetration was calculated. The percent filtration efficiency was obtained by subtracting the average percent penetration from 100%.

CHAPTER 5

RESULTS AND DISCUSSION

DIE SWELL STUDIES - INSTRON RHEOMETER

Earlier research at the University of Tennessee has indicated that increasing the polymer throughput rate resulted in average fiber diameters considerably higher than that for lower throughputs even when air flow rates were substantially increased [16]. It was suggested that the increase in die swell with increasing throughput might be the reason for this phenomenon. Bearing this in mind, experiments were conducted with two different L/D ratios (10/1 and 15/1) and two different hole diameters. Classical polymer rheology data indicates that larger the L/D ratio, the smaller the die swell [45].

The die swell measurements on extrudates from single orifice die tips fitted on an Instron Rheometer at different polymer throughputs are given in Table A.1 in Appendix A. It can be seen that as the polymer throughput rate increased for a constant die geometry, the die swell ratio increased. For a constant throughput as the L/D ratio increased, the die swell decreased. This is because the polymer has a greater flow path to dissipate the entry effects. Although in the case of the small hole die (0.25 mm) the die swell ratio was higher than the corresponding 0.4 mm die, the maximum diameter of the extrudate is lower at all throughputs. On the contrary, in the case of the step die, although the die swell appears to be much less, it was the geometry of the entry region (L/D = 10/1; D = 0.25 mm) which affects the die swell, and not the exit region (L/D = 5/1; D = 0.4 mm). Although the step die may help in molecular

relaxation, the true die swell (the ratio of the maximum swell diameter to the entry region diameter) was similar to the value obtained for L/D of 10 and hole diameter of 0.25 mm. The effects of polymer throughput and L/D ratio on die swell ratio are graphically represented in Figures A.1. and A.2 in Appendix A. Thus, it was assumed that increasing the L/D ratio to 15/1 from the standard 10/1 would reduce the die swell which in turn may produce finer fibers.

PHASE I - PRELIMINARY STUDY

Phase I was focused primarily on the effects of orifice diameter, orifice L/D ratio, air knife gap, PP melt flow rate (MFR), and polymer throughput rate on the fiber diameter in the web. The effects of these variables on melt blown web properties and filtration efficiency are also discussed. Table 5.1 lists the average fiber diameters, and physical and mechanical properties of the webs as well as the weight average molecular weight of PP in the web obtained from all the sample runs. Since it was not possible to maintain the same DCD for all runs due to fly generation, the effect of DCD on fiber diameters, with other processing parameters remaining constant, is also discussed. The analysis of the results obtained were carried out using a General Linear Models procedure on a SAS package available on the VAX main frame computer at the University of Tennessee. The model incorporated average fiber diameter, filtration efficiency, MD web tenacity, MD breaking elongation, bursting strength, air permeability, weight average molecular weight of the web, shot, and fly as the responses. The production variables were resin MFR, orifice size, resin throughput, L/D ratio, and air gap. The air temperature and the polymer temperature were not included in the analysis because of their confounding effects with the MFR and polymer

Table 5.1 Results Table - Phase I

Sample No.	Sample ID*	Average Fiber Dia, μm	MD Web Tenacity, g/Denier	MD Elongation-at-break, %	Bursting Strength, KPa	Air Permeability, $ft^3/ft^2/min$	Filtration Efficiency, %	Web Wt .av. molecular wt.
1	27[1]/23[2]/0.4/400/15/10	2.81	0.142	30.10	68.47	113.00	80	77818
2	36[1]/39[2]/0.4/400/15/15	2.77	0.122	13.60	43.68	112.60	76	78715
3	39[1]/39[2]/0.4/400/20/10	2.30	0.144	17.50	64.37	94.30	77	77020
4	36[1]/35[2]/0.4/400/20/15	1.82	0.063	17.80	61.30	63.70	89	61992
5	99[3]/64[4]/0.4/400/15/10	2.42	0.08	20.00	48.28	144.70	77	78059
6	118[3]/93[4]/0.4/400/15/15	2.55	0.092	19.00	55.70	136.00	78	75972
7	111[3]/85[4]/0.4/400/20/10	1.82	0.074	5.13	27.87	150.80	75	75613
8	108[3]/80[4]/0.4/400/20/15	2.11	0.097	24.50	62.41	89.90	88	61279
9	27[1]/23[2]/0.8/400/15/10	3.24	0.141	12.30	62.07	83.60	77	72495
10	36[1]/39[2]/0.8/400/15/15	2.66	0.141	4.25	29.06	90.60	72	75093

1-nominal air gap, 35 mil; 2-nominal setback, 34 mil; 3-nominal air gap, 110 mil; 4-nominal setback, 80 mil. * Air knife gap, mil/Setback, mil/Polymer throughput, g/hole/min/MFR/Orifice dia, mil/L/D ratio.

Table 5.1 (Contd.)

Sample No.	Sample ID*	Average Fiber Dia, μm	MD Web Tenacity, g/Denier	MD Elongation-at-break, %	Bursting Strength, KPa	Air Permeability, $ft^3/ft^2/min$	Filtration Efficiency, %	Web Wt .av. molecular wt.
11	$39^1/39^2$/0.8/400/20/10	2.59	0.129	24.90	52.76	110.60	81	73009
12	$36^1/35^2$/0.8/400/20/15	1.83	0.068	20.73	49.04	81.00	90	58156
13	$99^3/64^4$/0.8/400/15/10	2.11	0.095	3.38	23.03	134.90	78	73397
14	$118^3/93^4$/0.8/400/15/15	2.58	0.093	1.85	17.93	374.60	74	75929
15	$111^3/85^4$/0.8/400/20/10	2.34	0.091	2.50	22.07	175.20	72	75414
16	$108^3/80^4$/0.8/400/20/15	1.72	0.046	17.13	47.59	64.60	93	57945
17	$27^1/23^2$/0.4/35/15/10	2.48	0.140	34.60	54.48	111.70	83	106647
18	$36^1/39^2$/0.4/35/15/15	1.67	0.174	23.90	63.00	80.40	83	105156
19	$39^1/39^2$/0.4/35/20/10	1.79	0.133	24.90	57.37	122.20	74	107496
20	$36^1/35^2$/0.4/35/20/15	1.72	0.190	33.05	70.75	83.40	84	102707

Table 5.1 (Contd.)

Sample No.	Sample ID*	Average Fiber Dia, μm	MD Web Tenacity, g/Denier	MD Elongation-at-break, %	Bursting Strength, KPa	Air Permeability, $ft^3/ft^2/min$	Filtration Efficiency, %	Web Wt .av. molecular wt.
21	$99^3/64^4$/0.4/35/15/10	2.16	0.191	27.40	67.59	97.40	80	106235
22	$118^3/93^4$/0.4/35/15/15	1.94	0.173	18.40	62.76	103.80	85	104810
23	$111^3/85^4$/0.4/35/20/10	2.36	0.188	29.40	65.13	125.00	60	111029
24	$108^3/80^4$/0.4/35/20/15	2.37	0.167	35.25	55.98	132.00	75	110089
25	$27^1/23^2$/0.8/35/15/10	2.88	0.158	10.50	48.28	104.00	68	100824
26	$36^1/39^2$/0.8/35/15/15	2.10	0.186	12.30	57.47	89.30	71	106816
27	$39^1/39^2$/0.8/35/20/10	2.31	0.090	15.16	38.31	295.70	60	107080
28	$36^1/35^2$/0.8/35/20/15	1.93	0.159	23.30	66.38	95.90	76	104959
29	$99^3/64^4$/0.8/35/15/10	2.50	0.193	10.00	57.14	124.90	71	105064
30	$118^3/93^4$/0.8/35/15/15	2.48	0.217	8.90	45.98	122.30	74	102962
31	$111^3/85^4$/0.8/35/20/10	2.28	0.185	10.57	53.79	148.10	69	103950
32	$108^3/80^4$/0.8/35/20/15	2.91	0.182	12.40	54.14	142.00	72	104226

throughput. The nosetip setback was not included because it was tied to the air knife gap in that the air knives utilized were constructed in such a way that the air gap and the negative nose tip set back were collinear. The effects of orifice L/D, orifice diameter, and air knife gap with 35 and 400 MFR PP at 0.4 and 0.8 g/hole/min polymer throughput on fiber diameter, filtration efficiency, air permeability, weight average molecular weight of the web, bursting strength, MD tenacity, and MD breaking elongation are shown in bar charts for illustrative purposes.

Since some of the process variables such as the air temperature and melt temperature associated with each run were different, the bar graphs are provided for the purposes of qualitative comparisons. Wherever a process variable had a significant main effect on the response without any interactive effects in combination with another variable, the main effect least square means for that particular variable was taken from the 2x2 tables of the statistical output reproduced in Appendix B for the purpose of determining the direction of the trend. When a process variable had a main effect as well as an interactive effect on the response, then the trend was determined by examining the interactive effect least square means from the 2x2 tables of the statistical output. Comparing the least square means for a main effect implies that the average of 16 observations was compared against the average of the remaining 16 observations for the whole set of 32 observations.

Comparing the least square means for an interactive effect implies that the average of 8 observations is compared against the average of the remaining 8 observations within that subset of 16 observations. Only the main effects and the two-factor interactions were included in the statistical analysis to accommodate sufficient error terms in the analysis, which is usually at least as many terms as

the number of model terms. Table B.1 reveals the main effects and interactive effects of various production variables on average fiber diameter, shot and fly level, and other response variables such as filtration efficiency, air permeability, bursting strength, web tenacity and elongation, and weight average molecular weight of the web. The significant variables were prioritized according to F-value.

It is also very important to note that using the data out of this type of experimental methodology, only the trends of main effects and interactive effects can be obtained for a particular response. The magnitude of increase or decrease from the least square means tables is only a guideline for obtaining the general trend. The data from these experiments cannot be used for computing the estimator coefficients and predicting a particular response, as in the case of a regression model. Based on this statistical analysis, the process variables which seem to affect the response parameter may be obtained, and further experimentation designed to eliminate the confounding effects among the production variables will provide the precise equations to predict a particular response.

Process Conditions

The key melt blown conditions for each run are given in Tables 3.1 and 3.2. Generally, both 35 and 400 MFR resins processed well at 0.4 g/hole/min throughput with a 15 mil orifice diameter. At 0.8 g/hole/min throughput, not all the conditions resulted in a good web. As shown in Table 5.2 some webs had much shot and some gave excessive fly. Overall the 35 MFR PP appeared to process better with the 20 mil die tip, than with the 15 mil hole die tip in that less shot was

produced. The 400 MFR resin produced a great deal of fly with the 20 mil hole die tip at the lower throughput of 0.4 g/hole/min.

Shot and Fly Formation

Each sample web was visually rated on a four level subjective scale for incidence of visible shot and fly formation. The scale had levels for none, low, medium, and high incidence. The observations are summarized in Table 5.2.

Effect of Production Variables on Shot Generation. Visual observation during actual melt blowing indicated that in the case of the lower throughput (0.4 g/ hole/ min) there was very little incidence of shot formation.

The statistical analysis of the shot generation data indicates that the orifice size, polymer throughput, L/D ratio, MFR*L/D ratio, MFR*air gap, orifice size*polymer throughput, and orifice size*L/D ratio have a significant effect on the shot level of the web.

Effect of MFR*L/D ratio on the Shot level. From the 2x2 table for MFR*L/D ratio interaction in the statistical output in Appendix B it can be seen that at constant MFR, for both 35 and 400 MFR resins, the mean shot level decreased with the increase in L/D from 10/1 to 15/1. This may be due to the longer flow path for the molten polymer inside the orifice capillary with the 15/1 L/D, compared to the 10/1 L/D. Thus the polymeric chains may be less entangled and offer less resistance to attenuation with 15/1 L/D and hence produce finer fibers. This in turn may have given rise to a situation where 10/1 L/D resulted in coarser fiber diameters. Since coarser fibers carry more heat per unit length, there may

Table 5.2 Shot and Fly Rating of MB PP Webs - Phase I

Sample No.	Sample ID*	Shot				Fly			
		None	Low	Med	High	None	Low	Med	High
1	27[1]/23[2]/0.4/400/15/10		X			X			
2	36[1]/39[2]/0.4/400/15/15		X			X			
3	39[1]/39[2]/0.4/400/20/10		X			X			
4	36[1]/35[2]/0.4/400/20/15	X							X
5	99[3]/64[4]/0.4/400/15/10		X				X		
6	118[3]/93[4]/0.4/400/15/15		X					X	
7	111[3]/85[4]/0.4/400/20/10			X			X		
8	108[3]/80[4]/0.4/400/20/15	X							X
9	27[1]/23[2]/0.8/400/15/10			X		X			
10	36[1]/39[2]/0.8/400/15/15			X		X			
11	39[1]/39[2]/0.8/400/20/10			X		X			
12	36[1]/35[2]/0.8/400/20/15	X						X	
13	99[3]/64[4]/0.8/400/15/10			X			X		
14	118[3]/93[4]/0.8/400/15/15			X			X		
15	111[3]/85[4]/0.8/400/20/10				X	X			
16	108[3]/80[4]/0.8/400/20/15	X							X

* Air knife gap, mil/Setback, mil/Polymer throughput, g/hole/min/MFR/Orifice diameter, mil/L/D ratio. 1-nominal air gap, 35 mil; 2-nominal setback, 34 mil; 3-nominal air gap, 110 mil; 4-nominal setback, 80 mil.

Table 5.2 (Contd.)

Sample No.	Sample ID*	Shot				Fly			
		None	Low	Med	High	None	Low	Med	High
17	27[1]/23[2]/0.4/35/15/10		X			X			
18	36[1]/39[2]/0.4/35/15/15			X			X		
19	39[1]/39[2]/0.4/35/20/10				X		X		
20	36[1]/35[2]/0.4/35/20/15		X				X		
21	99[3]/64[4]/0.4/35/15/10	X					X		
22	118[3]/93[4]/0.4/35/15/15		X					X	
23	111[3]/85[4]/0.4/35/20/10	X				X			
24	108[3]/80[4]/0.4/35/20/15	X					X		
25	27[1]/23[2]/0.8/35/15/10				X			X	
26	36[1]/39[2]/0.8/35/15/15			X		X			
27	39[1]/39[2]/0.8/35/20/10			X				X	
28	36[1]/35[2]/0.8/35/20/15		X			X			
29	99[3]/64[4]/0.8/35/15/10			X			X		
30	118[3]/93[4]/0.8/35/15/15				X		X		
31	111[3]/85[4]/0.8/35/20/10		X			X			
32	108[3]/80[4]/0.8/35/20/15		X			X			

* Air knife gap, mil/Setback, mil/Polymer throughput, g/hole/min/MFR/Orifice diameter, mil/L/D ratio. 1-nominal air gap, 35 mil; 2-nominal setback, 34 mil; 3-nominal air gap, 110 mil; 4-nominal setback, 80 mil.

be more incidence of shot with 10/1 L/D than 15/1 L/D (15/1 L/D ratio has a lower viscosity as discussed in Phase IV).

Effect of MFR*Air Gap on Shot level. The 2x2 tables for MFR*Air gap interaction indicate that for the 35 MFR resin, the mean shot level decreased with the increase in the air gap from 35 to 110 mil, and for the 400 MFR resin the mean shot level increased with the same increase in the air gap. In the present air knife combination, since the increase in the air gap correspondingly increases the setback, the 35 MFR resin probably gets attenuated more easily and at the same time withstands the increase in setback and sustains the attenuation process in the hot region between the orifice exit and the face of the air knives. But the increase in the mean shot level for the 400 MFR resin with the increase in the air gap may be attributed to the fact that it is not able to withstand the attenuation process in the previously mentioned hot zone. This is probably due to the springing back of the broken filaments to form globules which are carried away by the air stream to the collector screen.

Effect of Orifice Size*Polymer Throughput on Shot level. The 2x2 orifice size*polymer throughput interaction table in Appendix B shows that at constant orifice diameter, for both 15 mil and the 20 mil orifices, the mean shot level increased with the increase in polymer throughput from 0.4 to 0.8 g/min/hole. This may be due to the formation of coarser fibers at higher polymer throughput rates, which carry more heat to the collector screen per unit time than finer fibers. But the increase in the mean shot level for the 20 mil orifice was less than the 15 mil orifice. Since the thermal degradation of 400 MFR resin processed through the 20 mil orifice was considerably greater in magnitude compared to 15 mil

orifice (as indicated by gel permeation chromatography [GPC] studies mentioned later in this chapter dealing with the effect of process variables on weight average molecular weight of the web), the least square means may be skewed and do not provide a true indication of the magnitude of change in shot level with the change in orifice diameter.

Effect of Orifice Size*L/D Ratio on Shot level. From the 2x2 orifice size*L/D ratio interaction table shown in Appendix B it can be seen that the mean shot level decreased notably with the increase in L/D ratio from 10/1 to 15/1 for the 20 mil orifice. On the other hand, the mean shot level for the 15 mil orifice increased with the increase in L/D ratio from 10/1 to 15/1. Because of complexity of the variables involved it becomes very difficult to ascertain a cause for this behavior.

Effect of Production Variables on Fly Generation. The statistical analysis of the fly generation data indicates that the L/D ratio, MFR*orifice size, MFR*L/D ratio, MFR*air gap, orifice size*air gap, polymer throughput*air gap, and orifice size*L/D ratio have a significant effect on the fly generation.

From the fly generation data in Table 5.2, it is evident that the 20 mil orifice with 15/1 L/D generated excessive fly with the 400 MFR resin. In spite of lowering the air temperatures to reduce the amount of fly, still much fly was generated. The above trend was consistent with the data from both the polymer throughputs and both the air knives. This may be due to an interactive effect of the orifice size with the L/D ratio. Since the combination of a 20 mil orifice size and 15/1 L/D offers the longest flow channel for the molten polymer, the possibility of thermal degradation within the orifice is the greatest for 20 mil orifice and 15/1 L/D ratio. This explanation is supported by the largest drop in weight

average molecular weight for the 20 mil orifice and 15/1 L/D ratio as shown in Table 5.1.

Effect of MFR*Orifice Size on Fly Generation. From the 2x2 tables in the statistical output for MFR*orifice size interaction it can be seen that for the 35 MFR resin conditions the mean fly level decreased with an increase in orifice size from 15 mil to 20 mil. Whereas, for the 400 MFR resin conditions, the mean fly level increased with an increase in orifice size. It is not clear as to why 35 and 400 MFR resins behave differently with change in orifice diameter form 15 to 20 mil. It is quite possible that in the case of 400 MFR the increased thermal degradation with 20 mil orifice resulted in better ease of attenuation and hence finer fibers (Table 5.1) carrying less heat to the collector than the slightly coarser fibers produced with 15 mil orifice. The decreased heat in the system associated with finer fibers overall, may have resulted in decreased shot generation for 400 MFR resin with an increase in orifice diameter.

Effect of MFR*L/D Ratio on Fly Generation. The 2x2 table for MFR*L/D ratio interaction (Appendix B) indicates the same trend as the MFR*orifice size interaction. For the 400 MFR resin, the mean fly level increased with the increase in L/D ratio from 10/1 to 15/1. Whereas for the 35 MFR resin, the mean fly level decreased with the increase in L/D ratio.

Effect of MFR*Air Gap on Fly Generation. From the 2x2 table for MFR*air gap interaction it is evident that the same trend as the MFR*orifice size interaction and the MFR*L/D ratio interaction is obtained. For the 400 MFR resin conditions, mean fly level increased with an increase in air gap from 35 to 110 mil. Since 400

MFR resin experienced a lot of thermal degradation, especially with 20 mil orifice diameter, the additional heat in the proximity of the nosetip created by slower quenching associated with slower primary air velocity at 110 mil (see discussion in phase II on the effect of primary air velocity on fiber diameter) is a probable reason for the increase in fly with an increase in air gap from 35 to 110 mil. Whereas for the 35 MFR resin, the mean fly level decreased with an increase in air gap. In the case of 35 MFR resin the slower velocity associated with the 110 mil air gap may have resulted in coarser fibers, thereby reducing fly generation at the larger air gap. It is probable that the greater heat stability of 35 MFR resin under the conditions employed (Table 5.1, weight average molecular weight of web) did not affect the attenuation characteristics of the melt as compared to 400 MFR, allowing the primary air to have a major influence on deciding the final fiber diameter.

Effect of Orifice Size*L/D Ratio on Fly Generation. For both orifice sizes, at constant orifice size, the mean fly level increased with the increase in the L/D ratio from 10/1 to 15/1, as evident from the 2x2 interactive table for orifice size*L/D ratio. Here again the effect of increased thermal degradation with 15/1 L/D ratio and 20 mil orifice tends to mask the individual effects. It is possible that the effect of larger orifice diameter and longer orifice length (higher L/D ratio) was high enough to give a net increase in fly generation although the individual MFR, orifice diameter, and L/D combinations may not necessarily exhibit the same behavior. Generally speaking, unless the molten polymer stream can with stand the attenuation process, broken filaments are likely to occur, which cause fly generation. The reason why the magnitude of increase in fly is drastically more for the 20 mil orifice than the 15 mil orifice lies in the increased thermal

degradation of 400 MFR resin with 20 mil orifice, 15/1 L/D ratio as evident from Table 5.1. The answer lies in the fact that in this interaction the average of 8 observations with the 10/1 L/D is compared to the average of 8 observations with the 15/1 L/D ratio with out regard to the resin MFRs. The same procedure is repeated for the two orifice sizes. From the marginal increase in the mean fly level with the increase in L/D ratio, for the 15 mil orifice, it can be said that the 35 MFR seems to survive the attenuation process, and only a relatively small portion of the 400 MFR resin breaks apart. With the 20 mil orifice, there was a considerable increase in the mean fly level, with the increase in L/D ratio, probably because the 400 MFR does not withstand the attenuation process at all (which seem to explain the highest fly rating for the 20 mil, 15/1 L/D combination for the 400 MFR resin). This appears to be the primary reason for such a drastic increase in the fly rating with the increase in L/D ratio with a 20 mil orifice for the 400 MFR resin.

Effect of Orifice Size*Air Gap on Fly Generation. From the 2x2 interaction table for the effect of orifice size*air gap on fly rating, it can be seen that with the 20 mil orifice die tip the mean fly rating decreased with the increase in the air gap from 35 to 110 mil. Whereas with the 15 mil orifice die tip, mean fly rating increased with an increase in air gap from 35 to 110 mil. The reasons for this phenomenon are not entirely understood.

Effect of Polymer Throughput*Air Gap on Fly Generation. For both polymer throughputs, at constant throughput, the mean fly rating increased with the increase in the air gap from 35 to 110 mil, with the magnitude of increase being much more for the lower throughput (0.4 g/hole/min) than for the higher

throughput (0.8 g/min/hole). Because of the lower primary air velocity at larger air gap, and for a constant volumetric flow rate of air, the quenching rate is likely to be slower (because the secondary air will be sucked in at a slower velocity and hence slower cooling of polymer jets) resulting in more heat in the system and thus increasing fly generation. Also, since the nosetip setback was confounded with air gap, the increased setback at larger air gap may have given rise to higher amount of fly.

To put things into perspective it can be said that with respect to shot and fly formation, for 400 MFR resin, the 15 mil hole seems to perform better for both 0.4 and 0.8 g/ hole/ min throughput. For 35 MFR the 20 mil hole seems to be better for both throughputs. In fact, to process 35 MFR at 0.8 g/ hole/ min, only the 20 mil hole seems appropriate. The 100 mil air knives gave more fly, especially with 400 MFR compared to the 35 mil air knives. Thus the DCDs had to be increased for the 110 mil air knives to prevent fly from accumulating all over the room. A possible explanation is the effect of reduced quenching at lower primary air velocities associated with the larger air gap.

Effect of Production Variables on Fiber Diameter

Figures 5.1-5.4 show the effect of the orifice L/D ratio on the average fiber diameter for 35 and 400 MFR resins processed with 35 mil and 110 mil air knives through two orifice diameters (15 mil and 20 mil). To take into account the variability of fiber diameters within a sample, 96% confidence intervals were created around the mean. A two-tailed t-test was performed to calculate the upper and lower confidence intervals.

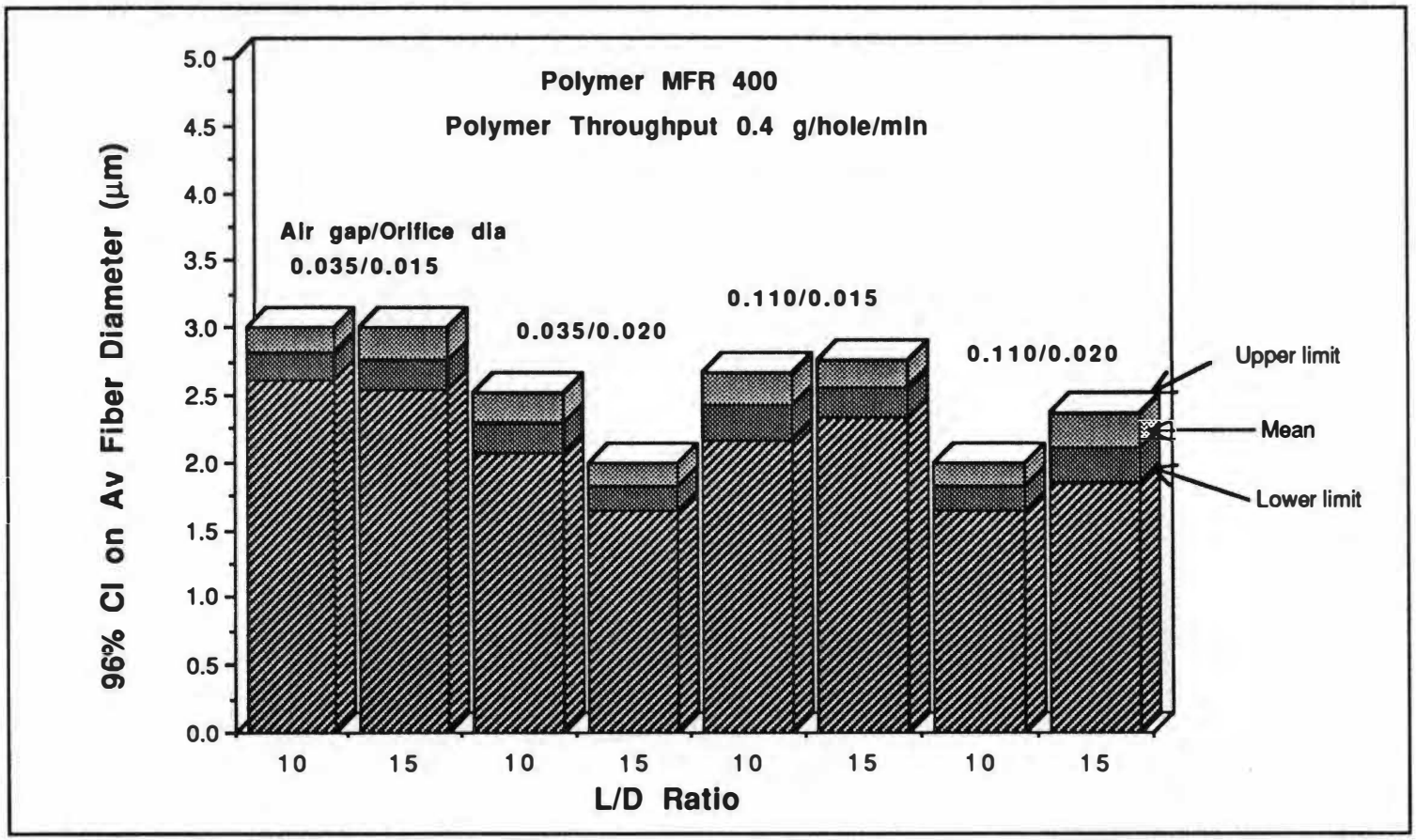


Figure 5.1 Effect of orifice L/D ratio, orifice diameter, and air knife gap on average fiber diameter showing the 96 % upper and lower confidence limits

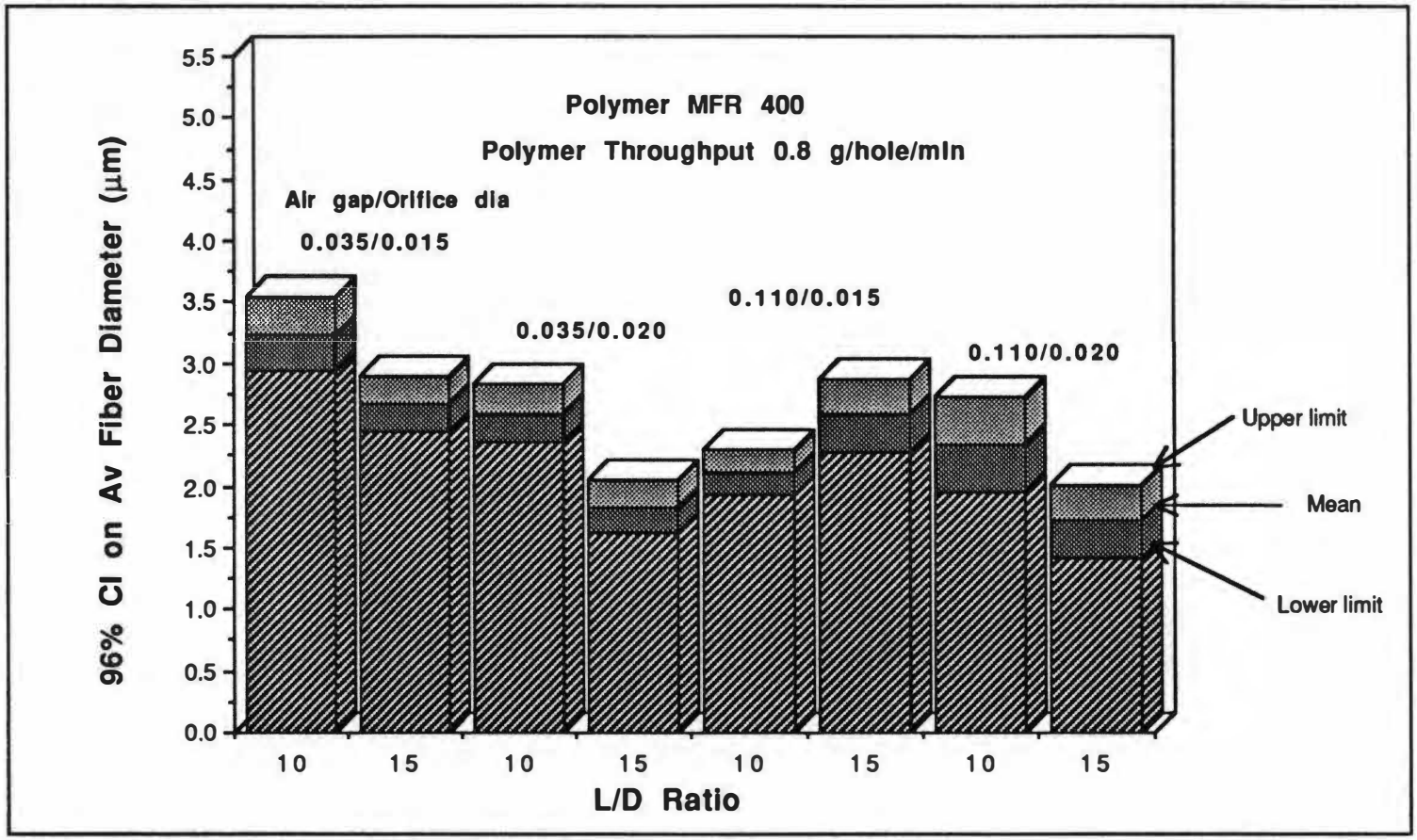


Figure 5.2 Effect of orifice L/D ratio, orifice diameter, and air knife gap on average fiber diameter showing the 96% upper and lower confidence limits

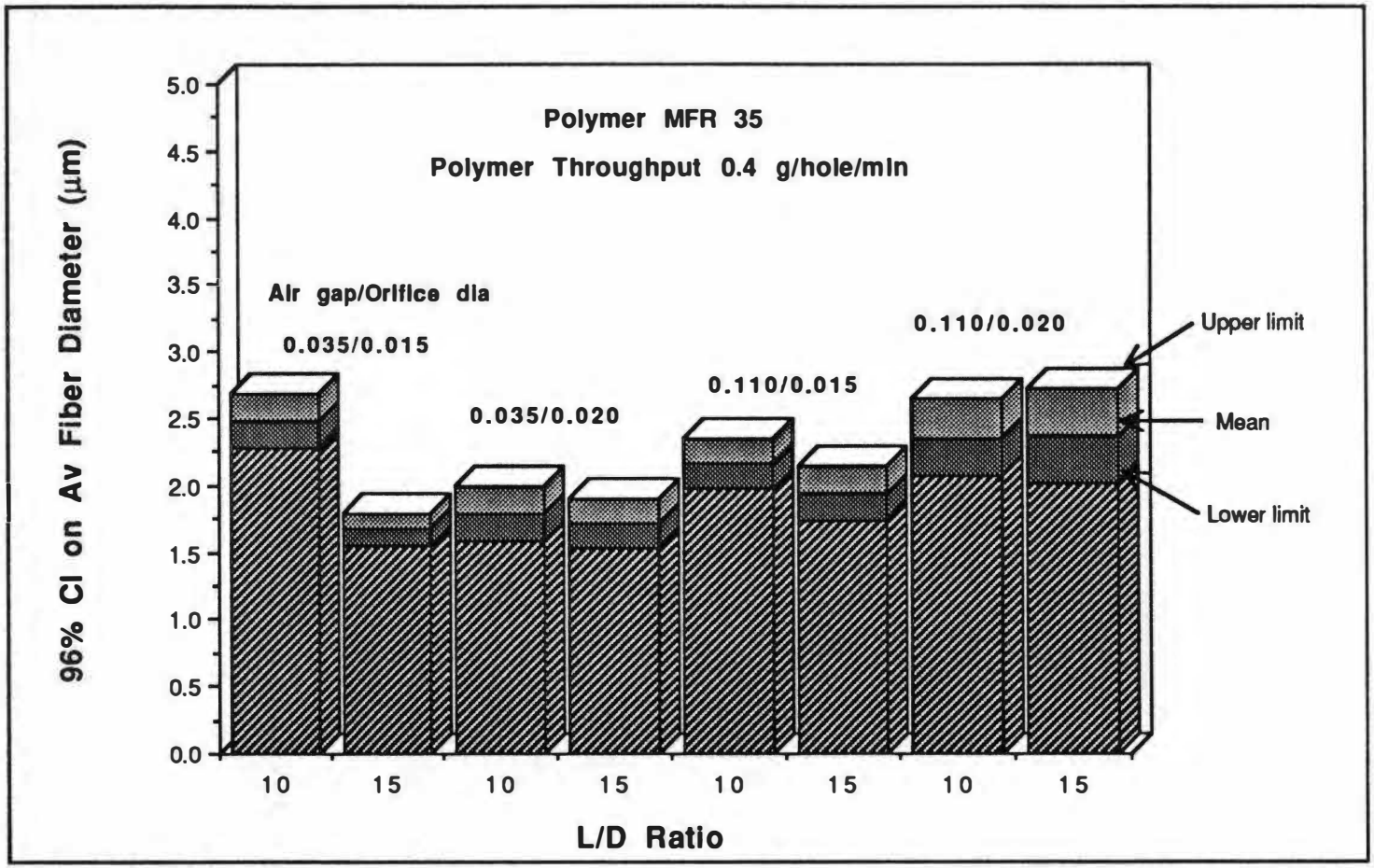


Figure 5.3 Effect of Orifice L/D ratio, orifice diameter, and air knife gap on average fiber diameter showing the 96 % upper and lower confidence limits

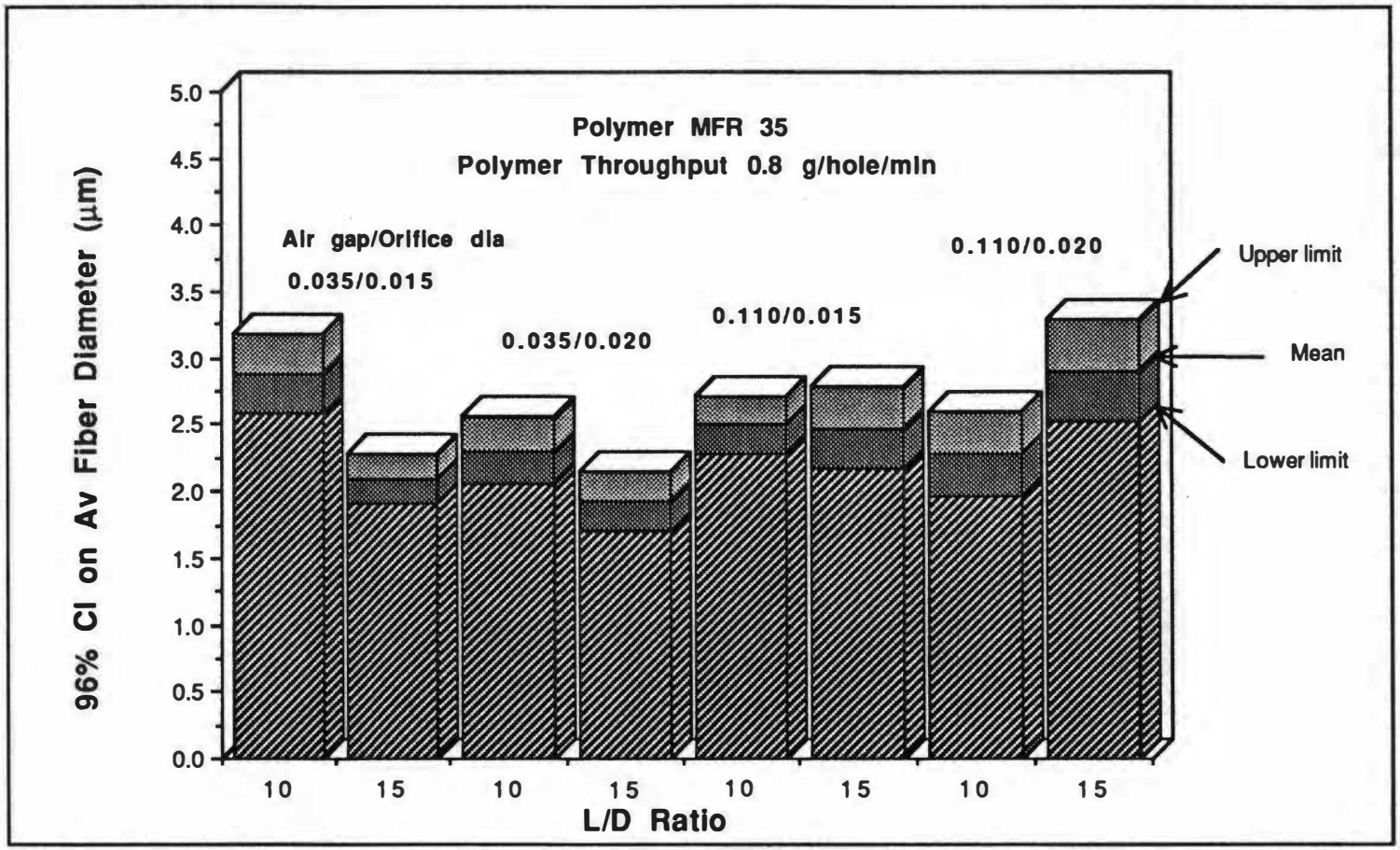


Figure 5.4 Effect of orifice L/D ratio, orifice diameter, and air knife gap on average fiber diameter showing the 96 % upper and lower confidence limits

The statistical analysis of the average fiber diameter data shown in Table 5.1 indicates that the orifice size, polymer throughput, L/D ratio, MFR*orifice size, MFR*air gap, orifice size*air gap, and L/D ratio*air gap have a significant effect on the average fiber diameter of the web.

Effect of Polymer Throughput on the Fiber Diameter. From the main effects table for the effect of polymer throughput on the average fiber diameter it is clear that the increase in the throughput from 0.4 to 0.8 g/hole/min resulted in an increase in the average fiber diameter. Although the increase in fiber diameter with throughput was statistically significant at the 0.05 level, the increase was comparatively small. As the polymer throughput increases, the average fiber diameter also increases, because the ratio of air-to-polymer decreases (at constant air flow rate). The differences in diameters depend on the processing temperature and the mass flow rate of the primary air. The experimental data shown in Table 5.1 and Figures 5.1-5.4 indicates less difference between the 0.4 and 0.8 g/hole/min throughputs, compared to earlier results obtained by Malkan [16]. This was probably because the polymer and air temperatures, and the air flow rate/inch of the die were much higher than that used by Malkan. At 40% air valve opening the scfm/inch with the 6-inch die used in this work was approximately 15 compared to 11.6 at 75% air valve opening in Malkan's study. At 70 % air valve opening in the present study the scfm/inch was 34.9 with the 6-inch die compared to 17.2 at 90% air valve opening in Malkan's study with the 20-inch die.

Effect of MFR*Orifice Size on the Fiber Diameter. It can be seen from the 2x2 interaction table in Appendix B for the effect of MFR*orifice size on the average

fiber diameter that there was a decrease in the average fiber diameter with the increase in the orifice size from 15 mil to 20 mil, at constant MFR, for both resins. The increased thermal degradation of 400 MFR resin (as evident from the weight average molecular weight data in Table 5.1) with a 20 mil orifice 15/1 L/D ratio, may have statistically contributed to finer fiber diameter for samples processed through a 20 mil orifice (both 10/1 and 15/1 L/D ratios). However the decrease in the average fiber diameter was only marginal for the 35 MFR resin, compared to the 400 MFR resin. This may be due to higher resistance of the 35 MFR resin to thermal degradation, resulting in only a marginal decrease in the average fiber diameter when the orifice diameter was increased from 15 to 20 mil. It is logical that at constant resin MFR and L/D ratio the 20 mil orifice will have a higher melt shear viscosity compared to 15 mil orifice (phase IV-viscosity studies), provided the processing conditions do not affect the thermal degradation of the resin differently at each orifice diameter. The reason for obtaining finer fiber diameter with 20 mil orifice may be the fact that 15/1 L/D ratio results in notably higher thermal degradation of the resin and thus the lowest shear viscosity.

Effect of MFR*Air Gap on the Fiber Diameter. From the 2x2 interaction table for the effect of MFR*air gap on the fiber diameter shown in Appendix B, it can be seen that for the 35 MFR resin the mean fiber diameter increased with the increase in the air gap from 35 to 110 mil. Whereas for the 400 MFR resin, the increase in the air gap resulted in the decrease in mean fiber diameter. It is possible that the 35 MFR resin with the 110 mil air gap may not attenuate to the same extent as with the 35 mil air gap because of the lower air velocity with the 110 mil air gap. It can be argued that since the setback increased along with the increase in the air gap that it may have served to offset the effect of the

decreased air velocity. Since the 35 MFR resin has longer chains it is quite possible that the increase in setback along with the increase in the air gap is not sufficient to offset the effect of the decreased velocity, associated with the larger air gap, resulting in the larger average fiber diameter. However for the 400 MFR resin, since the chains are much shorter, the setback might influence and offset the effect of the increased air gap, resulting in smaller average fiber diameters with the larger air gap. Also the effect of increased thermal degradation of 400 MFR resin under the processing conditions employed with 20 mil orifice and 15/1 L/D ratio combined with slower quenching rate at lower primary air velocity (larger air gap) may have influenced the overall arithmetic mean of the average fiber diameter, thus indicating smaller fiber diameter at 110 mil (larger air gap) compared to 35 mil (smaller air gap).

Effect of Orifice Size*Air Gap on the Fiber Diameter. With the 20 mil orifice the increase in air gap from 35 mil to 110 mil increased the average fiber diameter. With the 15 mil orifice, on the other hand, the average fiber diameter decreased with the increase in air gap. A possible explanation being, with the combination of the 20 mil orifice and the 110 mil air gap (setback), the polymer stream may have broken under the action of the hot air, but with the 15 mil orifice and 110 mil air gap combination, the polymer stream probably survived the attenuation process.

Effect of L/D Ratio*Air Gap on the Fiber Diameter. The effect of L/D ratio*air gap on the fiber diameter was similar to that of the orifice size*air gap interaction. The 15/1 L/D has a similar effect, as the 20 mil orifice, and the 10/1 L/D as the 15 mil orifice. Here again the effect of setback seems to be prominent over the air

velocity. This theory is justified by the fact that though the primary air velocity decreases with the increase in the air gap, finer average fiber diameter was produced.

Effect of Volumetric Flow Rate of Air on Fiber Diameter. Figures 5.5 and 5.6 show the effect of the flow rate of air on fiber diameters at constant air stagnation pressure in the die. At 5 psi air pressure, the volumetric flow rates at air valve openings of 40% and 70% were 119.2 scfm and 70% 279.2 scfm using the 35 mil and 110 mil air knives, respectively. The 110 mil air knives under these conditions gave a notably smaller average fiber diameter compared to the 35 mil air knives. Since the velocity was constant for both the air knives, the air to polymer mass flux ratio was higher for the 110 mil air knives. Thus the diameter was considerably finer and this result agrees well with the findings of Haynes [34].

Effect of Die-to-Collector Distance on Fiber Diameter. The result indicates that the DCD did not appear to affect the average fiber diameter. Figure 5.7 shows the effect of DCD on the average fiber diameter. Thus a study was conducted with the 35 MFR resin with the 20 mil orifice die and the 35 mil air knife gap to determine if DCD had an effect on the average fiber diameter.

Effect of Production Variables on Physical and Mechanical Properties of Melt blown PP webs

Filtration Efficiency. The values of filtration efficiency were plotted against the L/D ratio for four different polymer MFR/ polymer throughput combinations and

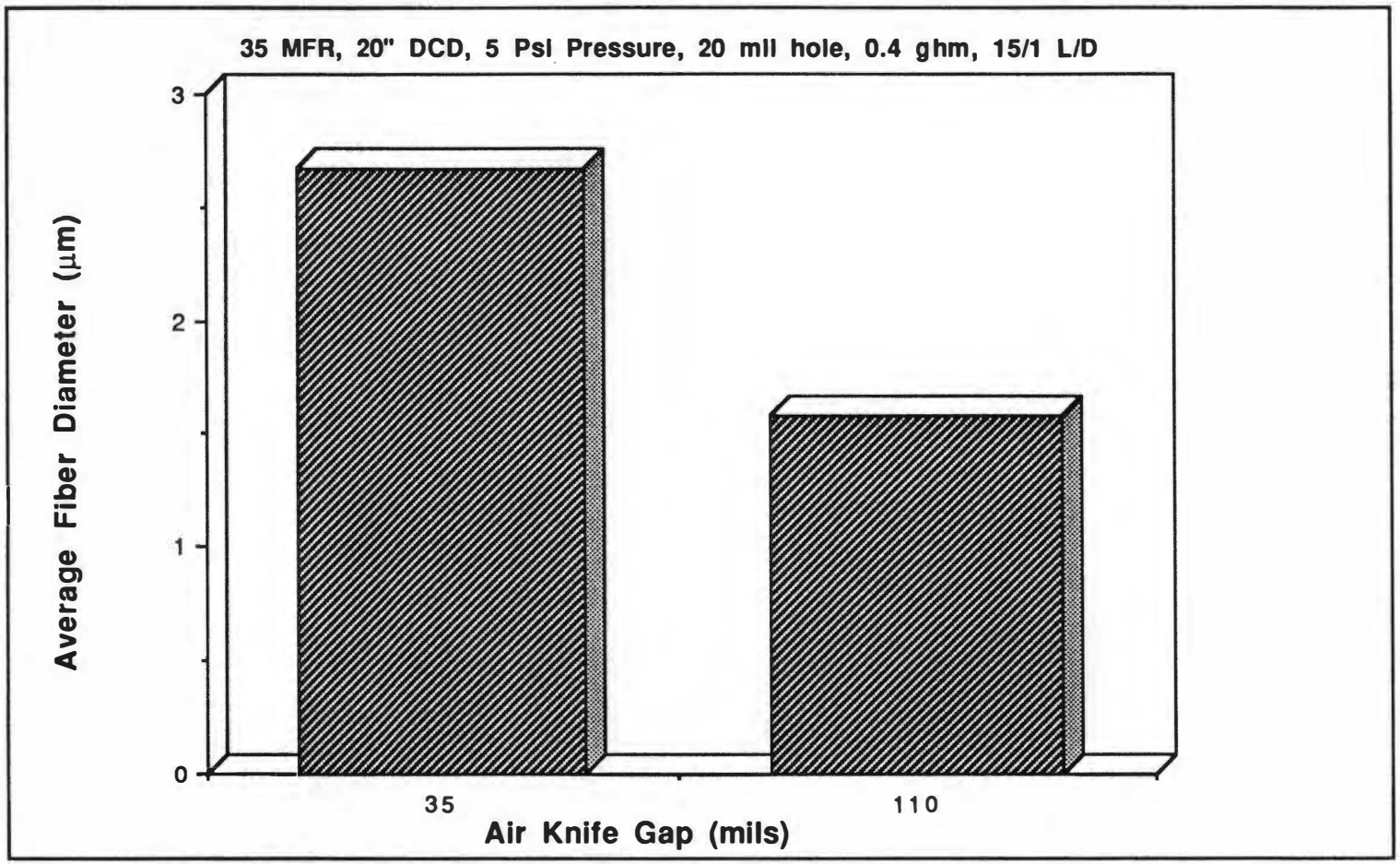


Figure 5.5 Effect of air knife gap on average fiber diameter at constant primary air stagnation pressure

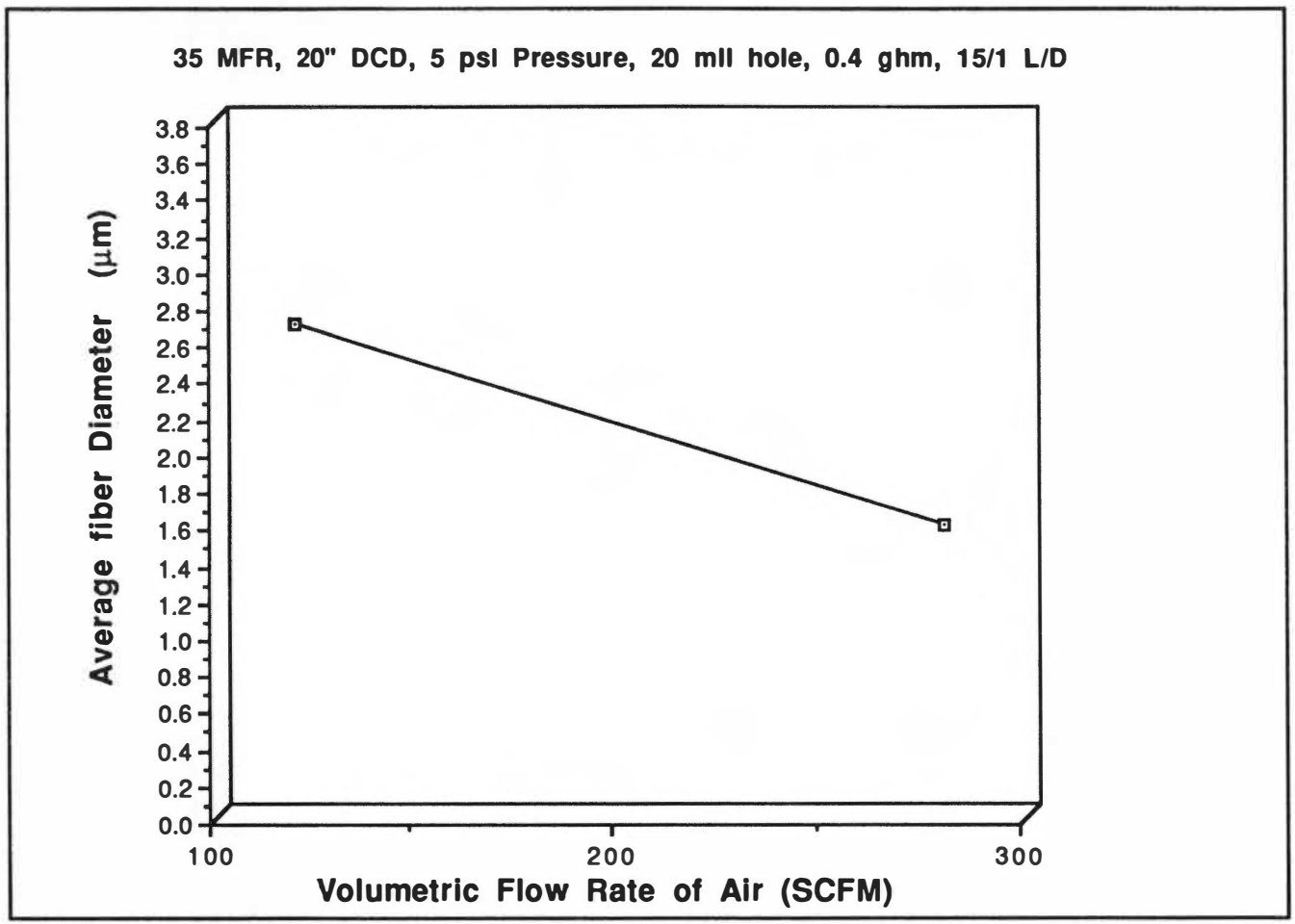


Figure 5.6 Effect of volumetric flow rate of air on average fiber diameter at constant primary air stagnation pressure

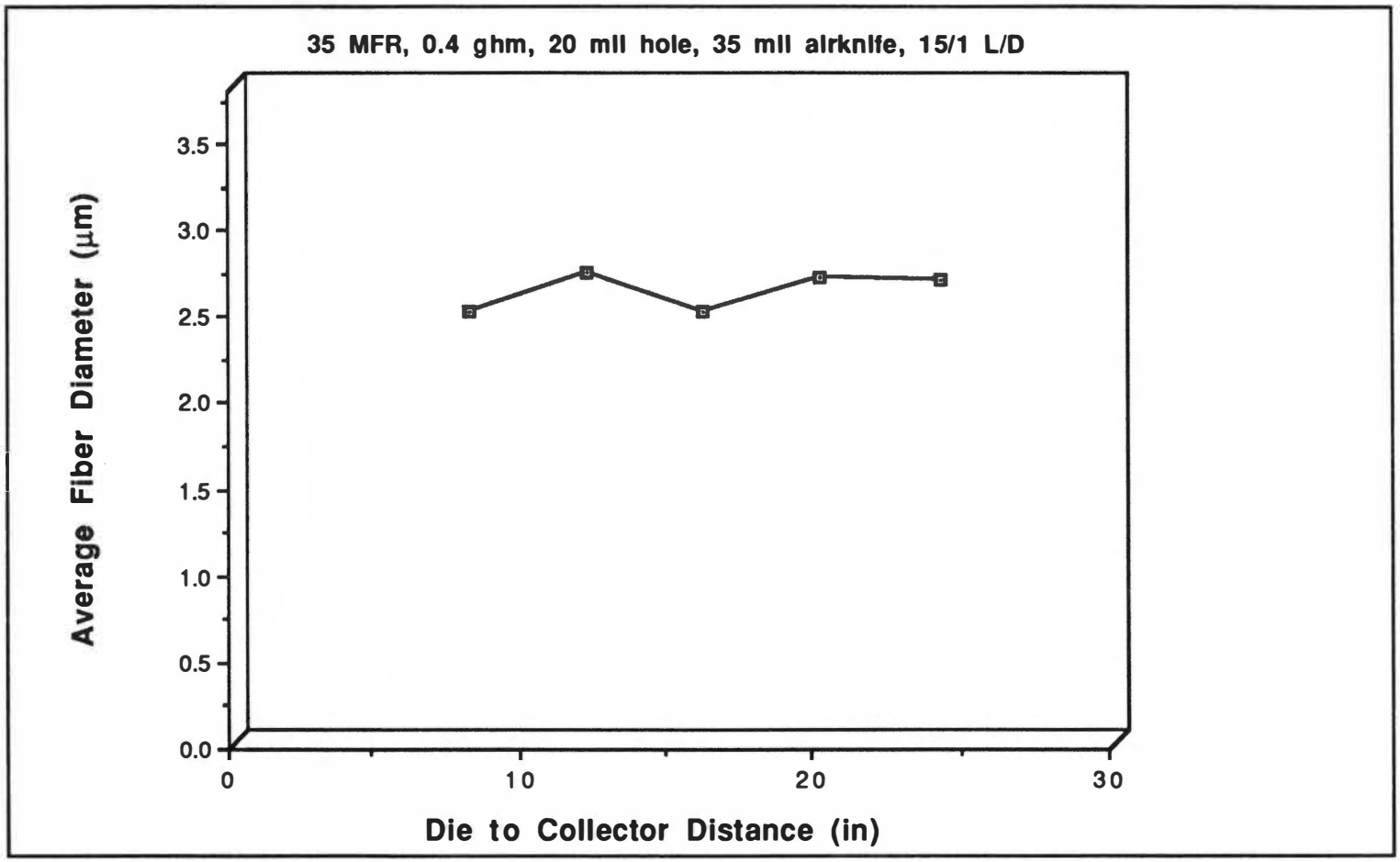


Figure 5.7 Effect of DCD on average fiber diameter

are shown in Figures 5.8-5.11. The corresponding data is shown in Table 5.1. From the statistical analysis it can be seen that the resin MFR, polymer throughput, L/D ratio, MFR*orifice size, MFR*polymer throughput, hole size*polymer throughput, and hole size*L/D ratio have a significant effect on the web filtration efficiency. As can be seen from the MFR*orifice size interaction relating to filtration efficiency, for the 35 MFR resin, the increase in orifice size from 15 to 20 mil decreased the filtration efficiency. Whereas for the 400 MFR resin, the filtration efficiency increased with the increase in orifice size.

The effect of MFR*polymer throughput interaction on the filtration efficiency indicates a decrease with the increase in polymer throughput from 0.4 to 0.8 g/hole/min for a constant MFR, for both MFRs. However the decrease in the filtration efficiency with the increase in polymer throughput was negligible for the 400 MFR.

With both the orifice sizes, at constant orifice size, the filtration efficiency decreased with the increase in the polymer throughput from 0.4 to 0.8 g/hole/min, as evident from the 2x2 interaction table shown in Appendix B for the effect of orifice size*polymer throughput on filtration efficiency.

The filtration efficiency increased with the increase in L/D ratio from 10/1 to 15/1 with the 20 mil orifice. Whereas with the 15 mil orifice the filtration efficiency remained unchanged with the increase in L/D ratio, as seen from the 2x2 interaction table for the effect of orifice size*L/D ratio on the filtration efficiency shown in Appendix B.

Air Permeability. The air flow rates under a constant head of 0.5 inches of water plotted against the L/D ratio for four different MFR/polymer throughput combinations are shown in Figures 5.12-5.15. The air flow rate data is given in

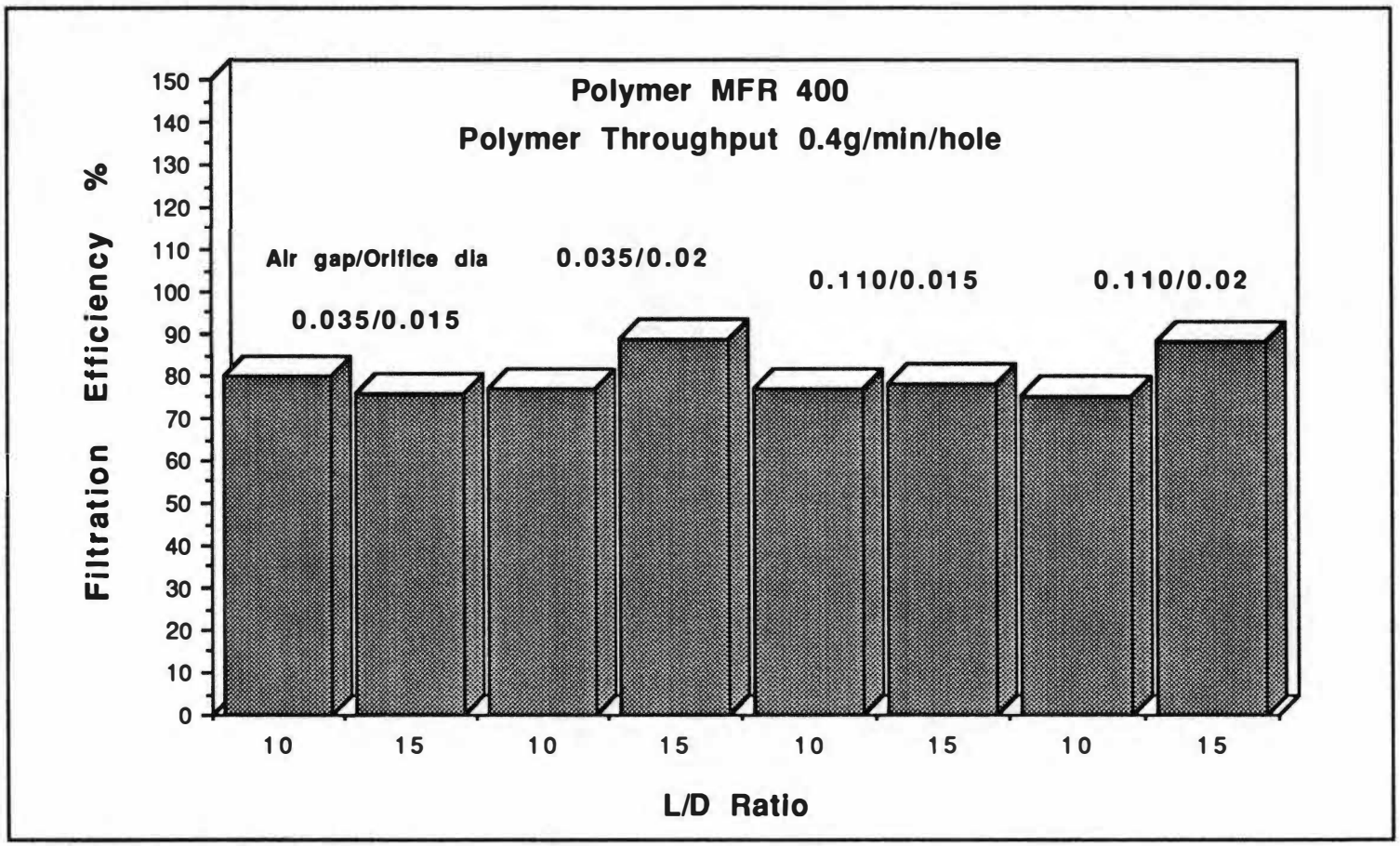


Figure 5.8 Effect of L/D ratio, orifice diameter, and air knife gap on filtration efficiency

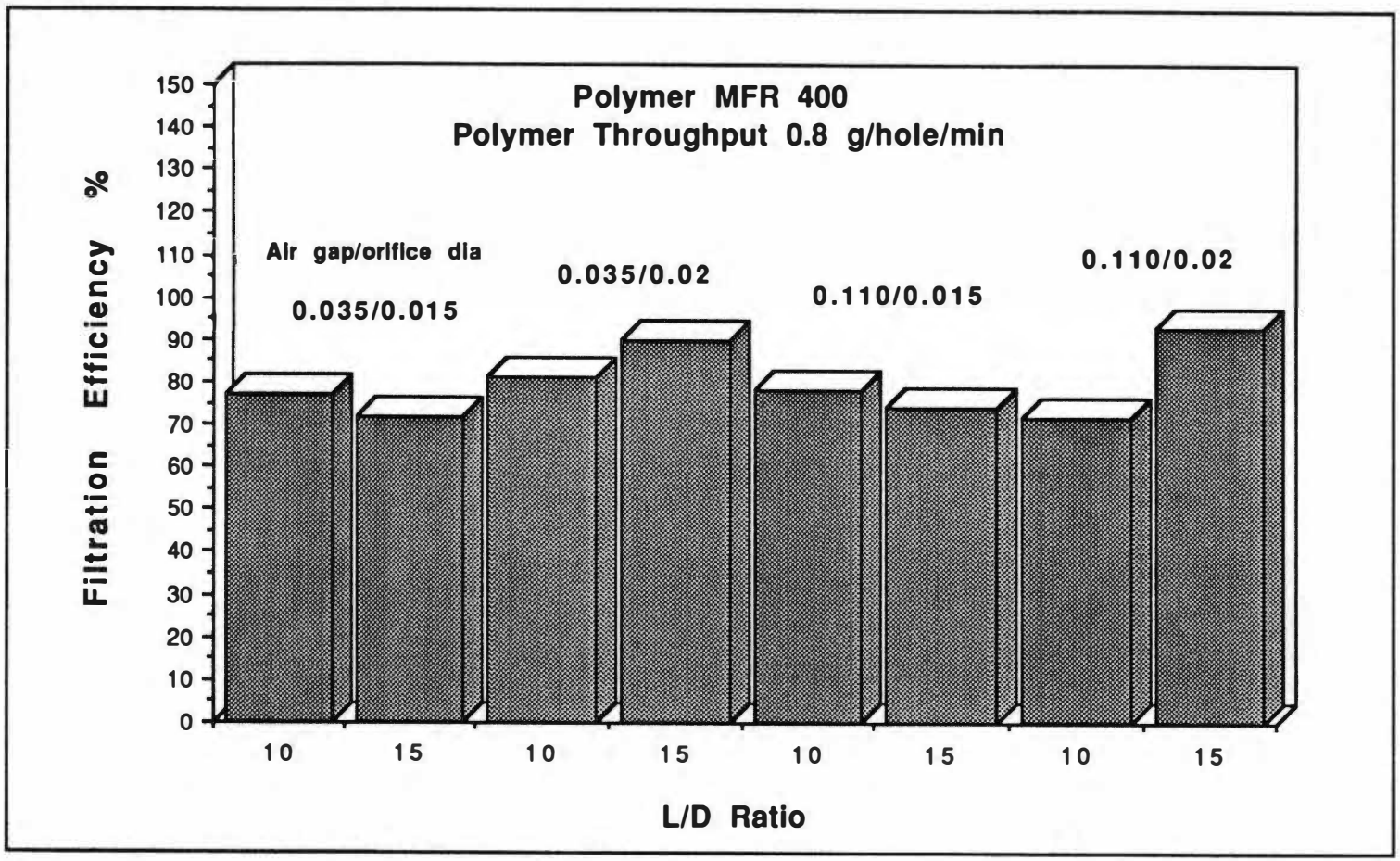


Figure 5.9 Effect of L/D ratio, orifice diameter, and air knife gap on filtration efficiency

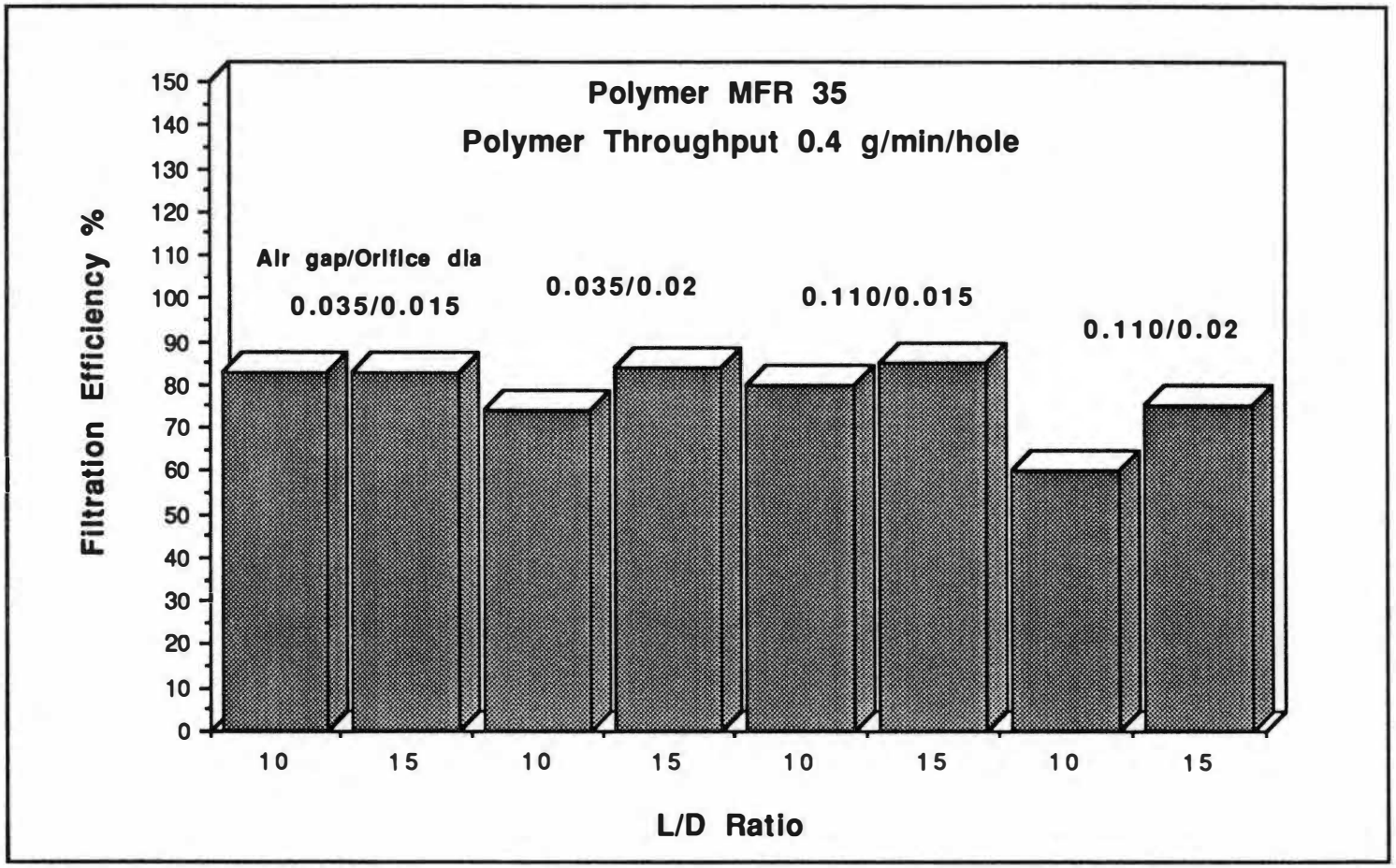


Figure 5.10 Effect of L/D ratio, orifice diameter, and air knife gap on filtration efficiency

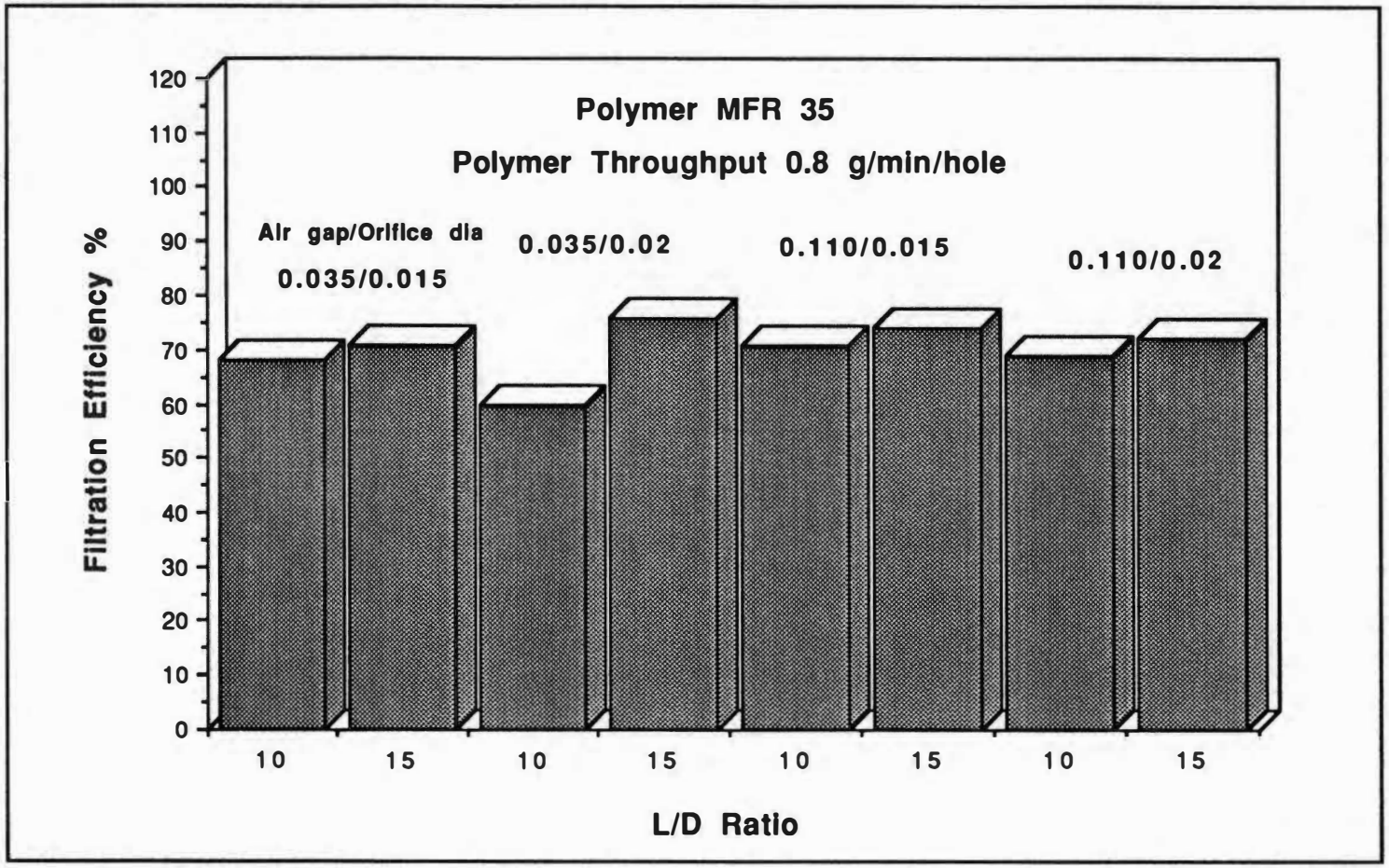


Figure 5.11 Effect of L/D ratio, orifice diameter, and air knife gap on filtration efficiency

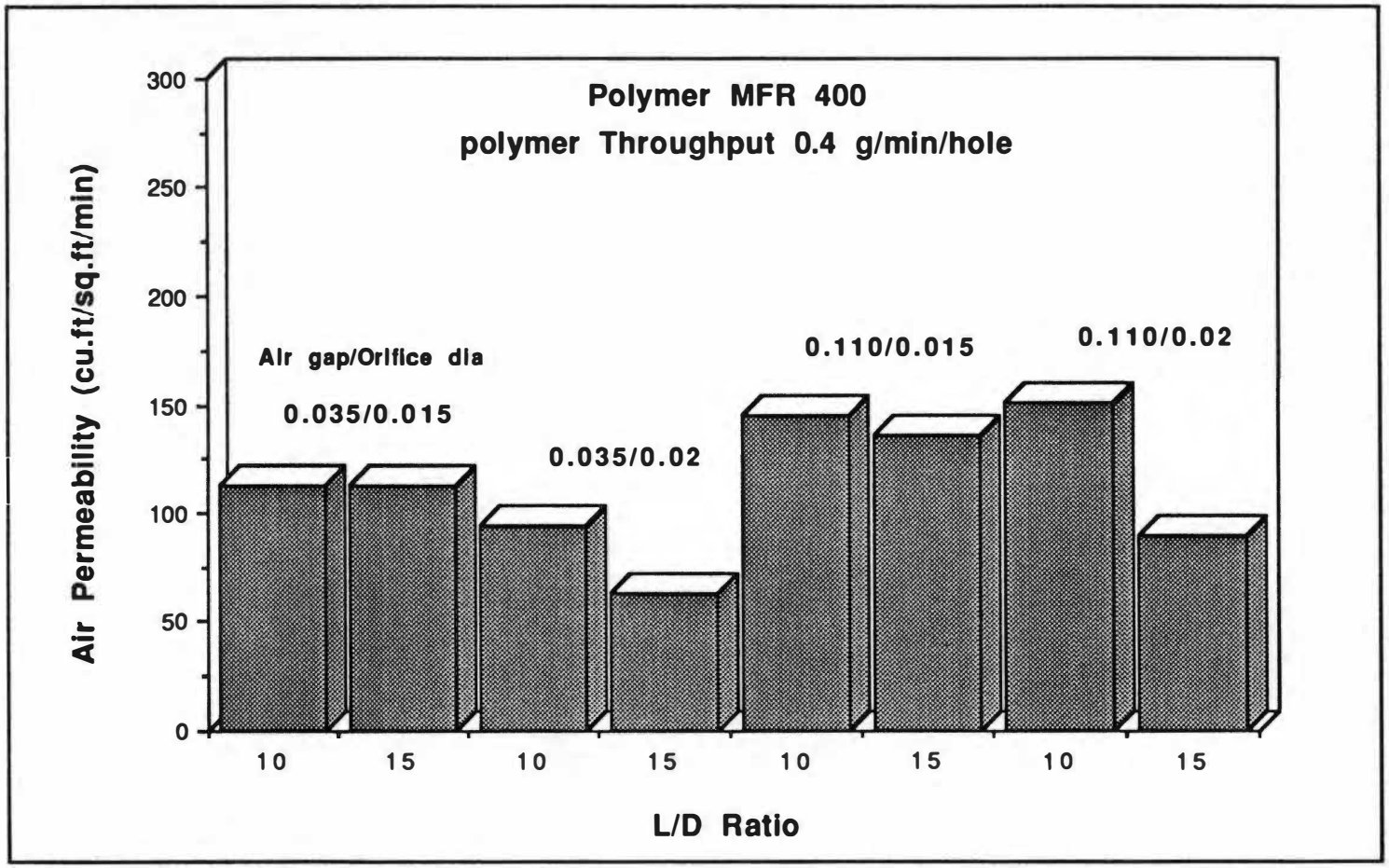


Figure 5.12 Effect of L/D ratio, orifice diameter, and air knife gap on air permeability

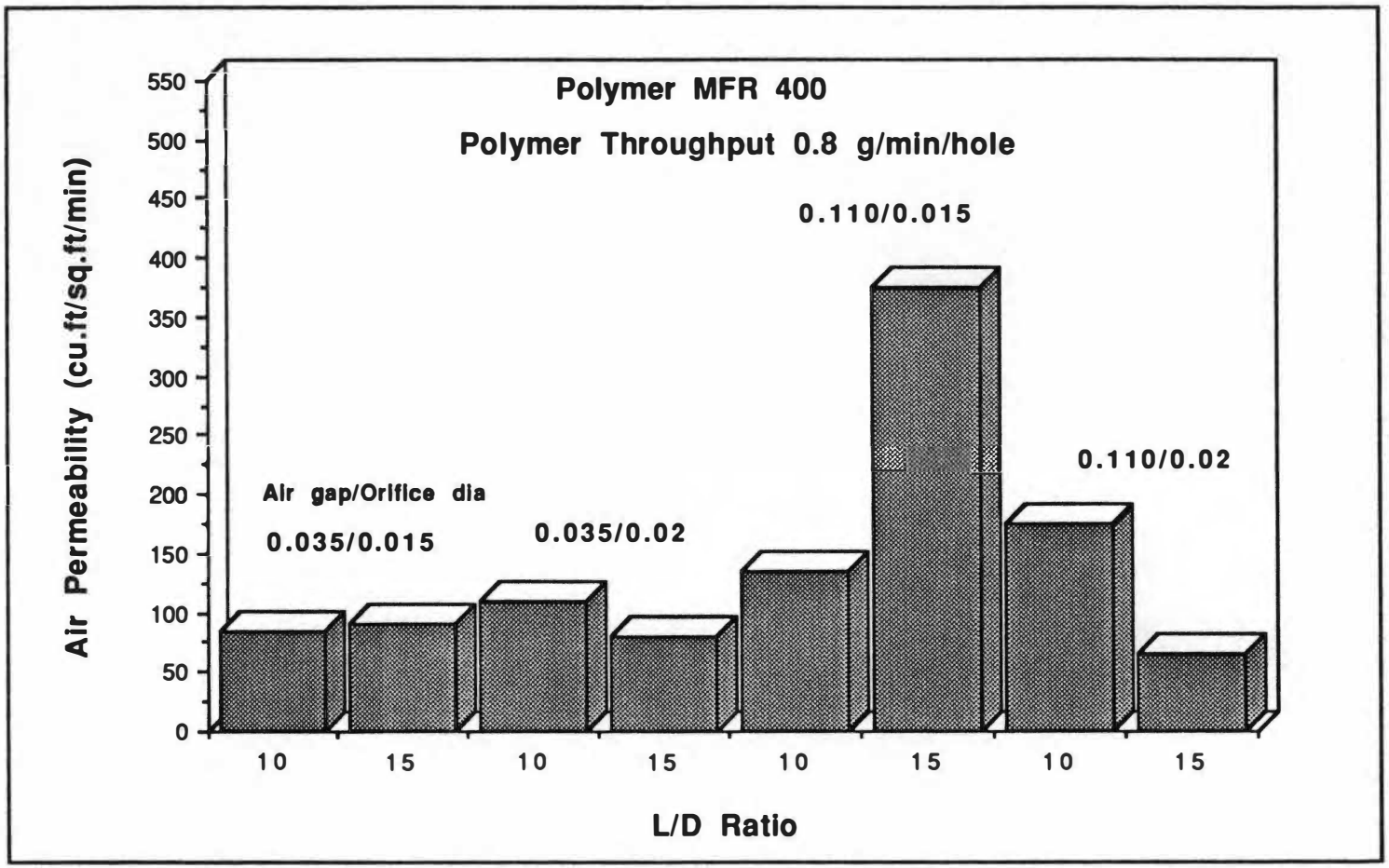


Figure 5.13 Effect of L/D ratio, orifice diameter, and air knife gap on air permeability

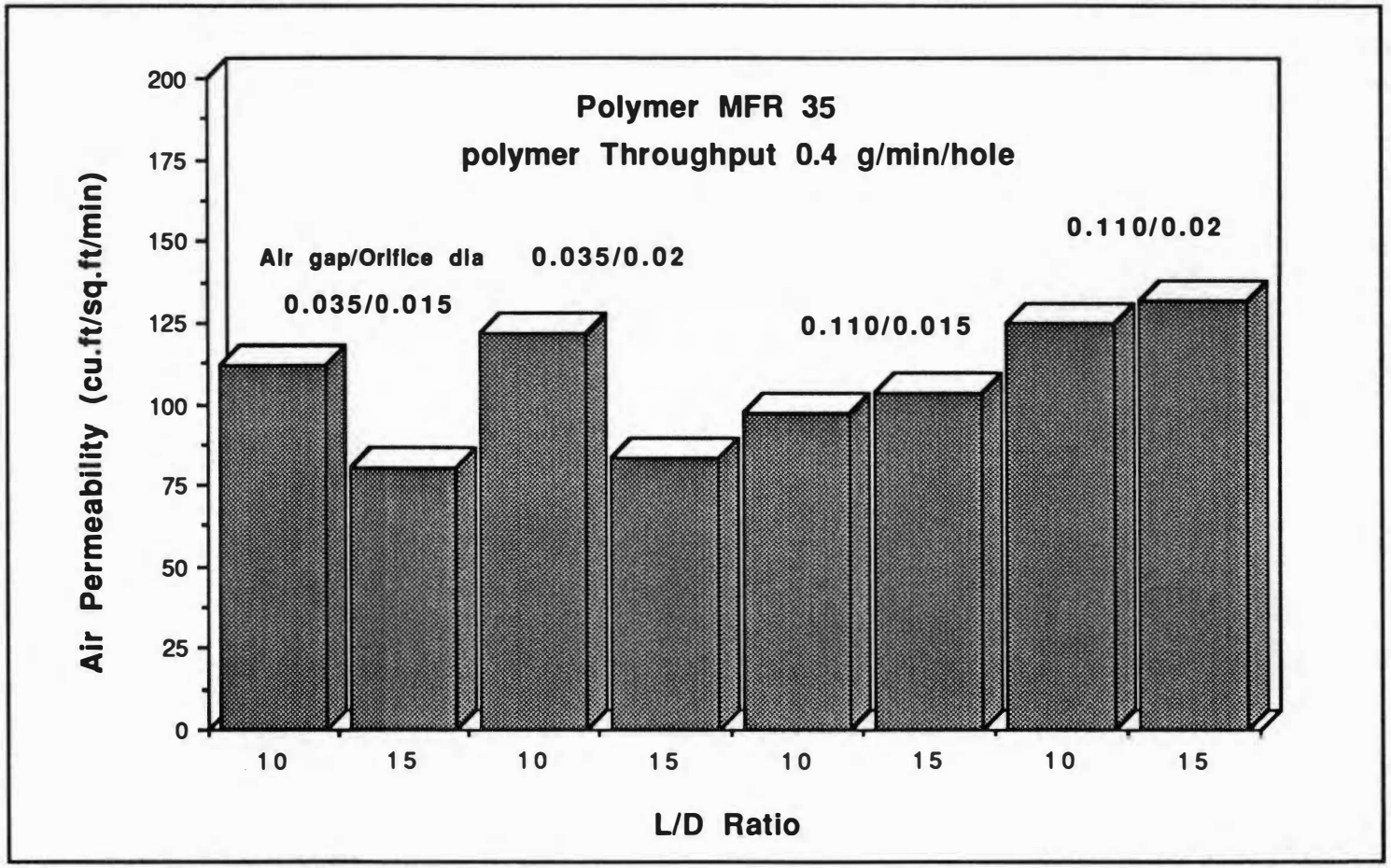


Figure 5.14 Effect of L/D ratio, orifice diameter, and air knife gap on air permeability

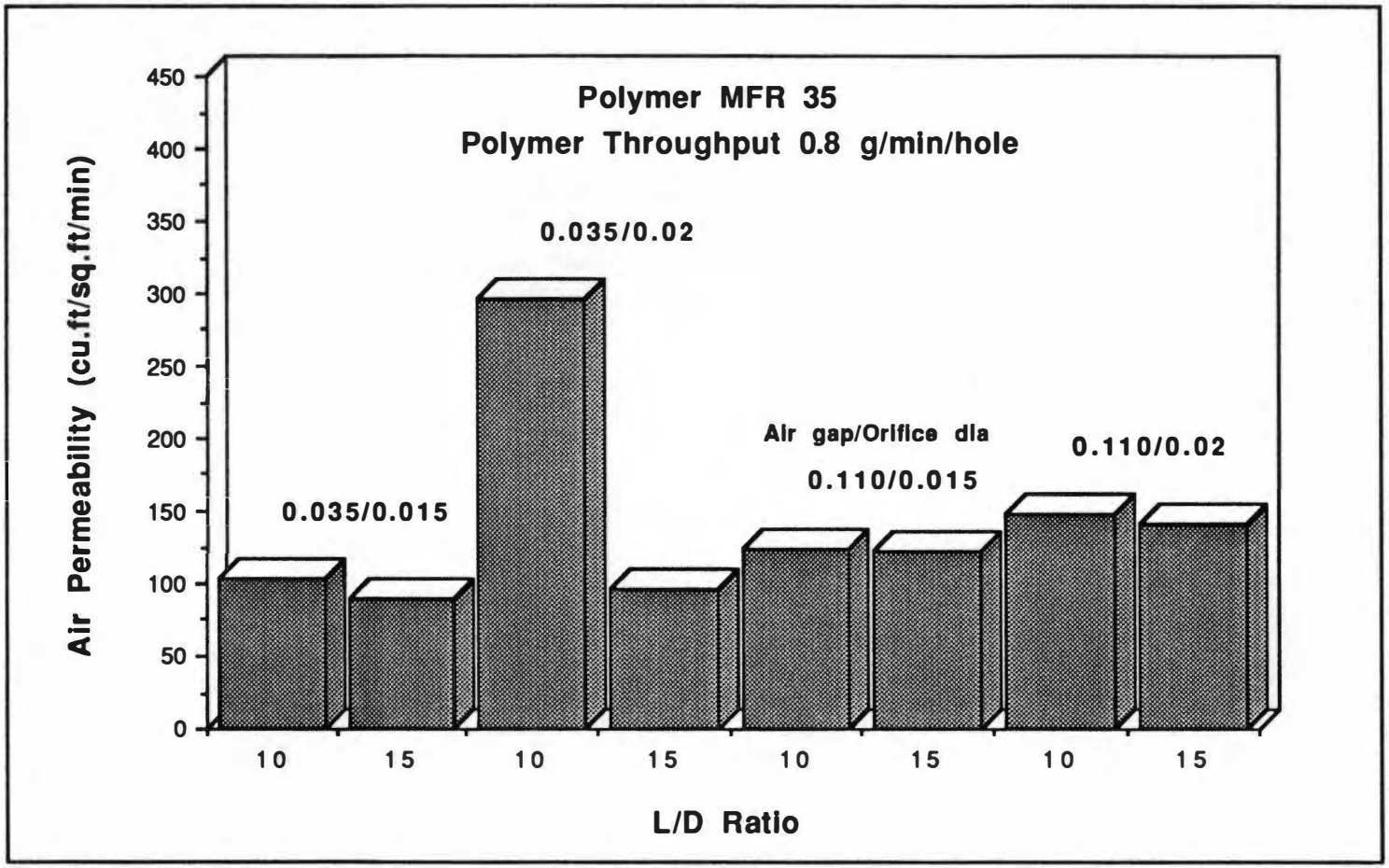


Figure 5.15 Effect of L/D ratio, orifice diameter, and air knife gap on air permeability

Table 5.1. From those values it is clear that for all MFRs and polymer throughputs the 110 mil air knives show a higher value of air permeability. This may be partly attributed to the fact that the die-to-collector distances in the case of 110 mil air gap were larger to reduce fly, than for the 35 mil air gap. Larger DCDs tend to give open structures because of increased ropiness. Since the air flow pattern is very different for the 110 mil air knives, it may have an influence on the web structure, which in turn affects the air permeability. The relationship between the fiber diameters and the air permeability must be used with caution when dealing with webs of different fiber arrangement. In other words although two webs have the same average fiber diameters, their air permeability may be very different if their web structures are wide apart.

The statistical analysis of the air permeability data indicates a very poor correlation. Thus it was not possible to evaluate the effects of the production variables on the response.

Bursting Strength. The values of bursting strength were plotted against the L/D ratio for four different polymer MFR/ polymer throughput combinations and are shown in Figures 5.16-5.19. It appears that there were no consistent trends that could be observed from the plots. However from the statistical analysis in Appendix B it can be seen that the resin MFR, polymer throughput, MFR*air gap, and orifice size*L/D ratio have a significant effect on the bursting strength of the web.

From the main effect table of the polymer throughput relating to the bursting strength, it appears that increasing the polymer throughput from 0.4 to 0.8 g/hole/min decreased the bursting strength. This may be due to greater

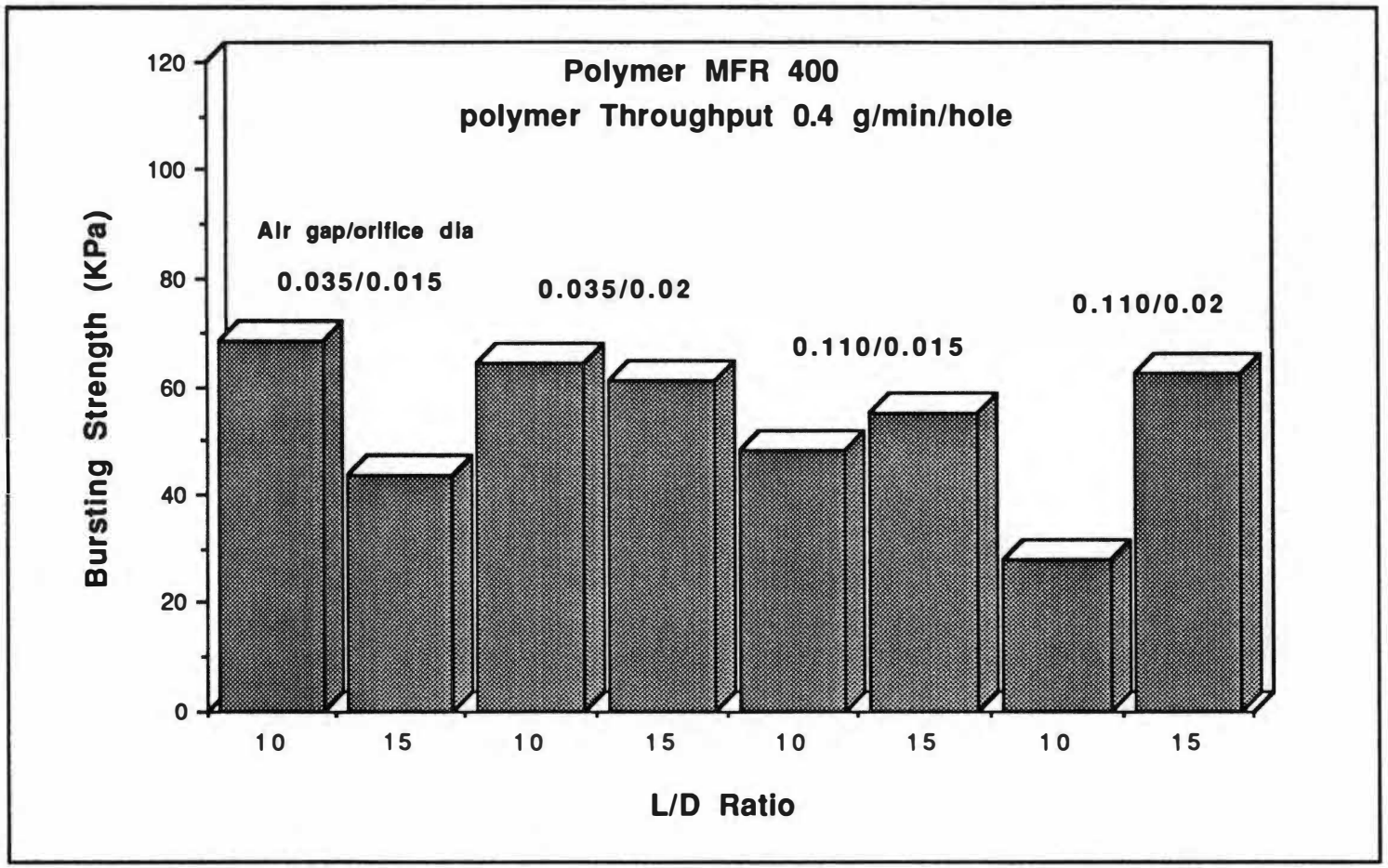


Figure 5.16 Effect of L/D ratio, orifice diameter, and air knife gap on bursting strength

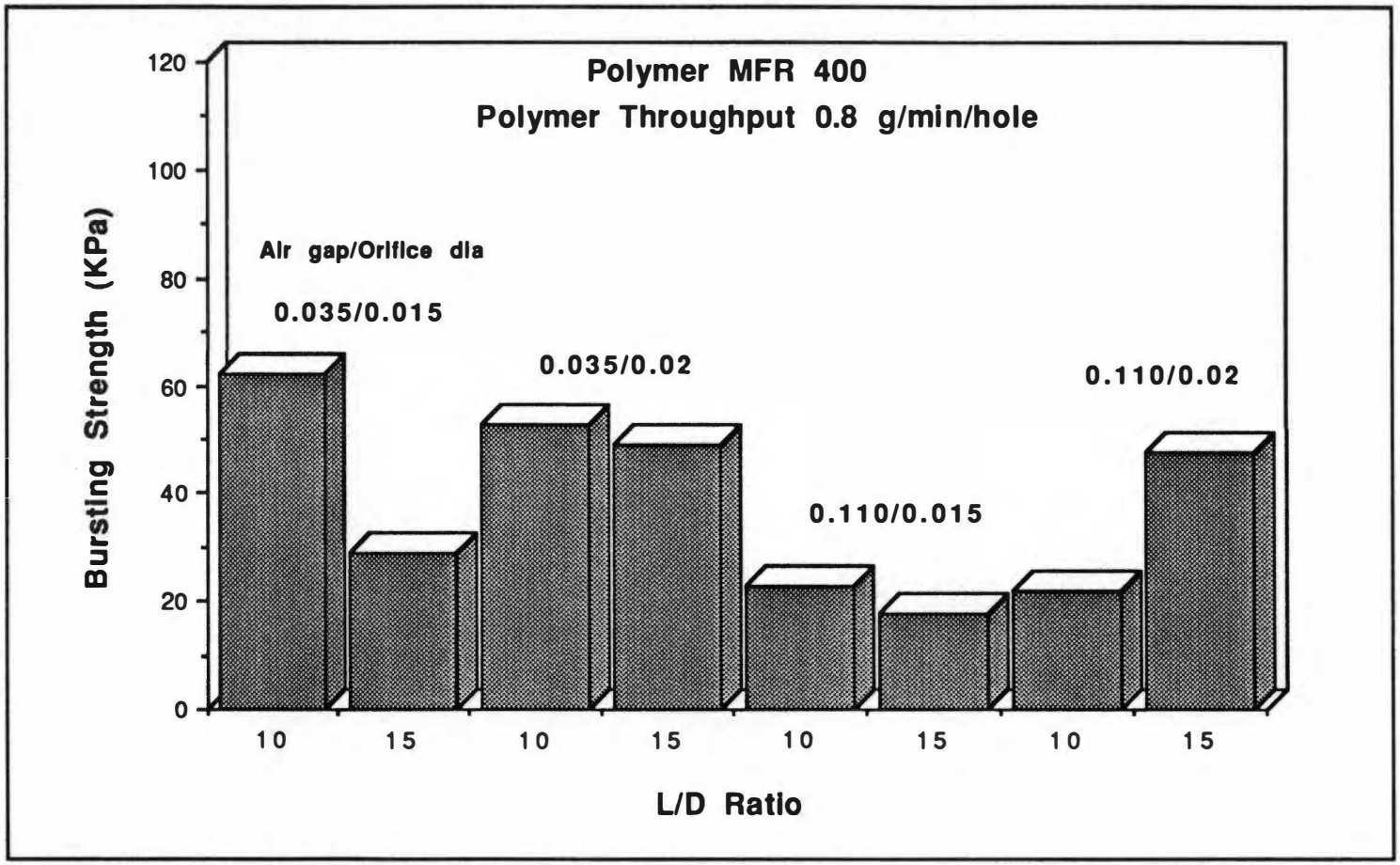


Figure 5.17 Effect of L/D ratio, orifice diameter, and air knife gap on bursting strength

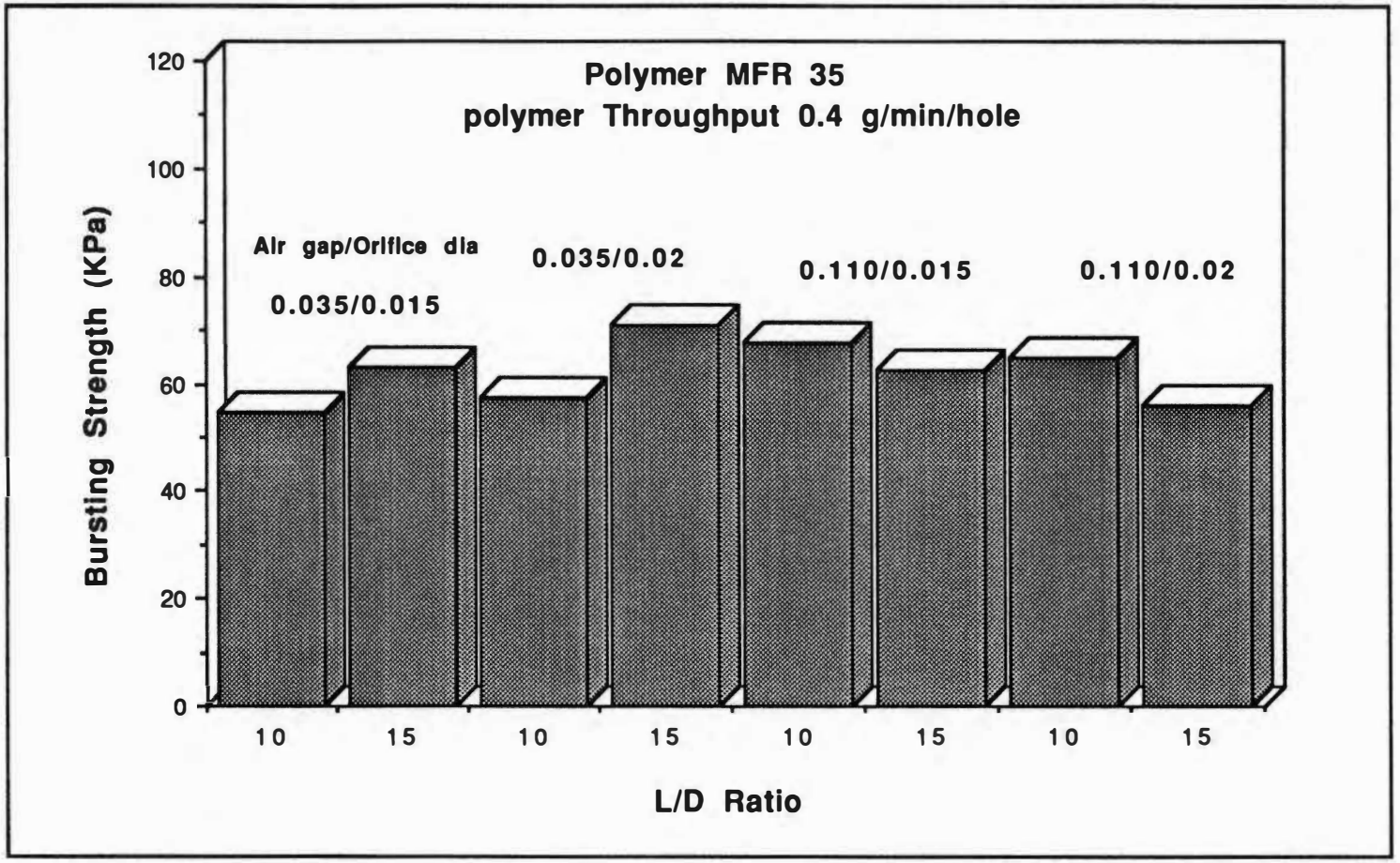


Figure 5.18 Effect of L/D ratio, orifice diameter, and air knife gap on bursting strength

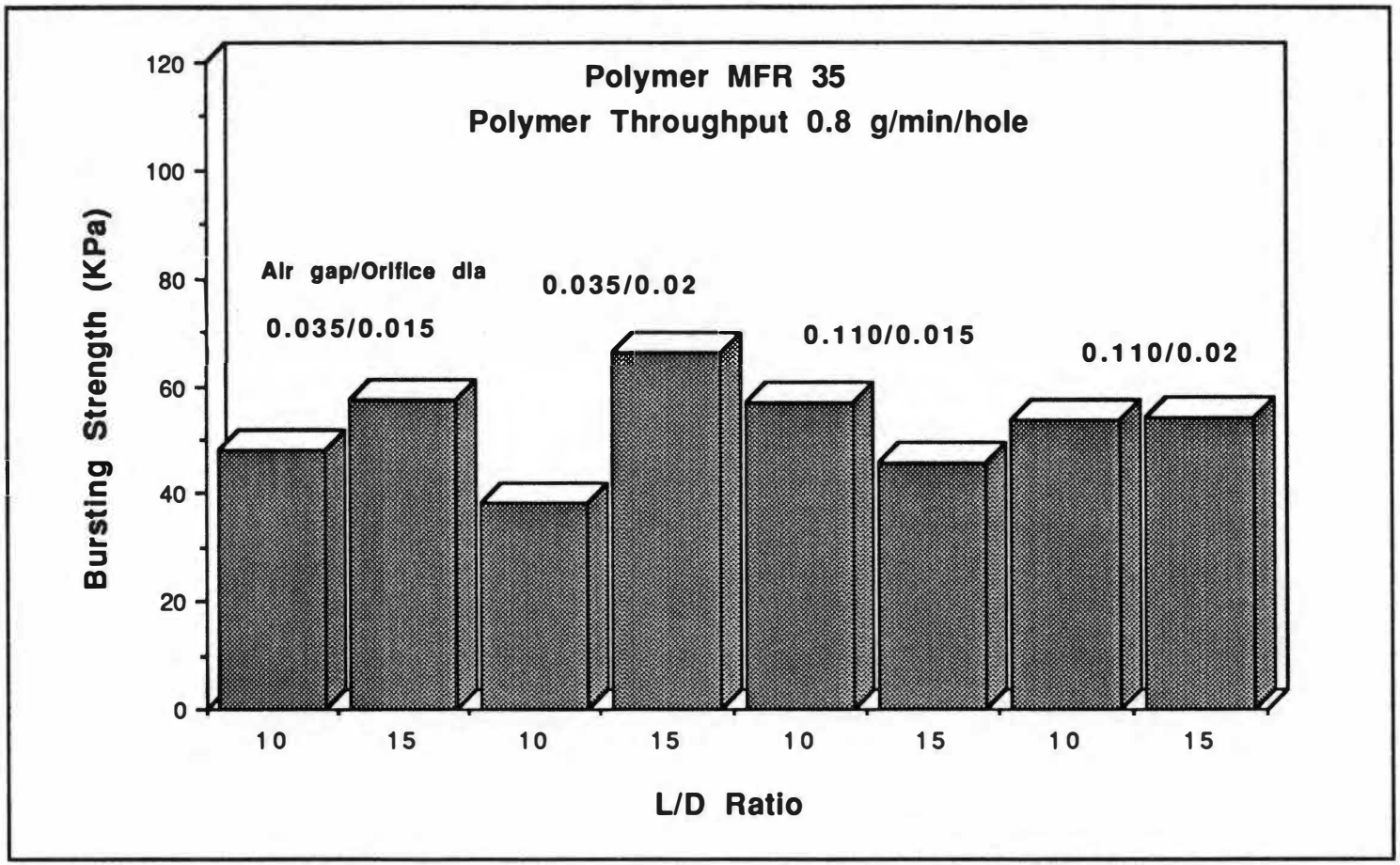


Figure 5.19 Effect of L/D ratio, orifice diameter, and air knife gap on bursting strength

thermal sticking with the higher throughput, which is likely to make the web stiff and hinder the sharing of load amongst the individual fibers.

From the MFR*air gap interaction, it can be seen that for 35 MFR resin, the average bursting strength remained unchanged with the increase in air gap from 35 to 110 mil. Whereas, for the 400 MFR resin, the average bursting strength decreased with the increase in air gap from 35 to 110 mil. The lower quenching rate associated with slower primary air velocity (larger air gap) is likely to contribute to greater heat in the filaments and hence more thermal sticking. Although this is true for both MFRs, the heat in the system for 35 MFR may have been very high to start with, which resulted in no noticeable change in thermal sticking behavior with increasing air gap.

The effect of orifice size*L/D ratio on bursting strength, as evident from the corresponding 2x2 table indicates an increase in the bursting strength with the increase in L/D ratio from 10/1 to 15/1, with a 20 mil orifice, and a decrease in the bursting strength with the increase in L/D ratio, with a 15 mil orifice.

MD Web Tenacity. Figures 5.20-5.23 show plots of MD web tenacity versus the L/D ratio for four different polymer MFR/ polymer throughput combinations. The corresponding data is shown in Table 5.1. The data shows that overall, the 35 MFR conditions produce webs of higher tensile strengths than the 400 MFR conditions. This agrees well with the previous findings [16]. Statistical analysis of the web tenacity data indicates a significant effect of resin MFR, orifice size, MFR*L/D ratio, and MFR*air gap on the response.

The larger orifice (20 mil) gave the higher average tenacity, as evident from the main effect table of orifice size relating to web tenacity. From the MFR*L/D ratio interaction it is clear, that for the 35 MFR resin the 15/1 L/D ratio

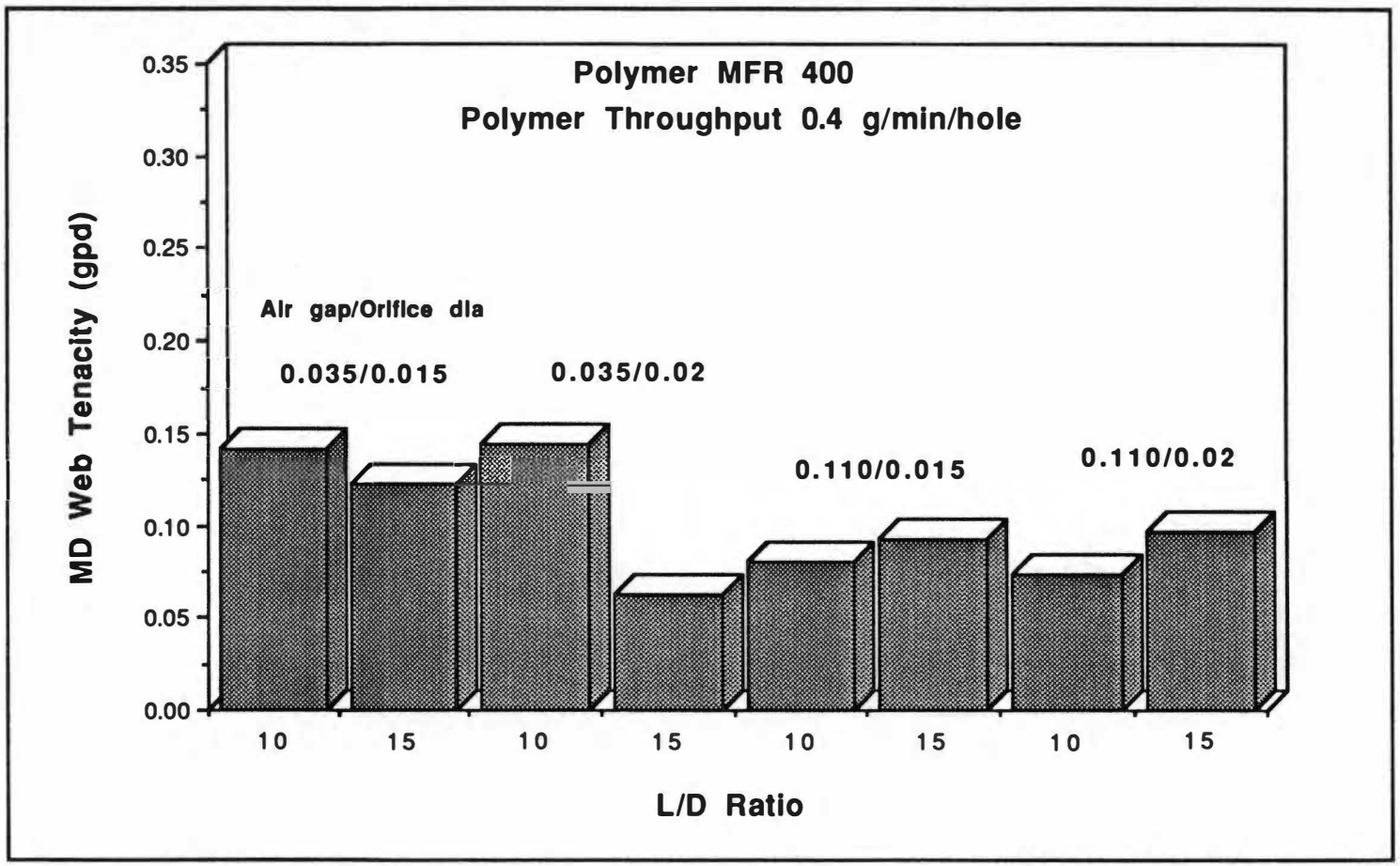


Figure 5.20 Effect of L/D ratio, orifice diameter, and air knife gap on MD web tenacity

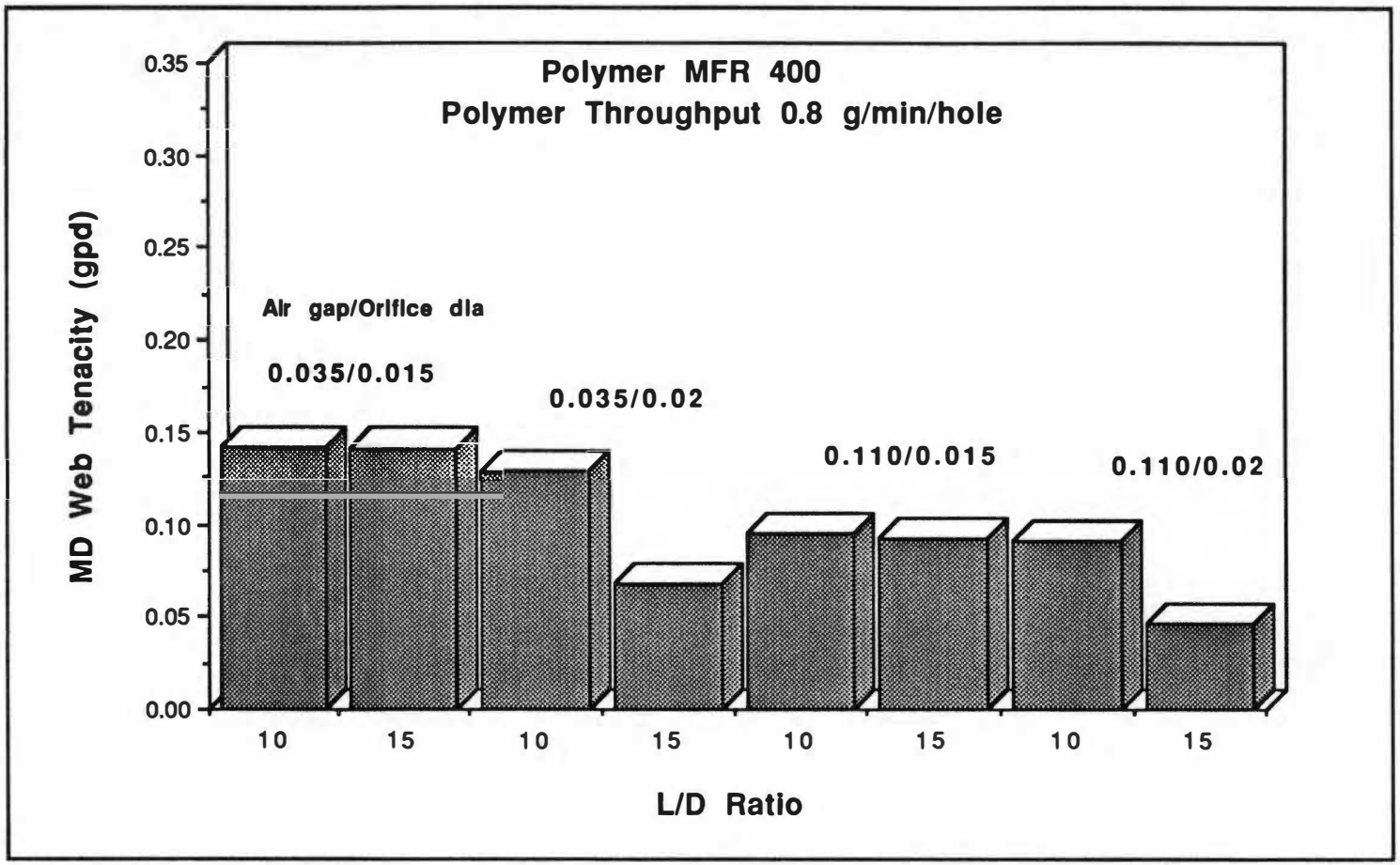


Figure 5.21 Effect of L/D ratio, orifice diameter, and air knife gap on MD web tenacity

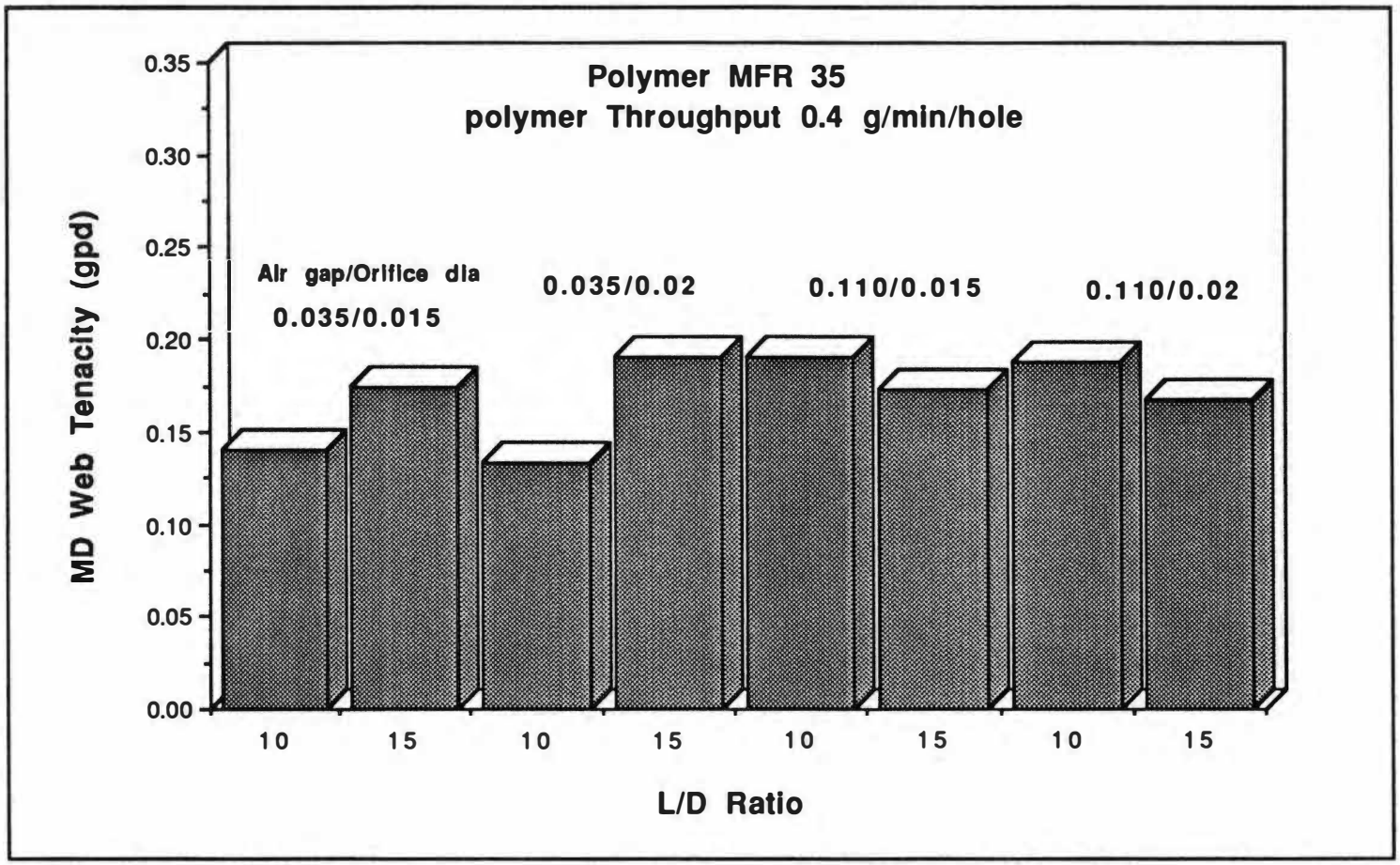


Figure 5.22 Effect of L/D ratio, orifice diameter, and air knife gap on MD web tenacity

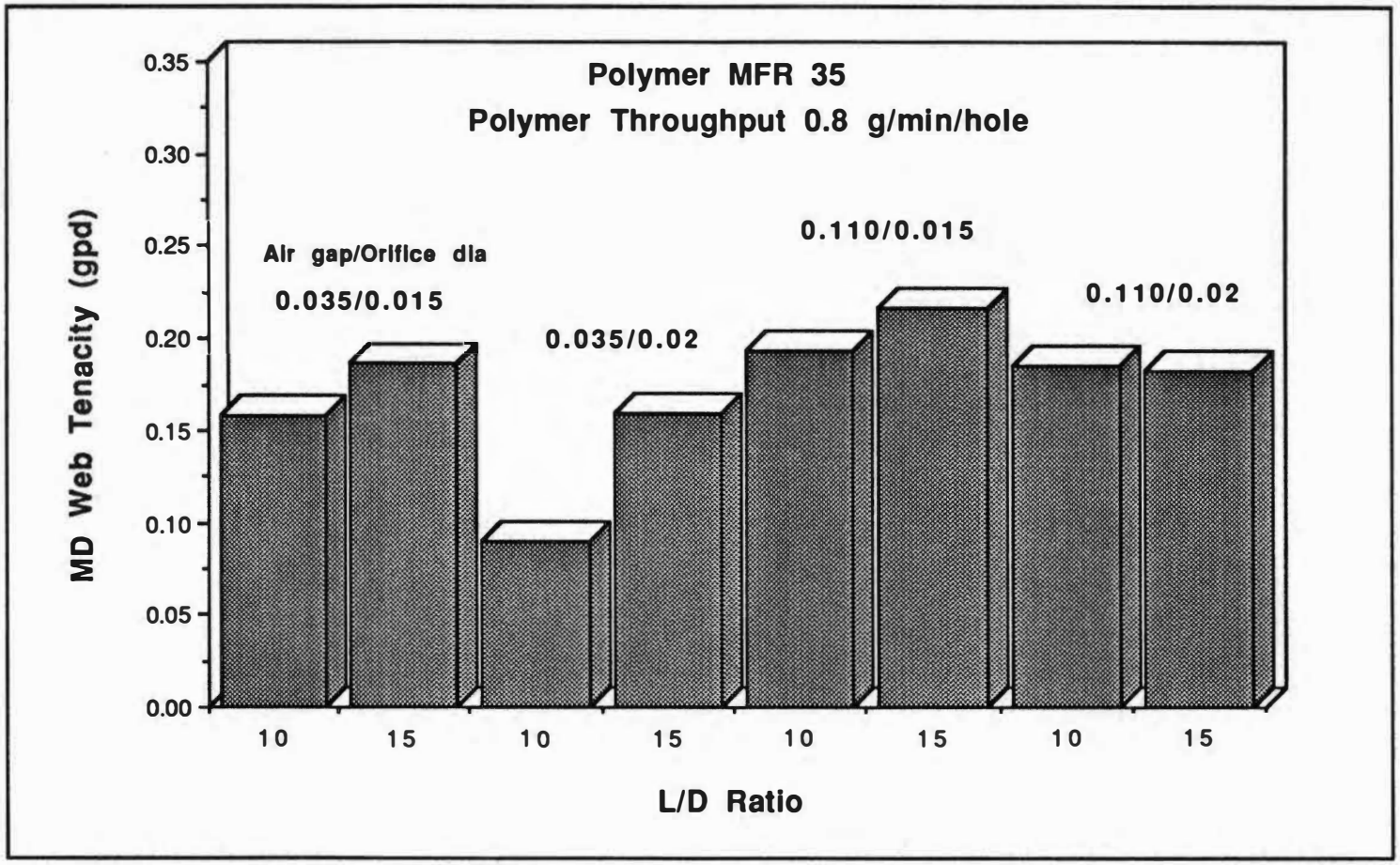


Figure 5.23 Effect of L/D ratio, orifice diameter, and air knife gap on MD web tenacity

gave the higher average tenacity. But for the 400 MFR resin, the 10/1 L/D gave the higher average tenacity. At constant L/D ratio, for both L/D ratios, the 35 MFR PP produced webs with a higher average tenacity than the 400 MFR. For the 35 MFR resin, the average tenacity increased with the increase in air gap from a nominal 30 to 100 mil, whereas, for the 400 MFR resin, the average tenacity decreased with the increase in air gap.

Although the individual fiber strength contributes to the final web strength, much depends on the way the fibers are bonded or entangled. This may be the reason for very weak webs produced with a nominal 100 mil air gap with a 400 MFR resin, although the fiber diameters were not very different from those of nominal 30 mil air gap. Also the effect of excessive degradation in the case of 400 MFR under some conditions may contribute to lower tenacities when computing average values.

MD Breaking Elongation. Figures 5.24-5.27 show the plots of MD breaking elongation versus the L/D ratio for four different polymer MFR/polymer throughput combinations. The corresponding data is shown in Table 5.1. In regards to the elongation-at-break, there do not seem to be any consistent trends. Since elongation-at-break is very sensitive to rate of loading, if the webs are greatly different in each case, very little can be interpreted from the data. Also the variability of the incidence of shot between different samples complicates the analyses. However, the statistical analysis indicates a significant effect of resin MFR, orifice size, polymer throughput, air gap, MFR*polymer throughput, orifice size*polymer throughput, and orifice size*L/D ratio on the MD breaking elongation.

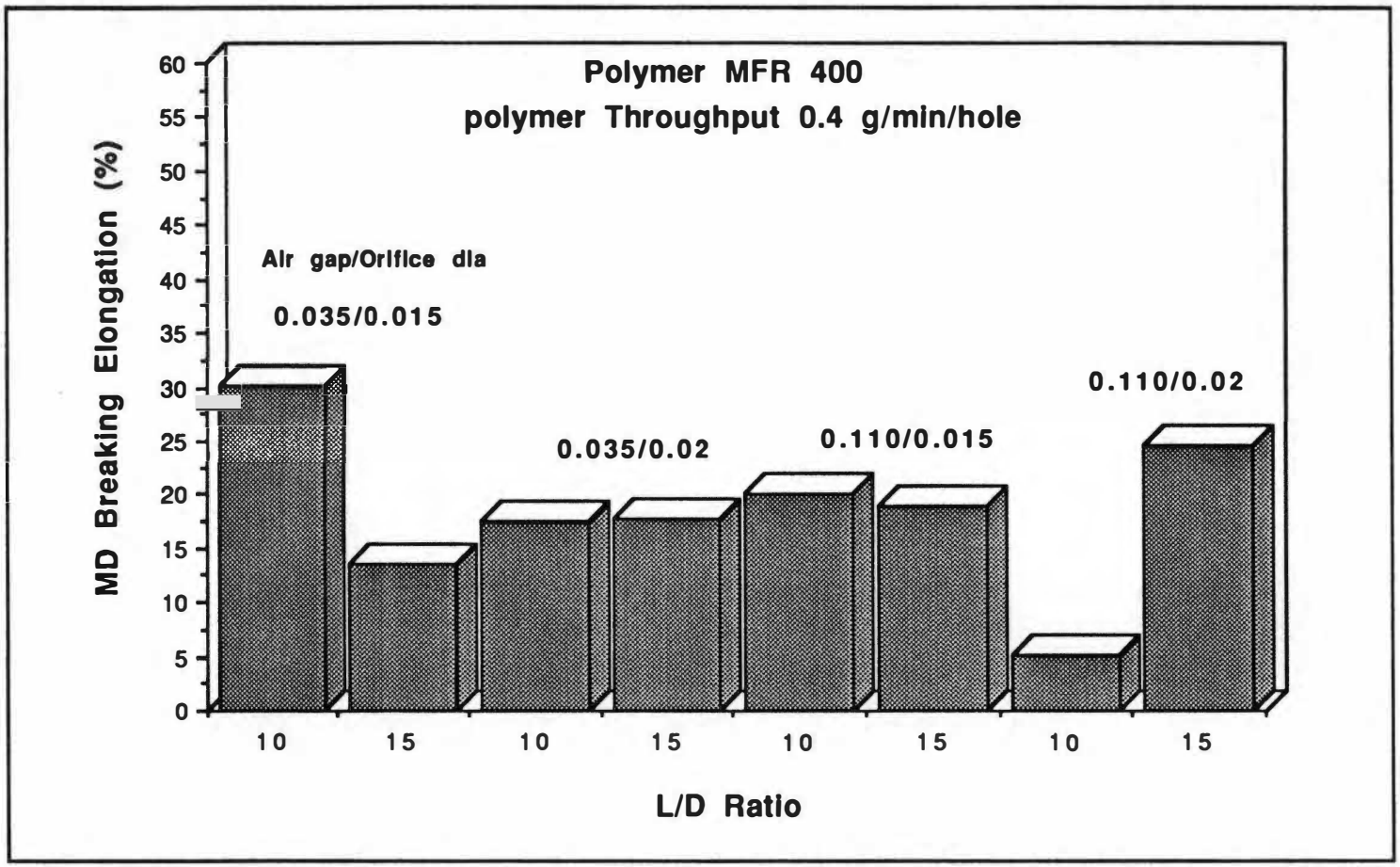


Figure 5.24 Effect of L/D ratio, orifice diameter, and air gap on MD breaking elongation

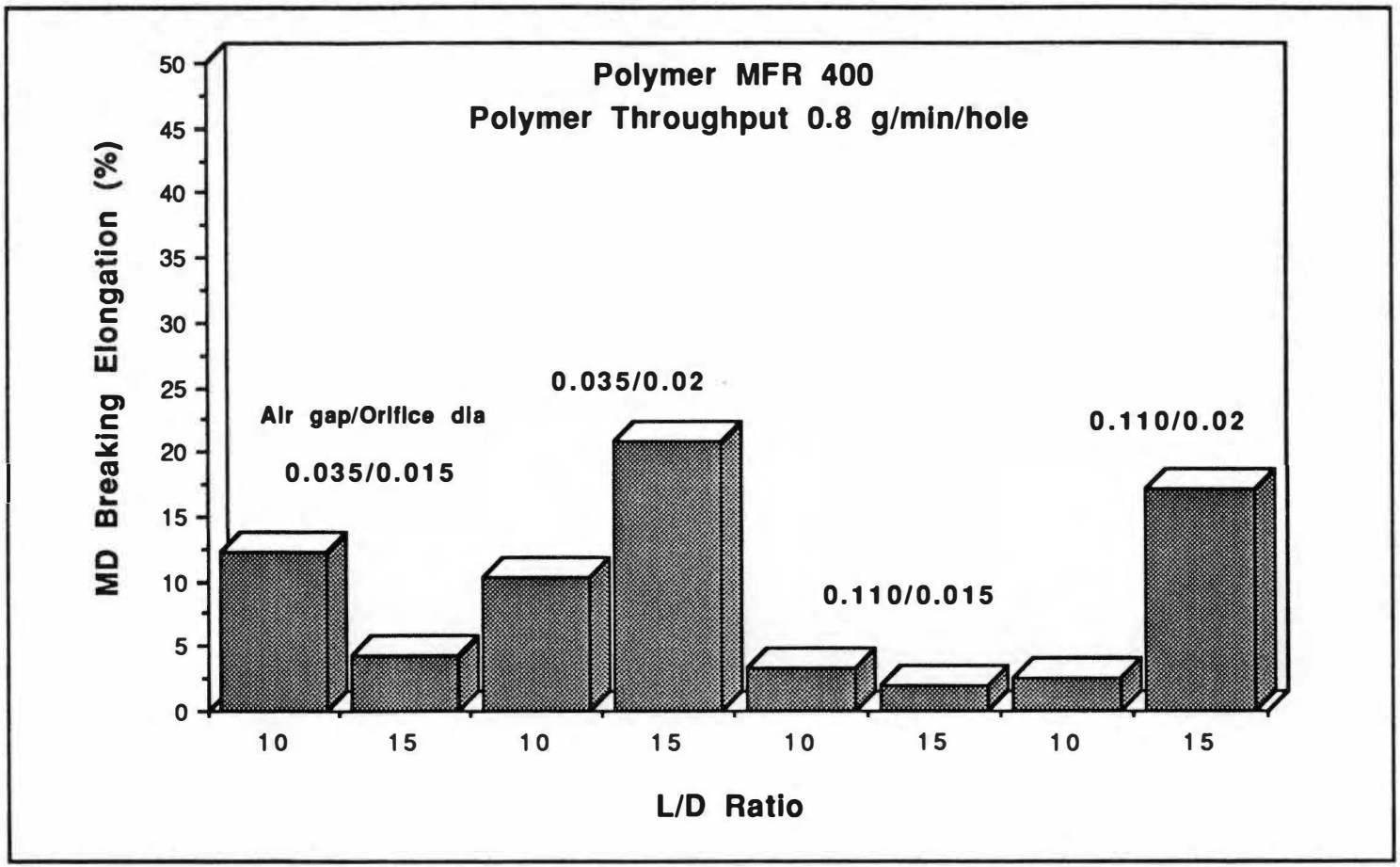


Figure 5.25 Effect of L/D ratio, orifice diameter, and air knife gap on MD breaking elongation

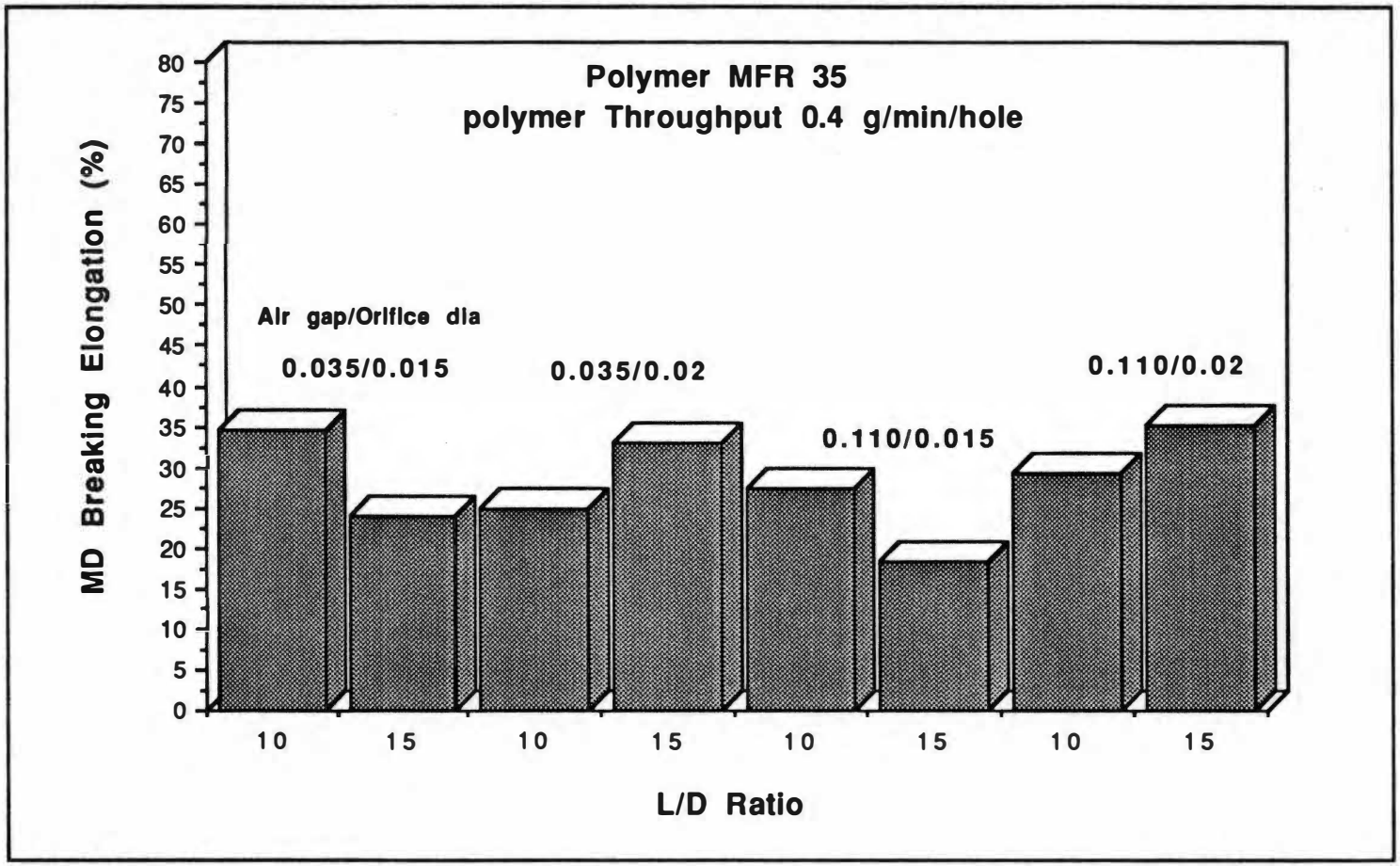


Figure 5.26 Effect of L/D ratio, orifice diameter, and air knife gap on MD breaking elongation

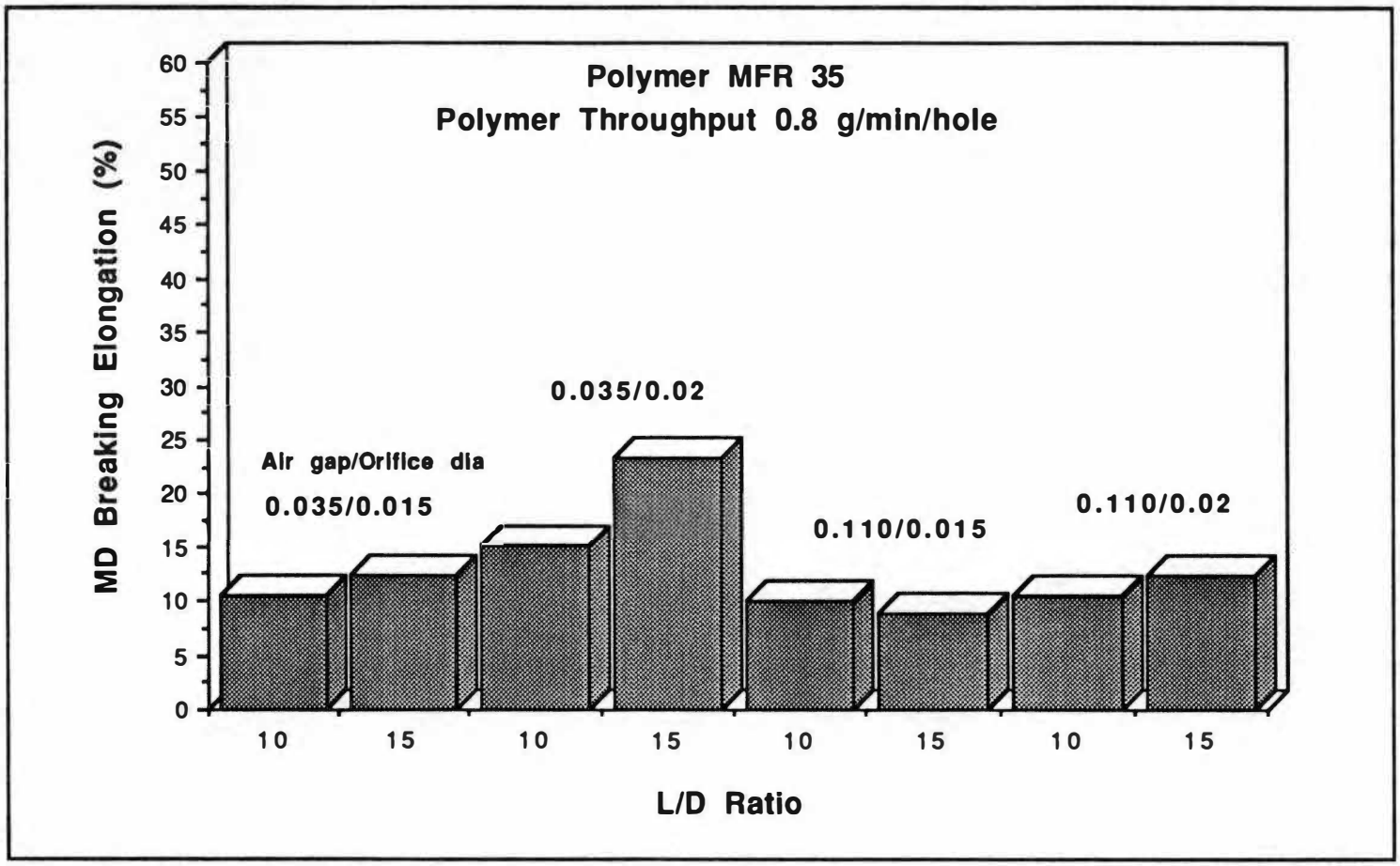


Figure 5.27 Effect of L/D ratio, orifice diameter, and air knife gap on MD breaking elongation

The air gap appears to have an independent main effect on the breaking elongation. The smaller air gap gave the higher mean breaking elongation. The effect of the MFR*polymer throughput interaction indicates that at constant MFR, for both MFRs, the elongation-to-break decreased with an increase in the throughput from 0.4 to 0.8 g/hole/min. This is quite logical, because at higher throughputs the polymer carries more heat which aids in sticking and results in a stiffer web which may not be able to stretch as much as a web formed with a throughput of 0.4 g/hole/min. At constant polymer throughput, for both the throughputs, the average elongation-to-break decreased with the increase in MFR from 35 to 400.

It can be seen from the interactive effects table of orifice size*throughput that at constant orifice size, and for both orifices, the average elongation-to-break decreased with the increase in polymer throughput from 0.4 to 0.8 g/hole/min. Whereas with the 0.4 g/hole/min throughput, the average elongation-to-break remained unaffected by the increase in the orifice size from 15 to 20 mil, and with the 0.8 g/hole/min throughput, the average elongation-to-break increased with the increase in orifice size.

With the 20 mil orifice, the mean elongation increased with the increase in L/D ratio from 10/1 to 15/1, and with the 15 mil orifice, the mean elongation-to-break decreased with the increase in L/D ratio. With 10/1 L/D, the mean elongation to break decreased with the increase in orifice size from 15 to 20 mil, whereas, with 15/1 L/D the mean elongation to break increased with the increase in orifice size.

Effect of Production Variables on the Weight Average Molecular Weight of the Web

The values of weight average molecular weight of the processed web were plotted against the L/D ratio for four different polymer MFR/ polymer throughput combinations and are shown in Figures 5.28-5.31. The corresponding data is shown in Table 5.1. From the statistical analysis it appears that hole size, L/D ratio, MFR*hole size, MFR*L/D ratio, and hole size*L/D ratio have a significant effect on the weight average molecular weight of the web.

As can be seen from the MFR* orifice size interaction relating to the weight average molecular weight of the web, for the 35 MFR resin the increase in orifice size from 15 to 20 mil has a negligible effect on the weight average molecular weight. Whereas for the 400 MFR resin the weight average molecular weight decreases notably with the increase in the orifice diameter from 15 to 20 mil. This may be due to thermal degradation as a result of the longer residence time inside the capillary with the larger orifice (at constant L/D). From the values it appears that the 35 MFR resin appears to withstand the passage through the longer capillary better than the 400 MFR resin.

The effect of MFR*L/D ratio interaction on the weight average molecular weight of the web indicates a decrease with an increase in L/D ratio from 10/1 to 15/1 at constant MFR, for both MFRs. This may be due to thermal degradation as a result of longer residence time inside the flow channel and also more shear (at constant orifice diameter). However the decrease in weight average molecular weight of the 35 MFR resin web was negligible. Here again the 35 MFR resin appears to be more resistant to decrease in weight average molecular weight compared to 400 MFR.

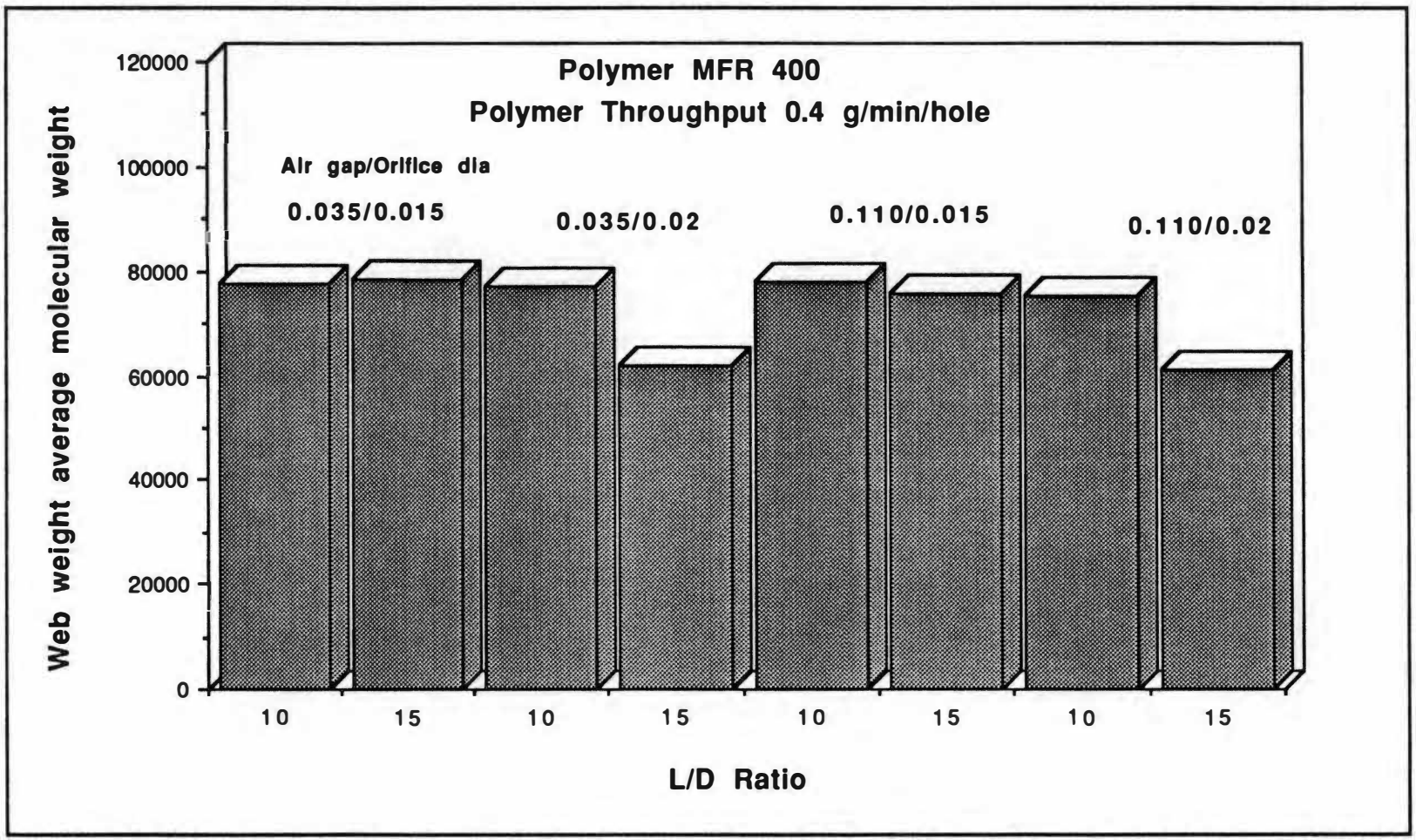


Figure 5.28 Effect of L/D ratio, orifice diameter, and air knife gap on weight average molecular weight of the web

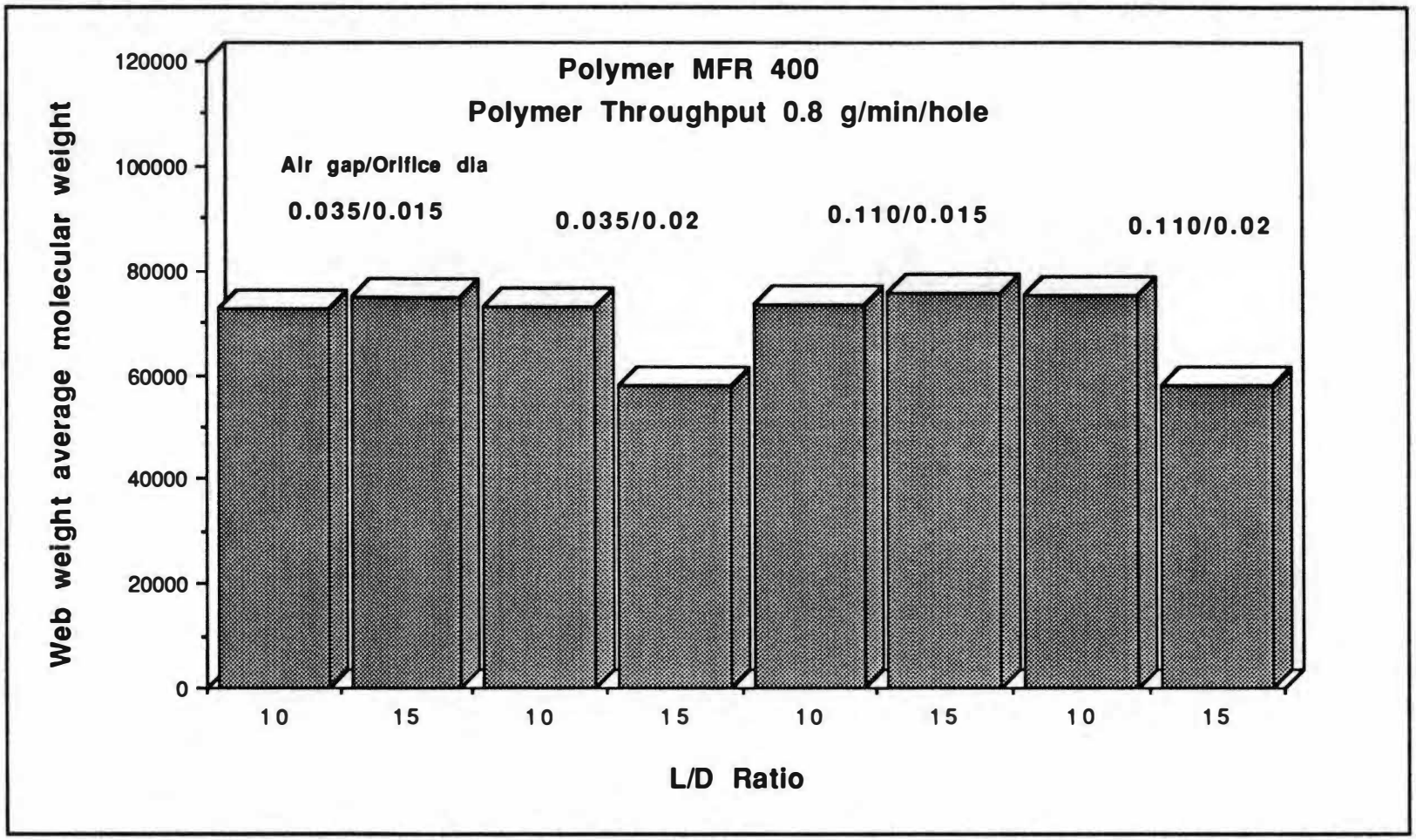


Figure 5.29 Effect of L/D ratio, orifice diameter, and air knife gap on weight average molecular weight of the web

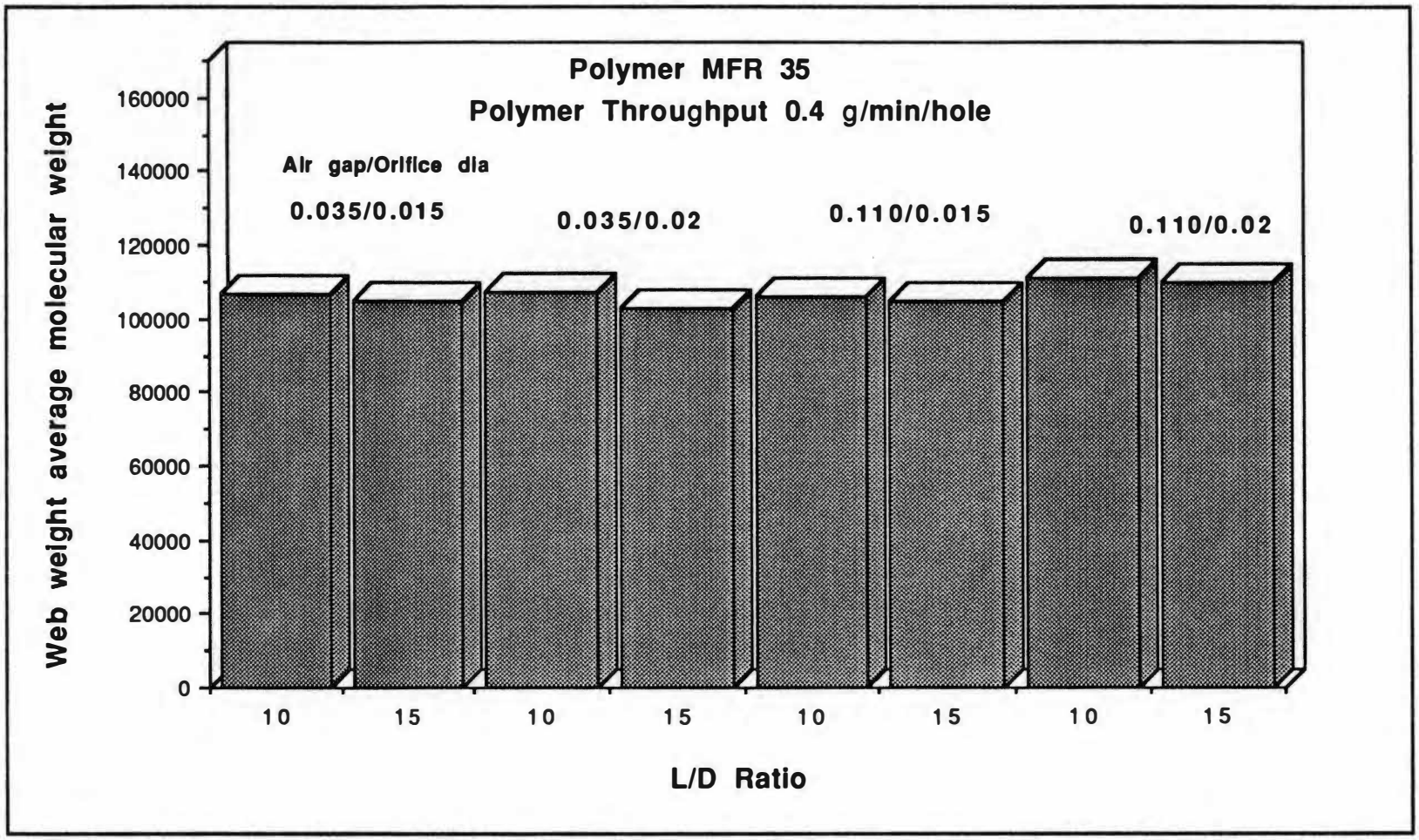


Figure 5.30 Effect of L/D ratio, orifice diameter, and air knife gap on weight average molecular weight of the web

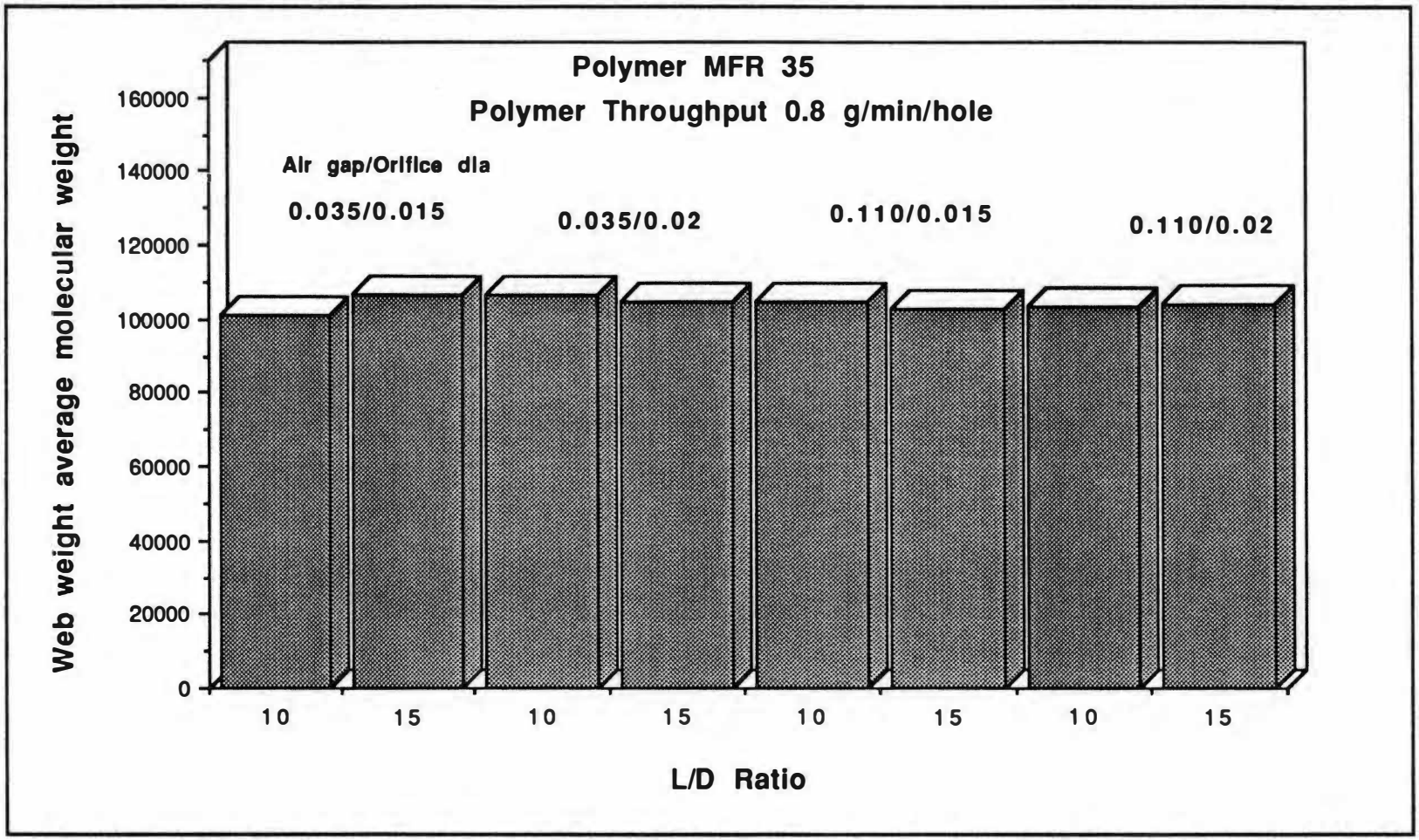


Figure 5.31 Effect of L/D ratio, orifice diameter, and air knife gap on weight average molecular weight of the web

From the orifice size*L/D ratio interaction it can be seen that for 15 mil orifice the increase in L/D ratio from 10/1 to 15/1 does not appear to have any notable effect on the weight average molecular weight. Whereas for the 20 mil orifice there is a large decrease in weight average molecular weight with an increase in L/D ratio. This phenomenon may be due to the longest residence time inside the capillary for the 20 mil 15/1 L/D combination, which in turn may have resulted in thermo-mechanical forces that the polymer could not withstand without chain cleavage. This result should be treated with caution because this interaction does not take into account the resin MFR. As indicated in Table 5.1 it is clear that only 400 MFR resin is sensitive to increase in orifice size and L/D ratio and not the 35 MFR resin. This was observed during processing and also by examining the manufactured web.

PHASE II - NOSETIP SETBACK STUDY

This study was focused primarily on the effects of nosetip setback (at constant air gap), polymer throughput rate, orifice diameter, and orifice L/D ratio at constant air-to-polymer flow rate ratio on average fiber diameter and shot level in the web.

Table 5.3 lists the average fiber diameter and shot rating of the webs obtained from all the sample runs. The analysis of the results obtained was carried out using a General Linear Models procedure on a SAS package available on the VAX mainframe computer at the University of Tennessee. The model incorporated average fiber diameter and shot rating as the responses. The production variables were resin MFR, orifice diameter, polymer throughput rate, L/D ratio, and nosetip setback. The air and the polymer temperatures were

Table 5.3

Average Fiber Diameter and Shot Rating of 650 MFR Melt Blown PP Webs

Sample No.	Sample ID*	Av. Fiber Dia (μm)	C.V. % of Fiber Dia	Shot Rating
1	0.8/20/10/+5/95.1	2.22	24.08	2
2	0.8/20/15/-39/67.6	2.67	24.5	3
3	0.4/15/10/+5/72.3	2.48	43.32	2
4	1.6/15/15/-28/74.6	2.14	25.5	3
5	2.0/15/10/+5/72.3	2.06	36.22	3
6	2.0/20/15/-39/67.6	2.6	31.41	4
7	1.2/20/10/-18/82.5	2.39	26.17	4
8	0.8/20/10/-28/71	2.49	24.18	2
9	1.6/15/15/-18/90.8	2.23	34.1	2
10	1.2/20/15/-5/91.9	2.32	23.28	3
11	1.6/15/15/-39/39.7	2.23	25.91	3
12	2.0/15/15/+5/105.4	2.19	27.00	2
13	0.4/15/15/-5/99.6	2.39	26.76	2
14	0.8/15/10/-18/52.6	1.98	33.71	2
15	1.2/15/10/-28/51.4	2.29	26.97	3
16	2.0/20/15/-18/66.9	2.56	25.19	4
17	1.2/15/15/-5/99.6	2.20	23.31	3
18	2.0/15/10/-39/39.69	2.32	29.05	4
19	1.6/20/10/-28/71	2.16	29.11	4
20	1.2/20/15/+5/96.7	2.12	26.70	2

• Nominal air gap, 31 mil.

* Polymer throughput, g/hole/min/Orifice dia, mil/L/D ratio/Setback, mil/Face gap, mil.

Table 5.3 (Contd.)

Sample No.	Sample ID*	Av. Fiber Dia (μm)	C.V. % of Fiber Dia	Shot Rating
21	0.8/15/15/-28/74.6	2.11	24.95	2
22	0.4/15/10/+5/72.3	2.35	34.27	2
23	0.4/15/10/-39/39.7	2.69	25.00	2
24	1.2/15/10/-18/52.6	2.08	24.59	2
25	1.6/15/10/-18/52.6	2.20	27.43	3
26	0.4/20/10/-5/94.5	2.40	43.80	3
27	2.0/20/10/-28/71	2.61	26.11	4
28	0.8/15/15/-5/99.6	2.58	28.13	2
29	0.4/20/10/-39/73.8	3.09	21.10	2
30	0.4/20/15/-28/66.9	3.34	20.80	3
31	0.4/20/15/-18/79	2.49	25.53	2
32	2.0/15/15/-28/74.6	2.30	28.19	4
33	1.6/20/15/+5/96.7	2.05	26.61	2
34	2.0/20/10/-5/94.5	2.55	29.74	4
35	1.2/20/10/-39/73.8	2.30	22.67	3
36	1.6/20/15/+5/96.72	2.29	26.71	2
37	0.8/20/15/-18/79	2.49	23.18	2
38	0.8/15/10/-5/77.9	2.23	75.51	2
39	1.2/15/15/-39/39.7	1.9	29.30	4
40	1.6/20/10/-5/94.5	2.24	31.65	4

• Nominal air gap, 31 mil.

* Polymer throughput, g/hole/min/Orifice dia, mil/L/D ratio/Setback, mil/Face gap, mil.

maintained constant for all the runs (520 and 500^{0}F respectively). The face gap was not separated out as a separate production variable because it was tied to the nosetip setback in that the air knives utilized were constructed in such a way that the face gap and nosetip set back were inversely collinear. That is, as the recessed setback increased the face gap decreased. The effects of orifice L/D, orifice diameter, nosetip setback, and polymer throughput rate (at constant air-to-polymer flow rate ratio) and their interactions on fiber diameter and shot level for 650 MFR PP are shown in Appendix B.

Wherever a process variable had a significant main effect on the response without any interactive effects in combination with another variable (obtained from Type III Sum of Squares in Appendix B), the main effect least square means for that particular variable was taken from the 2x2 tables of the statistical output shown in Appendix B for the purpose of determining the direction of the trend. When a process variable had a main effect as well as an interactive effect on the response, then the trend was determined by examining the interactive effect least square means from the 2x2 tables of the statistical output. Only the main effects and the two-factor interactions were included in the statistical analysis to accommodate sufficient error terms in the analysis, which is usually at least as many terms as the number of model terms.

In addition to the general linear models procedure, the fiber diameter data were analyzed using a multiple regression procedure. Since the design was fairly free of confounding variables, the data from these experiments can be used for computing the estimator coefficients and predicting a particular response. The fiber diameter data has been used to compute the estimator coefficients as shown in Appendix B, from which equations can be written showing the effect of the parameters on fiber diameter.

Effect of Production Variables on Fiber Diameter

The sample identification shown in Table 5.3 indicates the polymer throughput rate in g/hole/min, orifice diameter in mils, L/D ratio, nosetip setback in mils, and the face gap in mils. The summary of statistical analysis of the fiber diameter data shown in Table B.2 reveals that the nosetip setback, orifice diameter, and polymer throughput rate have a significant effect on the average fiber diameter of melt blown webs.

This fractional factorial study with 650 MFR PP at constant die and air temperatures and constant air to polymer ratio did not show that L/D had a statistically significant effect on fiber diameter as did phase I with the 35 and 400 MFR PP resins at different die and air temperatures and die geometry conditions. Phase I showed that the higher L/D ratio has an overall positive effect in reducing fiber diameter with 35 and 400 MFR PP resins at different temperatures and die geometry conditions. Although L/D had no notable effect on fiber diameter with the 400 MFR resin at 0.4 g/hole/min, it had a statistically significant and notable effect on producing finer fibers with higher L/D ratios at 0.8 g/hole/min. With the 35 MFR resin at 0.4 and 0.8 g/hole/min, increasing L/D also had an overall positive effect in reducing fiber size. However, the fact that changing from a 15 to 20 mil orifice diameter had little notable effect on fiber diameter indicates that the maximum swell diameter is not as important for producing fine fibers as originally believed [16].

Recent shear viscosity studies using sensitive pressure drop measurements indicate that the magnitude of decrease in melt shear viscosity with increasing L/D ratio at constant orifice diameter was higher as the resin MFR

decreased. For example, the decrease in shear viscosity for 35 MFR resin will be larger than for a 800 MFR resin. Also the lower MFR resins (35, 400) exhibit a higher viscosity to start with, and when the L/D ratio is increased they show a higher drop in viscosity. In contrast, the higher MFR resins (650, 800, etc.) have a very low viscosity to begin with and therefore the change in viscosity with increase in L/D ratio is small compared to low MFR resins. This is a probable reason as to why the 650 MFR did not show a statistically significant effect of L/D ratio on fiber diameter.

Figures 5.32-5.35 illustrate the effect of nosetip setback on average fiber diameter at each of the different, orifice diameters (15 and 20 mils) and L/D ratios (10 and 15). These results are interpreted and discussed in the following sections. The amount of fly was not taken into consideration. Generally the fly was not noticeable until after 1.2 g/hole/min when excessive fly was generated.

Effect of Polymer Throughput Rate on Fiber Diameter. From the main effects table for the effect of polymer throughput on average fiber diameter shown in Appendix B it can be seen that the average fiber diameter decreased from 2.7 to as low as 2.2 μm with an increase in polymer throughput rate. This was statistically significant. Although this result appears surprising initially, it should be remembered that the air-to-polymer flow rate ratio was maintained constant at all polymer throughput rates. The increased heat at higher polymer throughput rates probably resulted in reduced quenching thereby producing finer fiber diameters at higher polymer throughput rates, provided the air-to-polymer flow rate ratio was maintained constant. Also looking at Table 5.4 showing the primary air velocity and momentum data it appears that as the polymer throughput rate was increased from 0.4 to 1.2 g/hole/min, overall the air velocity

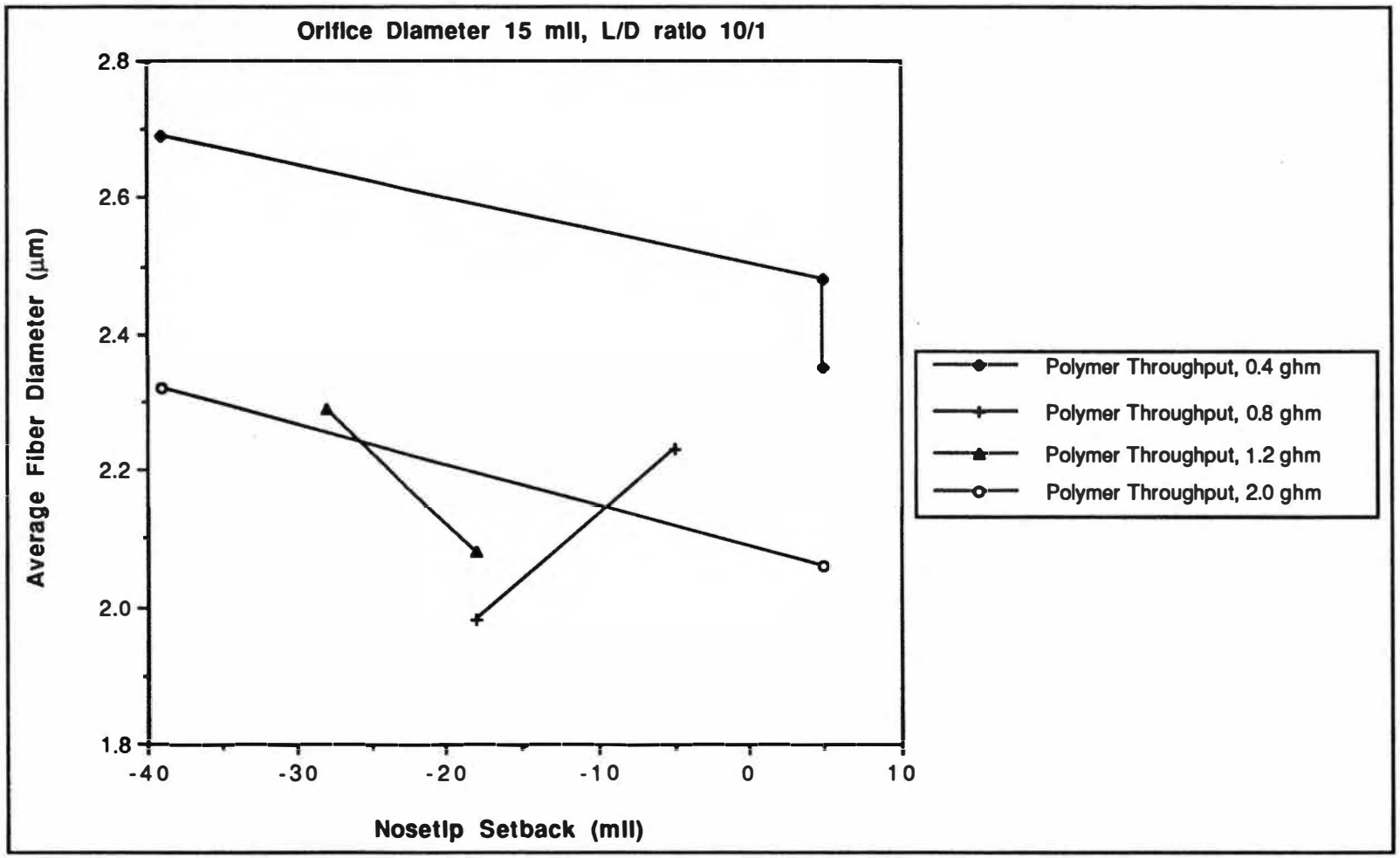


Figure 5.32 Effect of nosetip setback on average fiber diameter

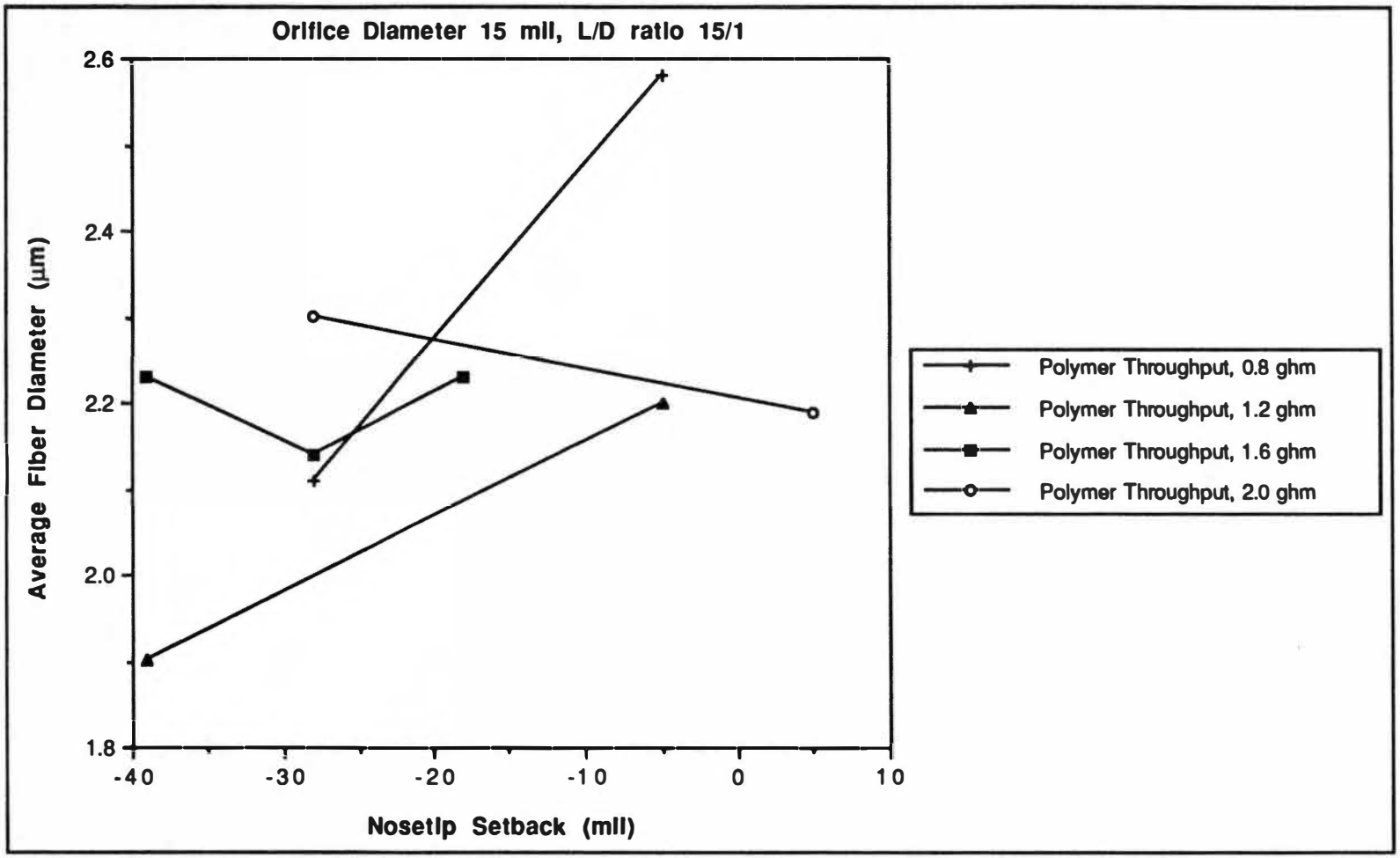


Figure 5.33 Effect of nosetip setback on average fiber diameter

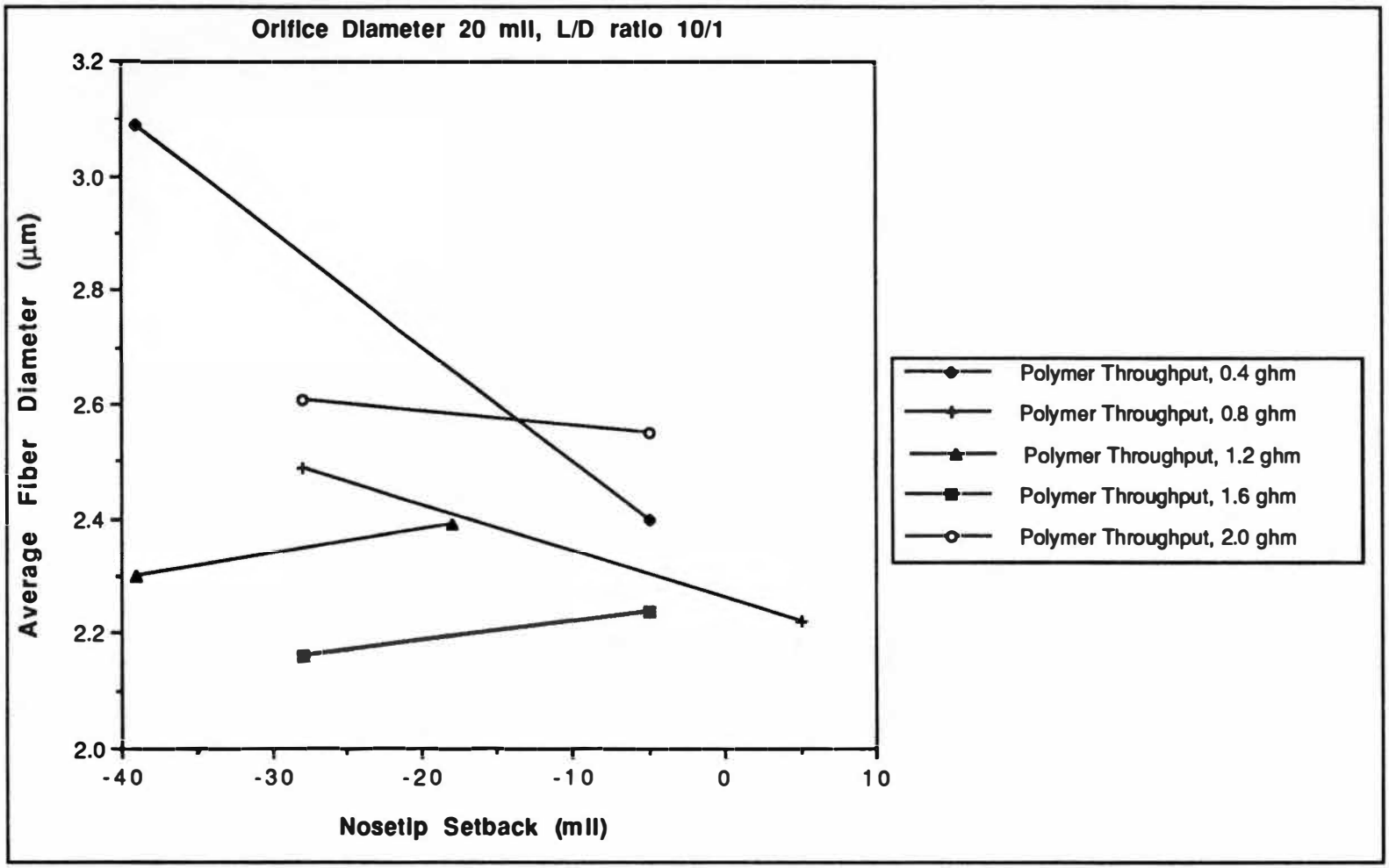


Figure 5.34 Effect of nosetip setback on average fiber diameter

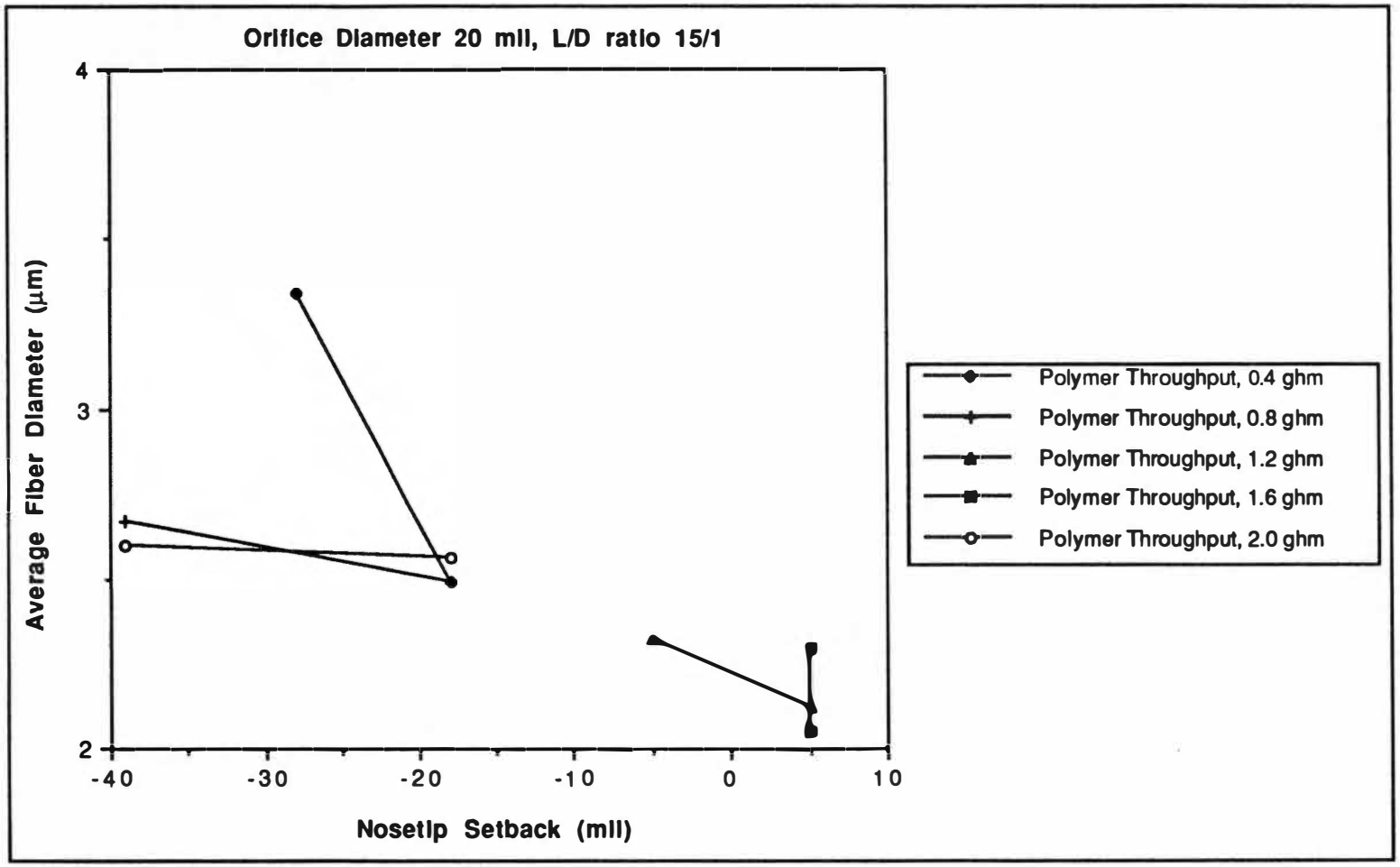


Figure 5.35 Effect of nosetip setback on average fiber diameter

Table 5.4 Actual CFM and Air Velocity Data for 0.4, 0.8, and 1.2 g/hole/min Polymer Throughput rates - Phase II

SAMPLE NO.	SAMPLE ID *	SCFM	ACFM	ACT. FACE GAP (MILS)	AIR SLOT AREA (FT^2)	AIR+ VELOCITY (FT/SEC)	AIR MOMENTUM LBS-FT/SEC	MOMENTUM/ GRAM of RESIN
1	0.8/20/10/+5/95.1	200	195.0	95.1	0.005282	614	154	95.5
2	0.8/20/15/-39/67.6	200	188.2	67.6	0.003756	835	209	129.6
3	0.4/15/10/+5/72.3	100	144.9	72.3	0.004018	601	75	93.0
7	1.2/20/10/-18/82.5	300	214.5	82.5	0.004586	779	292	120.1
8	0.8/20/10/-28/71	200	175.8	71.0	0.003944	740	185	114.7
10	1.2/20/15/-5/91.9	300	208.9	91.9	0.005106	682	256	105.8
13	0.4/15/15/-5/99.6	100	149.0	99.6	0.005535	449	56	69.4
14	0.8/15/10/-18/52.6	200	195.0	52.6	0.002922	1112	278	172.3
15	1.2/15/10/-28/51.4	300	193.8	51.4	0.002853	1132	425	175.6
17	1.2/15/15/-5/99.6	300	214.5	99.6	0.005535	644	242	100.0
20	1.2/20/15/+5/96.7	300	193.8	96.7	0.005373	599	225	93.0
21	0.8/15/15/-28/74.6	200	175.8	74.6	0.004146	706	177	109.7

+ Nominal air gap, 31 mil

* Polymer throughput, g/hole/min/Orifice dia, mil/L/D ratio/Setback, mil/Face gap, mil. + Air temperature at die and stagnation pressure in die manifold were used for calculation.

Table 5.4 (Contd.)

SAMPLE NO.	SAMPLE ID *	SCFM	ACFM	ACT. FACE GAP (MILS)	AIR SLOT AREA (FT^2)	AIR+ VELOCITY (FT/SEC)	AIR MOMENTUM LBS-FT/SEC	MOMENTUM/ GRAM of RESIN
22	0.4/15/10/+5/72.3	100	144.9	72.3	0.004018	601	75	93.0
23	0.4/15/10/-39/39.7	100	137.5	39.7	0.002205	1039	130	161.2
24	1.2/15/10/-18/52.6	300	198.6	52.6	0.002922	1154	433	178.9
26	0.4/20/10/-5/94.5	100	146.5	94.5	0.005247	465	58	71.9
28	0.8/15/15/-5/99.6	200	195.0	99.6	0.005535	587	147	91.1
29	0.4/20/10/-39/73.8	100	141.1	73.8	0.004100	573	72	89.3
30	0.4/20/15/-28/66.9	100	147.3	66.9	0.003717	633	79	97.9
31	0.4/20/15/-18/79	100	147.3	79.0	0.004389	560	70	86.8
35	1.2/20/10/-39/73.8	300	189.3	73.8	0.004100	770	289	119.4
37	0.8/20/15/-18/79	200	198.6	79.0	0.004389	755	189	117.2
38	0.8/15/10/-5/77.9	200	195.0	77.9	0.004328	751	188	116.5
39	1.2/15/15/-39/39.7	300	189.3	39.7	0.002050	1431	537	221.9

+ Nominal air gap, 31 mil

* Polymer throughput, g/hole/min/Orifice dia, mil/L/D ratio/Setback, mil/Face gap, mil. + Air temperature at die and stagnation pressure in die manifold were used for calculation.

and hence the momentum increased. Furthermore the momentum/g of resin throughput for 0.4, 0.8, and 1.2 g/hole/min increased on the average as the polymer throughput increased at constant air-to-polymer flow rate ratio, because of the increased air velocity (overcoming the effect of higher polymer throughput).

Perhaps the increased heat and momentum/g of resin at higher polymer throughput rates were the main factors contributing to the slight reduction in average fiber diameter. It can be said with fair accuracy that the average fiber diameter was maintained at all polymer throughput rates ranging from 0.4 to 2.0 g/hole/min, provided the air-to-polymer flow rate ratio was held constant at each polymer throughput rate. Another minor factor is the fact that as the screw speed increases with an increase in polymer throughput rate, the shear viscosity of the molten polymer is most likely to decrease. The drop in shear viscosity with increasing polymer throughput rate may have had a very slight effect on fiber diameter, contributing to slightly smaller average fiber diameter overall, as the polymer throughput was increased.

Effect of Nosetip Setback on Fiber Diameter. Upon reviewing the statistics associated with the p-value in Appendix B, for the effect of nosetip setback on fiber diameters it appears that the effect of nosetip setback on average fiber diameter was not significant. The work of Mancil Milligan at UTK has revealed that streamline drag contributes only a small fraction of the total draw-down, and that most of the attenuation was primarily due to form drag. The greater the setback, the longer will be the length of the polymer jet which remains straight, since the high speed photography studies by Milligan and Haynes [12] have confirmed that the molten polymer jet exhibits almost no vibrations until the filament strands are several centimeters forward of the knife edges.

It is most noteworthy that the average fiber diameter changed very little with nosetip setbacks ranging from -39 to +5 mils in that face gap which affects air jet exit velocity was directly coupled by geometry to nosetip setback. For example with the 15 mil diameter tip and 10/1 L/D, at nosetip setbacks of -39 and +5 mils, the face gaps are 40 and 72 mils, respectively. Consequently, the air jet velocity with the 40 mils face gap/-39 mils setback is approximately twice that of the 72 mils face gap/+5 mils setback geometry.

The plots of average fiber diameter versus the nosetip setback shown in Figures 5.32-5.35 indicate that there was no clear trend with respect to the effect of nosetip setback on average fiber diameter.

Effect of Orifice Diameter on Fiber Diameter. The effect of orifice diameter on average fiber diameter is evident from the 2x2 main effects table in Appendix B. The increase in orifice diameter from 15 to 20 mil resulted in a small but statistically significant increase in average fiber diameter. This is in contrast to the findings with 35 and 400 MFR PP resins during phase I, in which an increase in orifice diameter resulted in a small but statistically significant decrease in the average fiber diameter. The overall conclusion from these studies is that changing orifice diameter from 15 to 20 mils for 650 MFR PP resin has no effect of practical consequence on fiber diameter. Wadsworth et al. [20] have also shown the minimal differences in fiber diameter that were obtained in comparison of 10 and 15 mil orifices. Similarly, Bernd Kunze noted in a private discussion in 1991, that Reifenhauser had found that smaller fiber diameters were not obtained by decreasing orifice diameter [43].

Since the molecular weight of 650 MFR resin is much less compared to 35 or 400 MFR resins, it is possible that excessive degradation may have occurred

with the larger orifice diameter which would have a correspondingly greater capillary length, thereby resulting in premature breakage of the molten polymeric jet even before the attenuation was complete. Evidence from the Gel Permeation Chromatography (GPC) studies conducted during Phase I indicated that the higher MFR resin (400) was more sensitive to longer orifice length than the lower MFR resin (35). Additional evidence in support of the above theory can be found in the 2x2 main effects table for the effect of orifice diameter on shot generation. The larger orifice resulted in greater amount of shot, which may be probably due to fiber breakage in the hot attenuation zone.

Effect of Production Variables on Shot Generation

The statistical analysis of shot generation data shown in Table 5.3 indicates that the polymer throughput rate, orifice diameter, nosetip setback, and orifice L/D ratio*nosetip setback have a significant effect on the amount of shot formation. Figures 5.36-5.39 graphically illustrate the effect nosetip setback has on shot formation with each of the different orifice sizes (15 and 20 mils) and L/D ratios (10 and 15).

Effect of Polymer Throughput on Shot Generation. From the 2x2 tables for the effect of polymer throughput on shot generation, shown in Appendix B it can be seen that increasing the polymer throughput rate increases the amount of shot generated. In spite of the fact that the air-to-polymer flow rate ratio was maintained constant for all polymer throughput rates, the shot increased with an increase in polymer throughput rate. As seen earlier the average fiber diameter decreased with the increase in polymer throughput rate. Thus it appears that the

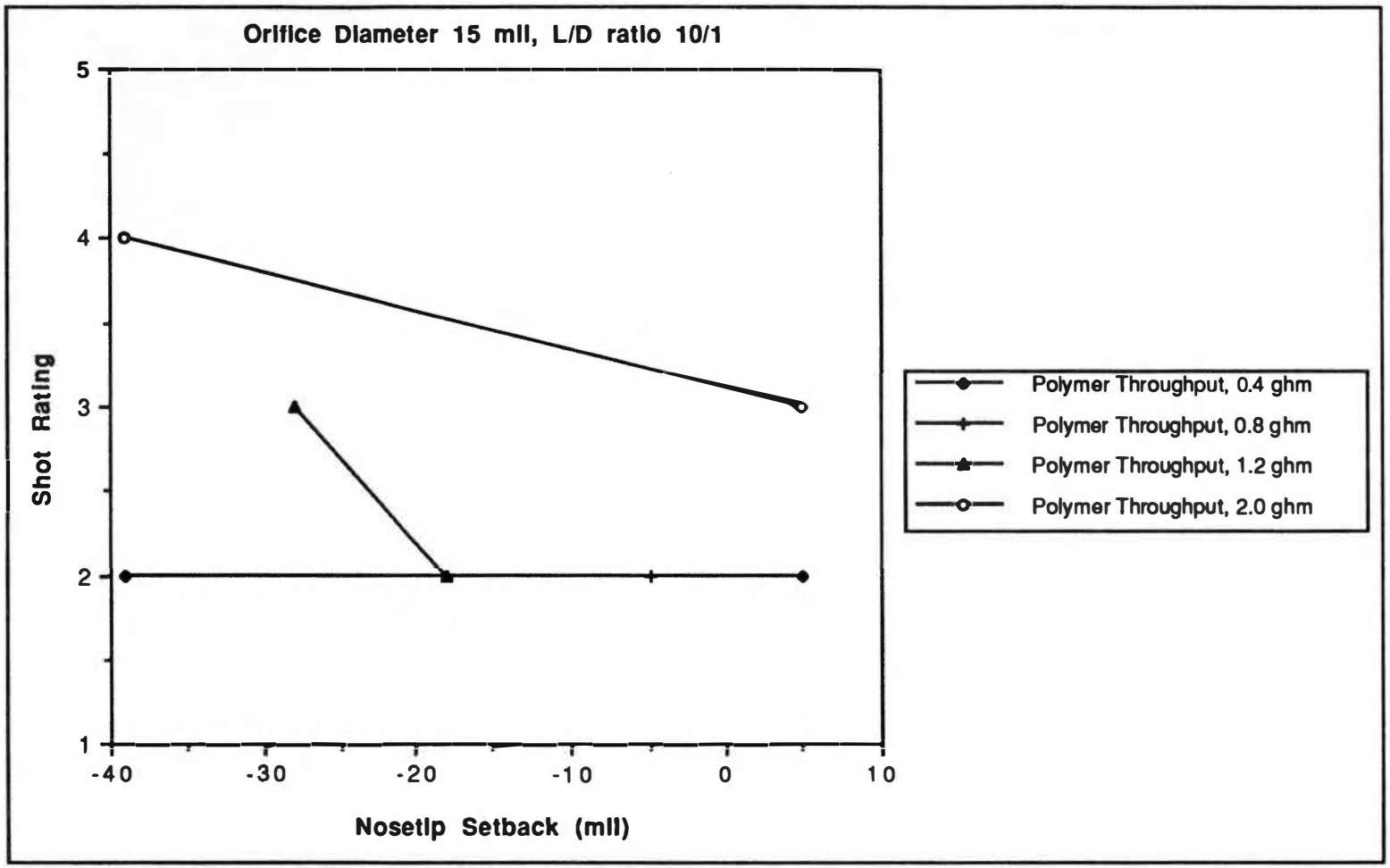


Figure 5.36 Effect of nosetip setback on shot

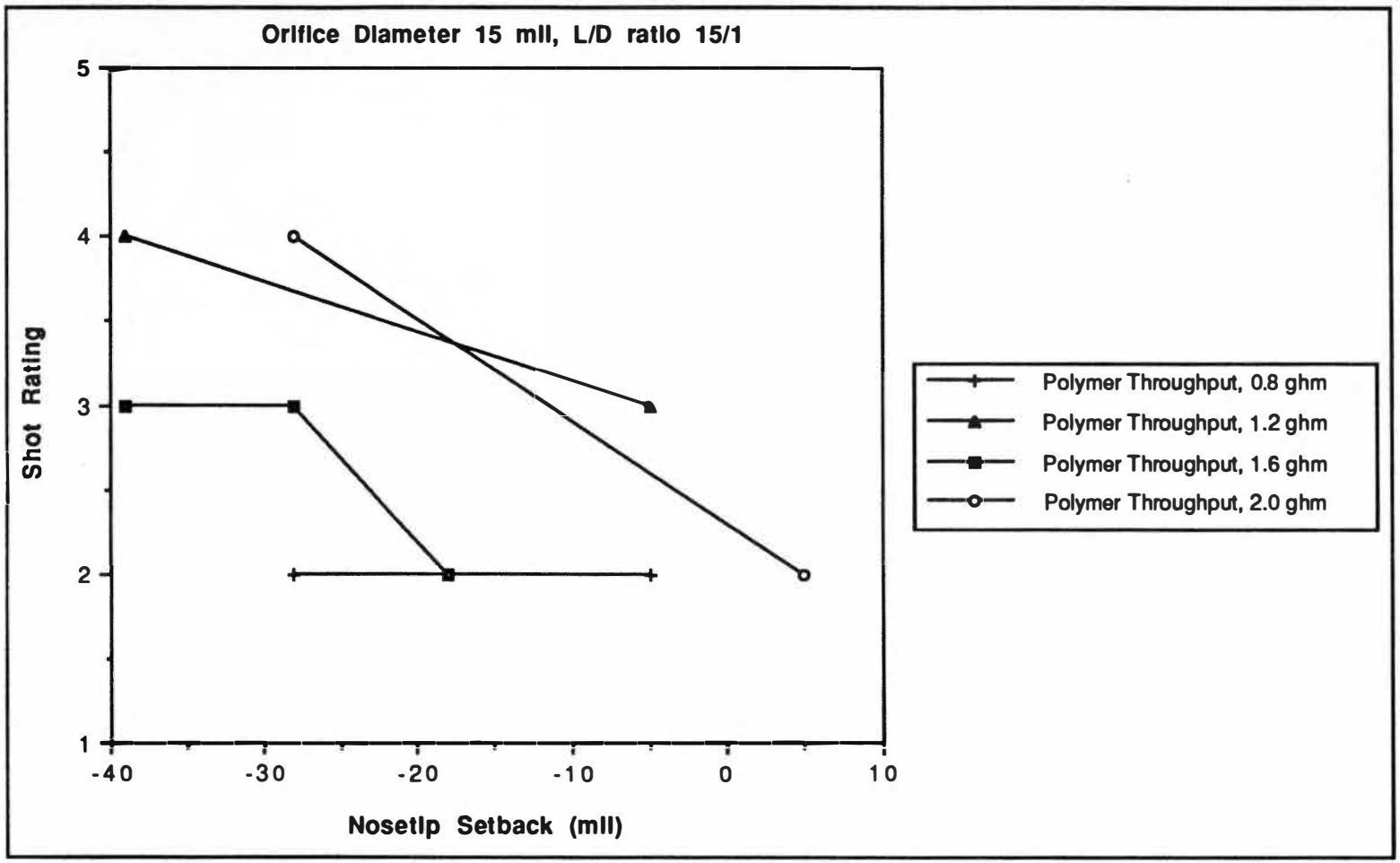


Figure 5.37 Effect of nosetip setback on shot

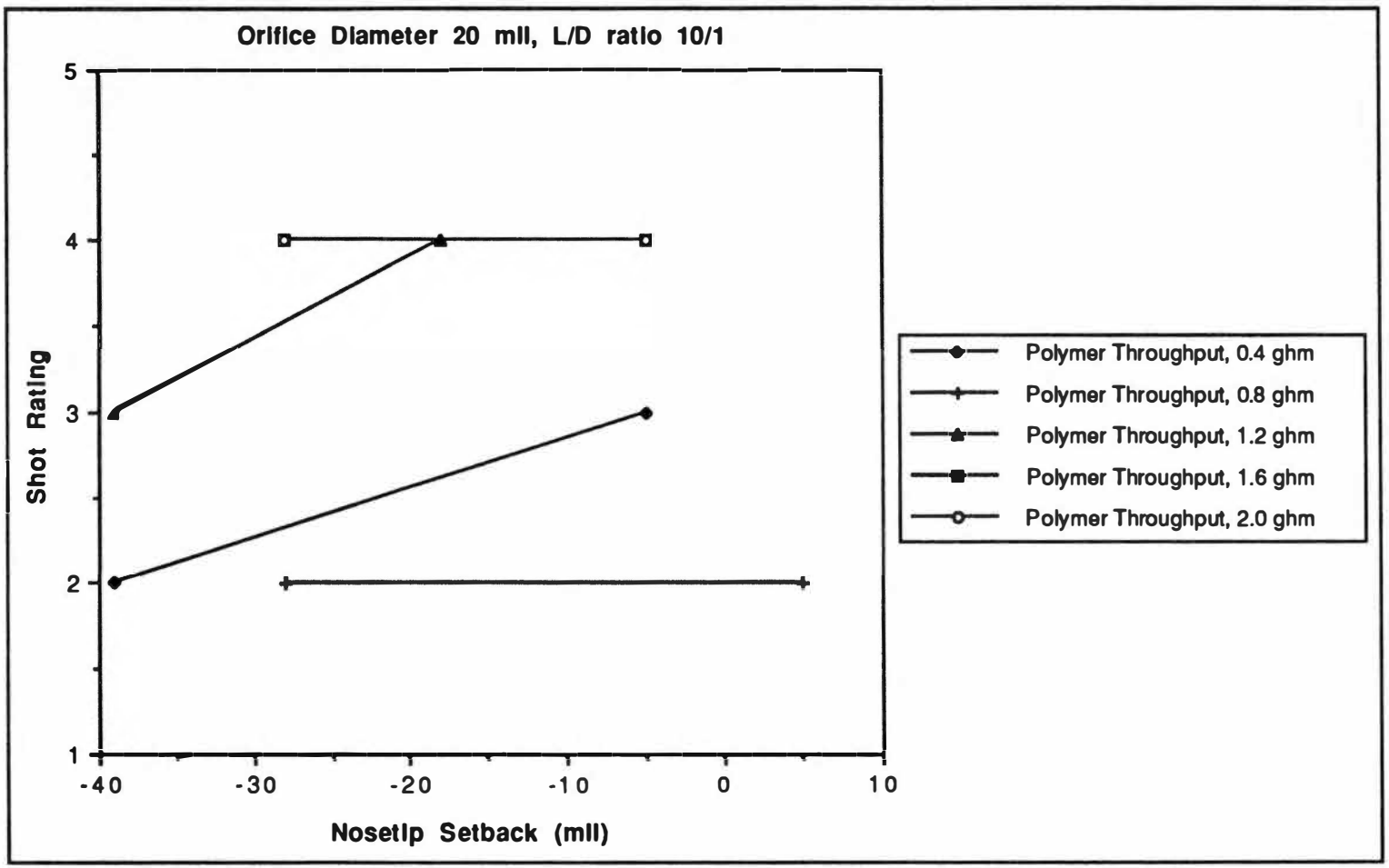


Figure 5.38 Effect of nosetip setback on shot

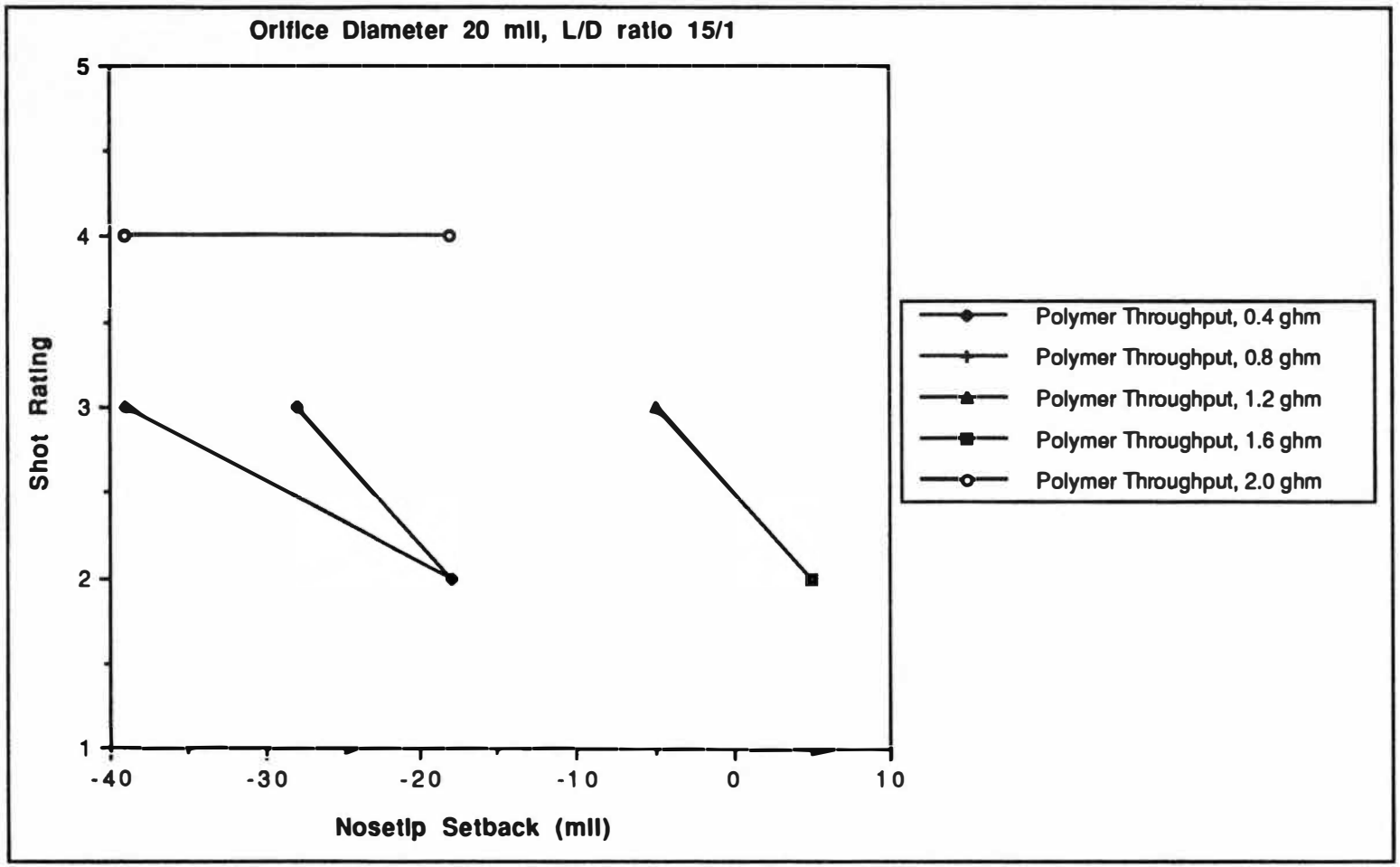


Figure 5.39 Effect of nosetip setback on shot

heat in the fibers does not get removed to the same extent at higher polymer throughput rates. The slower quenching could contribute to more shot by causing premature breakage of filaments and also to the deposition of the filaments on the collector which are still molten or which have enough heat to fuse to other fibers.

The plots of shot rating versus nosetip setback shown in Figures 5.36-5.39 support the results obtained from the statistical analysis. The plots are not comprehensive, since a fractional factorial experimental design was used. There were no corresponding points for all nosetip setbacks at each of the different polymer throughput rates.

Effect of Orifice Diameter on Shot Generation. As the orifice diameter increased from 15 to 20 mil, for both L/D ratios, the mean shot level increased. This may have been due to the increase in premature fiber breakage in the hot attenuation zone brought about by the possible increased degradation of the resin (650 MFR) at larger orifice diameters (which give rise to longer capillary lengths). Also, the heat would dissipate more slowly from the larger filaments exiting the orifices and would reduce the quenching rate. From the 2x2 tables in Appendix B it can be seen that the increase in nosetip setback resulted in the increase in the level of shot generated except for a few discrepancies. It is possible that longer heat exposure behind the air knives may contribute to shot by causing the filaments to be more susceptible to premature breakage. It is also possible that the hotter filaments may fuse together forming shot on the collector. Although the melt and primary air temperatures were held constant for all of the runs the effective heat transfer between the polymer jet and the attenuating air, in the proximity of the air jet exit is likely to be different for different setbacks.

Because of the way in which the air knives were constructed, as the setback was increased the face gap decreased proportionately which would increase the air jet exit velocity and thereby promote premature filament breakage. Finally, the more narrow face gap with increasing setback would increase the likelihood of the filaments colliding with the edges of the air knives causing shot and spitters (large shot).

Effect of Nosetip Setback on Shot Generation.

As shown in Figures 5.36-5.39, with the 20 mil orifice nosetip and the 15/1 L/D and the 15 mil die tip with both 10/1 and 15/1 L/D configurations, the degree of shot decreased as the setback changed from highly recessed to positive. With the 15 mil orifice diameter and 10/1 L/D, the level of shot either remained the same or increased with this type of change in setback.

Effect of Orifice L/D Ratio*Nosetip Setback on Shot Formation. The statistical analysis shown in Appendix B indicated a significant interaction of L/D ratio*setback on shot generation. But the 2x2 interactive effects table for L/D ratio*nosetip setback does not indicate a consistent trend. The complexity of this interaction might have masked any real trends. The orifice L/D ratio is likely to contribute towards the melt shear viscosity both by the pure shear thinning nature of polymer melts and degradation effects (because of the differences in residence time inside the capillary) and their interactions. This in combination with changing face gaps (hence different primary air exit velocities) at different nosetip setbacks may have complicated the effect of this interaction on the response, thereby not showing a consistent trend.

Effect of Primary Air Velocity and Momentum on Fiber Diameter and its Variability

The velocity of primary air is an important parameter affecting the draw-down of exiting molten polymer jets from the orifice. Air velocity creates a drag force on the filaments and also likely to affect the quenching process. The basic quenching mechanism is through the suction of ambient air (secondary air) by the expanding free flow jet of primary air exiting the air knives. The velocity at which the primary air moves through the immediate vicinity of the die will decide the velocity at which the ambient air rushes in (induced draft). If the primary air velocity is higher, the secondary air will be sucked in faster. It is essential to bear in mind that the convective heat transfer coefficient between the hot polymer streams and ambient air being sucked in increases with increasing velocity of rushing ambient air. It is very likely that the increased heat transfer coefficient arising from faster moving secondary air results in increased quenching rate thereby cooling the polymeric jets in a shorter time compared to slower moving secondary air. Therefore it must be borne in mind that higher primary air velocities (at constant mass flow rate of air) in addition to increasing the drag on the filament also may cool the polymer strands in a shorter time. The exact heat transfer characteristics will depend on primary air velocity, its temperature, the temperature of polymer melt, and the ambient air temperature. Also any effort to study the effect of velocity on fiber diameter in melt blowing must sort the data according to polymer throughput rates so that meaningful conclusions can be reached.

Most of the fiber diameter data obtained during the course of this research indicates that changes in primary air velocity (at constant mass flow rate) up to as

much as 200% produced little effect in terms of diameter changes. The above argument may partly explain this phenomena. The web bursting strength data shown in the statistical analysis of Phase I of this research and in Table 5.3 of the nosetip angle study (Phase III) lend credibility to the above argument that polymer strands cool faster at higher primary air velocities with other conditions remaining constant. The smaller air gap (higher primary air velocity) gave a higher bursting strength, indicating less thermal sticking between the filaments and hence greater load sharing. As the air gap gets larger the quenching rate is likely to decrease, thereby holding the filaments hotter for a longer period of time resulting in greater thermal sticking and hence lower bursting strength (because of poor load sharing between individual fibers).

Figures 5.40-5.45 show the effect of primary air momentum on average fiber diameter and C.V.% of fiber diameter. Table 5.4 shows the primary air velocity, momentum, and momentum/g of resin throughput calculated for the trials in Phase II (setback study) of this research. For actual volumetric flow rate and velocity calculations, primary air temperature at the die and stagnation pressure in the air manifold were used. Each plot has been sorted according to the polymer throughput rate. Polymer throughput rates of 1.6, and 2.0 g/hole/min could not be used because of the lack of stagnation pressure measurements at the die for air flow rates corresponding to those throughputs. Another criteria for these plots was the existence of at least two fiber diameter values at any particular nosetip setback for a given polymer throughput rate. As evident from Figures 5.40-5.43, overall the average fiber diameter decreased with an increase in the momentum of primary air. This result was logical because at greater momentum more force was imparted to the polymer jets and hence smaller average fiber diameters. It is interesting to note that the reduction in fiber

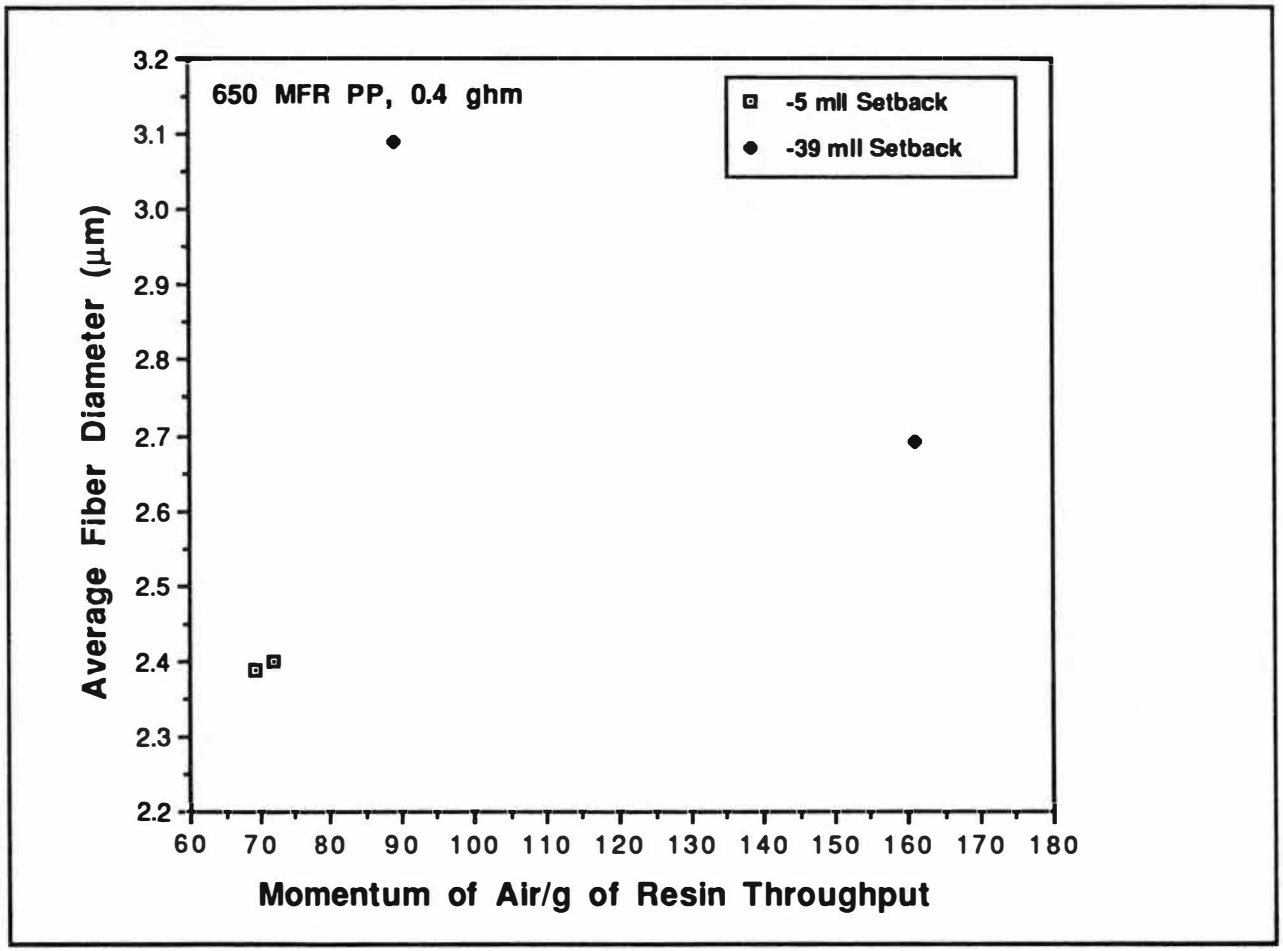


Figure 5.40 Effect of primary air momentum on average fiber diameter

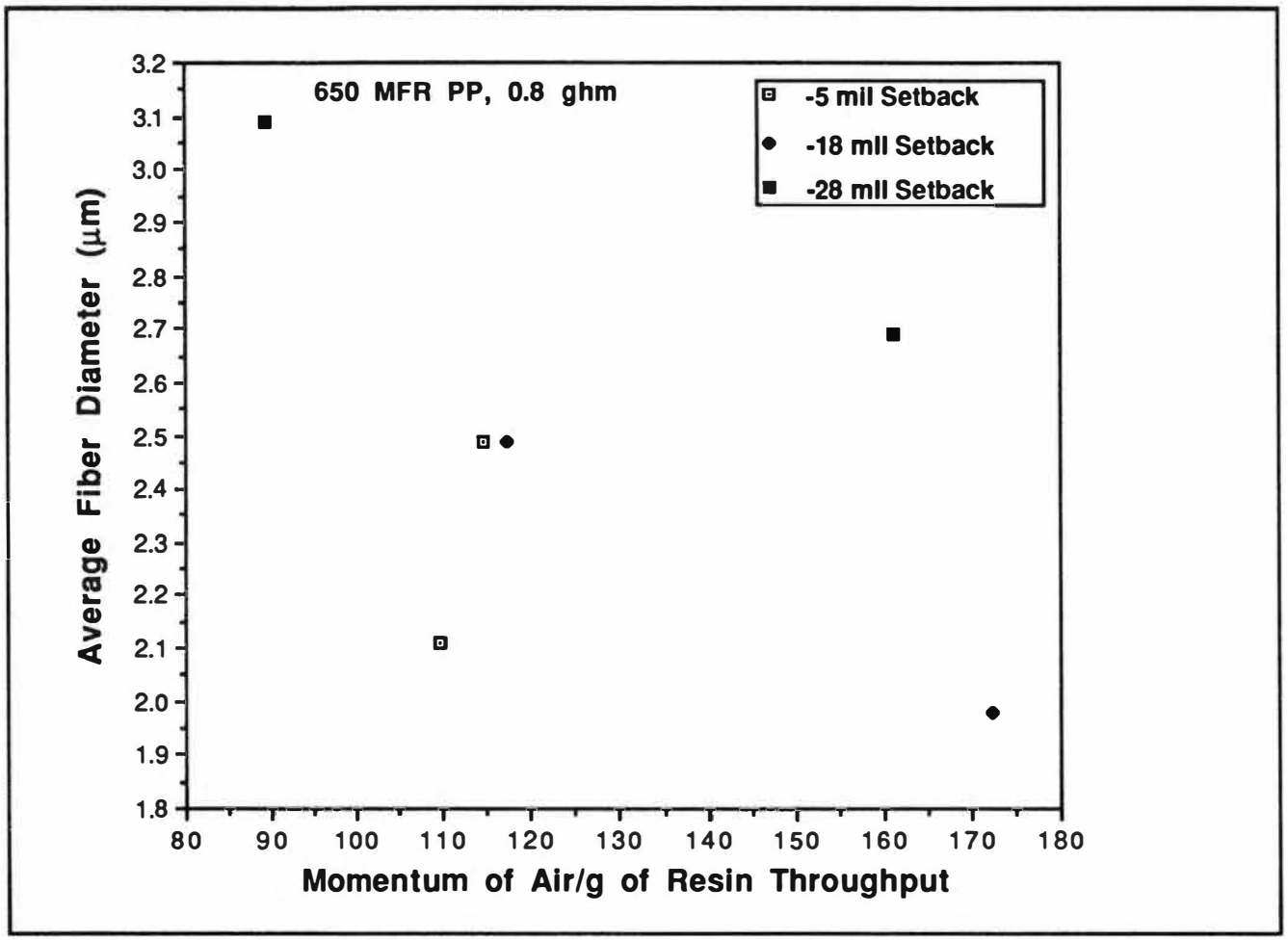


Figure 5.41 Effect of primary air momentum on average fiber diameter

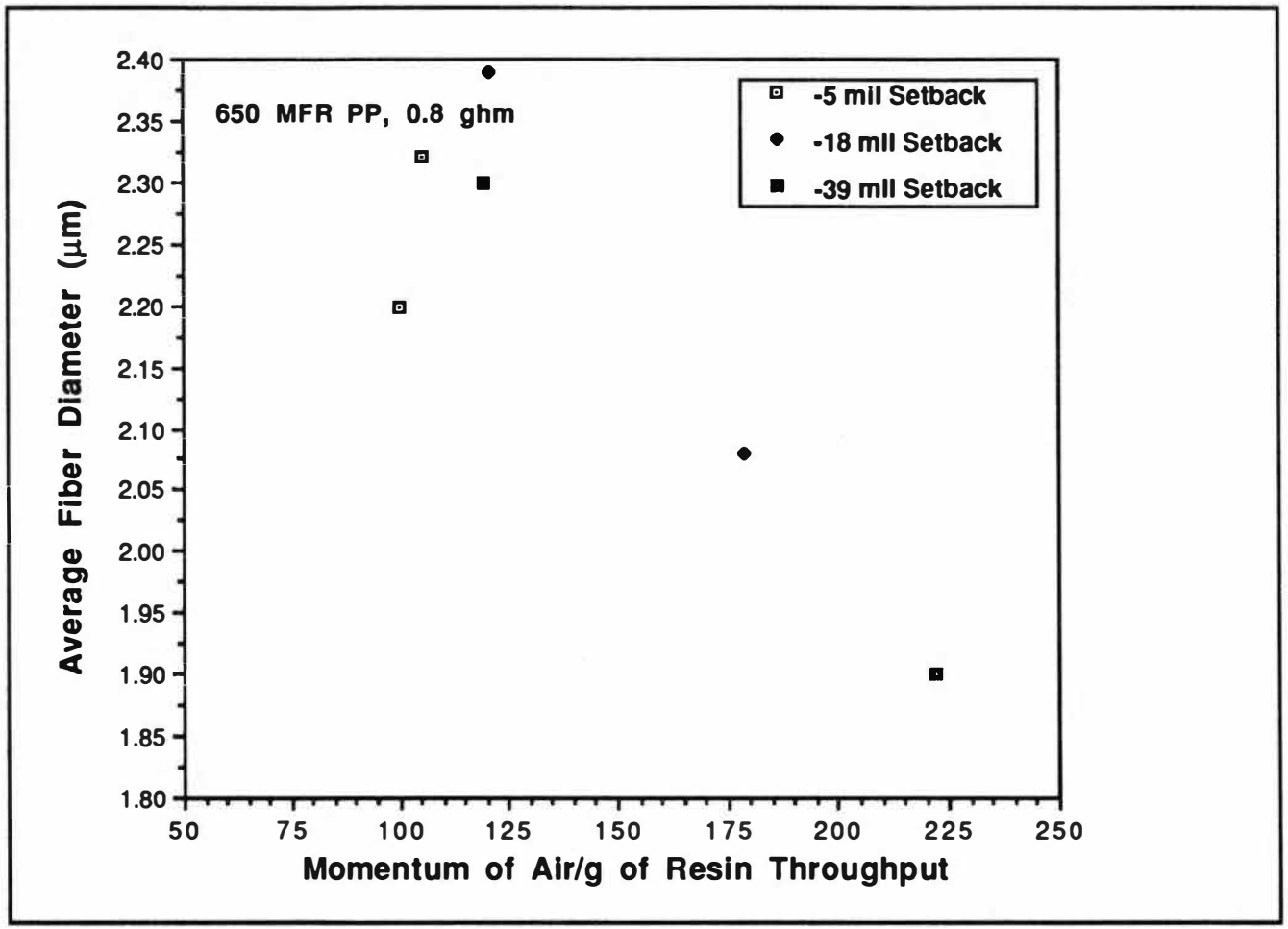


Figure 5.42 Effect of primary air momentum on average fiber diameter

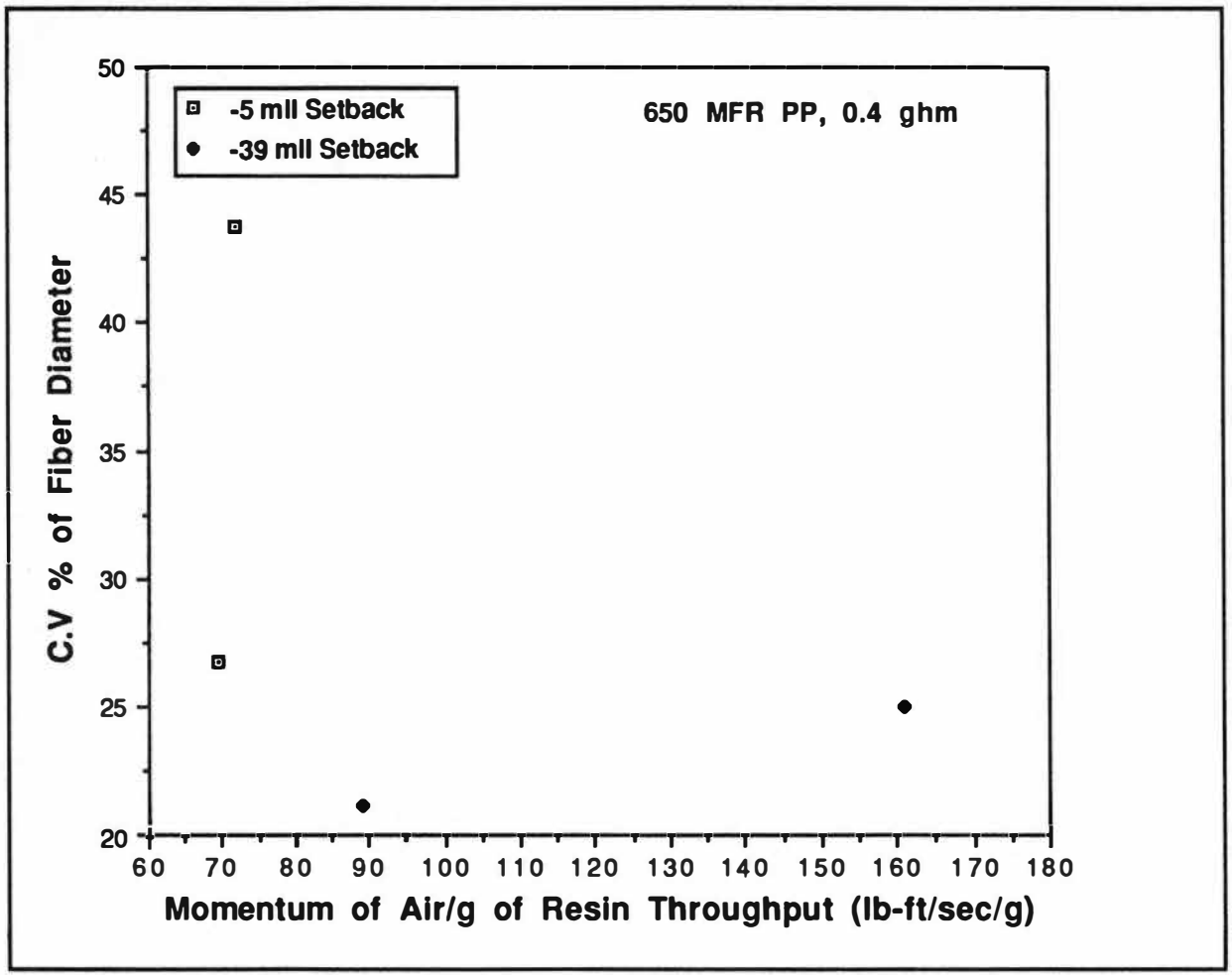


Figure 5.43 Effect of primary air momentum on C.V% of fiber diameter

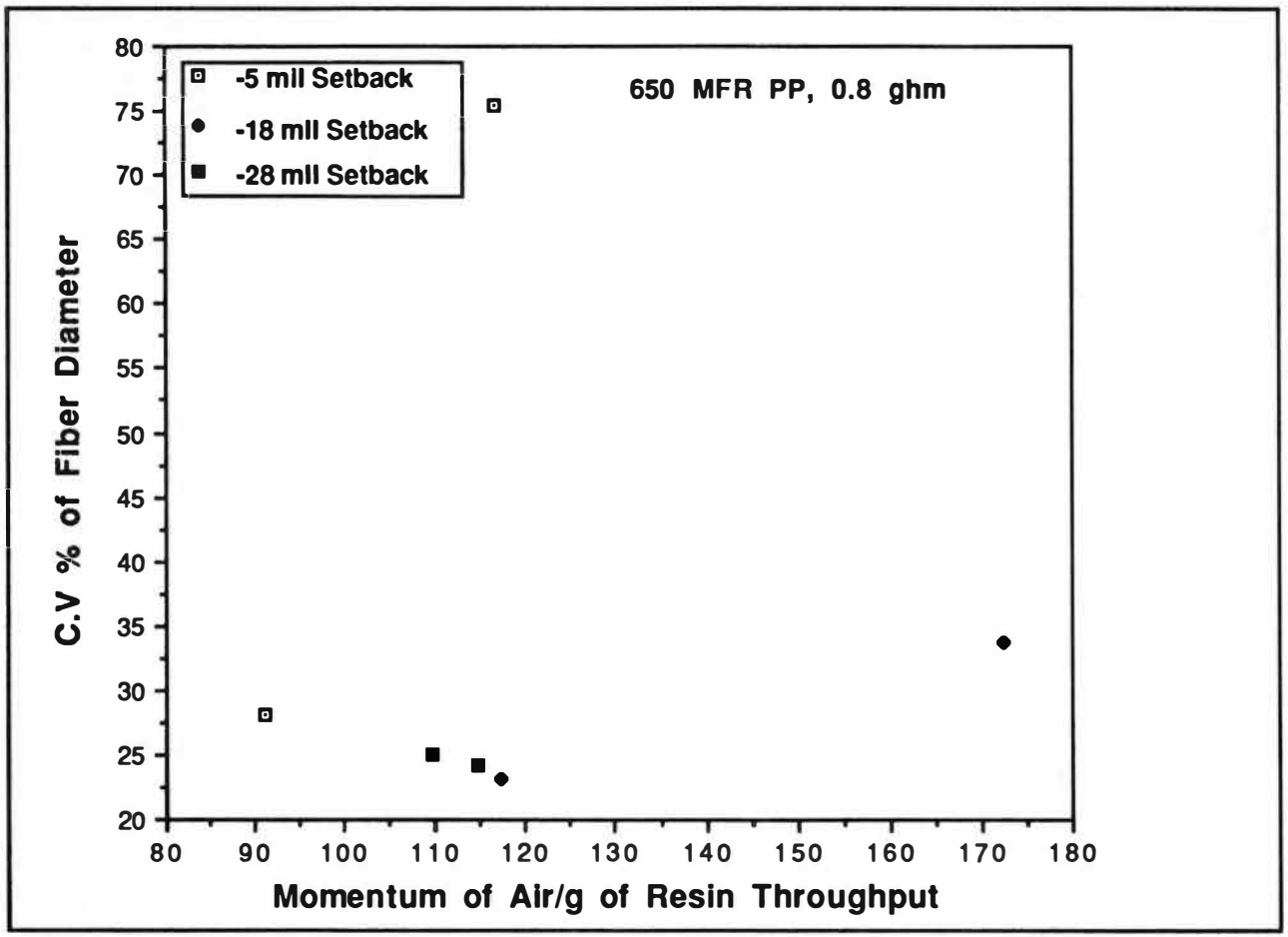


Figure 5.44 Effect of primary air momentum on C.V% of fiber diameter

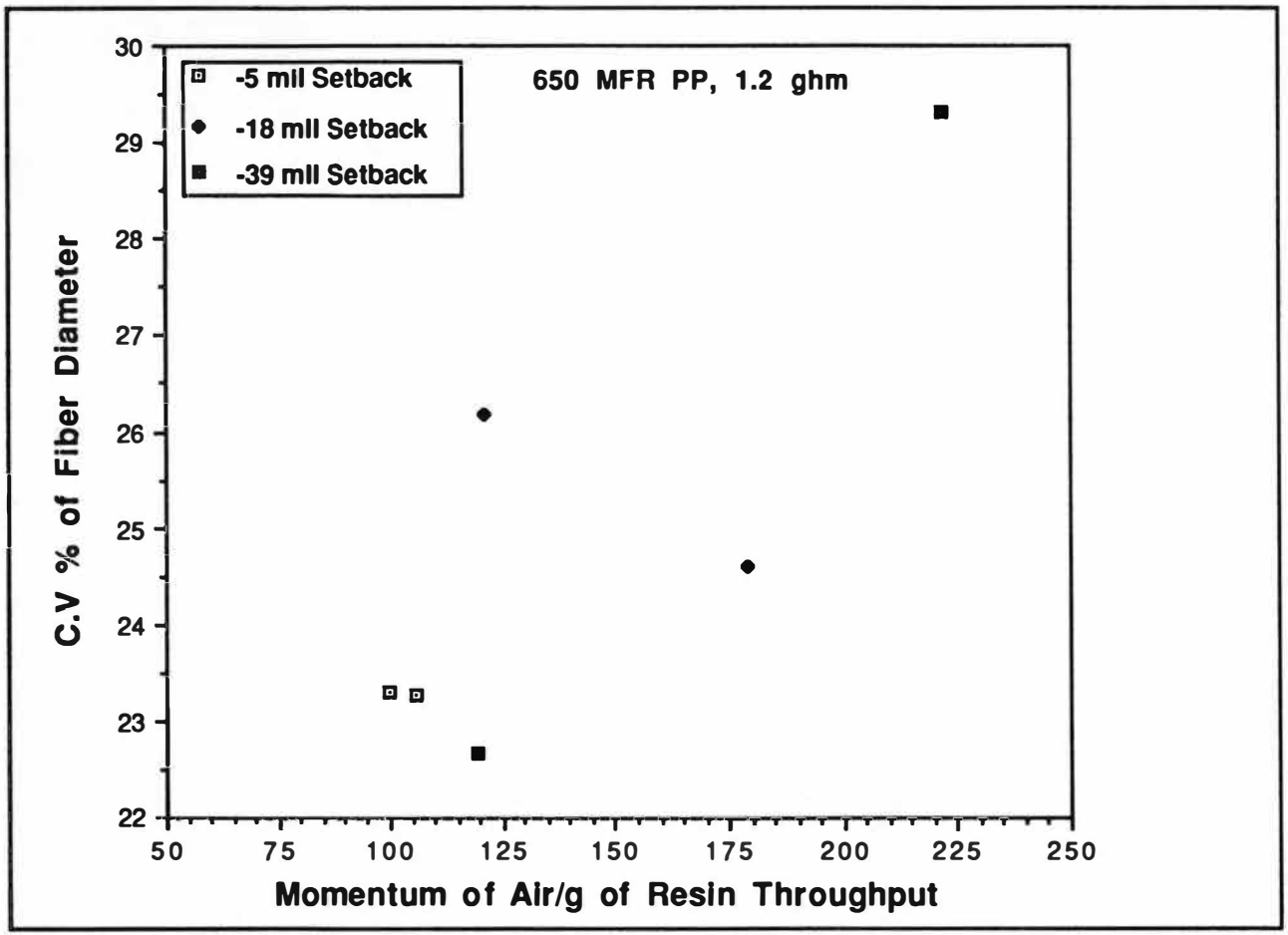


Figure 5.45 Effect of primary air momentum on C.V% of fiber diameter

diameter was quite small, which may have been the result of faster quenching at higher primary air velocities. A few exceptions seen in the plots may be due to mingling of fiber diameter data from 20 and 15 mil orifice diameter. 20 mil orifice gave slightly larger fibers compared to 15 mil orifice resulting in obscuring the effect of increasing primary air momentum.

On the other hand the coefficient of variation of fiber diameter increased with increase in momentum of primary air as shown in Figures 5.43-5.45, with some exceptions. The decrease in jet stability at higher primary air momentum may have caused greater variations in drag force acting on the filaments, thereby producing greater variability in fiber diameter. It is worth mentioning that the changes in C.V.% were only marginal to have any practical significance. A look at results in Table 5.3, reveal that only six out of the forty sample runs gave rise to a slightly larger range of C.V.%. The rest had C.V.% within a very narrow margin. This observation leaves room to believe that C.V.% is a fairly resilient characteristic and is not affected to a great degree by changes in air rate, polymer throughput, nosetip setback, and air momentum at constant resin MFR (which in this case was 650) and air-to-polymer flow rate ratio.

Figures 5.40-5.45 do not show a consistent trend for the effect of nosetip setback on average fiber diameter as well the coefficient of variation of fiber diameter. These findings were in agreement with the statistical analysis for the setback study shown in Appendix B. The GLM procedure does not indicate a significant main effect of the nosetip setback on average fiber diameter.

PHASE III - NOSETIP ANGLE (60^0 vs 90^0) STUDY

This study has focused primarily on the effects of nosetip angle (which decides the air injection angle; air injection angle = nosetip angle/2) on average fiber diameter and its coefficient of variation of melt blown webs made from 800 MFR polypropylene resin. Two 6-inch nosetips (one had a 60^0 and the other had a 90^0 nosetip angle) with a 15 mil orifice and a 10/1 L/D ratio were used in conjunction with three sets of air knives with nominal air gaps of 30, 60, and 110 mils, respectively. In addition, the effects of varying nosetip angle on key melt blown web properties such as filtration efficiency, air permeability, bursting strength, and packing factor have been discussed. Table 5.5 lists the average fiber diameter C.V.% of fiber diameter, filtration efficiency, air permeability, bursting strength, and packing factor of melt blown webs obtained from all the sample runs.

Effect of Nosetip Angle on Fiber Diameter and its Variability

The average fiber diameter and variability of fiber diameter obtained from the study were plotted against the nosetip angle as shown in Figures 5.46 and 5.47, respectively. It is evident from the plots, that in all cases, the 90^0 nosetip angle resulted in slightly larger average fiber diameter compared to 60^0 nosetip angle. Actual primary air exit velocities were calculated for all the sample runs and are shown in Table 5.6.

The air velocities were similar for both 60^0 and 90^0 nosetips with the nominal 30 mil air gap. Whereas, with the nominal 60 mil air gap, air velocity was considerably higher for the 90^0 nosetip angle (860 ft/sec) compared to the 60^0

Table 5.5 Results of the 60° Versus 90° Nosetip Angle Study [Phase III]

Primary Air Flow Rate = 130 Standard ft^3/min at 14.5 psi, 70° F

Sample No.	Sample ID *	Average Fiber Dia, μm	CV% of Fiber Dia	Frazier Air Permeab., $ft^3/ft^2/min$	Packing Factor	Bursting Strength, kPa	NaCl Aerosol Filt. Eff., %
1	0.4/15/10/54/-56/60	2.40	29.1	72.2	0.1218	58.28	48.07
2	0.8/15/10/54/-56/60	2.77	42.6	90.6	0.1351	41.38	45.42
3	0.8/15/10/27/-23/60	2.63	38.2	75.9	0.1268	41.04	42.88
4	0.8/15/10/100/-64/60	2.87	47.0	97.1	0.1364	25.17	42.72
5	0.4/15/10/54/-56/90	2.72	31.25	66.4	0.1222	66.07	55.47
6	0.8/15/10/54/-56/90	2.96	32.0	71.4	0.1326	59.04	47.74
7	0.8/15/10/27/-23/90	2.8	31.5	71.2	0.1262	56.49	50.41
8	0.8/15/10/100/-64/90	3.08	41.1	82.1	0.1394	35.31	49.87

* Polymer Throughput, g/hole/min/Orifice dia, mil/L/D ratio/Air gap, mil/Setback, mil/Nosetip angle, degrees

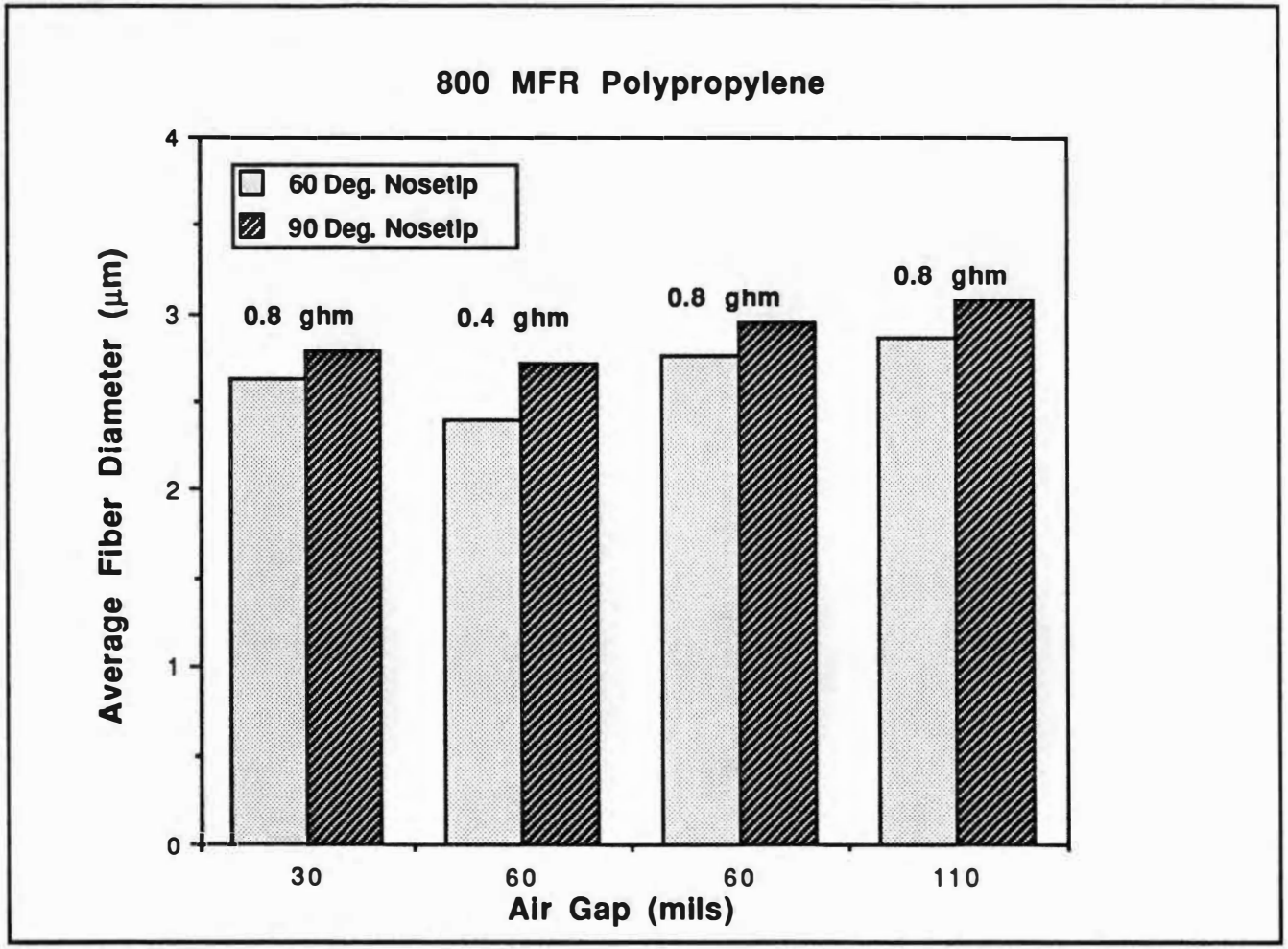


Figure 5.46 Effect of nosetip angle on average fiber diameter

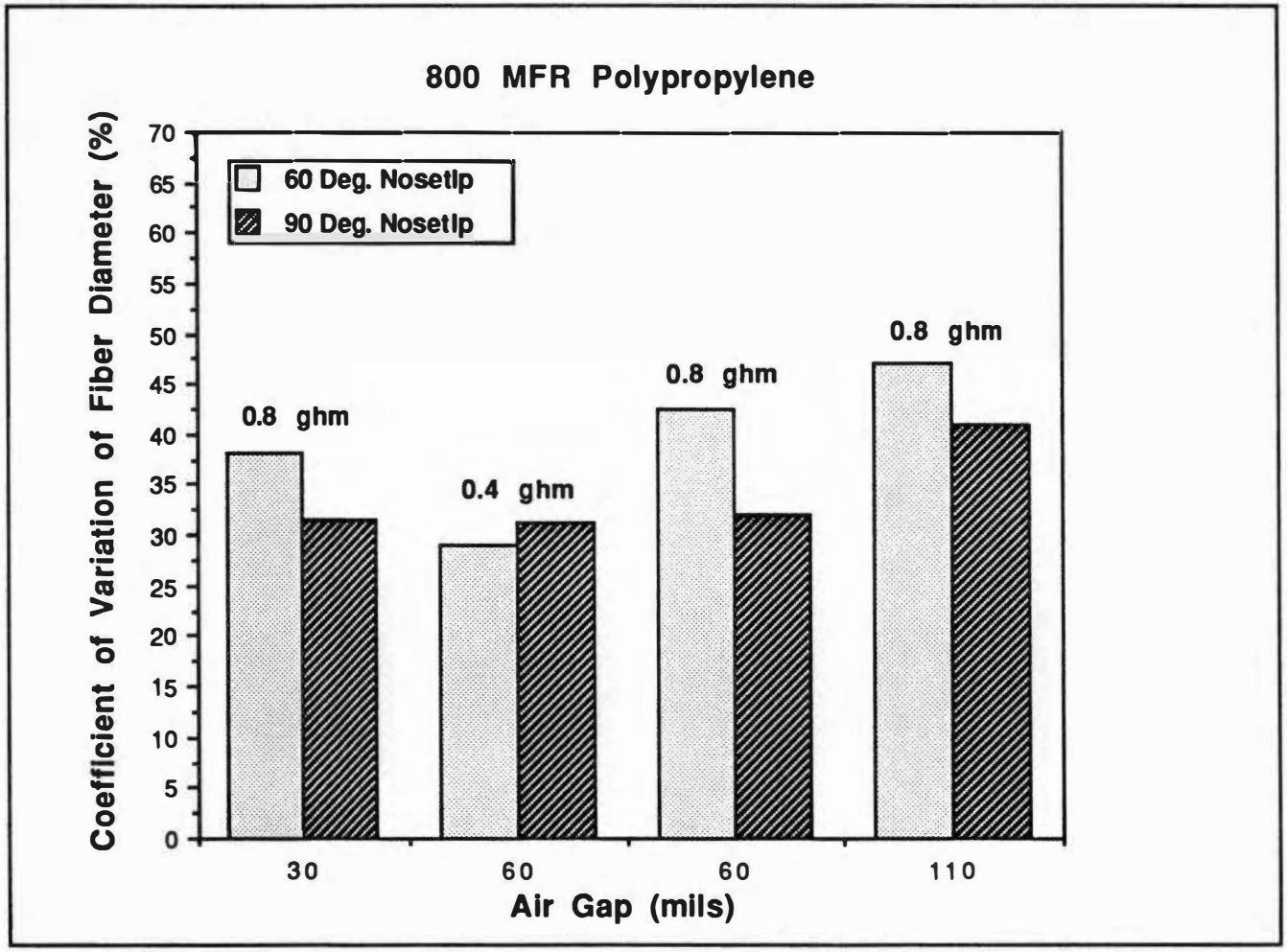


Figure 5.47 Effect of nosetip angle on C.V% of fiber diameter

Table 5.6 ACFM, Primary Air Velocity, and Momentum Calculations-60° vs 90° Nosetip Angle Study - Phase III

Primary Air Flow Rate = 130 Standard ft^3/min at 14.5 psi, 70° F

Sample No.	Sample ID*	Nosetip Angle °	Face Gap, mils	Slot Area, ft^2	Actual CFM	Primary Air+ Vel., (ft/sec)	Air Momentum, lb-ft/sec	Momentum/ g of resin, lb-ft/sec/g
1	0.4/15/10/54/-56	60	99.85	0.0055472	203.23	610.61	99.22	123.0
2	0.8/15/10/54/-56	60	99.85	0.0055472	203.23	610.61	99.22	61.5
3	0.8/15/10/27/-23	60	56.36	0.0031311	179.70	956.53	155.44	96.4
4	0.8/15/10/100/64	60	228.35	0.0126861	-	-	-	-
5	0.4/15/10/54/-56	90	53	0.0029444	151.75	858.98	139.58	173.0
6	0.8/15/10/54/-56	90	53	0.0029444	151.75	858.98	139.58	86.5
7	0.8/15/10/27/-23	90	42.5	0.0023611	133.90	945.18	153.59	95.2
8	0.8/15/10/100/-64	90	160	0.0088889	-	-	-	-

* Polymer Throughput, g/hole/min/Orifice dia, mil/L/D ratio/Air gap, mil/Nosetip setback, mil. + Air temperature at die and stagnation pressure in die manifold were used for calculation.

nosetip angle (611 ft/sec). Although the air gaps and corresponding setbacks were almost identical for the 60^0 and 90^0 nosetips with all three sets of air knives, the face gaps were different because of geometry constraints. In spite of the comparable velocity in the case of 30 mil air gap with both nosetip angles, and considerably higher velocity for 90^0 nosetip compared to 60^0 in the case of 60 mil air gap, the average fiber diameters were slightly smaller with the 60^0 nosetip (with all three air knives compared to 90^0 nosetip).

A logical explanation to this phenomena may lie in the magnitude of drag forces acting on the exiting molten polymer jets from the orifices. It has been observed by the author that the exiting polymer jet stays fairly straight for a short distance from the exit plane of the orifice. It is safe to assume that in this region the attenuation mechanism is through viscous drag between the hot primary air and the polymer jet. Since the horizontal drag component will be smaller in the case of 90^0 nosetip angle compared to the 60^0 nosetip angle, the resultant drag force may have been smaller resulting in slightly coarser fibers. This explanation is in agreement with the findings of Milligan and Haynes [42], where it has been said that the larger the air injection angle, the less is the drag force.

It can be seen from Figure 5.47 that overall, the coefficient of variation of fiber diameter was slightly smaller for the 90^0 nosetip in comparison to 60^0 nosetip (the only exception being the 0.4 g/hole/min throughput with 60 mil air gap). The smaller C.V.% for the 90^0 nosetip angle is indicative of slightly better jet stability during attenuation. The differences between 60^0 and 90^0 nosetips with respect to fiber diameter and its variability were too little to have a large practical significance.

Effect of Nosetip Angle on the Physical and Mechanical Properties of Melt Blown Webs

Figures 5.48-5.51 depict the effect of nosetip angle on the key properties of a melt blown web such as, Frazier air permeability, sodium chloride aerosol filtration efficiency, bursting strength, and the packing factor. The bursting strength, air permeability and filtration efficiency were all improved with the 90^0 nosetip angle. In all the cases air permeability was notably lower for webs made with the 90^0 nosetip than for the ones made with the 60^0 nosetip. Similar trends were observed in the case of bursting strength and filtration efficiency. There were no notable trends in the packing factors of webs produced from 60^0 and 90^0 nosetips. The packing factors were almost similar in both cases.

The slightly improved web properties in the case of 90^0 nosetip angle may be due to greater fiber entanglement. It is interesting to note that in the case of 90^0 nosetip, the primary air comes in contact with the exiting polymer stream at a greater angle, thereby increasing the chances of filament cross-over from face side to the screen side and vice versa. This process may result in greater filament entanglement resulting in improved web properties for the 90^0 nosetip although the fiber diameters are slightly larger. Also the slightly lower C.V. of fiber diameter for the 90^0 nosetip may have resulted in a more uniform pore structure and narrower diameter distribution in the webs, thereby contributing to the slight improvement in their properties. The similarity in packing factors among the webs obtained from 60^0 and 90^0 nosetips, in conjunction with improved filtration properties for the 90^0 nosetip webs indicates that overall, the 90^0 nosetip angle may result in slightly smaller pore structure.

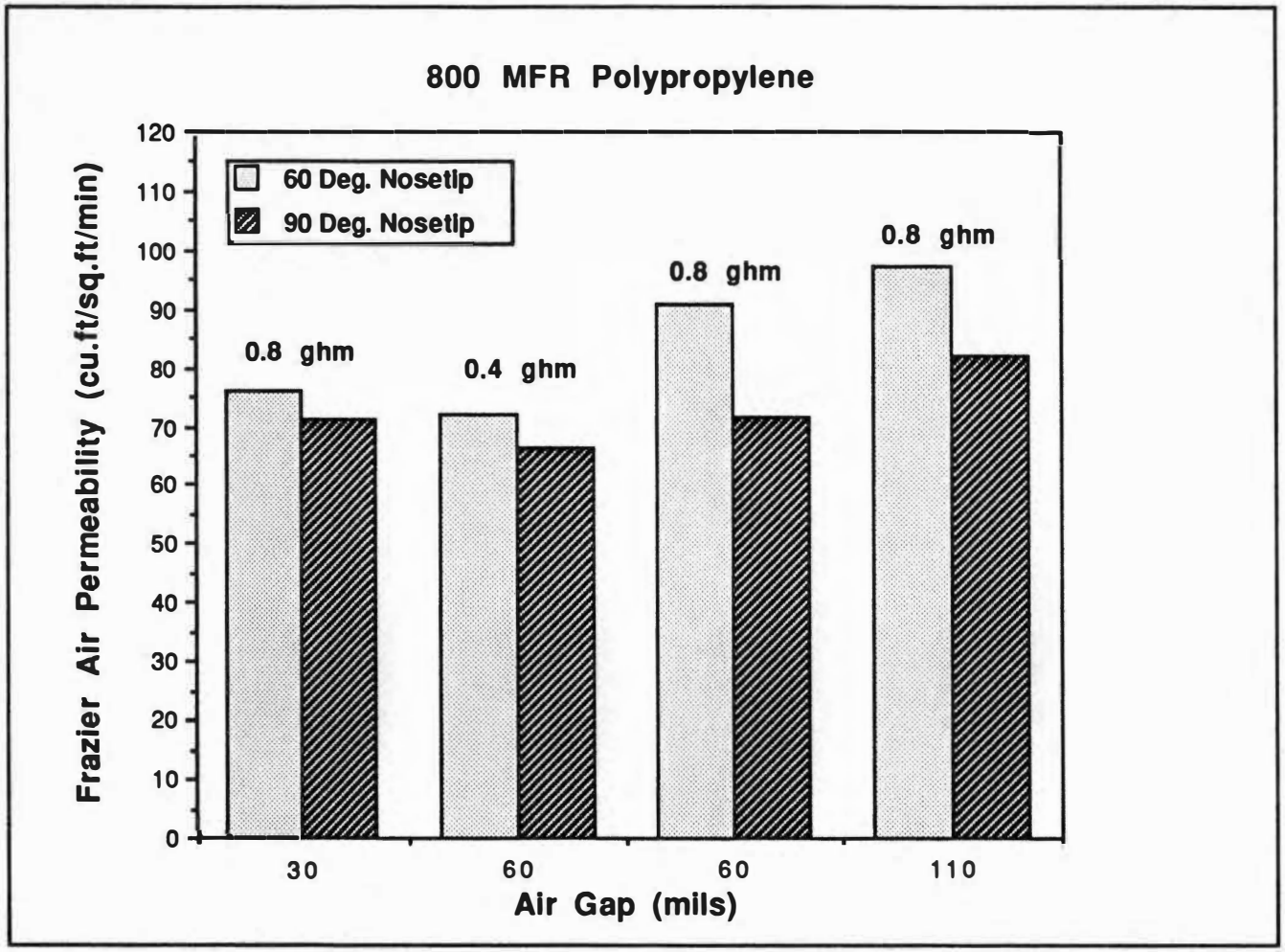


Figure 5.48 Effect of nosetip angle on air permeability

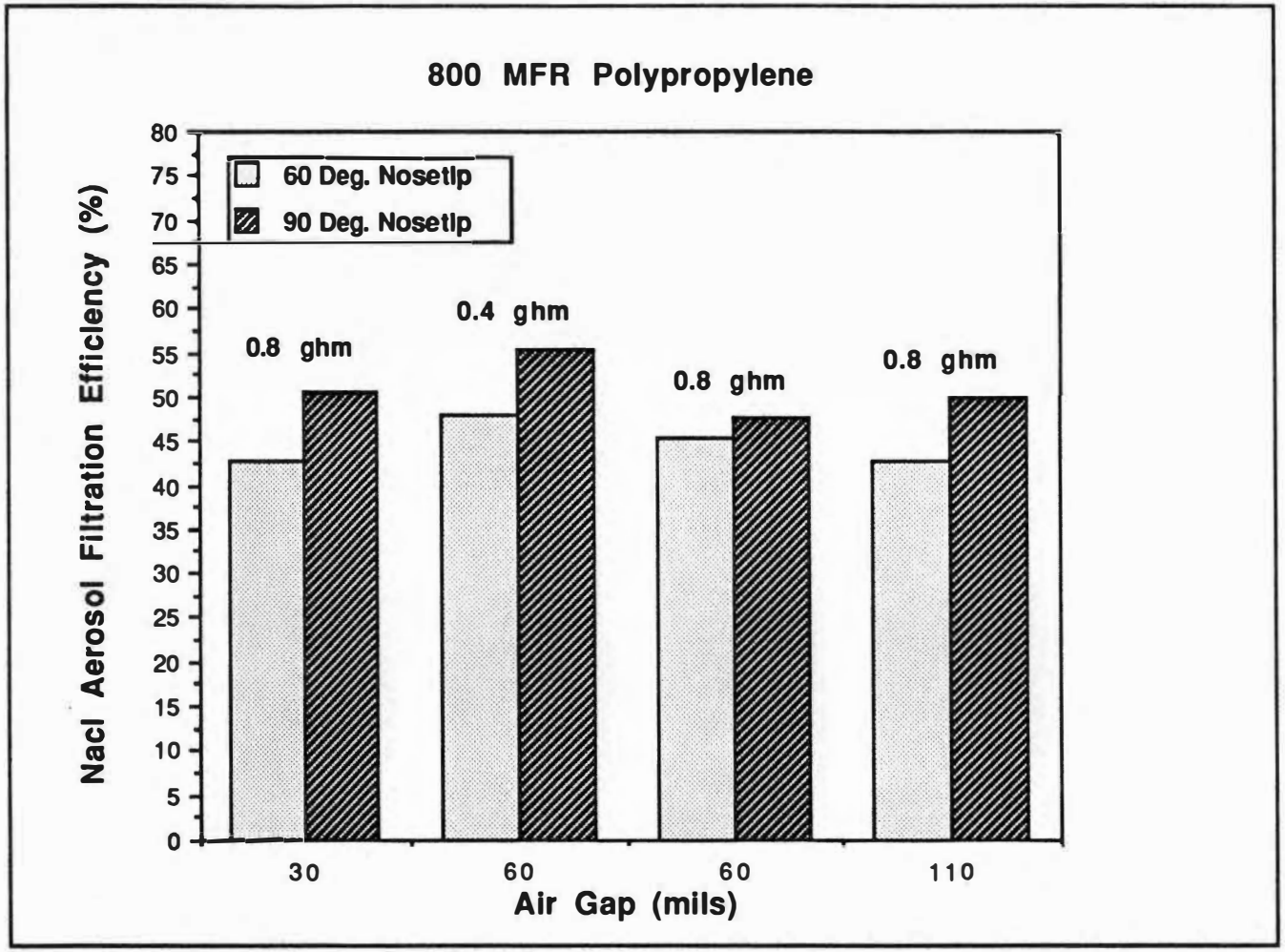


Figure 5.49 Effect of nosetip angle on NaCl aerosol filtration efficiency

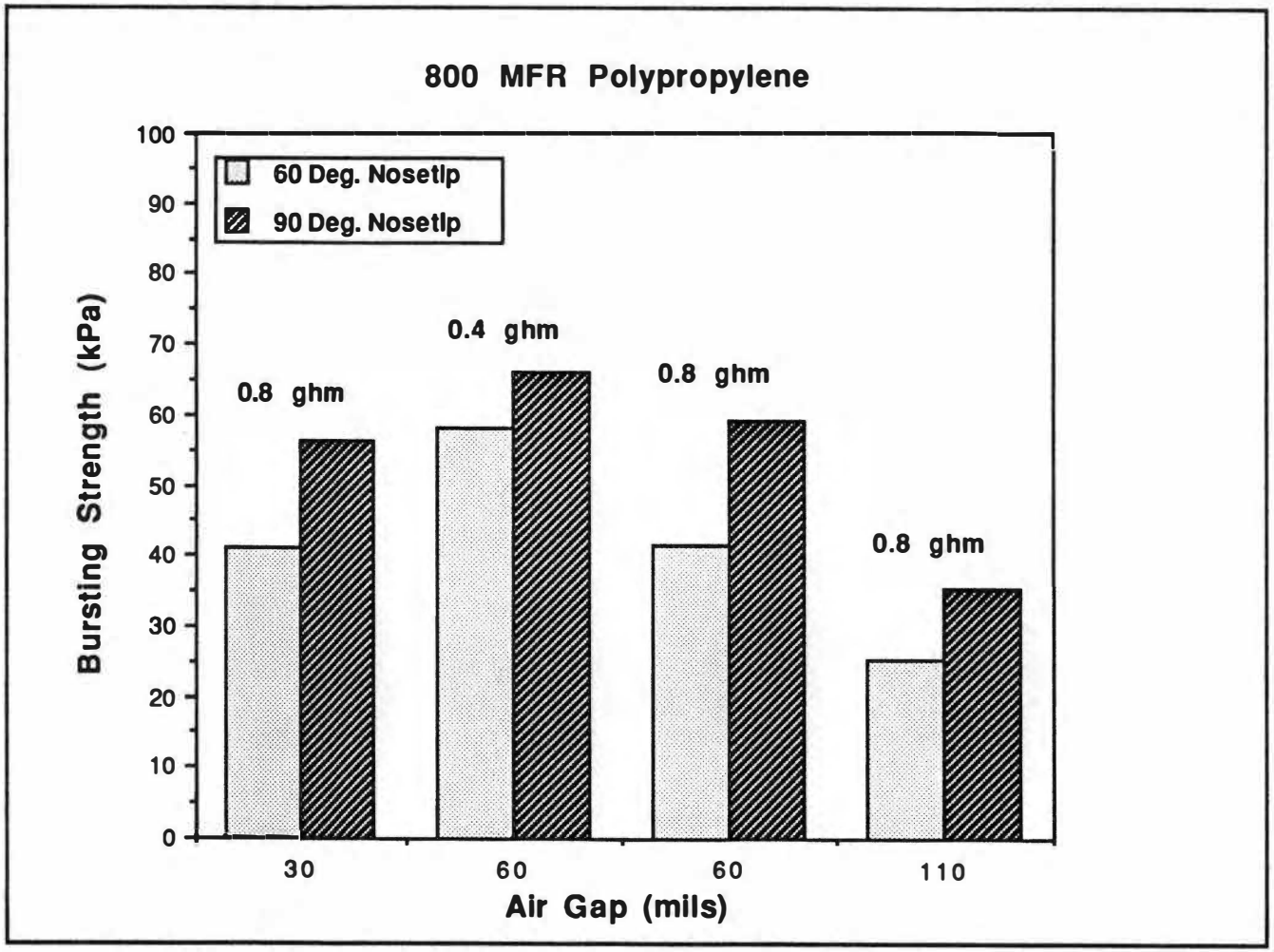


Figure 5.50 Effect of nosetip angle on bursting strength

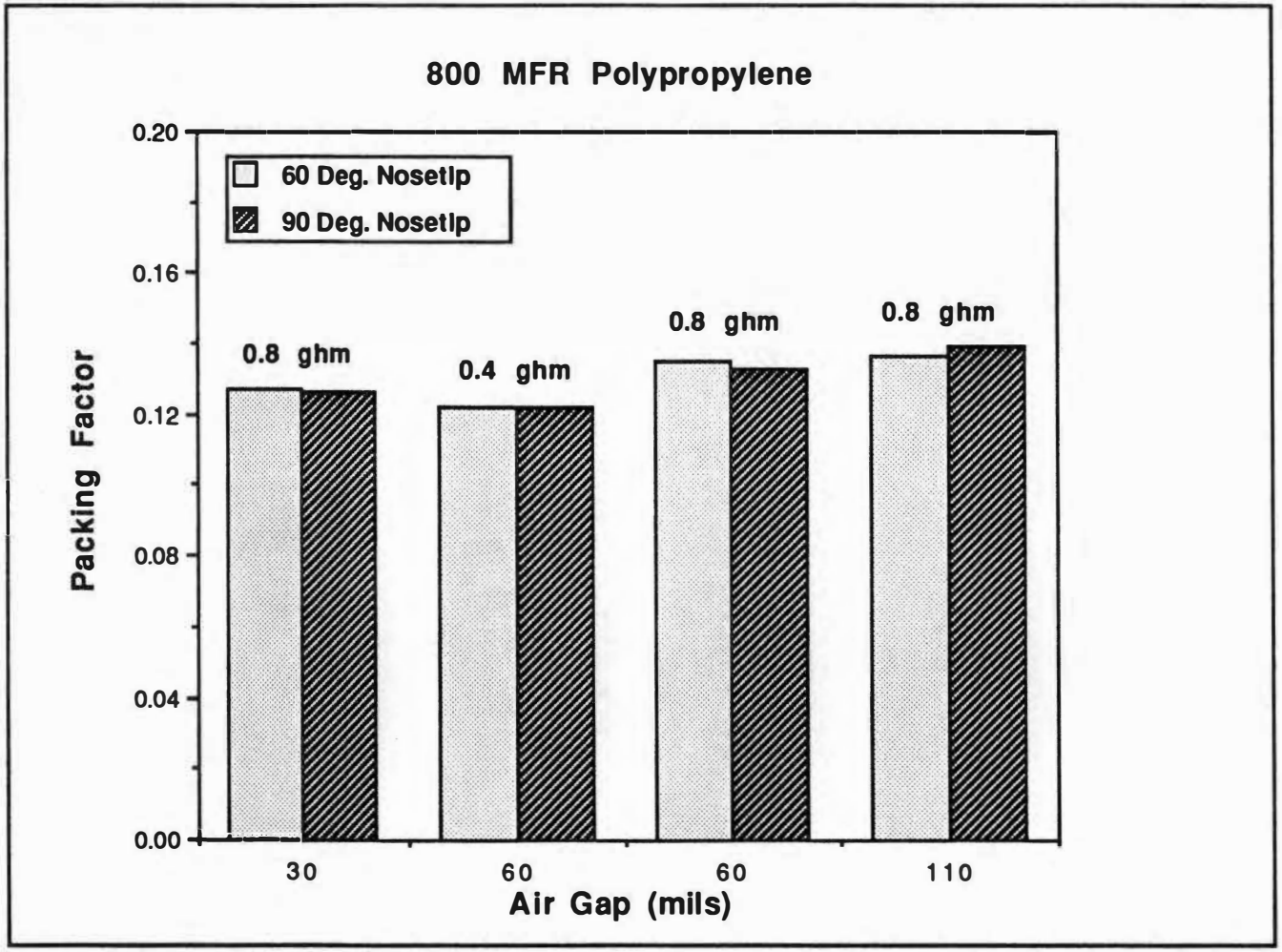


Figure 5.51 Effect of nosetip angle on web packing factor

PHASE IV - MELT SHEAR VISCOSITY STUDY OF 35 AND 800 MFR POLYPROPYLENE MELTS

The shear viscosity of 35 and 800 MFR polypropylene melts was determined using pressure readings obtained under actual melt blowing conditions on the 6-inch die utilizing different combinations of die temperatures, orifice diameters, L/D ratios, and polymer throughput rates as described in chapters 3 and 4. The importance of this study lies in the fact that actual melt blowing conditions were employed for pressure measurements, contrary to those utilized in the use of a more common plunger type rheometer. In the case of a plunger type rheometer (INSTRON Rheometer), the shear conditions existing between the screw and the barrel of a typical melt blowing extruder are absent. Therefore it was decided to use pressure measurements made during actual melt blowing trials to get a realistic estimate of the melt shear viscosity in the nosetip orifice.

The primary purpose of this study was to explain the results of the effects of orifice diameter and L/D ratio on fiber diameter from Phases I and II of the research. Since, both the orifice diameter and L/D ratio affect the shear properties of the melt, it becomes imperative to determine the magnitude of the effect, if the fiber diameter data has to be interpreted in terms of the variations in melt viscosity at different processing conditions.

A very elaborate data set containing shear rates, shear stresses, and Newtonian shear viscosities for both 35 and 800 MFR PP melts at different orifice diameters, L/D ratios, die temperatures, and resin throughputs is given in Table D.1 of Appendix D. From the main data set the shear stress and shear strain data for 35 and 800 MFR PP melts at 560 ^{0}F was plotted as shown in Figures 5.52

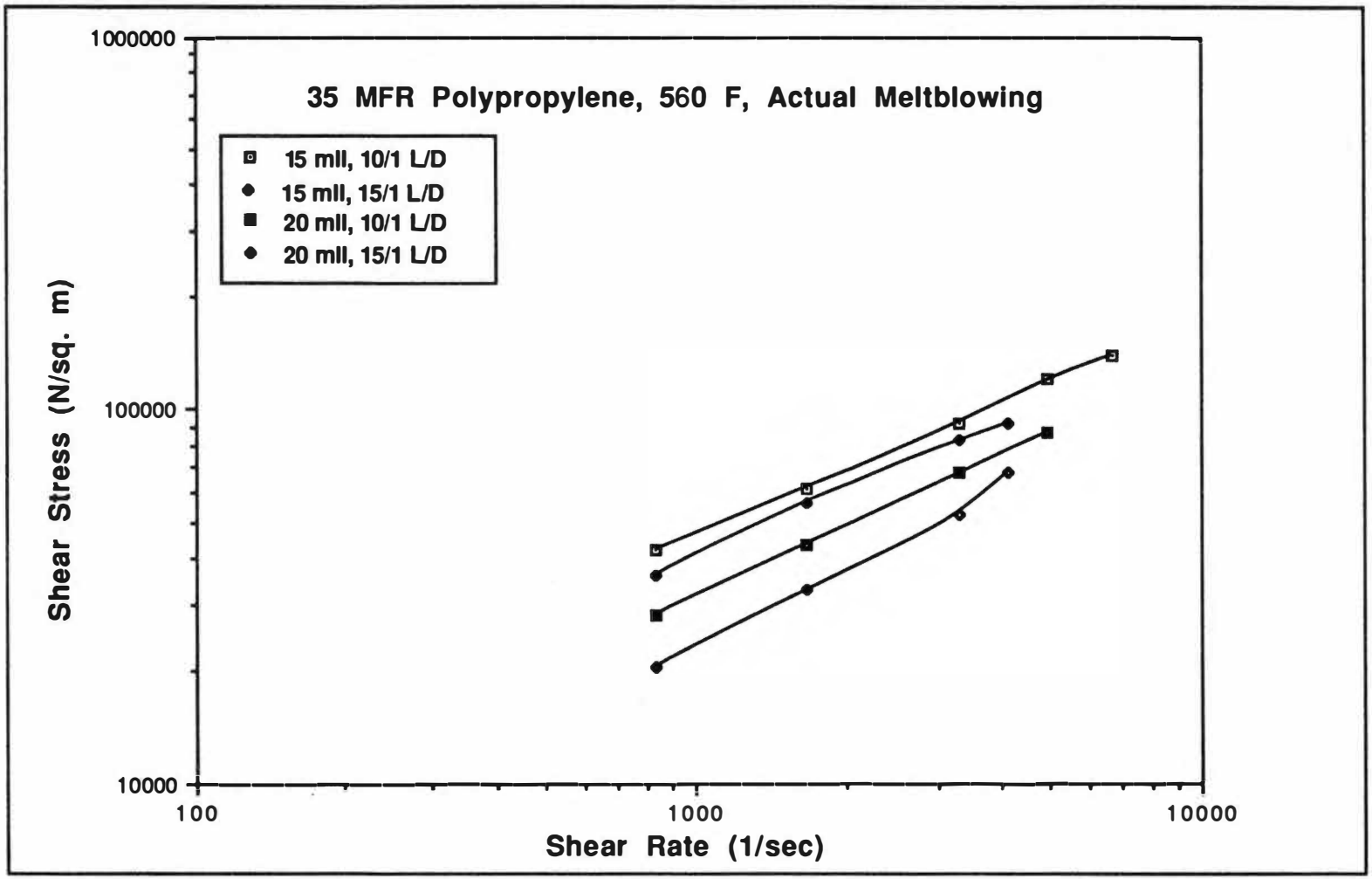


Figure 5.52 Effect of shear rate on shear stress of 35 MFR PP melt

and 5.53 at different polymer throughput rates and orifice diameter-L/D combinations. It is evident from the plots in Figures 5.52 and 5.53 that both 35 and 800 MFR PP melts under melt blowing conditions exhibit a fairly linear response between stress and strain (Newtonian behavior) inside the orifice. Therefore the shear viscosity obtained was not corrected for non-Newtonian behavior. The data pertaining to Figures 5.52 and 5.53 is shown in Table 5.7.

It is clear from Table 5.7 that for both MFRs, a 15/1 L/D ratio results in a lower shear viscosity compared to 10/1 L/D. This was true for both 15 and 20 mil orifice diameters at all polymer throughput rates. This may be due to the longer orifice in the case of 15/1 (at constant orifice diameter) resulting in greater chain orientation within the orifice and also a longer time for the entry stress to decay (at constant polymer throughput and orifice diameter). It is interesting to note that the decrease in viscosity for 35 MFR PP melt going from 10/1 to 15/1 L/D is considerably higher than for 800 MFR where the viscosity decreased only slightly.

The above observation may provide an answer as to why with 35 and 400 MFR resins (Phase I) a reduction in average fiber diameter with an increase in L/D ratio from 10/1 to 15/1 was seen, and failed to see a trend with 650 MFR PP resin (phase II). The viscosity of 650 MFR will be close to 800 MFR used for viscosity studies. Thus the behavior of 800 MFR resin shall provide clues to the viscosity behavior of 650 MFR PP resin. The viscosity of 650 MFR PP resin may have been so low to start with, changing L/D ratio did not give rise to any significant drop in shear viscosity and hence the lack of observable trends in fiber diameter with increasing L/D ratio.

Table 5.7 and Figures 5.52 and 5.53 indicate that the 20 mil orifice diameter results in higher shear viscosities for both 35 and 800 MFR resins

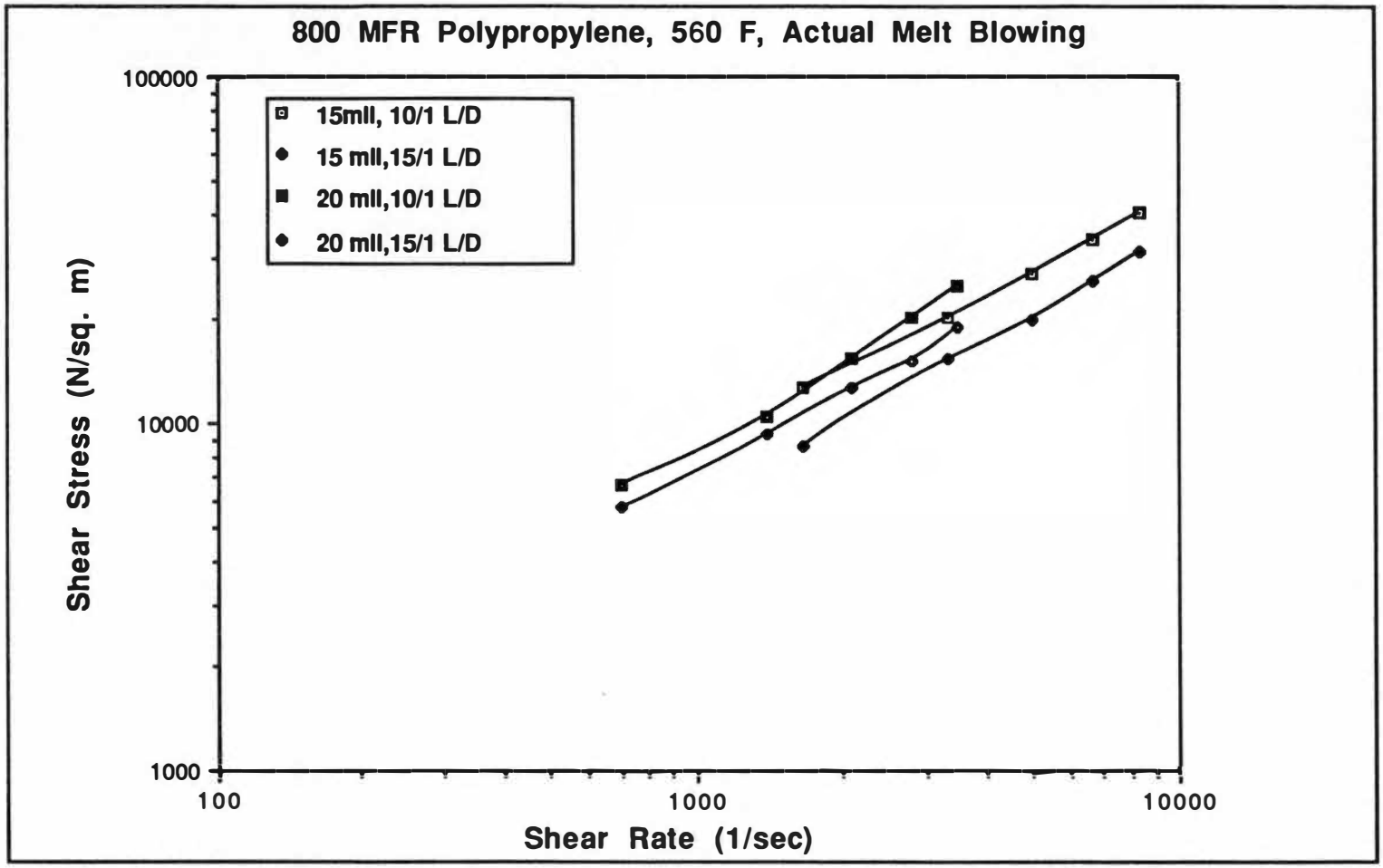


Figure 5.53 Effect of shear rate on shear stress of 800 MFR PP melt

Table 5.7 Melt Shear Viscosity (Newt) Data - Phase IV

[Parameters Measured During Actual Melt Blowing]

Melt Flow rate	Nosetip	Polymer Throughput (g/hole/min)	Pressure Drop (N/m^2)	Shear Stress (N/m^2)	Shear Viscosity Newt (Pa. Sec)	Shear Rate (sec^{-1})
35 Die temp 560^0 F	15 mil orifice diameter, 10/1 L/D	0.2	1.566×10^6	3.916×10^4	47.1	831.2
		0.4	2.449×10^6	6.123×10^4	36.8	1662.4
		0.8	3.740×10^6	9.349×10^4	28.1	3324.7
		1.2	4.857×10^6	1.214×10^5	24.4	4987.2
		1.6	5.733×10^6	1.433×10^5	21.6	6649.6
	15 mil orifice diameter, 15/1 L/D	0.2	2.056×10^6	3.426×10^4	41.2	831.2
		0.4	3.345×10^6	5.576×10^4	33.5	1662.4
		0.8	4.732×10^6	7.886×10^4	23.7	3324.7
		1.0	5.420×10^6	9.033×10^4	21.7	4156.0
35 Die temp 560^0 F	20 mil orifice diameter, 10/1 L/D	0.2	9.450×10^5	2.362×10^4	67.4	350.7
		0.4	1.545×10^6	3.863×10^4	55.1	701.3
		0.8	2.580×10^6	6.449×10^4	46.0	1402.6
		1.2	3.359×10^6	8.398×10^4	39.9	2103.9
	20 mil orifice diameter, 15/1 L/D	0.2	1.09×10^6	1.816×10^4	51.8	350.7
		0.4	1.793×10^6	2.989×10^4	42.6	701.3
		0.8	3.00×10^6	5.0×10^4	35.6	1402.6
		1.2	3.863×10^6	6.438×10^4	30.6	2103.9

Table 5.7 (Contd.)

Melt Flow rate	Nosetip	Polymer Throughput (g/hole/min)	Pressure Drop (N/m^2)	Shear Stress (N/m^2)	Shear Viscosity Newt (Pa. Sec)	Shear Rate (sec^{-1})
800 Die temp 560^0 F	15 mil orifice diameter, 10/1 L/D	0.4	5.104×10^5	1.276×10^4	7.68	1662.4
		0.8	8.07×10^5	2.02×10^4	6.07	3324.7
		1.2	1.09×10^6	2.724×10^4	5.46	4987.2
		1.6	1.366×10^6	3.414×10^4	5.13	6649.6
		2.0	1.628×10^6	4.07×10^4	4.9	8312
	15 mil orifice diameter, 15/1 L/D	0.4	5.173×10^5	8.622×10^3	5.31	1662.4
		0.8	9.243×10^5	1.54×10^4	4.63	3324.7
		1.2	1.193×10^6	1.99×10^4	3.99	4987.2
		1.6	1.552×10^6	2.587×10^4	3.89	6649.6
		2.0	1.89×10^6	3.15×10^4	3.79	8312
800 Die temp 560^0 F	20 mil orifice diameter, 10/1 L/D	0.4	2.69×10^5	6.725×10^3	9.59	701.3
		0.8	4.207×10^5	1.052×10^4	7.5	1402.6
		1.2	6.14×10^5	1.535×10^4	7.29	2103.9
		1.6	8.14×10^5	2.035×10^4	7.25	2805.2
		2.0	1×10^6	2.518×10^4	7.18	3506.5
	20 mil orifice diameter, 15/1 L/D	0.4	3.449×10^5	5.748×10^3	8.2	701.3
		0.8	5.587×10^5	9.312×10^3	6.64	1402.6
		1.2	7.656×10^5	1.276×10^4	6.06	2103.9
		1.6	9.105×10^5	1.517×10^4	5.41	2805.2
		2.0	1.138×10^6	1.897×10^4	5.41	3506.5

compared to 15 mil orifice diameter. The shear rate in the case of 20 mil orifice is considerably lower compared to 15 mil orifice, at constant polymer throughput rate and L/D ratio. Although the shear stress for a 20 mil orifice is lower than the 15 mil orifice at constant polymer throughput rate and L/D ratio the decrease is not low enough to compensate for the lower shear rate in the denominator of the viscosity equation, which results in higher viscosity for the 20 mil orifice. The findings of Phase II of this research indicate that overall, for 650 MFR PP resin, the average fiber diameter was slightly larger with the 20 mil orifice in comparison to 15 mil orifice and are in agreement with the viscosity study.

Whereas during Phase I (with 400 MFR PP) it was found that the 20 mil orifice produced a slightly smaller average fiber diameter compared to 15 mil orifice. This may be due to different temperatures used during Phase I which resulted in greater degradation during processing and hence drop in viscosity. In fact, gel permeation chromatography studies conducted during Phase I indicated a sharp drop in the weight average molecular weight for the 400 MFR resin with 20 mil orifice and 15/1 L/D ratio (the longest flow channel among the chosen nosetips). The resulting finer average fiber diameter with the larger orifice (20 mil) during Phase I of this research with 400 MFR appears to have been influenced by the thermal degradation of the polymer brought about by a combination of temperatures used in the extruder, the die tip, and the residence time inside the orifice.

CHAPTER 6

CONCLUSIONS

PHASE I - PRELIMINARY STUDY

1. The primary conclusion of Phase I of this study was that the orifice diameter, orifice L/D ratio, PP resin MFR, air gap, and polymer throughput all had a significant effect on the average fiber diameter. Only the polymer throughput had an independent main effect. The other production variables had interactive effects on the average fiber diameter. The statistical analysis indicated that MFR*orifice size, MFR*air gap, orifice size*air gap, and L/D ratio*air gap had a significant effect on the average fiber diameter.
2. The resin MFR, orifice size, MFR*L/D ratio, and MFR*air gap had a significant effect on the MD web tenacity. Overall, the 35 MFR resin produced stronger webs compared to the 400 MFR resin.
3. The resin MFR, polymer throughput, MFR*air gap, and orifice size*L/D ratio had a significant effect on the web bursting strength. The bursting strength decreased with increasing (0.4 to 0.8 g/hole/min) polymer throughput rate.
4. The shot generated was significantly affected by the orifice size, polymer throughput rate, L/D ratio, MFR*L/D ratio, MFR*air gap, orifice size*polymer throughput rate, and orifice size*L/D ratio.
5. The L/D ratio, MFR*orifice size, MFR*L/D ratio, MFR*air gap, orifice size*air gap, orifice size*L/D ratio, and polymer throughput rate*air gap had a significant effect on the amount of fly generated. The orifice size*L/D ratio had the strongest interactive effect with respect to the 400 MFR PP resin.

This was evident from the excessive fly generated with the 20 mil orifice and a 15/1 L/D for the 400 MFR resin.

6. With respect to the decrease in weight average molecular weight during melt blowing, the 400 MFR resin was affected more by the increase in orifice diameter and L/D ratio than the 35 MFR resin. In fact the 35 MFR resin, for all practical purposes is not affected by the increase in orifice diameter and L/D ratio. For the 400 MFR resin the maximum decrease in weight average molecular weight occurred with the processing conditions associated with the 20 mil orifice and 15/1 L/D. This was true with both air gap settings. MFR*orifice size, MFR*L/D ratio, orifice size*L/D ratio have a significant effect on the weight average molecular weight of the web.

PHASE II - NOSETIP SETBACK STUDY

1. The average fiber diameter was maintained within a range of 0.46 μm with increasing polymer throughput rate from 0.4-2.0 g/hole/min when the air-to-polymer flow rate ratio was maintained constant.
2. The effect of nosetip setback on fiber diameter was not statistically significant. There was no conclusive evidence that setback significantly affected the fiber diameter. Nevertheless, it is most noteworthy that average fiber diameter changed very little with nosetip setbacks ranging from -39 to +5 mils in which face gaps were directly coupled to setback resulting in air jet exit velocities which differed by a factor as great as 3.
3. The orifice diameter had a small but statistically significant effect on average fiber diameter with the 650 MFR PP, die geometry and processing conditions employed in this study. Overall, the average fiber diameter

increased with the increase in orifice diameter from 15 to 20 mils. This does not contradict directly with the results of Phase I where a slight reduction in average fiber diameter was noticed with the larger orifice (20 mil). It has been discussed in chapter 5 that the reason for the slight drop in average fiber diameter during Phase I was most likely the difference in thermal degradation characteristics of the melt in each case. This conclusion was supported by gel permeation chromatography studies conducted on the samples from Phase I to determine the weight average molecular weight of webs. The general conclusion was that orifice diameter in the range of 15-20 mils has no practical effect on final fiber diameter.

4. Shot notably increased with the increase in polymer throughput rate and orifice diameter. Overall, the shot generation increased slightly with an increase in nosetip setback.

PHASE III - 60^0 VS 90^0 NOSETIP ANGLE STUDY

1. The 60^0 nosetip angle produced melt blown webs with slightly smaller average fiber diameter compared to 90^0 nosetip angle. But the coefficient of variation of fiber diameter was smaller in the case of 90^0 nosetip angle.
2. The key properties of melt blown webs such as Frazier air permeability, bursting strength, and sodium chloride filtration efficiency were all higher for the 90^0 nosetip compared to the 60^0 tip. There was a notable improvement in those properties in the case of the 90^0 tip compared to the 60^0 nosetip. The packing factors did not show any consistent trends with changing nosetip angle, and they were almost similar for both nosetip angles.

PHASE IV - SHEAR VISCOSITY STUDIES ON 35 AND 800 MFR PP MELTS

1. Both 35 and 800 MFR resins exhibited a linear response between shear stress and shear rate (Newtonian) under actual melt blowing conditions with the chosen temperatures, orifice dimensions, and polymer throughput rates.
2. For both resins the shear viscosity decreased with an increase in L/D ratio from 10/1 to 15/1 at constant orifice diameter. In the case of 35 MFR, the decrease was notable, whereas 800 MFR showed only a marginal decrease with increasing L/D ratio. This may explain the decrease in average fiber diameter for 35 and 400 MFR PP (Phase I) when L/D ratio was increased from 10/1 to 15/1, and the lack of any noticeable effect of L/D ratio on 650 MFR PP (Phase II-setback study).
3. With an increase in orifice diameter from 15 to 20 mils the shear viscosity increased for both 35 and 800 MFR PP resins. The fiber diameter data from setback study (Phase II) with 650 MFR resin indicates a slightly larger average fiber diameter for webs produced with a 20 mil orifice compared to ones produced with a 15 mil orifice. Since the shear viscosity for the 20 mil orifice was higher, the fiber diameter was slightly larger.

LIST OF REFERENCES

LIST OF REFERENCES

1. Krcma, R., Manual of Nonwovens, Textile Trade Press, Manchester, England, 1971.

2. Drelich, A., Course Materials, Eighth Annual Nonwovens Workshop, The University of Tennessee, Knoxville, Tennessee, July 30-August 3, 1990, pp. 1-15.

3. Anonymous, Polymer Science and Engineering Encyclopedia, John Wiley and Sons, Inc., New York, 1987, pp. 204-226.

4. Wente, V. A., Industrial and Engineering Chemistry, Volume 48, 1956, pp. 1342-1346.

5. Buntin, R. R., Keller, J. P., and Harding, J. W., U. S. Patent 3,849, 241, November 19, 1974.

6. American Society of Testing and materials, Annual Book of Standards, Philadelphia, Pennsylvania, 1989.

7. Nonwovens - An Advanced Tutorial (Turbak, A. F. and Vigo, T. L., Editors), TAPPI Press, Atlanta, GA, 1989, pp.

8. Trimble, L. E., Melt blown Technology Today, Miller Freeman Publications, San Francisco, 1989, pp. 139-143.

9. Moore, G. K., Melt blown Technology Today, Miller Freeman Publications, San Francisco, 1989, pp. 150-158.

10. Wente, V. A., U. S. Dept. of Commerce, Office of Technical Services Report No. PB111437, NRL 4364, April 15, 1954.

11. Private Communications with Dr. Buntin, R. R., Exxon Chemical Company, July 1991.

12. Milligan, M. W. and Haynes, B., Proceedings, First Annual TANDEC Conference, The University of Tennessee, Knoxville, Tennessee, October 22-24, 1991.

13. Buntin, R. R. and Lohkamp, D. T., TAPPI, Volume 56, No. 4, 1973, pp. 74-77.

14. Private Communications with Dr. Milligan, M. W., The University of Tennessee, Knoxville and Dr. Buntin, R. R., Exxon Chemical Company, September 1990.

15. Warner, S. B. et al., INDA Journal of Nonwovens Research, Vol. 2, No. 2, 1990, pp. 33-40.

16. Malkan, S. R., Ph. D Dissertation, The University of Tennessee, Knoxville, May 1990.

17. Private Communications with Meade, R. A. and Spires, L. E., Textile Processing Laboratory, The University of Tennessee, Knoxville, September 1991.

18. Lau, J. C., U. S. Patent 4,526,733, Kimberly-Clark Corporation, July 2, 1985.

19. Jones, A. M., Book of Papers, 4th International Conference on Polypropylene Fibers and Textiles, Nottingham, England, September 23-25 1987, pp. 47.1-47.10.

20. Jones, A. M. and Wadsworth, L. C., TAPPI Proceedings, Atlanta, GA, April 21-24 1986, pp. 23-30.

21. Eaton, G. M. et al., Book of Papers, INDA-TEC, Hilton Head, SC, May 18-21 1987, pp. 221-231.

22. Shaumbagh, R. L., Industrial and Engineering Chemistry Research, Vol. 27, No. 12, 1988, pp. 2363-2372.

23. Wadsworth, L. C. and Jones, A. M., Nonwovens Industry, November 1986, pp. 44-51.

24. Wadsworth, L. C. and Muschelewicz, A. O., Book of Papers, 4th Intl. Conference on Polypropylene Fibers and Textiles, Nottingham, England, September 23-25 1987, pp. 41.11-47.20.

25. Wadsworth, L. C. et al., Book of Papers, Pira Paper and Board Fibramerics Programme, Vol. 1, Intl. Conference on Nonwovens in Healthcare Applications, Brighton, England, November 10-12 1987, pp. 1-19.

26. Wadsworth, L. C., Lee, Y., and Barboza, S. D., Book of Papers, INDA-TEC 1989, Philadelphia, PA, May 30-June 2 1989, pp. 585-600.

27. Choi, K. J. et al., Polymer Engineering and Science, Vol. 28, No. 2, 1988, pp. 81-89.

28. Malkan, S. R., et al., Nonwovens-An Advanced Tutorial (Turbak, A. F. and Vigo, T. L., Editors), TAPPI Press, Atlanta, GA, 1989, pp. 101-129.

29. Bodaghi, H., INDA Journal of Nonwovens Research, Vol. 1, No. 1, 1989, pp. 14.

30. Samuels, R. J., Journal of Polymer Science, Polymer Physics Edition, Vol. 13, 1975, pp. 1417-1446.

31. Straeffer, G. and Goswami, B. C., Book of Papers, INDA-TEC 1990, Baltimore, MD, June 5-8 1990, pp. 385-419.

32. Milligan, M. W. et al., Journal of Applied Polymer Science, Volume. 44, 1992, pp. 279-288.

33. Milligan, M. W. and Haynes, B. D., Paper Presented at the Winter Annual Meeting of the American Society of Mechanical Engineers, Boston, MA, December 13-18, 1987.

34. Haynes, B. D., Ph.D. Dissertation, The University of Tennessee, Knoxville, TN, September 1991, pp. 59-64.

35. Narasimhan, K. M. and Shaumbagh, R. L., Book of Papers, INDA-TEC 1987, Hilton Head, SC, May 18-21 1987, pp. 189-205.

36. Uyttendaele, M. A. and Shaumbagh, R. L., AIChE Journal, Vol. 36, No. 2, February 1992, pp. 175-186.

37. Majumdar, B. and Shaumbagh, R. L., Journal of Rheology, Vol. 34, No. 4, May 1990, pp. 591-601.

38. Milligan, M. W. and Haynes, B. D., American Society of Mechanical Engineers Publication, Vol. 54, pp. 47-50.
39. Milligan, M. W. et al., Nonwovens-An Advanced Tutorial (Turbak, A. F. and Vigo, T. L., Editors), TAPPI Press, Atlanta, GA, 1989.

40. Milligan, M. W., Book of Papers, INDA-TEC 1989, Philadelphia, PA, May 30-June 2 1989, pp. 573-583.

41. Anonymous, Flow Measurement, American Society of Mechanical Engineers, Power Test Code, PTC 19.5;4-1959.

42. Milligan, M. W. and Haynes, B. D., 1986 Annual Report to Exxon Chemical Company, The University of Tennessee, Knoxville, January 1987.

43. Kunze, B., Private Communication, Reifenhauser GmbH and Company, Troisdorf, Germany, September 1991.

44. Wadsworth, L. C. and Hill, G. J., Book of Papers, INDA 13th Annual Technical Symposium, Boston, MA, June 4-6 1985, pp. 41-54.

45. Han, C. D., Charles, M., and Philippoff, W., Transactions of the Society of Rheology, 14:3, 1970, pp. 393-408.

APPENDIXES

APPENDIX A- DIE SWELL STUDIES (INSTRON RHEOMETER)

Table A.1

Die Swell Data for Different Polymer Throughputs and L/D Ratios - Instron Rheometer

Temperature=240 ^{0}C; 400 MFR Polypropylene

Die Geometry	Cross Head Speed, Inches/min	Melt Pressure, psi	Polymer Throughput, g/min	Swell Diameter d, mm	Die Swell Ratio, d/D
L/D ratio=5; D=0.4mm	0.20	42.42	0.24	0.69	1.74
	0.50	76.35	0.64	0.73	1.82
	1.00	123.00	1.32	0.76	1.90
	2.00	186.64	2.68	0.79	1.98
L/D ratio=10; D=0.4mm	0.20	74.36	0.24	0.66	1.65
	0.50	101.81	0.64	0.69	1.74
	1.00	152.70	1.32	0.73	1.82
	2.00	229.06	2.68	0.76	1.90
L/D ratio=15; D=0.4mm	0.20	78.05	0.24	0.5953	1.488
	0.50	112.00	0.64	0.6284	1.571
	1.00	169.67	1.32	0.6610	1.6536
	2.00	250.26	2.68	0.6945	1.736

Table A.1 (Contd.)

Die Geometry	Cross Head Speed Inches/min	Melt Pressure, psi	Polymer Throughput, g/min	Swell Diameter d, mm	Die Swell Ratio, d/D
L/D ratio=20; D=0.4mm	0.20	78.05	0.24	0.529	1.323
	0.50	138.28	0.64	0.562	1.405
	1.00	220.57	1.32	0.595	1.488
	2.00	326.62	2.68	0.628	1.571
L/D ratio=10; D=0.25mm	0.20	220.58	0.24	0.463	1.72
	0.50	339.35	0.64	0.496	1.852
	1.00	453.88	1.32	0.529	1.984
	2.00	619.32	2.68	0.562	2.12
Step Die Entry region L/D=10; D=0.25 mm Exit Region L/D=5; D=0.4 mm	0.20	220.58	0.24	0.459	1.148
	0.50	339.35	0.64	0.488	1.220
	1.00	471.61	1.32	0.517	1.290
	2.00	649.85	2.68	0.545	1.363

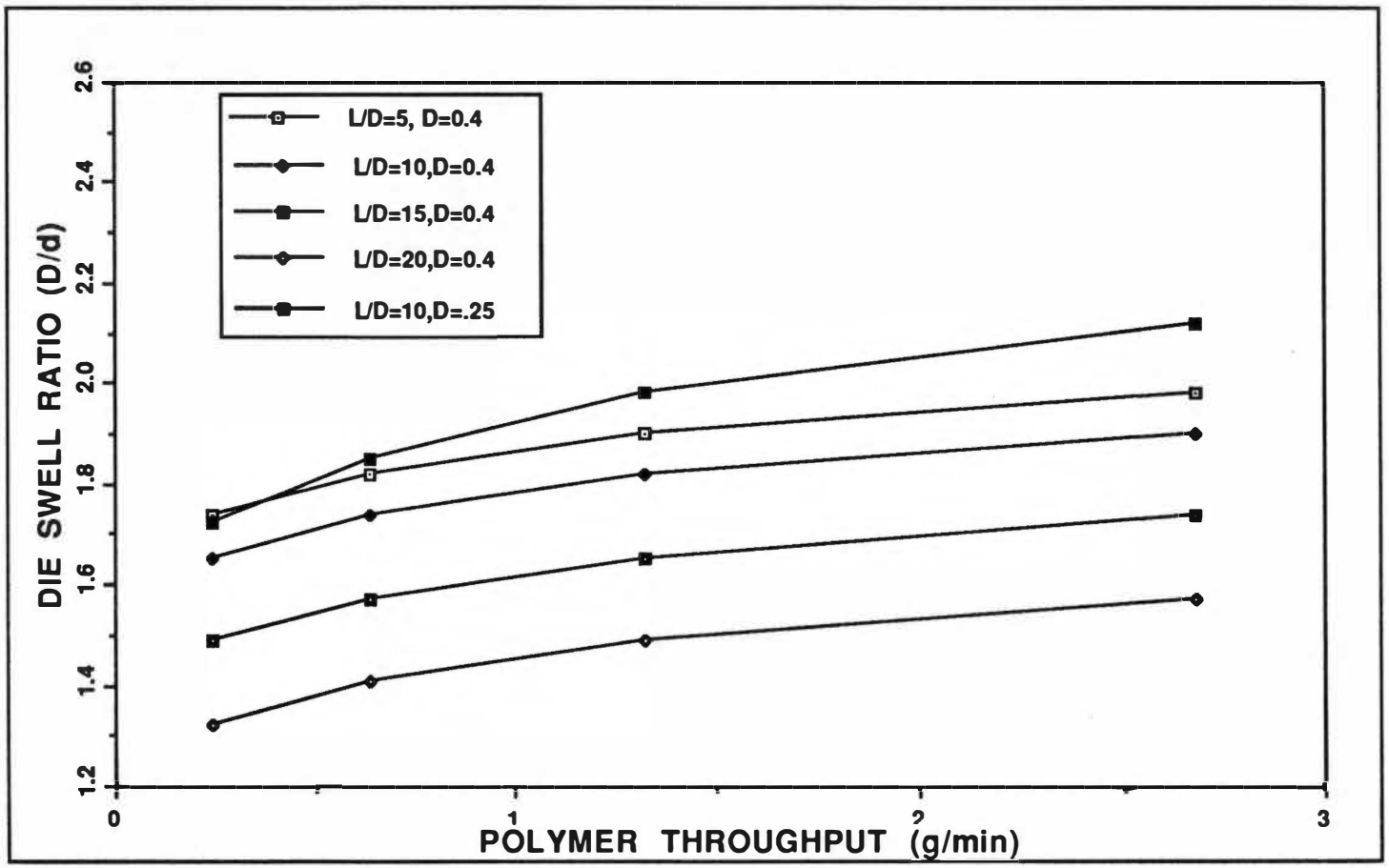


Figure A.1 Effect of polymer throughput and L/D ratio on die swell ratio

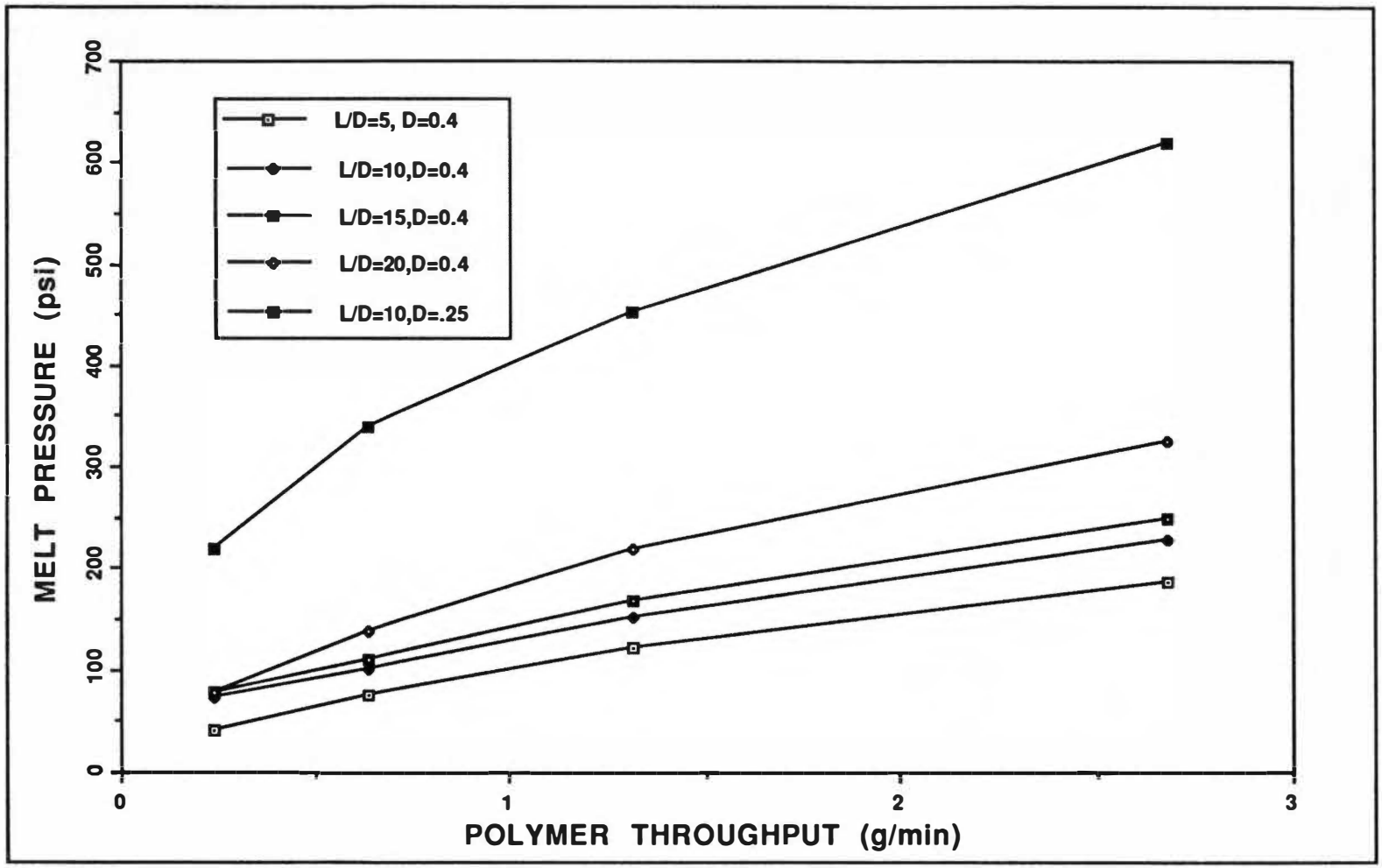


Figure A.2 Effect of polymer throughput and L/D ratio on melt pressure

APPENDIX B - STATISTICAL ANALYSES

Table B.1 Summary of Main Effects and Interactive Effects on the Response Variables - PHASE I

PARAMETER	MAIN EFFECTS	INTERACTIVE EFFECTS
1. Fiber Diameter	Hole Size Polymer throughput L/D Ratio	L/D Ratio*Air Gap MFR*Air Gap MFR*Hole Size Hole Size*Air Gap
2. Filtration Efficiency	L/D Ratio MFR Polymer throughput	Hole Size*L/D Ratio MFR*Hole Size MFR*Polymer Throughput Hole Size*Polymer Throughput
3. MD Web Tenacity	MFR Hole Size	MFR*Air Gap MFR*L/D Ratio
4. MD Elongation	Polymer Throughput MFR Air Gap Hole Size	Hole Size*L/D Ratio MFR*Polymer Throughput Hole Size*Polymer Throughput
5. Bursting Strength	Polymer Throughput MFR	Hole Size*L/D Ratio MFR*Air Gap
6. Shot	Polymer Throughput Hole Size L/D Ratio	Hole Size*L/D Ratio MFR*Air gap MFR*L/D Ratio Hole Size*Polymer Throughput
7.Fly	L/D Ratio	MFR*L/D Ratio MFR*Hole Size MFR*Air Gap Hole Size*L/D Ratio Hole Size*Air Gap Polymer Throughput*Air Gap
8. Weight average Molecular weight of the web	L/D ratio Hole Size Polymer Throughput	MFR*Hole Size Hole Size*L/D Ratio MFR*L/D Ratio

Table B.2

Summary of Main Effects and Interactive Effects on the Response Variables - PHASE II (Nosetip Setback Study)

PARAMETER	MAIN EFFECTS	INTERACTIVE EFFECTS
1. Fiber Diameter	Orifice Diameter Polymer Throughput	None
2. Shot Level	Polymer Throughput Orifice Diameter Nosetip Setback	L/D Ratio*Nosetip Setback

The SAS System
15:40 Wednesday, September 4, 1991

General Linear Models Procedure
Class Level Information

Class	Levels	Values
MFR	2	35 400
HOLESIZE	2	0.02 0.015
THRUPUT	2	0.4 0.8
LDRATIO	2	10 15
AIRGAP	2	0.110 0.035

Number of observations in data set = 32

General Linear Models Procedure

Dependent Variable: FIBERDIA

Source	DF	Sum of Squares	Mean Square	F Value	Pr > F
Model	15	4.0380219	0.2692015	4.64	0.0021
Error	16	0.9292000	0.0580750		
Corrected Total	31	4.9672219			

R-Square	C.V.	Root MSE	FIBERDIA Mean
0.812934	10.48484	0.2410	2.2984

Source	DF	Type I SS	Mean Square	F Value	Pr > F
HOLESIZE	1	0.8288281	0.8288281	14.27	0.0016
THRUPUT	1	0.3549031	0.3549031	6.11	0.0250
LDRATIO	1	0.3260281	0.3260281	5.61	0.0307
AIRGAP	1	0.0019531	0.0019531	0.03	0.8568
MFR	1	0.1001281	0.1001281	1.72	0.2077
MFR*HOLESIZE	1	0.5176531	0.5176531	8.91	0.0087
MFR*THRUPUT	1	0.1845281	0.1845281	3.18	0.0936
MFR*LDRATIO	1	0.0000781	0.0000781	0.00	0.9712
MFR*AIRGAP	1	0.6300031	0.6300031	10.85	0.0046
HOLESIZE*THRUPUT	1	0.0005281	0.0005281	0.01	0.9252
HOLESIZE*LDRATIO	1	0.0069031	0.0069031	0.12	0.7348
HOLESIZE*AIRGAP	1	0.3806281	0.3806281	6.55	0.0210
THRUPUT*LDRATIO	1	0.0225781	0.0225781	0.39	0.5417
THRUPUT*AIRGAP	1	0.0306281	0.0306281	0.53	0.4782
LDRATIO*AIRGAP	1	0.6526531	0.6526531	11.24	0.0040

Source	DF	Type III SS	Mean Square	F Value	Pr > F
HOLESIZE	1	0.8288281	0.8288281	14.27	0.0016
THRUPUT	1	0.3549031	0.3549031	6.11	0.0250
LDRATIO	1	0.3260281	0.3260281	5.61	0.0307
AIRGAP	1	0.0019531	0.0019531	0.03	0.8568
MFR	1	0.1001281	0.1001281	1.72	0.2077
MFR*HOLESIZE	1	0.5176531	0.5176531	8.91	0.0087
MFR*THRUPUT	1	0.1845281	0.1845281	3.18	0.0936
MFR*LDRATIO	1	0.0000781	0.0000781	0.00	0.9712
MFR*AIRGAP	1	0.6300031	0.6300031	10.85	0.0046
HOLESIZE*THRUPUT	1	0.0005281	0.0005281	0.01	0.9252
HOLESIZE*LDRATIO	1	0.0069031	0.0069031	0.12	0.7348
HOLESIZE*AIRGAP	1	0.3806281	0.3806281	6.55	0.0210
THRUPUT*LDRATIO	1	0.0225781	0.0225781	0.39	0.5417
THRUPUT*AIRGAP	1	0.0306281	0.0306281	0.53	0.4782
LDRATIO*AIRGAP	1	0.6526531	0.6526531	11.24	0.0040

General Linear Models Procedure

Dependent Variable: FILTEFF

Source	DF	Sum of Squares	Mean Square	F Value	Pr > F
Model	15	1603.7500	106.9167	7.99	0.0001
Error	16	214.1250	13.3828		
Corrected Total	31	1817.8750			

R-Square	C.V.	Root MSE	FILTEFF Mean
0.882211	4.754837	3.6583	76.938

Source	DF	Type I SS	Mean Square	F Value	Pr > F
HOLESIZE	1	2.00000	2.00000	0.15	0.7042
THRUPUT	1	136.12500	136.12500	10.17	0.0057
LDRATIO	1	300.12500	300.12500	22.43	0.0002
AIRGAP	1	12.50000	12.50000	0.93	0.3482
MFR	1	264.50000	264.50000	19.76	0.0004
MFR*HOLESIZE	1	300.12500	300.12500	22.43	0.0002
MFR*THRUPUT	1	112.50000	112.50000	8.41	0.0105
MFR*LDRATIO	1	4.50000	4.50000	0.34	0.5701
MFR*AIRGAP	1	1.12500	1.12500	0.08	0.7756
HOLESIZE*THRUPUT	1	72.00000	72.00000	5.38	0.0339
HOLESIZE*LDRATIO	1	312.50000	312.50000	23.35	0.0002
HOLESIZE*AIRGAP	1	36.12500	36.12500	2.70	0.1199
THRUPUT*LDRATIO	1	1.12500	1.12500	0.08	0.7756
THRUPUT*AIRGAP	1	40.50000	40.50000	3.03	0.1011
LDRATIO*AIRGAP	1	8.00000	8.00000	0.60	0.4507

Source	DF	Type III SS	Mean Square	F Value	Pr > F
HOLESIZE	1	2.00000	2.00000	0.15	0.7042
THRUPUT	1	136.12500	136.12500	10.17	0.0057
LDRATIO	1	300.12500	300.12500	22.43	0.0002
AIRGAP	1	12.50000	12.50000	0.93	0.3482
MFR	1	264.50000	264.50000	19.76	0.0004
MFR*HOLESIZE	1	300.12500	300.12500	22.43	0.0002
MFR*THRUPUT	1	112.50000	112.50000	8.41	0.0105
MFR*LDRATIO	1	4.50000	4.50000	0.34	0.5701
MFR*AIRGAP	1	1.12500	1.12500	0.08	0.7756
HOLESIZE*THRUPUT	1	72.00000	72.00000	5.38	0.0339
HOLESIZE*LDRATIO	1	312.50000	312.50000	23.35	0.0002
HOLESIZE*AIRGAP	1	36.12500	36.12500	2.70	0.1199
THRUPUT*LDRATIO	1	1.12500	1.12500	0.08	0.7756
THRUPUT*AIRGAP	1	40.50000	40.50000	3.03	0.1011
LDRATIO*AIRGAP	1	8.00000	8.00000	0.60	0.4507

General Linear Models Procedure.

Dependent Variable: TENACITY

Source	DF	Sum of Squares	Mean Square	F Value	Pr > F
Model	15	0.0577015	0.0038468	6.74	0.0002
Error	16	0.0091365	0.0005710		
Corrected Total	31	0.0668380			

R-Square	C.V.	Root MSE	TENACITY Mean
0.863304	17.60314	0.0239	0.1358

Source	DF	Type I SS	Mean Square	F Value	Pr > F
HOLESIZE	1	0.0034445	0.0034445	6.03	0.0259
THRUPUT	1	0.0000005	0.0000005	0.00	0.9768
LDRATIO	1	0.0000005	0.0000005	0.00	0.9768
AIRGAP	1	0.0000080	0.0000080	0.01	0.9073
MFR	1	0.0383645	0.0383645	67.18	0.0001
MFR*HOLESIZE	1	0.0000980	0.0000980	0.17	0.6842
MFR*THRUPUT	1	0.0000180	0.0000180	0.03	0.8613
MFR*LDRATIO	1	0.0036980	0.0036980	6.48	0.0216
MFR*AIRGAP	1	0.0093845	0.0093845	16.43	0.0009
HOLESIZE*THRUPUT	1	0.0014580	0.0014580	2.55	0.1296
HOLESIZE*LDRATIO	1	0.0004500	0.0004500	0.79	0.3878
HOLESIZE*AIRGAP	1	0.0004805	0.0004805	0.84	0.3726
THRUPUT*LDRATIO	1	0.0000180	0.0000180	0.03	0.8613
THRUPUT*AIRGAP	1	0.0001805	0.0001805	0.32	0.5818
LDRATIO*AIRGAP	1	0.0000980	0.0000980	0.17	0.6842

Source	DF	Type III SS	Mean Square	F Value	Pr > F
HOLESIZE	1	0.0034445	0.0034445	6.03	0.0259
THRUPUT	1	0.0000005	0.0000005	0.00	0.9768
LDRATIO	1	0.0000005	0.0000005	0.00	0.9768
AIRGAP	1	0.0000080	0.0000080	0.01	0.9073
MFR	1	0.0383645	0.0383645	67.18	0.0001
MFR*HOLESIZE	1	0.0000980	0.0000980	0.17	0.6842
MFR*THRUPUT	1	0.0000180	0.0000180	0.03	0.8613
MFR*LDRATIO	1	0.0036980	0.0036980	6.48	0.0216
MFR*AIRGAP	1	0.0093845	0.0093845	16.43	0.0009
HOLESIZE*THRUPUT	1	0.0014580	0.0014580	2.55	0.1296
HOLESIZE*LDRATIO	1	0.0004500	0.0004500	0.79	0.3878
HOLESIZE*AIRGAP	1	0.0004805	0.0004805	0.84	0.3726
THRUPUT*LDRATIO	1	0.0000180	0.0000180	0.03	0.8613
THRUPUT*AIRGAP	1	0.0001805	0.0001805	0.32	0.5818
LDRATIO*AIRGAP	1	0.0000980	0.0000980	0.17	0.6842

General Linear Models Procedure

Dependent Variable: ELONGTN

Source	DF	Sum of Squares	Mean Square	F Value	Pr > F
Model	15	2361.9817	157.4654	5.43	0.0008
Error	16	463.9596	28.9975		
Corrected Total	31	2825.9413			

R-Square	C.V.	Root MSE	ELONGTN Mean
0.835821	30.51492	5.3849	17.647

Source	DF	Type I SS	Mean Square	F Value	Pr > F
HOLESIZE	1	126.9621	126.9621	4.38	0.0527
THRUPUT	1	1062.1441	1062.1441	36.63	0.0001
LDRATIO	1	2.0100	2.0100	0.07	0.7957
AIRGAP	1	166.8964	166.8964	5.76	0.0290
MFR	1	284.1728	284.1728	9.80	0.0065
MFR*HOLESIZE	1	4.7432	4.7432	0.16	0.6912
MFR*THRUPUT	1	124.7410	124.7410	4.30	0.0546
MFR*LDRATIO	1	0.1152	0.1152	0.00	0.9505
MFR*AIRGAP	1	15.5403	15.5403	0.54	0.4747
HOLESIZE*THRUPUT	1	122.7744	122.7744	4.23	0.0563
HOLESIZE*LDRATIO	1	313.6260	313.6260	10.82	0.0046
HOLESIZE*AIRGAP	1	1.9208	1.9208	0.07	0.8002
THRUPUT*LDRATIO	1	7.1064	7.1064	0.25	0.6273
THRUPUT*AIRGAP	1	50.8536	50.8536	1.75	0.2040
LDRATIO*AIRGAP	1	78.3752	78.3752	2.70	0.1197

Source	DF	Type III SS	Mean Square	F Value	Pr > F
HOLESIZE	1	126.9621	126.9621	4.38	0.0527
THRUPUT	1	1062.1441	1062.1441	36.63	0.0001
LDRATIO	1	2.0100	2.0100	0.07	0.7957
AIRGAP	1	166.8964	166.8964	5.76	0.0290
MFR	1	284.1728	284.1728	9.80	0.0065
MFR*HOLESIZE	1	4.7432	4.7432	0.16	0.6912
MFR*THRUPUT	1	124.7410	124.7410	4.30	0.0546
MFR*LDRATIO	1	0.1152	0.1152	0.00	0.9505
MFR*AIRGAP	1	15.5403	15.5403	0.54	0.4747
HOLESIZE*THRUPUT	1	122.7744	122.7744	4.23	0.0563
HOLESIZE*LDRATIO	1	313.6260	313.6260	10.82	0.0046
HOLESIZE*AIRGAP	1	1.9208	1.9208	0.07	0.8002
THRUPUT*LDRATIO	1	7.1064	7.1064	0.25	0.6273
THRUPUT*AIRGAP	1	50.8536	50.8536	1.75	0.2040
LDRATIO*AIRGAP	1	78.3752	78.3752	2.70	0.1197

General Linear Models Procedure

Dependent Variable: BSTRNGTH

Source	DF	Sum of Squares	Mean Square	F Value	Pr > F
Model	15	4403.7769	293.5851	2.34	0.0509
Error	16	2006.6360	125.4148		
Corrected Total	31	6410.4129			

R-Square	C.V.	Root MSE	BSTRNGTH Mean
0.686972	21.66414	11.199	51.693

Source	DF	Type I SS	Mean Square	F Value	Pr > F
HOLESIZE	1	61.4386	61.4386	0.49	0.4940
THRUPUT	1	1301.7753	1301.7753	10.38	0.0053
LDRATIO	1	32.3208	32.3208	0.26	0.6186
AIRGAP	1	445.5112	445.5112	3.55	0.0778
MFR	1	1045.6165	1045.6165	8.34	0.0107
MFR*HOLESIZE	1	36.2101	36.2101	0.29	0.5984
MFR*THRUPUT	1	87.6488	87.6488	0.70	0.4155
MFR*LDRATIO	1	41.8155	41.8155	0.33	0.5717
MFR*AIRGAP	1	547.3086	547.3086	4.36	0.0530
HOLESIZE*THRUPUT	1	54.8628	54.8628	0.44	0.5178
HOLESIZE*LDRATIO	1	609.7032	609.7032	4.86	0.0424
HOLESIZE*AIRGAP	1	16.8200	16.8200	0.13	0.7190
THRUPUT*LDRATIO	1	4.4105	4.4105	0.04	0.8536
THRUPUT*AIRGAP	1	60.5000	60.5000	0.48	0.4973
LDRATIO*AIRGAP	1	57.8350	57.8350	0.46	0.5068

Source	DF	Type III SS	Mean Square	F Value	Pr > F
HOLESIZE	1	61.4386	61.4386	0.49	0.4940
THRUPUT	1	1301.7753	1301.7753	10.38	0.0053
LDRATIO	1	32.3208	32.3208	0.26	0.6186
AIRGAP	1	445.5112	445.5112	3.55	0.0778
MFR	1	1045.6165	1045.6165	8.34	0.0107
MFR*HOLESIZE	1	36.2101	36.2101	0.29	0.5984
MFR*THRUPUT	1	87.6488	87.6488	0.70	0.4155
MFR*LDRATIO	1	41.8155	41.8155	0.33	0.5717
MFR*AIRGAP	1	547.3086	547.3086	4.36	0.0530
HOLESIZE*THRUPUT	1	54.8628	54.8628	0.44	0.5178
HOLESIZE*LDRATIO	1	609.7032	609.7032	4.86	0.0424
HOLESIZE*AIRGAP	1	16.8200	16.8200	0.13	0.7190
THRUPUT*LDRATIO	1	4.4105	4.4105	0.04	0.8536
THRUPUT*AIRGAP	1	60.5000	60.5000	0.48	0.4973
LDRATIO*AIRGAP	1	57.8350	57.8350	0.46	0.5068

General Linear Models Procedure

Dependent Variable: AIRPERM

Source	DF	Sum of Squares	Mean Square	F Value	Pr > F
Model	15	67137.228	4475.815	1.39	0.2608
Error	16	51569.751	3223.109		
Corrected Total	31	118706.979			

R-Square	C.V.	Root MSE	AIRPERM Mean
0.565571	45.43840	56.772	124.94

Source	DF	Type I SS	Mean Square	F Value	Pr > F
HOLESIZE	1	76.261	76.261	0.02	0.8797
THRUPUT	1	7092.405	7092.405	2.20	0.1574
LDRATIO	1	2346.125	2346.125	0.73	0.4062
AIRGAP	1	8917.801	8917.801	2.77	0.1157
MFR	1	55.125	55.125	0.02	0.8976
MFR*HOLESIZE	1	14044.880	14044.880	4.36	0.0532
MFR*THRUPUT	1	98.701	98.701	0.03	0.8633
MFR*LDRATIO	1	2552.551	2552.551	0.79	0.3867
MFR*AIRGAP	1	8077.205	8077.205	2.51	0.1330
HOLESIZE*THRUPUT	1	23.120	23.120	0.01	0.9336
HOLESIZE*LDRATIO	1	13811.220	13811.220	4.29	0.0550
HOLESIZE*AIRGAP	1	4338.461	4338.461	1.35	0.2630
THRUPUT*LDRATIO	1	51.511	51.511	0.02	0.9010
THRUPUT*AIRGAP	1	591.680	591.680	0.18	0.6740
LDRATIO*AIRGAP	1	5060.180	5060.180	1.57	0.2282

Source	DF	Type III SS	Mean Square	F Value	Pr > F
HOLESIZE	1	76.261	76.261	0.02	0.8797
THRUPUT	1	7092.405	7092.405	2.20	0.1574
LDRATIO	1	2346.125	2346.125	0.73	0.4062
AIRGAP	1	8917.801	8917.801	2.77	0.1157
MFR	1	55.125	55.125	0.02	0.8976
MFR*HOLESIZE	1	14044.880	14044.880	4.36	0.0532
MFR*THRUPUT	1	98.701	98.701	0.03	0.8633
MFR*LDRATIO	1	2552.551	2552.551	0.79	0.3867
MFR*AIRGAP	1	8077.205	8077.205	2.51	0.1330
HOLESIZE*THRUPUT	1	23.120	23.120	0.01	0.9336
HOLESIZE*LDRATIO	1	13811.220	13811.220	4.29	0.0550
HOLESIZE*AIRGAP	1	4338.461	4338.461	1.35	0.2630
THRUPUT*LDRATIO	1	51.511	51.511	0.02	0.9010
THRUPUT*AIRGAP	1	591.680	591.680	0.18	0.6740
LDRATIO*AIRGAP	1	5060.180	5060.180	1.57	0.2282

General Linear Models Procedure

Dependent Variable: SHOT

Source	DF	Sum of Squares	Mean Square	F Value	Pr > F
Model	15	23.718750	1.581250	4.60	0.0021
Error	16	5.500000	0.343750		
Corrected Total	31	29.218750			

R-Square	C.V.	Root MSE	SHOT Mean
0.811765	43.63177	0.5863	1.3438

Source	DF	Type I SS	Mean Square	F Value	Pr > F
HOLESIZE	1	2.5312500	2.5312500	7.36	0.0153
THRUPUT	1	5.2812500	5.2812500	15.36	0.0012
LDRATIO	1	2.5312500	2.5312500	7.36	0.0153
AIRGAP	1	0.7812500	0.7812500	2.27	0.1512
MFR	1	0.2812500	0.2812500	0.82	0.3791
MFR*HOLESIZE	1	0.0312500	0.0312500	0.09	0.7669
MFR*THRUPUT	1	0.0312500	0.0312500	0.09	0.7669
MFR*LDRATIO	1	1.5312500	1.5312500	4.45	0.0509
MFR*AIRGAP	1	2.5312500	2.5312500	7.36	0.0153
HOLESIZE*THRUPUT	1	1.5312500	1.5312500	4.45	0.0509
HOLESIZE*LDRATIO	1	5.2812500	5.2812500	15.36	0.0012
HOLESIZE*AIRGAP	1	0.0312500	0.0312500	0.09	0.7669
THRUPUT*LDRATIO	1	0.2812500	0.2812500	0.82	0.3791
THRUPUT*AIRGAP	1	0.7812500	0.7812500	2.27	0.1512
LDRATIO*AIRGAP	1	0.2812500	0.2812500	0.82	0.3791

Source	DF	Type III SS	Mean Square	F Value	Pr > F
HOLESIZE	1	2.5312500	2.5312500	7.36	0.0153
THRUPUT	1	5.2812500	5.2812500	15.36	0.0012
LDRATIO	1	2.5312500	2.5312500	7.36	0.0153
AIRGAP	1	0.7812500	0.7812500	2.27	0.1512
MFR	1	0.2812500	0.2812500	0.82	0.3791
MFR*HOLESIZE	1	0.0312500	0.0312500	0.09	0.7669
MFR*THRUPUT	1	0.0312500	0.0312500	0.09	0.7669
MFR*LDRATIO	1	1.5312500	1.5312500	4.45	0.0509
MFR*AIRGAP	1	2.5312500	2.5312500	7.36	0.0153
HOLESIZE*THRUPUT	1	1.5312500	1.5312500	4.45	0.0509
HOLESIZE*LDRATIO	1	5.2812500	5.2812500	15.36	0.0012
HOLESIZE*AIRGAP	1	0.0312500	0.0312500	0.09	0.7669
THRUPUT*LDRATIO	1	0.2812500	0.2812500	0.82	0.3791
THRUPUT*AIRGAP	1	0.7812500	0.7812500	2.27	0.1512
LDRATIO*AIRGAP	1	0.2812500	0.2812500	0.82	0.3791

General Linear Models Procedure

Dependent Variable: FLY

Source	DF	Sum of Squares	Mean Square	F Value	Pr > F
Model	15	23.250000	1.550000	3.74	0.0063
Error	16	6.625000	0.414063		
Corrected Total	31	29.875000			

R-Square	C.V.	Root MSE	FLY Mean
0.778243	68.63753	0.6435	0.9375

Source	DF	Type I SS	Mean Square	F Value	Pr > F
HOLESIZE	1	0.5000000	0.5000000	1.21	0.2881
THRUPUT	1	0.5000000	0.5000000	1.21	0.2881
LDRATIO	1	3.1250000	3.1250000	7.55	0.0143
AIRGAP	1	1.1250000	1.1250000	2.72	0.1188
MFR	1	0.5000000	0.5000000	1.21	0.2881
MFR*HOLESIZE	1	3.1250000	3.1250000	7.55	0.0143
MFR*THRUPUT	1	0.1250000	0.1250000	0.30	0.5903
MFR*LDRATIO	1	4.5000000	4.5000000	10.87	0.0046
MFR*AIRGAP	1	2.0000000	2.0000000	4.83	0.0430
HOLESIZE*THRUPUT	1	0.1250000	0.1250000	0.30	0.5903
HOLESIZE*LDRATIO	1	2.0000000	2.0000000	4.83	0.0430
HOLESIZE*AIRGAP	1	2.0000000	2.0000000	4.83	0.0430
THRUPUT*LDRATIO	1	2.0000000	2.0000000	4.83	0.0430
THRUPUT*AIRGAP	1	0.5000000	0.5000000	1.21	0.2881
LDRATIO*AIRGAP	1	1.1250000	1.1250000	2.72	0.1188

Source	DF	Type III SS	Mean Square	F Value	Pr > F
HOLESIZE	1	0.5000000	0.5000000	1.21	0.2881
THRUPUT	1	0.5000000	0.5000000	1.21	0.2881
LDRATIO	1	3.1250000	3.1250000	7.55	0.0143
AIRGAP	1	1.1250000	1.1250000	2.72	0.1188
MFR	1	0.5000000	0.5000000	1.21	0.2881
MFR*HOLESIZE	1	3.1250000	3.1250000	7.55	0.0143
MFR*THRUPUT	1	0.1250000	0.1250000	0.30	0.5903
MFR*LDRATIO	1	4.5000000	4.5000000	10.87	0.0046
MFR*AIRGAP	1	2.0000000	2.0000000	4.83	0.0430
HOLESIZE*THRUPUT	1	0.1250000	0.1250000	0.30	0.5903
HOLESIZE*LDRATIO	1	2.0000000	2.0000000	4.83	0.0430
HOLESIZE*AIRGAP	1	2.0000000	2.0000000	4.83	0.0430
THRUPUT*LDRATIO	1	2.0000000	2.0000000	4.83	0.0430
THRUPUT*AIRGAP	1	0.5000000	0.5000000	1.21	0.2881
LDRATIO*AIRGAP	1	1.1250000	1.1250000	2.72	0.1188

General Linear Models Procedure

Dependent Variable: MWWA

Source	DF	Sum of Squares	Mean Square	F Value	Pr > F
Model	15	9.933E+09	6.622E+08	63.33	0.0001
Error	16	1.673E+08	1.046E+07		
Corrected Total	31	1.010E+10			

R-Square	C.V.	Root MSE	MWWA Mean
0.983437	3.646003	3233.5	88686

Source	DF	Type I SS	Mean Square	F Value	Pr > F
HOLESIZE	1	9.119E+07	9.119E+07	8.72	0.0093
THRUPUT	1	5.861E+07	5.861E+07	5.61	0.0308
LDRATIO	1	1.293E+08	1.293E+08	12.37	0.0029
AIRGAP	1	1.118E+06	1.118E+06	0.11	0.7479
MFR	1	9.185E+09	9.185E+09	878.45	0.0001
MFR*HOLESIZE	1	2.003E+08	2.003E+08	19.16	0.0005
MFR*THRUPUT	1	1.417E+06	1.417E+06	0.14	0.7176
MFR*LDRATIO	1	8.171E+07	8.171E+07	7.82	0.0130
MFR*AIRGAP	1	1.702E+06	1.702E+06	0.16	0.6920
HOLESIZE*THRUPUT	1	8.456E+04	8.456E+04	0.01	0.9295
HOLESIZE*LDRATIO	1	1.719E+08	1.719E+08	16.44	0.0009
HOLESIZE*AIRGAP	1	2.129E+06	2.129E+06	0.20	0.6579
THRUPUT*LDRATIO	1	6.177E+06	6.177E+06	0.59	0.4533
THRUPUT*AIRGAP	1	8.093E+05	8.093E+05	0.08	0.7844
LDRATIO*AIRGAP	1	1.429E+06	1.429E+06	0.14	0.7164

Source	DF	Type III SS	Mean Square	F Value	Pr > F
HOLESIZE	1	9.119E+07	9.119E+07	8.72	0.0093
THRUPUT	1	5.861E+07	5.861E+07	5.61	0.0308
LDRATIO	1	1.293E+08	1.293E+08	12.37	0.0029
AIRGAP	1	1.118E+06	1.118E+06	0.11	0.7479
MFR	1	9.185E+09	9.185E+09	878.45	0.0001
MFR*HOLESIZE	1	2.003E+08	2.003E+08	19.16	0.0005
MFR*THRUPUT	1	1.417E+06	1.417E+06	0.14	0.7176
MFR*LDRATIO	1	8.171E+07	8.171E+07	7.82	0.0130
MFR*AIRGAP	1	1.702E+06	1.702E+06	0.16	0.6920
HOLESIZE*THRUPUT	1	8.456E+04	8.456E+04	0.01	0.9295
HOLESIZE*LDRATIO	1	1.719E+08	1.719E+08	16.44	0.0009
HOLESIZE*AIRGAP	1	2.129E+06	2.129E+06	0.20	0.6579
THRUPUT*LDRATIO	1	6.177E+06	6.177E+06	0.59	0.4533
THRUPUT*AIRGAP	1	8.093E+05	8.093E+05	0.08	0.7844
LDRATIO*AIRGAP	1	1.429E+06	1.429E+06	0.14	0.7164

2X2 TABLES

General Linear Models Procedure
Least Squares Means

HOLESIZE	TENACITY LSMEAN
0.02	0.12537500
0.015	0.14612500

THRUPUT	FIBERDIA LSMEAN
0.4	2.19312500
0.8	2.40375000

THRUPUT	BSTRNGTH LSMEAN
0.4	58.0712500
0.8	45.3150000

AIRGAP	ELONGTN LSMEAN
0.110	15.3631250
0.035	19.9306250

MFR	HOLESIZE	FIBERDIA LSMEAN
35	0.02	2.20875000
35	0.015	2.27625000
400	0.02	2.06625000
400	0.015	2.64250000

MFR	HOLESIZE	FILTEFF LSMEAN
35	0.02	71.2500000
35	0.015	76.8750000
400	0.02	83.1250000
400	0.015	76.5000000

MFR	HOLESIZE	FLY LSMEAN
35	0.02	0.62500000
35	0.015	1.00000000
400	0.02	1.50000000
400	0.015	0.62500000

MFR	HOLESIZE	MWWA LSMEAN
35	0.02	106442.000
35	0.015	104814.250
400	0.02	67554.625
400	0.015	75934.750

MFR	THRUPUT	FILTEFF LSMEAN
35	0.4	78.0000000
35	0.8	70.1250000
400	0.4	80.0000000
400	0.8	79.6250000

MFR	THRUPUT	ELONGTN LSMEAN
35	0.4	28.3625000
35	0.8	12.8912500
400	0.4	18.4537500
400	0.8	10.8800000

MFR	LDRATIO	TENACITY LSMEAN
35	10	0.15975000
35	15	0.18100000
400	10	0.11200000
400	15	0.09025000

MFR	LDRATIO	SHOT LSMEAN
35	10	1.50000000
35	15	1.37500000
400	10	1.75000000
400	15	0.75000000

MFR	LDRATIO	FLY LSMEAN
35	10	0.87500000
35	15	0.75000000
400	10	0.37500000
400	15	1.75000000

MFR	LDRATIO	MWWA LSMEAN
35	10	106040.625
35	15	105215.625
400	10	75353.125
400	15	68136.250

MFR	AIRGAP	FIBERDIA LSMEAN
35	0.110	2.37500000
35	0.035	2.11000000
400	0.110	2.20625000
400	0.035	2.50250000

MFR	AIRGAP	TENACITY LSMEAN
35	0.110	0.18700000
35	0.035	0.15375000
400	0.110	0.08350000
400	0.035	0.11875000

MFR	AIRGAP	BSTRNGTH LSMEAN
35	0.110	57.8137500
35	0.035	57.0050000
400	0.110	38.1100000
400	0.035	53.8437500

MFR	AIRGAP	SHOT LSMEAN
35	0.110	1.00000000
35	0.035	1.87500000
400	0.110	1.37500000
400	0.035	1.12500000

MFR	AIRGAP	FLY LSMEAN
35	0.110	0.75000000
35	0.035	0.87500000
400	0.110	1.50000000
400	0.035	0.62500000

HOLESIZE	THRUPUT	FILTEFF LSMEAN
0.02	0.4	77.7500000
0.02	0.8	76.6250000
0.015	0.4	80.2500000
0.015	0.8	73.1250000

HOLESIZE	THRUPUT	ELONGTN LSMEAN
0.02	0.4	23.4412500
0.02	0.8	15.8362500
0.015	0.4	23.3750000
0.015	0.8	7.9350000

HOLESIZE	THRUPUT	SHOT LSMEAN
0.02	0.4	0.87500000
0.02	0.8	1.25000000
0.015	0.4	1.00000000
0.015	0.8	2.25000000

HOLESIZE	LDRATIO	FILTEFF LSMEAN
0.02	10	71.0000000
0.02	15	83.3750000
0.015	10	76.7500000
0.015	15	76.6250000

HOLESIZE	LDRATIO	ELONGTN LSMEAN
0.02	10	16.2575000
0.02	15	23.0200000
0.015	10	18.5350000
0.015	15	12.7750000

HOLESIZE	LDRATIO	BSTRNGTH LSMEAN
0.02	10	47.7087500
0.02	15	58.4487500
0.015	10	53.6675000
0.015	15	46.9475000

HOLESIZE	LDRATIO	SHOT LSMEAN
0.02	10	1.75000000
0.02	15	0.37500000
0.015	10	1.50000000
0.015	15	1.75000000

HOLESIZE	LDRATIO	FLY LSMEAN
0.02	10	0.50000000
0.02	15	1.62500000
0.015	10	0.75000000
0.015	15	0.87500000

HOLESIZE	LDRATIO	MWWA LSMEAN
0.02	10	91326.3750
0.02	15	82670.2500
0.015	10	90067.3750
0.015	15	90681.6250

HOLESIZE	AIRGAP	FIBERDIA LSMEAN
0.02	0.110	2.23875000
0.02	0.035	2.03625000
0.015	0.110	2.34250000
0.015	0.035	2.57625000

HOLESIZE	AIRGAP	FLY LSMEAN
0.02	0.110	1.00000000
0.02	0.035	1.12500000
0.015	0.110	1.25000000
0.015	0.035	0.37500000

THRUPUT	AIRGAP	FLY LSMEAN
0.4	0.110	1.37500000
0.4	0.035	0.75000000
0.8	0.110	0.87500000
0.8	0.035	0.75000000

LDRATIO	AIRGAP	FIBERDIA LSMEAN
10	0.110	2.24875000
10	0.035	2.55000000
15	0.110	2.33250000
15	0.035	2.06250000

General Linear Models Procedure
Class Level Information

Class	Levels	Values
SETBACK	5	5 -5 -18 -28 -39
POLTHPUT	5	2 0.4 0.8 1.2 1.6
ORIDIAM	2	15 20
LDRATIO	2	10 15

Number of observations in data set = 40

General Linear Models Procedure

Dependent Variable: FIBERDIA

Source	DF	Sum of Squares	Mean Square	F Value	Pr > F
Model	11	2.0222606	0.1838419	5.13	0.0002
Error	28	1.0031169	0.0358256		
Corrected Total	39	3.0253775			

R-Square	C.V.	Root MSE	FIBERDIA Mean
0.668432	8.026144	0.1893	2.3583

Source	DF	Type I SS	Mean Square	F Value	Pr > F
SETBACK	4	0.3282400	0.0820600	2.29	0.0846
POLTHPUT	4	1.1482579	0.2870645	8.01	0.0002
ORIDIAM	1	0.4906225	0.4906225	13.69	0.0009
LDRATIO	1	0.0251567	0.0251567	0.70	0.4091
ORIDIAM*LDRATIO	1	0.0299834	0.0299834	0.84	0.3681

Source	DF	Type III SS	Mean Square	F Value	Pr > F
SETBACK	4	0.3733290	0.0933323	2.61	0.0572
POLTHPUT	4	1.0813810	0.2703453	7.55	0.0003
ORIDIAM	1	0.4906225	0.4906225	13.69	0.0009
LDRATIO	1	0.0233202	0.0233202	0.65	0.4266
ORIDIAM*LDRATIO	1	0.0299834	0.0299834	0.84	0.3681

General Linear Models Procedure

Dependent Variable: FIBERDIA

Source	DF	Sum of Squares	Mean Square	F Value	Pr > F
Model	6	1.9425487	0.3237581	9.87	0.0001
Error	33	1.0828288	0.0328130		
Corrected Total	39	3.0253775			

R-Square	C.V.	Root MSE	FIBERDIA Mean
0.642085	7.681271	0.1811	2.3583

Source	DF	Type I SS	Mean Square	F Value	Pr > F
POLTHPUT	1	0.3524513	0.3524513	10.74	0.0025
POLTHPUT*POLTHPUT	1	0.7772223	0.7772223	23.69	0.0001
ORIDIAM	1	0.4906225	0.4906225	14.95	0.0005
LDRATIO	1	0.0238898	0.0238898	0.73	0.3997
ORIDIAM*LDRATIO	1	0.0000187	0.0000187	0.00	0.9811
SETBACK	1	0.2983441	0.2983441	9.09	0.0049

Source	DF	Type III SS	Mean Square	F Value	Pr > F
POLTHPUT	1	0.9789877	0.9789877	29.84	0.0001
POLTHPUT*POLTHPUT	1	0.7919971	0.7919971	24.14	0.0001
ORIDIAM	1	0.0053786	0.0053786	0.16	0.6882
LDRATIO	1	0.0016188	0.0016188	0.05	0.8256
ORIDIAM*LDRATIO	1	0.0039575	0.0039575	0.12	0.7306
SETBACK	1	0.2983441	0.2983441	9.09	0.0049

Parameter	Estimate	T for H0: Parameter=0	Pr > |T|	Std Error of Estimate
INTERCEPT	2.521705814	2.43	0.0209	1.03905493
POLTHPUT	-1.446835689	-5.46	0.0001	0.26488266
POLTHPUT*POLTHPUT	0.529948910	4.91	0.0001	0.10786862
ORIDIAM	0.024054133	0.40	0.6882	0.05941230
LDRATIO	-0.018357706	-0.22	0.8256	0.08265114
ORIDIAM*LDRATIO	0.001619669	0.35	0.7306	0.00466378
SETBACK	-0.005544603	-3.02	0.0049	0.00183880

General Linear Models Procedure

Dependent Variable: SHOT

Source	DF	Sum of Squares	Mean Square	F Value	Pr > F
Model	14	22.768960	1.626354	9.67	0.0001
Error	25	4.206040	0.168242		
Corrected Total	39	26.975000			

R-Square	C.V.	Root MSE	SHOT Mean
0.844076	14.78100	0.4102	2.7750

Source	DF	Type I SS	Mean Square	F Value	Pr > F
POLTHPUT	4	11.850000	2.962500	17.61	0.0001
ORIDIAM	1	1.225000	1.225000	7.28	0.0123
SETBACK	4	5.929257	1.482314	8.81	0.0001
LDRATIO	1	0.480366	0.480366	2.86	0.1035
LDRATIO*SETBACK	4	3.284337	0.821084	4.88	0.0048

Source	DF	Type III SS	Mean Square	F Value	Pr > F
POLTHPUT	4	13.418960	3.354740	19.94	0.0001
ORIDIAM	1	1.930227	1.930227	11.47	0.0023
SETBACK	4	6.026395	1.506599	8.95	0.0001
LDRATIO	1	0.513090	0.513090	3.05	0.0930
LDRATIO*SETBACK	4	3.284337	0.821084	4.88	0.0048

The SAS System
20:16 Monday, March 23, 1992

General Linear Models Procedure
Least Squares Means

SETBACK	FIBERDIA LSMEAN	Std Err LSMEAN	Pr > |T| H0:LSMEAN=0
5	2.18063703	0.06976688	0.0001
-5	2.36520715	0.07006550	0.0001
-18	2.32948016	0.06999194	0.0001
-28	2.46262761	0.06943043	0.0001
-39	2.45329805	0.06758459	0.0001

POLTHPUT	FIBERDIA LSMEAN	Std Err LSMEAN	Pr > |T| H0:LSMEAN=0
2	2.39602341	0.06756743	0.0001
0.4	2.66149657	0.06862431	0.0001
0.8	2.33592939	0.06759797	0.0001
1.2	2.19084558	0.06756777	0.0001
1.6	2.20695505	0.06894580	0.0001

ORIDIAM	FIBERDIA LSMEAN	Std Err LSMEAN	Pr > |T| H0:LSMEAN=0
15	2.24750000	0.04232352	0.0001
20	2.46900000	0.04232352	0.0001

LDRATIO	FIBERDIA LSMEAN	Std Err LSMEAN	Pr > |T| H0:LSMEAN=0
10	2.33377292	0.04261512	0.0001
15	2.38272708	0.04261512	0.0001

ORIDIAM	LDRATIO	FIBERDIA LSMEAN	Std Err LSMEAN	Pr > |T| H0:LSMEAN=0
15	10	2.25431761	0.06286104	0.0001
15	15	2.24068239	0.06286104	0.0001
20	10	2.41322824	0.06174325	0.0001
20	15	2.52477176	0.06174325	0.0001

General Linear Models Procedure
Least Squares Means

POLTHPUT	SHOT LSMEAN	Std Err LSMEAN	Pr > |T| H0:LSMEAN=0
2	3.64849118	0.14980668	0.0001
0.4	2.22252804	0.16207378	0.0001
0.8	1.95840443	0.14891547	0.0001
1.2	3.01970106	0.16133647	0.0001
1.6	3.02587529	0.15614888	0.0001

ORIDIAM	SHOT LSMEAN	Std Err LSMEAN	Pr > |T| H0:LSMEAN=0
15	2.52606647	0.09801663	0.0001
20	3.02393353	0.09801663	0.0001

SETBACK	SHOT LSMEAN	Std Err LSMEAN	Pr > |T| H0:LSMEAN=0
5	2.05351319	0.14667476	0.0001
-5	3.01554581	0.14669070	0.0001
-18	2.66512740	0.14678075	0.0001
-28	3.08652864	0.14667729	0.0001
-39	3.05428497	0.14657206	0.0001

LDRATIO	SHOT LSMEAN	Std Err LSMEAN	Pr > |T| H0:LSMEAN=0
10	2.89016736	0.09249398	0.0001
15	2.65983264	0.09249398	0.0001

LDRATIO	SETBACK	SHOT LSMEAN	Std Err LSMEAN	Pr > |T| H0:LSMEAN=0
10	5	2.63647884	0.22119707	0.0001
10	-5	3.18670850	0.21208618	0.0001
10	-18	2.89354630	0.22050568	0.0001
10	-28	2.98741525	0.21215756	0.0001
10	-39	2.74668792	0.21619868	0.0001
15	5	1.47054753	0.22081585	0.0001
15	-5	2.84438312	0.22094524	0.0001
15	-18	2.43670850	0.21208618	0.0001
15	-28	3.18564203	0.21111322	0.0001
15	-39	3.36188201	0.20842090	0.0001

APPENDIX C - PRIMARY AIR FLOW RATE AND VELOCITY DETERMINATION

PRIMARY AIR FLOW RATE AND VELOCITY DETERMINATION

The standardized volumetric flow rate of air was determined according to the American Society of Mechanical Engineers (ASME) standard procedure [41]. The following equation was used to calculate the air mass flow rate [41]:

$$W_h = 359\ C\ F\ d^2\ [\text{sq.root of } (Y\ h_w)] \qquad \text{(C-1)}$$

Where

W_h is the air mass flow rate in lb/hour,

C is the discharge coefficient,

d is the diameter of the orifice in inches,

h_w is the differential pressure in inches of water,

Y is the weight of air in lb/ft^3 entering the orifice, and

F is the velocity approach factor and is expressed as

$$F = 1/[\text{sq. root of } (1-b^4)]\ ;\ b = d/D \qquad \text{(C-2)}$$

Where

d is the orifice plate diameter and D is the pipe diameter.

The orifice diameter, d, is 1.335 inches and the pipe diameter, D, is 2.9 inches (ID). Therefore the diameter ratio b is 0.46. Evaluation of equation C-2 gives a velocity approach factor, F = 1.023. Thus, equation C-1 becomes:

$$W_h = 654.64\ C\ [\text{sq. root of } (Y\ h_w)] \qquad \text{(C-3)}$$

The specific weight of air entering the orifice, Y, can be determined from the ideal gas equation of state:

$$Y = P/RT \qquad \text{(C-4)}$$

Where

P is the absolute pressure in lb/ft^2,

T is the absolute temperature in ^oR, and

R is the gas constant of air, 53.34 ft-lb/lbm-^oR.

The absolute pressure upstream of the orifice is given by:

$$P_1 = P_2 + rgh_w + P_a \qquad \text{(C-5)}$$

Where

P_1 is the pressure upstream of orifice in psia,

P_2 is the pressure downstream of orifice in psig,

rg is the specific weight of Water, 0.0361 lb/in^3, and

P_a is the ambient pressure in psia.

The coefficient of discharge, c, is a function of b and the Reynolds number, R_e, based on inside diameter of the pipe. The expression for the Reynolds number is given by:

$$R_e = (Y\ V\ D)/\mu \qquad \text{(C-6)}$$

Where

V is the air velocity in the pipe in ft/sec,

μ is the dynamic viscosity of air in lb/ft-sec, and

D is the inside diameter of pipe in feet.

The viscosity of air is a function of the temperature. The viscosity in terms of the absolute temperature is given by the expression

$$\mu = 1.3183 \times 10^{-6}\, T^{1.5}/(T+200) \text{ lb/ft-sec} \qquad \text{(C-7)}$$

Equation C-8 gives the air velocity in the pipe:

$$V = W_h/[Y\,(\pi D^2/4) \times 3600) \qquad \text{(C-8)}$$

The air flow rate (equation C-3), can be converted to standard cubic feet per minute (SCFM) using a standard density, evaluated at P = 14.7 psia and T = 68 °F. The standard density of air at 68 °F is 0.07516 lb/ft^3. The volumetric flow rate of air, Q, in SCFM is given by:

$$Q = W_h/60\, Y_s \text{ in SCFM} \qquad \text{(C-9)}$$

Sample Calculation

The following is a sample calculation to compute the volumetric flow rate of air in SCFM at a given air valve opening. The following measured values at a given air valve opening will be used in this sample calculation [16]:

P_2 = 25 psig

T_1 = 100 °F

h_w = 10.5 inches of water

P_a = 14.5 psia (ambient pressure)

Step 1 Determine the pressure upstream of the orifice using equation C-5.

$P_1 = 25 + 0.0361\ (10.5) + 14.5 = 39.88$ psia

Step 2 Calculate the air density from equation C-4. The pressure should be in lb/ft^2 and the temperature in ^oR for consistency in units.

$P_1 = (39.88)\ (144) = 5742.6\ lb/ft^2$

$T_1 = 100 + 460 = 560\ ^oR$

$Y = 5742.61/[53.34(550)] = 0.20\ lb/ft^3$

Step 3 Assuming a value of 0.61 for the discharge coefficient c calculate the flow rate using equation C-3.

$W_h = 654.64(0.61)$ sq. root of $[10.5(0.20)] = 578.7$ lb/hour

Step 4 Calculate the air velocity in the pipe using equation C-8 with the pipe internal cross sectional area in ft^2.

$\pi D^2/4 = [\pi(2.9)^2/4] \times 1/144 = 0.0459\ ft^2$

$V = 578.7/[0.20(0.0459)]x1/3600 = 17.5$ ft/sec

Step 5 Calculate the volumetric flow rate of air in SCFM using equation C-9.

$Q = 578.85/60(0.07516) = 128.36$ SCFM

Determination of Actual Primary Air Velocity at the Air Knife Exit of 6-inch Melt Blown Die

Using the Standard flow rate of air in SCFM calculated at the orifice plate, the actual flow rate at the air knife exit can be calculated, knowing the actual air temperature and pressure at the die. The actual flow rate (ACFM) is essential to calculate the air velocity at the air knife exit, since air expands when heated. Assuming the hot air passing through the air knives at the die to follow the ideal gas law equation, the actual flow rate of air at the air knife exit, Q_a in ACFM is given by the equation:

$$Q_a = Q(T_a/T_s)(P_s/P_a) \qquad \text{(C-10)}$$

Where

Q is the standard air flow rate in SCFM at 14.5 psi and 70 ^oF,

T_a is the actual air temperature at the die in ^oR,

T_s is the standard air temperature, 530 ^oR,

P_s is the standard air pressure, 14.5 psia, and

P_a is the actual air pressure at the die in psia

actual air pressure=(14.5+stagnation pressure, psi)

For ACFM calculations, primary air temperature at the die and stagnation pressure in the air manifold were used.

The actual air velocity, V in ft/sec, at the die (air knife exit) is given by,

$V = Q_a$/air knife exit slot area (ft^2).

The momentum of the air at air knife exit is the product of the actual air velocity in ft/sec and the mass of air passing through the die per second.

APPENDIX D - MELT SHEAR VISCOSITY DATA [PHASE IV]

Table D.1 Melt Shear Viscosity Data (Newtonian) for 35 (PP3445) and 800 (PD 3545G) MFR Polypropylene Resins - Phase IV

[Parameters Measured Under Actual Melt Blowing Conditions]

Melt Flow Rate	Nosetip	Polymer Throughput (g/hole/min)	Pressure Drop (N/m^2)	Shear Stress (N/m^2)	Shear Viscosity Newt (Pa. Sec)	Shear Rate (sec^{-1})
35 Die temp 540° F	15 mil orifice diameter, 10/1 L/D	0.2	1.683×10^6	4.208×10^4	50.6	831.2
		0.4	2.483×10^6	6.208×10^4	37.3	1662.4
		0.8	3.711×10^6	9.278×10^4	27.9	3324.7
		1.2	4.891×10^6	1.223×10^5	24.5	4987.2
		1.6	5.656×10^6	1.414×10^5	21.3	6649.6
	15 mil orifice diameter, 15/1 L/D	0.2	2.18×10^6	3.633×10^4	43.7	831.2
		0.4	3.40×10^6	5.667×10^4	34.1	1662.4
		0.8	4.993×10^6	8.322×10^4	25.0	3324.7
		1.0	5.552×10^6	9.253×10^4	22.3	4156.0
35 Die temp 540° F	20 mil orifice diameter, 10/1 L/D	0.2	1.138×10^6	2.845×10^4	81.1	350.7
		0.4	1.752×10^6	4.380×10^4	62.5	701.3
		0.8	2.725×10^6	6.811×10^4	48.6	1402.6
		1.2	3.504×10^6	8.760×10^4	41.6	2103.9
	20 mil orifice diameter, 15/1 L/D	0.2	1.235×10^6	2.058×10^4	58.7	350.7
		0.4	1.980×10^6	3.30×10^4	47.1	701.3
		0.8	3.160×10^6	5.267×10^4	37.6	1402.6
		1.2	4.098×10^6	6.830×10^4	39.0	2103.9

Table D.1 (Contd.)

Melt Flow Rate	Nosetip	Polymer Throughput (g/hole/min)	Pressure Drop (N/m^2)	Shear Stress (N/m^2)	Shear Viscosity Newt (Pa. Sec)	Shear Rate (sec^{-1})
35 Die temp 560° F	15 mil orifice diameter, 10/1 L/D	0.2	1.566×10^6	3.916×10^4	47.1	831.2
		0.4	2.449×10^6	6.123×10^4	36.8	1662.4
		0.8	3.740×10^6	9.349×10^4	28.1	3324.7
		1.2	4.857×10^6	1.214×10^5	24.4	4987.2
		1.6	5.733×10^6	1.433×10^5	21.6	6649.6
	15 mil orifice diameter, 15/1 L/D	0.2	2.056×10^6	3.426×10^4	41.2	831.2
		0.4	3.345×10^6	5.576×10^4	33.5	1662.4
		0.8	4.732×10^6	7.886×10^4	23.7	3324.7
		1.0	5.420×10^6	9.033×10^4	21.7	4156.0
35 Die temp 560° F	20 mil orifice diameter, 10/1 L/D	0.2	9.450×10^5	2.362×10^4	67.4	350.7
		0.4	1.545×10^6	3.863×10^4	55.1	701.3
		0.8	2.580×10^6	6.449×10^4	46.0	1402.6
		1.2	3.359×10^6	8.398×10^4	39.9	2103.9
	20 mil orifice diameter, 15/1 L/D	0.2	1.09×10^6	1.816×10^4	51.8	350.7
		0.4	1.793×10^6	2.989×10^4	42.6	701.3
		0.8	3.00×10^6	5.0×10^4	35.6	1402.6
		1.2	3.863×10^6	6.438×10^4	30.6	2103.9

Table D.1 (Contd.)

Melt Flow Rate	Nosetip	Polymer Throughput (g/hole/min)	Pressure Drop (N/m^2)	Shear Stress (N/m^2)	Shear Viscosity Newt (Pa. Sec)	Shear Rate (sec^{-1})
35 Die temp 580^0 F	15 mil orifice diameter, 10/1 L/D	0.2	1.408×10^6	3.519×10^4	42.3	831.2
		0.4	2.277×10^6	5.692×10^4	34.2	1662.4
		0.8	3.629×10^6	9.073×10^4	27.3	3324.7
		1.2	4.485×10^6	1.121×10^5	22.5	4987.2
		1.6	5.319×10^6	1.330×10^5	20.0	6649.6
	15 mil orifice diameter, 15/1 L/D	0.2	1.821×10^6	3.036×10^4	36.5	831.2
		0.4	3.022×10^6	5.037×10^4	30.3	1662.4
		0.8	4.595×10^6	7.659×10^4	23.0	3324.7
		1.0	5.216×10^6	8.693×10^4	20.9	4156.0
35 Die temp 580^0 F	20 mil orifice diameter, 10/1 L/D	0.2	8.555×10^5	2.139×10^4	61.0	350.7
		0.4	1.483×10^6	3.709×10^4	52.9	701.3
		0.8	2.477×10^6	6.193×10^4	44.2	1402.6
		1.2	3.229×10^6	8.073×10^4	38.4	2103.9
	20 mil orifice diameter, 15/1 L/D	0.2	1.007×10^6	1.679×10^4	47.9	350.7
		0.4	1.656×10^6	2.76×10^4	39.4	701.3
		0.8	2.815×10^6	4.692×10^4	33.5	1402.6
		1.2	3.691×10^6	6.152×10^4	29.2	2103.9

Table D.1 (Contd.)

Melt Flow Rate	Nosetip	Polymer Throughput (g/hole/min)	Pressure Drop (N/m^2)	Shear Stress (N/m^2)	Shear Viscosity Newt (Pa. Sec)	Shear Rate (sec^{-1})
35 Die temp 600° F	15 mil orifice diameter, 10/1 L/D	0.2	1.104×10^6	2.760×10^4	33.2	831.2
		0.4	2.022×10^6	5.054×10^4	30.4	1662.4
		0.8	3.298×10^6	8.245×10^4	24.8	3324.7
		1.2	4.278×10^6	1.069×10^5	21.4	4987.2
		1.6	5.175×10^6	1.294×10^5	19.5	6649.6
	15 mil orifice diameter, 15/1 L/D	0.2	1.628×10^6	2.714×10^4	32.7	831.2
		0.4	2.787×10^6	4.646×10^4	27.9	1662.4
		0.8	4.450×10^6	7.417×10^4	22.3	3324.7
		1.0	5.085×10^6	8.475×10^4	20.4	4156.0
35 Die temp 600° F	20 mil orifice diameter, 10/1 L/D	0.2	7.865×10^5	1.966×10^4	56.1	350.7
		0.4	1.345×10^6	3.363×10^4	48.0	701.3
		0.8	2.347×10^6	5.868×10^4	41.8	1402.6
		1.2	3.195×10^6	7.988×10^4	38.0	2103.9
	20 mil orifice diameter, 15/1 L/D	0.2	8.831×10^5	1.472×10^4	42.0	350.7
		0.4	1.532×10^6	2.553×10^4	36.4	701.3
		0.8	2.642×10^6	4.404×10^4	31.4	1402.6
		1.2	3.622×10^6	6.037×10^4	28.7	2103.9

Table D.1 (Contd.)

Melt Flow Rate	Nosetip	Polymer Throughput (g/hole/min)	Pressure Drop (N/m^2)	Shear Stress (N/m^2)	Shear Viscosity Newt (Pa. Sec)	Shear Rate (sec^{-1})
35 Die temp 620° F	15 mil orifice diameter, 10/1 L/D	0.2	1.00×10^6	2.50×10^4	30.1	831.2
		0.4	1.807×10^6	4.518×10^4	27.2	1662.4
		0.8	3.104×10^6	7.760×10^4	23.3	3324.7
		1.2	4.118×10^6	1.029×10^5	20.6	4987.2
		1.6	5.021×10^6	1.255×10^5	18.9	6649.6
	15 mil orifice diameter, 15/1 L/D	0.2	1.303×10^6	2.172×10^4	26.1	831.2
		0.4	2.586×10^6	4.310×10^4	25.9	1662.4
		0.8	4.207×10^6	7.012×10^4	21.1	3324.7
		1.0	4.848×10^6	8.081×10^4	19.4	4156.0
35 Die temp 620° F	20 mil orifice diameter, 10/1 L/D	0.2	7.034×10^5	1.759×10^4	50.2	350.7
		0.4	1.193×10^6	2.983×10^4	42.5	701.3
		0.8	2.138×10^6	5.345×10^4	38.1	1402.6
		1.2	2.917×10^6	7.293×10^4	34.7	2103.9
	20 mil orifice diameter, 15/1 L/D	0.2	7.241×10^5	1.207×10^4	34.4	350.7
		0.4	1.317×10^6	2.195×10^4	31.3	701.3
		0.8	2.448×10^6	4.080×10^4	29.1	1402.6
		1.2	3.310×10^6	5.517×10^4	26.2	2103.9

Table D.1 (Contd.)

Melt Flow Rate	Nosetip	Polymer Throughput (g/hole/min)	Pressure Drop (N/m^2)	Shear Stress (N/m^2)	Shear Viscosity Newt (Pa. Sec)	Shear Rate (sec^{-1})
800 Die temp 480^0 F	15 mil orifice diameter, 10/1 L/D	0.4	6.208×10^5	1.552×10^4	9.34	1662.4
		0.8	9.657×10^5	2.414×10^4	7.26	3324.7
		1.2	1.248×10^6	3.121×10^4	6.26	4987.2
		1.6	1.586×10^6	3.966×10^4	5.96	6649.6
		2.0	1.904×10^6	4.759×10^4	5.73	8312
	15 mil orifice diameter, 15/1 L/D	0.4	6.967×10^5	1.161×10^4	6.98	1662.4
		0.8	1.131×10^6	1.885×10^4	5.67	3324.7
		1.2	1.517×10^6	2.529×10^4	5.07	4987.2
		1.6	1.876×10^6	3.127×10^4	4.7	6649.6
		2.0	2.276×10^6	3.794×10^4	4.56	8312
800 Die temp 480^0 F	20 mil orifice diameter, 10/1 L/D	0.4	3.035×10^5	7.587×10^3	10.82	701.3
		0.8	4.897×10^5	1.224×10^4	8.73	1402.6
		1.2	7.036×10^5	1.759×10^4	8.36	2103.9
		1.6	9.243×10^5	2.311×10^4	8.24	2805.2
		2.0	1.159×10^6	2.897×10^4	8.26	3506.5
	20 mil orifice diameter, 15/1 L/D	0.4	4.483×10^5	7.472×10^3	10.66	701.3
		0.8	7.173×10^5	1.196×10^4	8.52	1402.6
		1.2	9.381×10^5	1.563×10^4	7.43	2103.9
		1.6	1.159×10^6	1.931×10^4	6.88	2805.2
		2.0	1.393×10^6	2.322×10^4	6.62	3506.5

Table D.1 (Contd.)

Melt Flow Rate	Nosetip	Polymer Throughput (g/hole/min)	Pressure Drop (N/m^2)	Shear Stress (N/m^2)	Shear Viscosity Newt (Pa. Sec)	Shear Rate (sec^{-1})
800 Die temp 500^0 F	15 mil orifice diameter, 10/1 L/D	0.4	6.000×10^5	1.500×10^4	9.02	1662.4
		0.8	9.036×10^5	2.259×10^4	6.79	3324.7
		1.2	1.248×10^6	3.121×10^4	6.26	4987.2
		1.6	1.531×10^6	3.828×10^4	5.76	6649.6
		2.0	1.835×10^6	4.587×10^4	5.52	8312
	15 mil orifice diameter, 15/1 L/D	0.4	6.346×10^5	1.058×10^4	6.36	1662.4
		0.8	1.048×10^6	1.747×10^4	5.26	3324.7
		1.2	1.435×10^6	2.391×10^4	4.79	4987.2
		1.6	1.800×10^6	3.000×10^4	4.51	6649.6
		2.0	2.152×10^6	3.587×10^4	4.32	8312
800 Die temp 500^0 F	20 mil orifice diameter, 10/1 L/D	0.4	2.828×10^5	7.070×10^3	10.08	701.3
		0.8	4.897×10^5	1.224×10^4	8.73	1402.6
		1.2	7.173×10^5	1.793×10^4	8.52	2103.9
		1.6	9.105×10^5	2.276×10^4	8.11	2805.2
		2.0	1.117×10^6	2.794×10^4	7.97	3506.5
	20 mil orifice diameter, 15/1 L/D	0.4	4.208×10^5	7.013×10^3	10.0	701.3
		0.8	6.760×10^5	1.127×10^4	8.03	1402.6
		1.2	8.622×10^5	1.437×10^4	6.83	2103.9
		1.6	1.055×10^6	1.759×10^4	6.27	2805.2
		2.0	1.331×10^6	2.219×10^4	6.33	3506.5

Table D.1 (Contd.)

Melt Flow Rate	Nosetip	Polymer Throughput (g/hole/min)	Pressure Drop (N/m^2)	Shear Stress (N/m^2)	Shear Viscosity Newt (Pa. Sec)	Shear Rate (sec^{-1})
800 Die temp 520° F	15 mil orifice diameter, 10/1 L/D	0.4	5.587×10^5	1.397×10^4	8.40	1662.4
		0.8	8.829×10^5	2.207×10^4	6.64	3324.7
		1.2	1.179×10^6	2.949×10^4	5.91	4987.2
		1.6	1.442×10^6	3.604×10^4	5.42	6649.6
		2.0	1.759×10^6	4.397×10^4	5.29	8312
	15 mil orifice diameter, 15/1 L/D	0.4	5.863×10^5	9.772×10^3	5.88	1662.4
		0.8	1.007×10^6	1.678×10^4	5.05	3324.7
		1.2	1.373×10^6	2.288×10^4	4.59	4987.2
		1.6	1.724×10^6	2.874×10^4	4.32	6649.6
		2.0	2.069×10^6	3.449×10^4	4.15	8312
800 Die temp 520° F	20 mil orifice diameter, 10/1 L/D	0.4	2.897×10^5	7.242×10^3	10.33	701.3
		0.8	4.897×10^5	1.224×10^4	8.73	1402.6
		1.2	6.691×10^5	1.673×10^4	7.95	2103.9
		1.6	8.691×10^5	2.173×10^4	7.75	2805.2
		2.0	1.083×10^6	2.707×10^4	7.72	3506.5
	20 mil orifice diameter, 15/1 L/D	0.4	4.001×10^5	6.668×10^3	9.51	701.3
		0.8	6.346×10^5	1.058×10^4	7.54	1402.6
		1.2	8.277×10^5	1.380×10^4	6.56	2103.9
		1.6	1.000×10^6	1.667×10^4	5.94	2805.2
		2.0	1.269×10^6	2.115×10^4	6.03	3506.5

Table D.1 (Contd.)

Melt Flow Rate	Nosetip	Polymer Throughput (g/hole/min)	Pressure Drop (N/m^2)	Shear Stress (N/m^2)	Shear Viscosity Newt (Pa. Sec)	Shear Rate (sec^{-1})
800 Die temp 540° F	15 mil orifice diameter, 10/1 L/D	0.4	5.656×10^5	1.414×10^4	8.50	1662.4
		0.8	8.139×10^5	2.035×10^4	6.12	3324.7
		1.2	1.138×10^6	2.845×10^4	5.71	4987.2
		1.6	1.400×10^6	3.500×10^4	5.26	6649.6
		2.0	1.669×10^6	4.173×10^4	5.02	8312
	15 mil orifice diameter, 15/1 L/D	0.4	5.518×10^5	9.197×10^3	5.53	1662.4
		0.8	9.657×10^5	1.609×10^4	4.84	3324.7
		1.2	1.283×10^6	2.138×10^4	4.29	4987.2
		1.6	1.607×10^6	2.679×10^4	4.03	6649.6
		2.0	1.987×10^6	3.311×10^4	3.98	8312
800 Die temp 540° F	20 mil orifice diameter, 10/1 L/D	0.4	2.690×10^5	6.725×10^3	9.60	701.3
		0.8	4.552×10^5	1.138×10^4	8.11	1402.6
		1.2	6.484×10^5	1.621×10^4	7.70	2103.9
		1.6	8.277×10^5	2.069×10^4	7.38	2805.2
		2.0	1.042×10^6	2.604×10^4	7.42	3506.5
	20 mil orifice diameter, 15/1 L/D	0.4	3.725×10^5	6.208×10^3	8.85	701.3
		0.8	6.000×10^5	1.000×10^4	7.13	1402.6
		1.2	7.794×10^5	1.299×10^4	6.17	2103.9
		1.6	9.794×10^5	1.632×10^4	5.82	2805.2
		2.0	1.200×10^6	2.000×10^4	5.70	3506.5

Table D.1 (Contd.)

Melt Flow Rate	Nosetip	Polymer Throughput (g/hole/min)	Pressure Drop (N/m^2)	Shear Stress (N/m^2)	Shear Viscosity Newt (Pa. Sec)	Shear Rate (sec^{-1})
800 Die temp 560^0 F	15 mil orifice diameter, 10/1 L/D	0.4	5.104×10^5	1.276×10^4	7.68	1662.4
		0.8	8.07×10^5	2.02×10^4	6.07	3324.7
		1.2	1.09×10^6	2.724×10^4	5.46	4987.2
		1.6	1.366×10^6	3.414×10^4	5.13	6649.6
		2.0	1.628×10^6	4.07×10^4	4.90	8312
	15 mil orifice diameter, 15/1 L/D	0.4	5.173×10^5	8.622×10^3	5.31	1662.4
		0.8	9.243×10^5	1.54×10^4	4.63	3324.7
		1.2	1.193×10^6	1.99×10^4	3.99	4987.2
		1.6	1.552×10^6	2.587×10^4	3.89	6649.6
		2.0	1.89×10^6	3.15×10^4	3.79	8312
800 Die temp 560^0 F	20 mil orifice diameter, 10/1 L/D	0.4	2.69×10^5	6.725×10^3	9.59	701.3
		0.8	4.207×10^5	1.052×10^4	7.50	1402.6
		1.2	6.14×10^5	1.535×10^4	7.29	2103.9
		1.6	8.14×10^5	2.035×10^4	7.25	2805.2
		2.0	1×10^6	2.518×10^4	7.18	3506.5
	20 mil orifice diameter, 15/1 L/D	0.4	3.449×10^5	5.748×10^3	8.20	701.3
		0.8	5.587×10^5	9.312×10^3	6.64	1402.6
		1.2	7.656×10^5	1.276×10^4	6.06	2103.9
		1.6	9.105×10^5	1.517×10^4	5.41	2805.2
		2.0	1.138×10^6	1.897×10^4	5.41	3506.5

APPENDIX E- MASTER DATA TABLE

Table E.1 Master Data Table

Sample ID*	Face Gap, mils	Air Pressure at Die, psi	Die Temp., °F	Primary Air Temp., °F	SCFM/ inch+	Average Fiber Dia, μm
27[1]/-23[2]/0.4/400/15/10/60	57.1	6	504	582	15.5	2.81
36[1]/-39[2]/0.4/400/15/15/60	66.6	6	525	595	15.1	2.77
39[1]/-39[2]/0.4/400/20/10/60	75.9	5	527	594	17.0	2.30
36[1]/-35[2]/0.4/400/20/15/60	71.2	5	527	540	16.2	1.82
99[3]/-64[4]/0.4/400/15/10/60	233.0	1	525	596	15.8	2.42
118[3]/-93[4]/0.4/400/15/15/60	258.4	2	525	595	15.1	2.55
111[3]/-85[4]/0.4/400/20/10/60	246.0	1	527	594	14.9	1.82
108[3]/-80[4]/0.4/400/20/15/60	242.4	1	527	459	16.6	2.11
27[1]/-23[2]/0.8/400/15/10/60	57.1	6	558	577	15.9	3.24
36[1]/-39[2]/0.8/400/15/15/60	66.6	6	560	578	15.9	2.66
39[1]/-39[2]/0.8/400/20/10/60	75.9	5	561	578	16.8	2.59
36[1]/-35[2]/0.8/400/20/15/60	71.2	5	561	488	16.2	1.83
99[3]/-64[4]/0.8/400/15/10/60	233.0	1	560	577	16.3	2.11

Table E.1 (Contd.)

Sample ID*	Face Gap, mils	Air Pressure at Die, psi	Die Temp., °F	Primary Air Temp., °F	SCFM/ inch+	Average Fiber Dia, μm
118[3]/-93[4]/0.8/400/15/15/60	258.4	2	560	578	15.9	2.58
111[3]/-85[4]/0.8/400/20/10/60	246.0	1	561	578	14.6	2.34
108[3]/-80[4]/0.8/400/20/15/60	242.4	1	561	484	16.2	1.72
27[1]/-23[2]/0.4/35/15/10/60	57.1	6	595	608	15.8	2.48
36[1]/-39[2]/0.4/35/15/15/60	66.6	5	595	608	16.4	1.67
39[1]/-39[2]/0.4/35/20/10/60	75.9	5	597	608	16.4	1.79
36[1]/-35[2]/0.4/35/20/15/60	71.2	5	597	608	16.4	1.72
99[3]/-64[4]/0.4/35/15/10/60	233.0	1	596	609	15.7	2.16
118[3]/-93[4]/0.4/35/15/15/60	258.4	2	596	608	15.8	1.94
111[3]/-85[4]/0.4/35/20/10/60	246.0	1	597	609	15.7	2.36
108[3]/-80[4]/0.4/35/20/15/60	242.4	1	597	609	16.1	2.37
27[1]/-23[2]/0.4/35/15/10/60	57.1	6	625	640	15.9	2.88
36[1]/-39[2]/0.4/35/15/15/60	66.6	5	625	645	16.3	2.10

Table E.1 (Contd.)

Sample ID*	Face Gap, mils	Air Pressure at Die, psi	Die Temp., °F	Primary Air Temp., °F	SCFM/ inch+	Average Fiber Dia, μm
39[1]/-39[2]/0.4/35/20/10/60	75.9	5	624	645	15.3	2.31
36[1]/-35[2]/0.4/35/20/15/60	71.2	5	624	644	15.3	1.93
99[3]/-64[4]/0.4/35/15/10/60	233.0	1	627	645	16.4	2.50
118[3]/-93[4]/0.4/35/15/15/60	258.4	2	625	645	16.0	2.48
111[3]/-85[4]/0.4/35/20/10/60	246.0	1	624	645	16.1	2.28
108[3]/-80[4]/0.4/35/20/15/60	242.4	1	624	643	16.1	2.91
32[5]/+5/0.8/650/20/10/60	95.1	13	500	520	25.0	2.22
37[5]/-39/0.8/650/20/15/60	67.6	14	500	520	25.0	2.67
22[5]/+5/0.4/650/15/10/60	72.3	4	500	520	12.5	2.48
35[5]/-28/1.6/650/15/15/60	-	-	500	520	50.0	2.14
22[5]/+5/2.0/650/15/10/60	-	-	500	520	62.5	2.06
37[5]/-39/2.0/650/20/15/60	-	-	500	520	62.5	2.60
32[5]/-18/1.2/650/20/10/60	82.5	23	500	520	37.5	2.39

Table E.1 (Contd.)

Sample ID*	Face Gap, mils	Air Pressure at Die, psi	Die Temp., °F	Primary Air Temp., °F	SCFM/ inch+	Average Fiber Dia, μm
32^5/-28/0.8/650/20/10/60	71.0	16	500	520	25.0	2.49
36^5/-18/1.6/650/15/15/60	-	-	500	520	50.0	2.23
33^5/-5/1.2/650/20/15/60	91.9	24	500	520	37.5	2.32
36^5/-39/1.6/650/15/15/60	-	-	500	520	50.0	2.23
34^5/+5/2.0/650/15/15/60	-	-	500	520	62.5	2.19
34^5/-5/0.4/650/15/15/60	99.6	3.5	500	520	12.5	2.39
23^5/-18/0.8/650/15/10/60	52.6	13	500	520	25.0	1.98
27^5/-28/1.2/650/15/10/60	51.4	26	500	520	37.5	2.29
32^5/-18/2.0/650/20/15/60	-	-	500	520	62.5	2.56
34^5/-5/1.2/650/15/15/60	99.6	23	500	520	37.5	2.20
27^5/-39/2.0/650/15/10/60	-	-	500	520	62.5	2.32
32^5/-28/1.6/650/20/10/60	-	-	500	520	50.0	2.16
31^5/+5/1.2/650/20/15/60	96.7	27	500	520	37.5	2.12

Table E.1 (Contd.)

Sample ID*	Face Gap, mils	Air Pressure at Die, psi	Die Temp., °F	Primary Air Temp., °F	SCFM/ inch+	Average Fiber Dia, μm
35[5]/-28/0.8/650/15/15/60	74.6	16	500	520	25.0	2.11
22[5]/+5/0.4/650/15/10/60	72.3	4	500	520	12.5	2.35
27[5]/-39/0.4/650/15/10/60	39.7	5	500	520	12.5	2.69
23[5]/-18/1.2/650/15/10/60	52.6	26	500	520	37.5	2.08
23[5]/-18/1.6/650/15/10/60	-	-	500	520	50.0	2.20
32[5]/-5/0.4/650/20/10/60	94.5	3.8	500	520	12.5	2.40
32[5]/-28/2.0/650/20/10/60	-	-	500	520	62.5	2.61
34[5]/-5/0.8/650/15/15/60	99.6	13	500	520	25.0	2.58
39[5]/-39/0.4/650/20/10/60	73.8	4.5	500	520	12.5	3.09
32[5]/-28/0.4/650/20/15/60	66.9	4.5	500	520	12.5	3.34
32[5]/-18/0.4/650/20/15/60	79.0	3.7	500	520	12.5	2.49
35[5]/-28/2.0/650/15/15/60	-	-	500	520	62.5	2.30
31[5]/+5/1.6/650/20/15/60	-	-	500	520	50.0	2.05

Table E.1 (Contd.)

Sample ID*	Face Gap, mils	Air Pressure at Die, psi	Die Temp., °F	Primary Air Temp., °F	SCFM/ inch+	Average Fiber Dia, μm
32[5]/-5/2.0/650/20/10/60	-	-	500	520	62.5	2.55
39[5]/-39/1.2/650/20/10/60	73.8	28	500	520	37.5	2.30
31[5]/+5/1.6/650/20/15/60	-	-	500	520	50.0	2.29
32[5]/-18/0.8/650/20/15/60	79.0	12.5	500	520	25.0	2.49
27[5]/-5/0.8/650/15/10/60	77.9	13	500	520	25.0	2.23
36[5]/-39/1.2/650/15/15/60	39.7	28	500	520	37.5	1.90
32[5]/-5/1.6/650/20/10/60	-	-	500	520	50.0	2.24
54/-56/0.4/800/15/10/60	99.9	2.3	500	500	16.3	2.40
54/-56/0.8/800/15/10/60	99.9	2.3	500	500	16.3	2.77
27/-23/0.8/800/15/10/60	56.4	4.5	500	500	16.3	2.63
100/-64/0.8/800/15/10/60	228.4	1	500	500	16.3	2.87
54/-56/0.4/800/15/10/90	53.0	8	500	500	16.3	2.72
54/-56/0.8/800/15/10/90	53.0	8	500	500	16.3	2.96

Table E.1 (Contd.)

Sample ID*	Face Gap, mils	Air Pressure at Die, psi	Die Temp., °F	Primary Air Temp., °F	SCFM/ inch+	Average Fiber Dia, μm
27/-23/0.8/800/15/10/90	42.5	11	500	500	16.3	2.80
100/-64/0.8/800/15/10/90	160.0	1	500	500	16.3	3.08

1-nominal air gap, 35 mil; 2-nominal setback, 34 mil; 3-nominal air gap, 110 mil; 4-nominal setback, 80 mil; 5-nominal air gap, 31 mil. * Air knife gap, mil/Nosetip setback, mil/Polymer throughput, g/hole/min/MFR/Orifice dia, mil/Orifice L/D ratio/Nosetip angle, degrees. + Air slot width = 8 inches.

VITA

Ahamad Yacub Khan was born in Coimbatore, India on October 19, 1966. After attending A.G.B. Higher Secondary School in Dharmapuri, India he went to P.S.G. College of Technology, Coimbatore, a well respected engineering institution for higher learning in September 1983 to earn a Bachelor's degree in textile technology. He graduated in May 1987 with a first class and distinction. He secured a government of India scholarship in August 1987 towards a master of technology degree in fiber science at the Indian Institute of Technology, New Delhi, India, a prestigious institution of international reputation. In January 1989 he earned his master's degree. He then went to work in March 1989 as an Assistant Director at the Bureau of Indian Standards (BIS) attached to the ministry of commerce, Government of India. During his tenure at BIS he was responsible for monitoring quality licenses issued for textile and apparel items out of the southern regional office located in Madras, India. The author left India in August 1989 for the United States of America to join the doctoral program at the University of Tennessee, Knoxville. He worked in the area of melt blowing towards his dissertation. The author is a member of the Textile Institute, Manchester, UK. His hobbies include photography, travel, hiking, and fishing.